The regulation of L-selectin activity by proteolysis

A thesis submitted to Cardiff University in candidature for the degree of Doctor of Philosophy.

Andrew Charles John Newman

Institute of Infection and Immunity, School of Medicine

Cardiff University

May 2017

DECLARATION

This work has not been submitted in substance for any other degree or award at this or any other university or place of learning, nor is being submitted concurrently in candidature for any degree or other award.

Signed …… (candidate) Date ……

STATEMENT 1

This thesis is being submitted in partial fulfillment of the requirements for the degree of PhD

Signed …… (candidate) Date ……

STATEMENT 2

This thesis is the result of my own independent work/investigation, except where otherwise stated.

Other sources are acknowledged by explicit references. The views expressed are my own.

Signed …… (candidate) Date ……

STATEMENT 3

I hereby give consent for my thesis, if accepted, to be available online in the University's Open Access repository and for inter-library loan, and for the title and summary to be made available to outside organisations.

Signed …… (candidate) Date ……

STATEMENT 4: PREVIOUSLY APPROVED BAR ON ACCESS

I hereby give consent for my thesis, if accepted, to be available online in the University's Open Access repository and for inter-library loans **after expiry of a bar on access previously approved by the Academic Standards & Quality Committee.**

Signed …… (candidate) Date ……

Acknowledgements

I dedicate my PhD thesis to my inspirational Grandfather Malcolm Campbell

I would like to thank Sophie Wehenkel, Tim Wanger, Caroline Tinsley, Rosie Collings, Miriam Vigar and Pierre Rizkallah for their help throughout the project.

Most importantly, I would also like to thank my supervisors Ann Ager and Vera Knäuper for always offering the highest level of supervision, motivation and support during my PhD

Abstract

L-selectin (CD62L) is a type I transmembrane protein expressed by lymphocytes which directs their migration from the bloodstream into lymph nodes and infected tissues.

Stimulation of the T cell receptor (TCR) activates the enzyme A Disintegrin and Metalloproteinase 17 (ADAM 17), which cleaves L-selectin at the ectodomain generating a metalloproteinase product (MP product) comprising of a transmembrane region and a 17-amino acid intracellular domain (ICD). ϒ-secretase is a multi-subunit protease that cleaves up to 90 identified type I transmembrane proteins in the intramembrane region following ectodomain proteolysis by metalloproteinases. Presenilin (PS), the catalytic component of γ-secretase is activated during an intramolecular cleavage called endoproteolysis separating the carboxy (C) and amino (N) termini. The catalytically active C-terminal fragment of PS then induces intramembrane proteolysis of substrates. The aim of my thesis was to firstly determine whether the MP product of L-selectin was a substrate for PS. Subsequently, I analysed whether stimulation of the TCR activates PS, inducing intramembrane proteolysis of the MP product releasing the ICD into the intracellular region.

My data showed for the first time that in a resting T-cell, L-selectin forms a multi-component complex with both ADAM 17 and PS. TCR-activation induces ADAM 17 dependent proteolysis of L-selectin generating an MP product. Stimulation of the TCR also causes endoproteolysis of PS, where activated PS then cleaves the bound MP product. After PS cleavage, the released ICD was unstable and therefore difficult to detect, however I was able to block its formation using either PS inhibitor treatment or

generating I351W mutated L-selectin, which was resistant to intramembrane proteolysis.

Abbreviations

A Disintegrin And Metalloproteinase 17	ADAM 17
A DIYGs and peptidase homologous region	DAPs
Activated protein kinase B	Akt
Adaptor complex	AP-2
Adult respiratory distress syndrome	ARDS
Albumin-coated latex beads	ACLB
Alzheimer's disease	AD
Amino	N
Amyloid precursor protein	APP
Anterior pharynx defective-1	Aph-1
B regulatory	Breg
Bacterial/permeability increasing protein	BPI
Base pairs	bp
Calcium	Ca^{2+}
Calmodulin	CaM
cAMP response element binding	CREB
Carboxyl	C
Carboxyl-terminal fragment	CTF
Cardiac microvascular endothelial cells	HCMECs
Chemokine ligand	CCL
c-Jun N-terminal kinase	JNK

Cluster of differentiation	CD
Colony stimulating factor-1	CSF-1
Conserved ADAM seventeen dynamic interaction sequence that binds substrates	CANDIS
C-type lectin domain	CTLD
C-X-C motif chemokine	CXCL
Cyclic guanosine monophosphate	cGMP
Dendritic cells	DC
Ectodomain	ECD
Endoglycosidase-H	endo-H
Endoplasmic reticulum	ER
Endothelial protein C receptor	EPCR
Endotoxin-stimulated human umbilical vein endothelial cells	HUVECs
Eph receptor B4	EphB4
Epidermal growth factor like domain	EGF
Epidermal growth factor receptor	EGFR
Extracellular signal-regulated kinase	Erk
Ezrin-radixin-moesin	ERM
F for 4.1 protein, E for ezrin, R for radixin and M for moesin	FERM
F-box/WD repeat containing protein 7	FBXW7
Fibroblast growth factor	FGF
Forkhead box protein O1	FOXO1
Four and Half LIM domain 2 protein	FHL2

Glycosylation-dependent cell adhesion molecule-1	GlyCAM-1
Graft vs host disease	GVHD
Granulocyte colony stimulating factor	G-CSF
Growth factor receptor-bound protein 2	Grb-2
Heat shock protein 90	Hsp90
Heparin-binding EGF-like growth factor	HB-EGF
High endothelial venule	HEV
Human embryonic kidney	HEK 293
Human epidermal growth factor -2	Her-2
Hydrophobic domain VII	HDVII
Hydrogen peroxide	H_2O_2
Hypochlorous acid	HClO
Immunoreceptor tyrosine based activation motifs	ITAMs
Intercellular adhesion molecule	ICAM
Interferon-γ	IFN-γ
Interleukin	IL
interleukin receptor	IL-R
Intracellular domain	ICD
Keratinocyte chemoattractant	KC
Kit ligand 2	KitL2
Krüppel-like Factor 2	KLF-2
L1 cell adhesion molecule	L1CAM
Large extracellular loop	LEL

Lipopolysaccharide	LPS
Lymph node	LN
Lymphocyte specific tyrosine kinase	Lck
Magnetic activated cells sorting	MACS
Major histocompatibility complex	MHC
Matrix metalloproteinase	MMP
Mechanistic target of rapamycin	mTOR
Membrane proximal region	MPR
Metalloproteinase	MP
Mitogen and stress activated kinase	MSK
Mitogen-activating protein	MAP
Monoclonal antibody	mAb
Mouse embryonic fibroblasts	MEFs
Myeloid-derived suppressor cells	MDSCs
Natural killer	NK
Neutrophil extracellular traps	NETs
N-Formylmethionine-leucyl-phenylalanine	fMLP
Nitric oxide	NO
Nitric oxide synthase	iNOS
Nuclear factor kappa-light-chain-enhancer of activated B cells	NF-kB
Nuclear factor of activated T-cells	NFAT
Pathogen-activated molecular patters	PAMPs
Peptidylarginine deiminase 4	PAD4

Peripheral lymph node addressin	PNAd
Peripheral lymph node	PLN
Phorbol 12-myristate 13-acetate	PMA
Phosphatase and tensin homolog	PTEN
Phosphatidylserine	Ptd-L-Ser
Phosphofurin acidic cluster sorting protein 2	PACS-2
Phosphoinositide (3,4,5) trisphosphate	$PI(3,4,5)P_3$
Phosphoinositide 3-kinase	PI3K
Platelet activating factor	PAF
Platelet-derived growth factor	PDGF
Platelet-derived growth factor receptor-alpha	PDGFRA
Polymerase chain reaction	PCR
Premelanosome protein	PMEL
Presenilin	PS
Presenilin enhancer-2	Pen-2
Proline-alanine-leucine	PAL
Protease activated receptor-1	PAR-1
Protein disulphide isomerase	PDI
Protein kinase C	PKC
Protein kinase G	PKG
P-selectin glycoprotein ligand-1	PSGL-1
Ras-related C3 botulinum toxin substrate 2	Rac-2
Rat cluster of differentiation 2	rCD2

Reactive oxygen species	ROS
Real time quantitative polymerase chain reaction	q-PCR
Receptor tyrosine kinase	Ryk
Short complement like repeat domains	SCR
Sialyl Lewis X	sLex
Soluble L-selectin ECD	sL-selectin
Son of Sevenless	SOS
Synapse associated protein-9	SAP-9
T cell acute lymphoblastic leukaemia	T-ALL
T cell immunoglobulin and mucin domain 3	Tim-3
T cell receptor	TCR
T regulatory cells (Tregs)	Tregs
Tetraspanin	TSPAN
Tetratricopeptide repeat	TPR
Tissue metalloproteinase inhibitor 3	TIMP-3
TNF-α receptor associated periodic febrile syndrome	TRAPS
Toll-like receptor 4	TLR-4
Transforming growth factor-α	TGF-α
Transmembrane domains	TMDs
Tumour necrosis factor-α	TNF-α
Tumour necrosis factor-α receptor-1	TNFR-1
Tyrosine kinase with immunoglobulin-like and EGF-like domains-2	Tie-2

Wild type	WT
Zinc finger nuclease-1	ZFN-1

Table of contents

Figures

Tables

1 Introduction

1.1 The immune system

The immune system is divided into two parts named the innate and adaptive responses. The innate response is a form of immunity that is activated immediately and is non-specific in nature to the invading microorganism involving components of the immune system such as monocytes, macrophages and neutrophils. Unlike the innate immune system, the adaptive immune system is specific to an antigen which has been presented to T-lymphocytes that induces long-lasting protection to the host (Hoebe, *et al.* 2004).

1.1.1 The innate immune response

During innate immunity, macrophages express cell surface toll-like receptors at the site of infection which interact with invading pathogens causing the plasma membrane to restructure around the microbe forming a pseudopodium (Ribes, *et al.* 2010). The pseudopodium then engulfs the microbe during endocytosis which forms an intracellular vesicle called a phagosome that later fuses with a lysosome generating a phagolysosome (Weiss and Schaible, 2015). The phagolysosome contains lytic enzymes such as lysozyme that degrades the microbe (Ip *et al.* 2010). Activated macrophages then release cytokines such as granulocyte colony stimulating factor (G-CSF) and tumour necrosis factor-α (TNF-α), which recruits neutrophils and extends their life-span at the site of infection from 6-12 to 24-72 h by inhibiting apoptosis (Selders, *et al.* 2017). Neutrophils contain three types of granules known as azurophilic (primary), specific (secondary) and tertiary, which encompasses proteins with antimicrobial properties (Lacy, *et al*. 2006). Specifically, azurophilic granules contain myeloperoxidase, bactericidal/permeability-

increasing protein (BPI), defensins and the serine proteases cathepsin G and neutrophil elastase (Loria, *et al. 2008;* Calafat, *et al.* 2000; Faurschou, *et al.* 2002; Hanson, *et al.* 1990; Korkmaz, *et al.* 2010). Specific granules comprise of alkaline phosphatase, lysozyme, NAPDH oxidase, collagenase, lactoferrin and cathelicidin (Parmley, *et al.* 1986; Saito, *et al.* 1987; Steadman, *et al.* 1996; Esaguy, *et al.* 1989; Tan, *et al.* 2006), while tertiary granules hold cathepsin, gelatinase and collagenase (Wysocka, *et al.* 2001; Faurschou, *et al.* 2003). Upon encounter with a pathogen, neutrophils release these antimicrobial proteins from azurophilic, specific and tertiary granules in an immunological process called degranulation, which helps combat infection (Lacy, *et al.* 2006). Additionally, during an encounter with pathogens, NAPDH oxidase in neutrophils becomes activated and reduces oxygen to form reactive oxygen species (ROS) (Karlsson, *et al.* 2002). ROS are then degraded by enzymes such as superoxide dismutases to form hydrogen peroxide (H_2O_2) which is subsequently converted to hypochlorous acid (HClO) by myeloperoxidase (Segal, 2005; Kettle and Winterbourn, 1990). Neutrophils then engulf pathogens which are then later lysed in intracellular phagosomes by H_2O_2 and HClO (Robinson, 2008). After intracellular lysis of pathogens, neutrophils then activate peptidylarginine deiminase 4 (PAD4), which decondenses chromatin and ejects the DNA coils to the extracellular space to form neutrophil extracellular traps (NETs) in an immunological process called NETosis (Martinod, *et al.* 2013; Mohanty, *et al.* 2015). These NETs are impregnated by microbial agents such as myeloperoxidase, neutrophil elastase, defensins and cathepsin G. Circulating pathogens are then trapped by NETs which are subsequently degraded by the associated microbial proteins (Mohanty, *et al.* 2015). Neutrophils then release chemokine ligand 2 (CCL2), interleukin 2 (IL-2), chemokine (C-X-C motif) ligand 1 (CXCL1), macrophage inflammatory protein 1-α and

interferon-γ (IFN-γ), which causes the recruitment of monocytes to the site of inflammation and their differentiation to macrophages (Blidberg, *et al.* 2012; Scapini *et al.* 2000). The recruited macrophages then engulf both non-apoptotic and apoptotic neutrophils to regulate the immune response (Selders, *et al.* 2017).

1.1.2 The adaptive immune response

For a naïve T cell to induce an adaptive immune response, the T cell receptor (TCR) needs to recognize a specific antigen presented within the major histocompatibility complex (MHC) at the cell surface of dendritic cells (DC). However, the amount of T cells specific for a cognate antigen is low (1:5,000 to 1:50,000) and only a small subpopulation of DCs present the cognate peptide on MHC molecules (Westermann*, et al.* 2001). Consequently, T cells enter lymph nodes (LNs) after transmigration across post-capillary vascular endothelium called high endothelial venules (HEVs) and search for resident DCs that present cognate peptide in the T cell zone (paracortex) (Hay*, et al.* 1977; Gretz*, et al.* 1997; Bajenoff*, et al.* 2003). Naïve T cells then interact with the dendritic cells, become activated and then prime into an effector T cell. Effector T cells change expression of cell surface adhesion molecules and chemokine receptors which alters their migratory pattern from lymphoid organs to sites of inflammation and non-lymphoid tissue where they have the capacity to induce an immune response (Lipp*, et al.* 2002; Sallusto*, et al.* 2000; Sallusto*, et al.* 1999; Mora and von Andrian, 2006; Lefrançois and Marzo, 2006) (Fig 1.1).

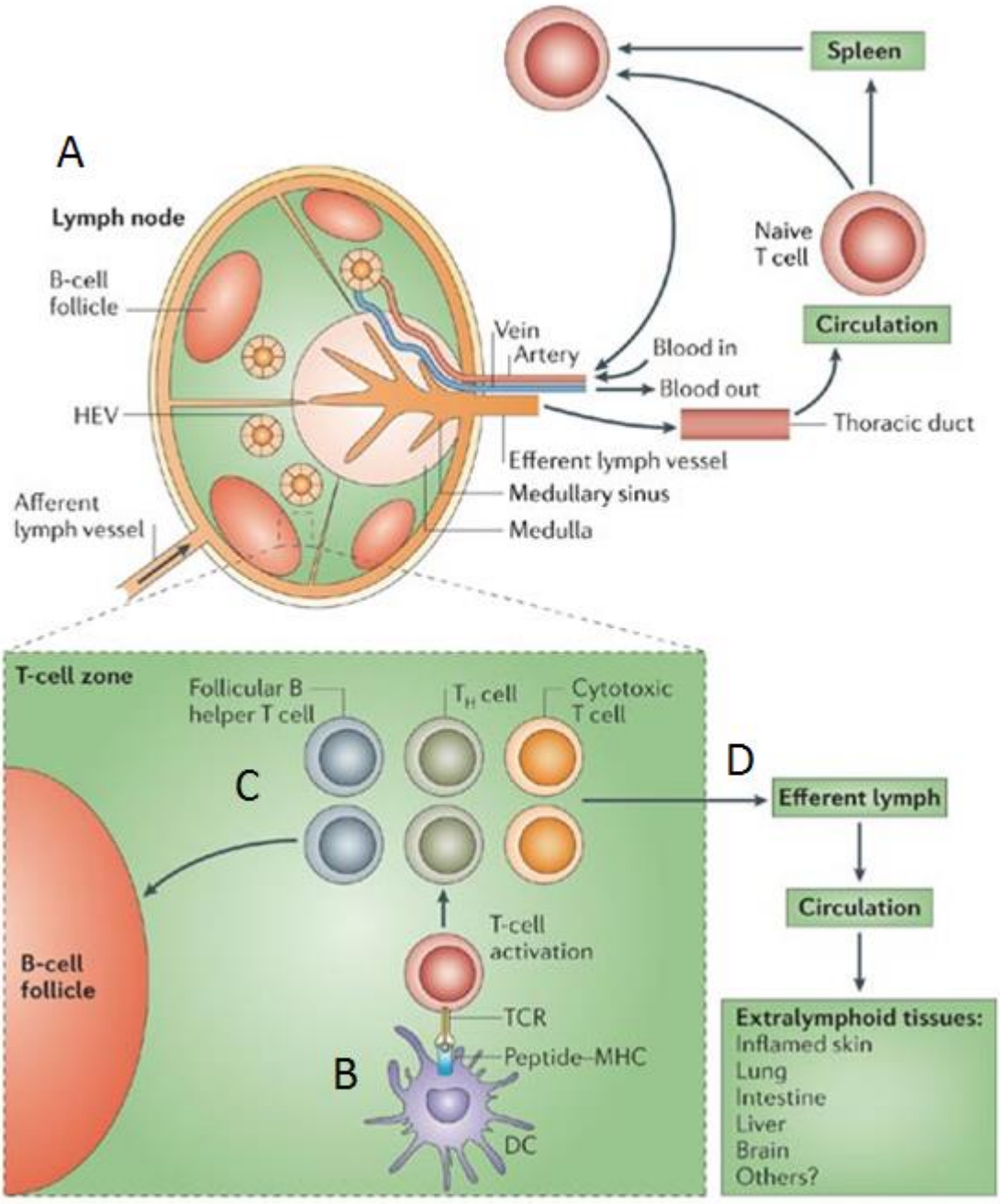

Figure 1.1: Naive T cell activation in the peripheral LNs during adaptive immunity. (A) Naïve T cells transmigrate across HEVs to enter LNs. (B) At the T-cell zone within the LN, the naïve T cell encounters a DC presenting cognate peptide. The TCR of the naïve T cell interacts with cognate peptide presented with MHC on the surface of dendritic cells. (C) The TCR becomes activated and naïve T cells differentiate into effector T cells (such as cytotoxic T cells or T helper (TH) cells) some of which are recruited to the B-cell follicle to help B cells (follicular B helper T cells). (D) Effector T cells egress from the LN through efferent lymph vessels and migrate towards infected tissue to induce an immune response (Agace, 2006).

1.2 L-selectin

1.2.1 The structure of L-selectin

L-selectin is a type I transmembrane protein found on the cell surface of leucocytes, comprised of an ectodomain (ECD), a transmembrane helix and a 17-amino acid intracellular domain (ICD). The ECD contains a C-type lectin domain (CTLD), an epidermal growth factor like domain (EGF), two short complement like repeat domains (SCR) followed by a membrane proximal metalloproteinase cleavage site (Kansas, 1992) (Fig 1.2).

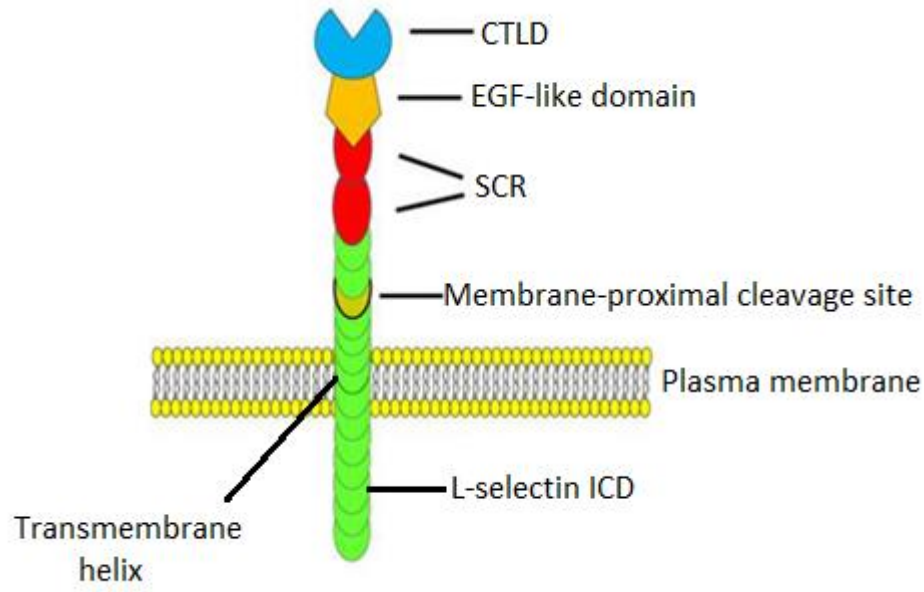

Figure 1.2: The structure of L-selectin. L-selectin is a type I transmembrane protein located at the cell surface of leucocytes. L-selectin contains an ECD comprised of a C-type lectin domain (CTLD), an epidermal growth factor like domain (EGF-like domain), two short complement like repeat domains (SCR) followed by a transmembrane region which spans the membrane leading to a 17-amino acid ICD (L-selectin ICD) localized intracellularly (Modified from Ivetic, 2013).

1.2.2 Microvillar localization of L-selectin is regulated by ERM proteins.

L-selectin localizes to both microvillar tips and the actin cytoskeleton via its ICD. The L-selectin ICD interaction with α-actinin is disrupted upon truncation of 11-amino acids at the carboxyl (C) terminus and consequently, L-selectin cannot bind to the cortical actin cytoskeleton (Palvalko*, et al.* 1995). However, L-selectin localizes at microvillar tips regardless of its interaction with α-actinin, showing that other cytoskeletal proteins link L-selectin to microvilli (Dwir*, et al.* 2001; Palvalko*, et al.* 1995, Ivetic and Ridley, 2004). Ezrin-radixin-moesin (ERM) proteins use their amino (N) terminus to bind intracellular domains (ICDs) of membrane proteins (such as cluster of differentiation 43 and 44 (CD43 and CD44)) and their C terminus to bind F-actin which links these adhesion molecules to the cortical actin cytoskeleton (Ivetic and Ridley, 2004). Ezrin and moesin were firstly shown to bind the L-selectin ICD using affinity chromatography with lymphocyte extracts (Ivetic*, et al.* 2002). The positively charged polar residues Arg^{357} and Lys^{362} in the L-selectin ICD bind with ezrin and moesin and disruption of this interaction using alanine mutants (R357A and K362A) significantly reduces microvillar localization (Ivetic*, et al.* 2002; Ivetic*, et al.* 2004).

1.3 The function of L-selectin during leucocyte homing to lymphoid organs and inflamed tissues

1.3.1 Lymphocyte recruitment to lymphoid organs

Gallatin *et al* firstly showed that L-selectin is a lymphocyte-homing receptor which regulates lymphocyte migration into peripheral LNs (Gallatin*, et al.* 1983). The importance of L-selectin was demonstrated by Arbonés*, et al.* where truncation of the N-terminal lectin domain prevented lymphocyte adherence to HEVs and localization in PLNs. Additionally, in L-selectin deficient mice, lymphocyte recruitment to LNs was significantly reduced, yet migration to the spleen was elevated (Arbonés*, et al.* 1994).

Sulphated glycoproteins such as glycosylation-dependent cell adhesion molecule-1 (GlyCAM-1), CD34 and podocalyxin were initially established as adhesion ligands expressed on HEVs surrounding lymphoid organs (Imai*, et al.* 1991; Lasky, 1992; Baumhueter*, et al.* 1993; Sassetti*, et al.* 1998) which interacted with MECA-79 monoclonal antibody (mAb) inhibiting lymphocyte adherence to HEVs (Streeter*, et al.* 1988). These ligands express 6-sulphated Sialyl Lewis X (sLex) tetrasaccharide structures and collectively are called peripheral lymph node addressin (PNAd) (Streeter*, et al.* 1988; van Zante and Rosen, 2003). L-selectin on the surface of naïve T cells forms weak glycosidic bonds with these endothelial ligands causing the leucocyte to tether to the inside of the blood vessel wall (Giblin*, et al.* 1997). The microvillus contains lipid rafts, rich in cholesterol micoodomains and glycosphingolipids. These lipid rafts promote L-selectin clustering which encourages multivalent tethering with endothelial ligands increasing the strength of interaction during blood flow (Abbal*, et al.* 2006; Phong*, et al.* 2003). Initially, L-selectin intermittently interacts

with its endothelial ligands, with interactions lasting between 10^{-2} and 10^{0} seconds, causing leukocytes to roll in the direction of blood flow (Alon*, et al.* 1997). The rolling leucocyte then encounters chemokines such as CXCL12 which cause activation of integrins (β_1 and β_2) on the surface of leucocytes (Hartmann*, et al.* 2008). These integrins bind stably to the endothelial ligands, intercellular adhesion molecule (ICAM-1 and ICAM-2) decelerating the velocity of cell rolling until cells arrest (Gopalan*, et al.* 1997), which occurs after 1-3 seconds (Bjerknes*, et al.* 1986). The leucocyte then enters the peripheral LN by transmigrating across the endothelial cell layer (Fig 1.3) (Vestweber and Blanks, 1999).

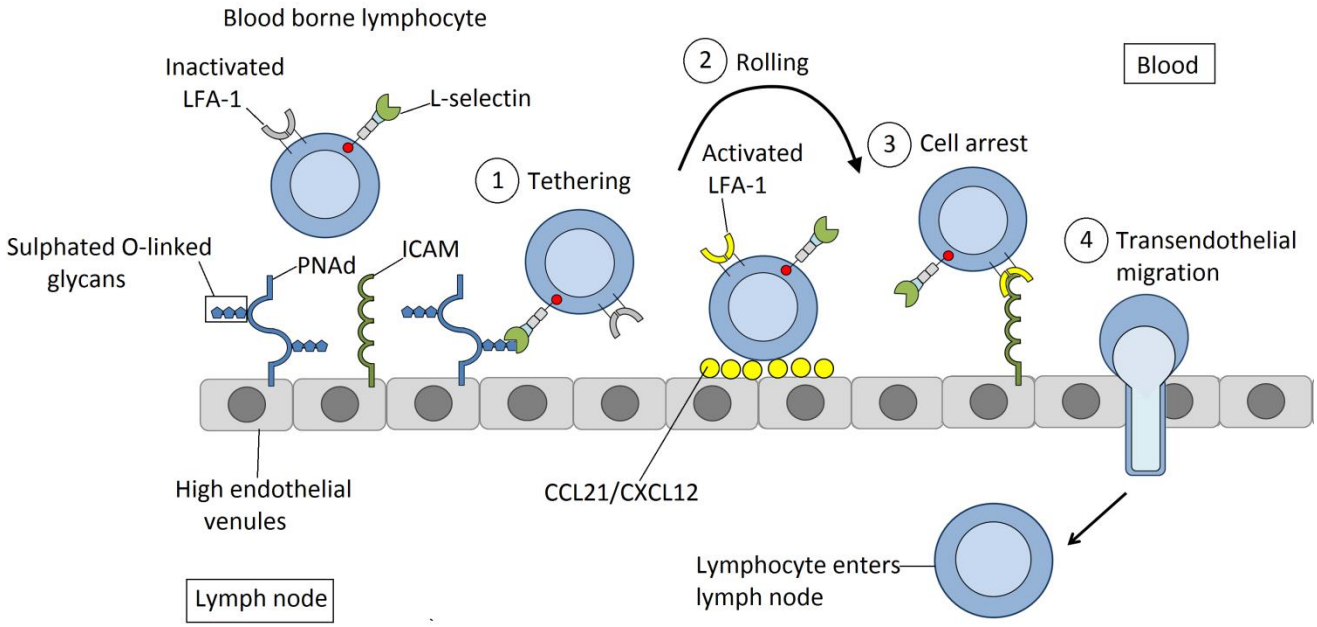

Figure 1.3: The various stages of the multi-step adhesion cascade. (1) Tethering – L-selectin, expressed on the surface of lymphocytes induces weak glycosidic bonds with sulphated O-linked glycans presented on endothelial ligands such as PNAd. These interactions allow lymphocytes to be recruited from the circulation to the surface of HEVs inside lymph nodes. (2) Rolling –The strong hydrodynamic force of blood flow causes dissociation between L-selectin and PNAd. L-selectin constantly dissociates and re-associates with HEV endothelial ligands causing the lymphocyte to roll along the endothelial wall. During rolling, chemokines such as CCL21 and CXCL12, presented on the apical aspect of the endothelium via anchorage to glycosaminoglycans contact lymphocytes and activate integrins such as LFA-1 (shown in diagram as grey (inactivated) to yellow (activated)). (3) Cell arrest -Activated LFA-1 binds stably to the HEV endothelial ligand ICAM. This interaction causes deceleration of lymphocyte rolling causing cell arrest. (4) Transendothelial migration- The arrested lymphocyte starts to transmigrate across the HEV allowing entry into the lymph node.

1.3.2 L-selectin and PSGL-1 interactions regulate secondary tethering of leucocytes

During the course of inflammation, leucocytes accumulate on the vascular wall and reduce the amount of available endothelial ligands for newly arriving leucocytes preventing further tethering with the inflamed endothelium monolayer. To allow continued influx of leucocytes in inflamed tissue beyond these adhesive events following the induction of inflammation, adherent leucocytes themselves act as adhesive substrates to allow further recruitment of additional leucocytes (Bargatze, *et al.* 1994). P-selectin glycoprotein ligand-1 (PSGL-1) expressed on the surface of leucocytes interacts with L-selectin which allows flowing leucocytes in circulation to attach adherent leucocytes on the endothelium in a process called secondary tethering (Fig 1.4) (Tu, *et al.* 1996; Spertini, *et al.* 1996).

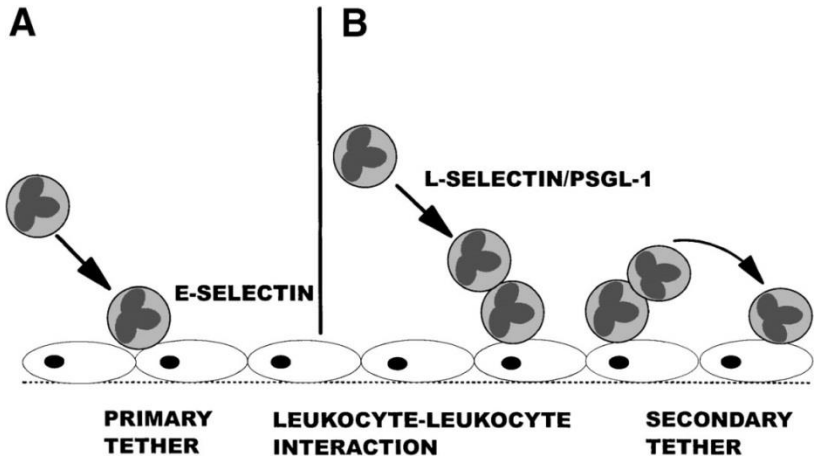

Figure 1.4: L-selectin and PSGL-1 interactions mediate secondary tethering. (A) In a primary tether, lymphocytes bind to E-selectin presented on the endothelial surface. (B) In secondary tethering, a free-flowing lymphocyte in circulation binds to an adherent lymphocyte on the endothelium and is regulated by interactions between L-selectin and PSGL-1 (Mitchell*, et al.* 2000).

1.3.3 Leucocyte recruitment to inflamed tissues

L-selectin also regulates leucocyte recruitment to non-lymphoid tissues which correlates with acute inflammation. Studies using L-selectin blocking antibodies which disrupt interactions with endothelial ligands prevent leucocyte rolling along exposed rat mesentery (Ley*, et al.* 1991) and rabbit mesenteric venules (von Andrian*, et al.* 1991). L-selectin deficient mice showed a reduction of neutrophil (52-62 %), lymphocyte (70-75 %) and monocyte (72-79 %) migration into inflamed peritoneum after 24 to 48 h thioglycollate challenge. Furthermore, inflammation in the footpad by red blood cell challenge and ear after oxazolone treatment were reduced 75 % and 69 % respectively in comparison to wild type (WT) mice. L-selectin deficient mice also showed a 90 % survival rate after lipopolysaccharide (LPS)-induced toxic shock in comparison to a 90 % mortality rate in WT mice (Tedder*, et al.* 1995).

L-selectin endothelial ligands presented on non-lymphoid organs have been researched for many years. Adherence of human and mouse B cells on human TNF-α activated cardiac microvascular endothelial cells (HCMECs) increased 80 % after transfection with human L-selectin cDNA in comparison to non-transfected cells. Also, B cell adherence was disrupted by $NaClO_3$, which inhibits posttranslational sulfation showing that TNF-α activation upregulates sulphated ligands on HCMECs (Zakrzewicz*, et al.* 1997). Sulfoglucuronyl glycosphingolipids presented on the surface of the brain microvascular endothelium was also shown to bind L-selectin allowing leucocyte recruitment to the central nervous system (Needham*, et al.* 1993). Later studies then identified sulphates presented on the surface on non-lymphoid organs that bind to L-selectin. Firstly, Kawashima *et al* established versican as the chondroitin sulphate presented on the surface of human renal adenocarcinoma cells of

the kidney (Kawashima, *et al.* 1999). Collagen XVIII was then recognised as the heparan sulphate proteoglycan expressed in rat kidneys that interacted with L-selectin causing infiltration of monocytes (Kawashima, *et al.* 2003). Also, the dermatan sulphate biglycan was shown to be presented on the surface of endometrial microvascular endothelial cells in human uterine endometrium which bound to L-selectin on natural killer (NK) cells allowing adherence and rolling (Kitaya*, et al.* 2009).

1.3.4 The role of L-selectin during inflammatory diseases

L-selectin dependent lymphocyte recruitment during inflammation either attenuates or intensifies immune disease progression (table 1.1).

Immune disease	Immunological role for L-selectin
Encephalomyelitis	L-selectin ligands are abundantly expressed on myelin sheaths causing leucocyte homing to myelinated axons (Huang, *et al.* 1991; Huang, *et al.* 1994). L-selectin causes infiltration of macrophages to the parenchyma initiating myelin damage in the central nervous system leading to encephalomyelitis. L-selectin deficient mice did not develop encephalomyelitis, however adoptive transfer of WT macrophages initiated development of encephalomyelitis correlated with destruction of myelin (Grewal, *et al.* 2001).
Graft vs host disease	The definite role of L-selectin during graft vs host disease (GVHD) is conflicting depending on the cell type. In lymphocytes, L-selectin deficient BALB/c mice showed reduced rates of rejection to both primary and secondary allogeneic skin grafts in comparison to WT correlated with less CD4+ and CD8+ T cells localized at the dermis and graft bed (Tang*, et al.* 1997). However, increased L-selectin expression in T regulatory cells (Tregs) reduced expansion of alloreactive T effector cells which protected the host against GVHD allowing engraftment of the transplanted bone marrow. Injected Tregs with high cell surface L-selectin expression migrated to lymph nodes and interfered with expansion, activation and priming of alloreactive T cells. In contrast, Tregs with low cell surface L-selectin expression migrated directly to the GVHD tissue allowing alloreactive T cells to become activated and expand in the

	lymph node before migrating to the graft initiating autoimmune destruction (Taylor, *et al.* 2004).
Atherosclerosis	L-selectin causes migration of Treg and B regulatory (Breg) cells to aortas inducing a pro-atherogenic role. L-selectin also recruits splenic B cells such as B1aB cells to the aorta which release a natural antibody named T15 that interacts to oxidative-specific epitopes preventing macrophages endocytosing oxidized low-density lipoproteins reducing foam cell accumulation in the aorta. Other L-selectin recruited splenic Breg cells secrete IL-10, which suppresses the progression of atherosclerosis. (Galkina*, et al.* 2006; Doran*, et al.* 2012; Caligiuri*, et al.* 2002; Major*, et al.* 2002; Kyaw*, et al.* 2011; Binder*, et al.* 2005). The pathology of atherosclerosis was accelerated in L-selectin deficient mice (Rozenberg*, et al.* 2011) with 74 % increased plaque formation in the aorta alongside lower numbers of recruited B1a and Breg cells (Gjurich *, et al.* 2014).
Asthma	L-selectin is not required for recruitment of neutrophils, monocytes and eosinophils into the airway-lung during an allergic inflammatory response. However, L-selectin mediates infiltration of CD3+ T cells to the airway-lung and sensitizes mice to airway hyperresponsiveness after allergic airway disease was stimulated with ovalbumin (Fiscus, *et al.* 2001).

Table 1.1: Immune diseases correlated with L-selectin dependent leucocyte recruitment to affected tissues.

1.3.5 L-selectin clustering induces signalling pathways that increases integrin β_2 expression

L-selectin clustering causes activation of the mitogen-activating protein (MAP) kinase pathway, superoxide generation, elevated intracellular calcium (Ca^{2+}) and increased mRNA expression of TNF-α and IL-8 (Brenner*, et al.* 1996; Brenner*, et al.* 1997a; Crockett-Torabi*, et al.* 1995; Waddell*, et al.* 1994; Waddell*, et al.* 1995).

Brenner *et al* demonstrated that L-selectin clustering in Jurkat T cells induces lymphocyte-specific tyrosine kinase (p56 Lck) dependent phosphorylation at terminal Tyr^{372} in the L-selectin ICD causing association to both growth factor receptor-bound protein 2 (Grb-2) and Son of Sevenless (SOS) leading to activation of Ras and Ras-related C3 botulinum toxin substrate 2 (Rac-2), which increased O^{2-} synthesis (Brenner, *et al.* 1996). In later studies, they also found that activated Ras and Rac-2 induced by L-selectin clustering caused a tenfold increase in actin filament polymerization which remained stable for 45 min, possibly correlated with firm leucocyte adhesion to endothelial cells (Brenner, *et al.* 1997).

In other studies, L-selectin cross-linking in neutrophils was linked to increased cell surface expression of β_2 integrin CD11b/CD18. Simon *et al* showed that L-selectin clustering sensitized neutrophils to platelet activating factor (PAF) mediated CD11b/CD18 expression which doubled the numbers of neutrophils that transmigrated across endotoxin-stimulated human umbilical vein endothelial cells (HUVECs) (Simon, *et al.* 1995). Elevated CD11b/CD18 expression after L-selectin engagement also increased neutrophil adherence to enteroendocrine L cells previously transfected with ICAM-1 and human E-selectin (Gopalan, *et al.* 1997). Tsang *et al* further demonstrated that both L-selectin clustering and IL-8 expression increased neutrophil adherence to albumin-coated latex beads (ACLB) and also increased neutrophil transmigration across IL-1 stimulated HUVECs (Tsang, *et al.* 1997). Based on previous studies that show increased transcription of IL-8 and ICAM-1 in IL-1 stimulated endothelial cells (Zimmerman, *et al.* 1990; Sica, *et al.* 1990), Tsang *et al* suggested that IL-1 stimulates endothelial cells to release IL-8 which acts in synergy with L-selectin to induce CD11b /CD18 dependent neutrophil adhesion on upregulated endothelial ICAM-1 allowing transmigration (Tsang, *et al.* 1997). Simon *et al* then found that closely associated L-selectin and CD18 were uniformly distributed along the circumference of

resting neutrophils. L-selectin engagement caused rapid induction of F-actin assembly causing co-localization of L-selectin and CD18 at the site of the neutrophil membrane in contact with endothelium enhancing β_2 expression for firm adhesion (Simon, *et al.* 1999).

Phosphorylation of p38 MAP kinase after L-selectin clustering also elevates the immune response by causing neutrophils to secrete both secondary and tertiary granules in response to IL-8 (Smolen, *et al.* 2000). Additionally, L-selectin cross-linking activates nuclear factor of activated T-cells (NFAT) which is recruited to the nucleus and interacts with the colony stimulating factor-1 (CSF-1) gene to activate transcription (Chen*, et al.* 2008; Chen*, et al.* 2010). CSF-1 regulates cell development and activity of monocytes enhancing the immune response (Konicek, *et al.* 1998).

1.4 Regulation of cell surface L-selectin expression levels

1.4.1 Ectodomain proteolysis of L-selectin by ADAM 17

Following protein kinase C (PKC) activation with phorbol 12-myristate 13-acetate (PMA), L-selectin is cleaved in the ectodomain between the membrane proximal site and second short consensus repeat between residues Lys^{321} and Ser^{322} (Kahn, *et al.* 1994). The enzyme responsible is A Disintegrin and Metalloproteinase 17 (ADAM 17) (Peschon, *et al.* 1998). After release of the 68 kDa ECD, an 8 kDa metalloproteinase (MP) product remains in the plasma membrane which comprises the transmembrane region and 17-amino acid L-selectin ICD (Kahn, *et al.* 1994) (Fig 1.5).

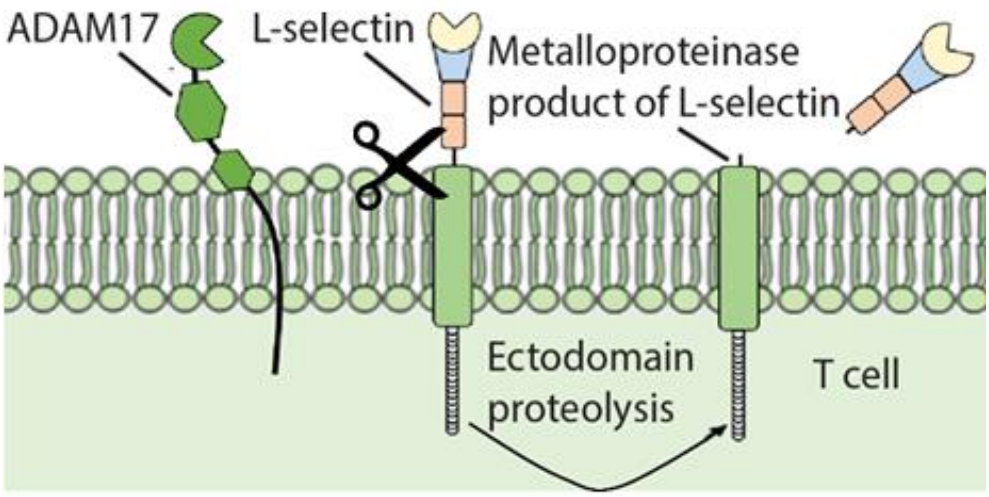

Figure 1.5: Ectodomain shedding of L-selectin mediated by ADAM 17. PMA activates ADAM 17 which cleaves L-selectin at the ectodomain generating an MP product comprising of a transmembrane region and a 17-amino acid L-selectin ICD.

1.4.2 Activation of the TCR modulates proteolysis and gene transcription of L-selectin

Studies have shown that TCR-activation modulates cell surface expression of L-selectin on lymphocytes. For instance, TCR-activation in response to immunization of mice (Bradley, *et al.* 1991), antigens derived from Sendai virus pneumonitis (Hou, *et al.* 1993) or allogeneic skin grafts (Mobley, *et al.* 1992) correlated with reduced cell surface L-selectin expression. Within 3-4 h of TCR activation, L-selectin proteolyzes rapidly which decreases expression by 90 %. After 48 h, expression levels increase 3-4 fold due to increased mRNA stability and de novo protein synthesis. High cell surface L-selectin expression levels persist for 3 days and finally lower at days 6-7 due to a combination of proteolysis and a decline in mRNA levels resulting in loss of gene transcription (Chao, *et al.* 1997).

Sinclair *et al* found that TCR activation initiates the phosphoinositide 3-kinase (PI3K) and mechanistic target of rapamycin (mTOR) signalling pathway to downregulate L-selectin by increased proteolysis and reduced transcription (Sinclair*, et al.* 2008) (Fig 1.6).

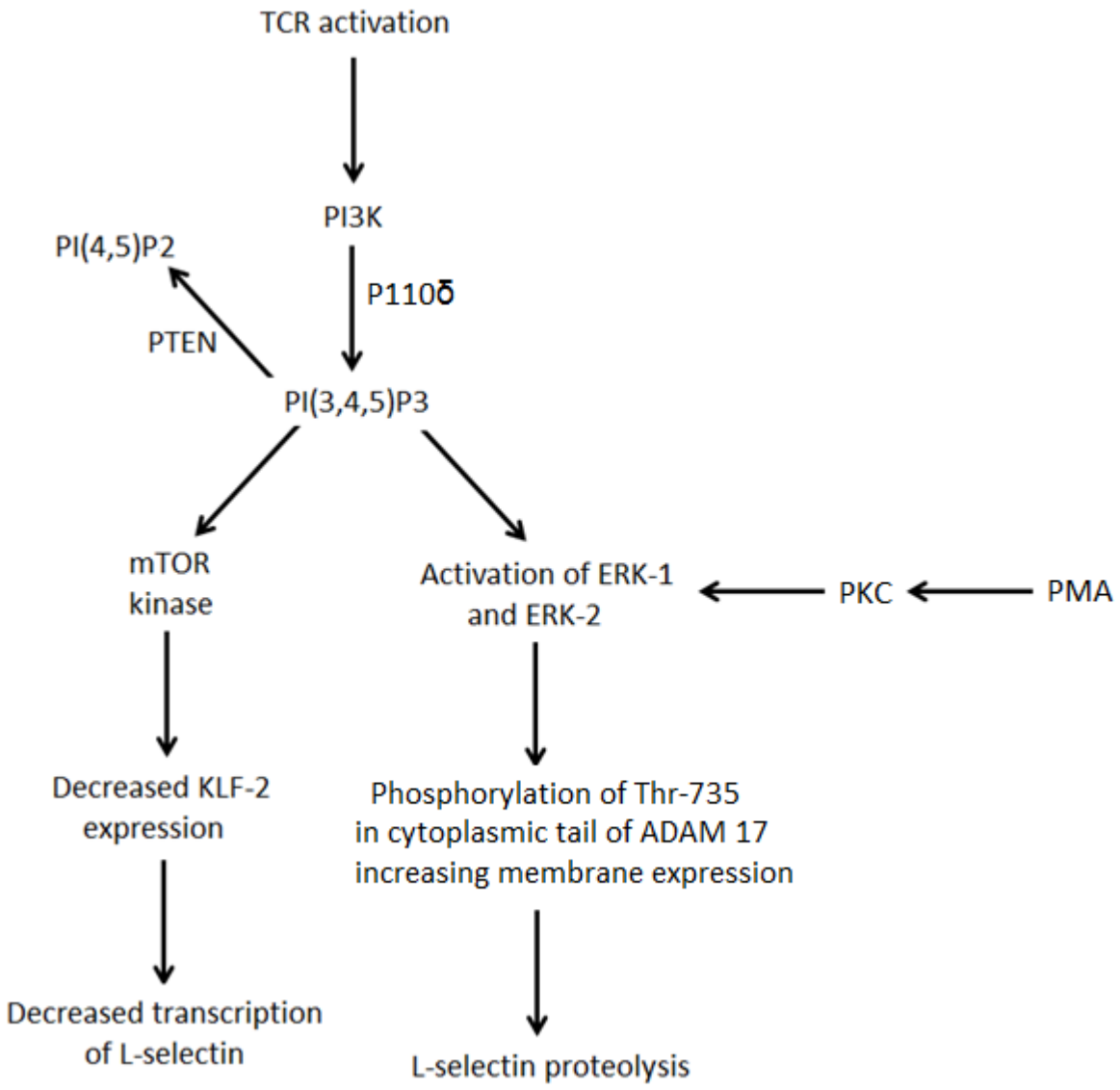

Figure 1.6: TCR activation upregulate the PI3K and mTOR signalling pathway regulating L-selectin expression. After TCR activation, the P110δ subunit of PI3K produces phosphoinositide (3,4,5) trisphosphate ($PI(3,4,5)P_3$) after phosphorylation by PI3K. $PI(3,4,5)P_3$ induces two signalling pathways which decrease expression of L-selectin. Firstly, $PI(3,4,5)P_3$ activates mTOR kinase which decreases Krüppel-like Factor 2 (KLF2) expression, which is a transcriptional factor for L-selectin. Consequently, lower levels of L-selectin are transcribed. Secondly, $PI(3,4,5)P_3$ activates the mitogen activated protein kinases (MAPK), extracellular signal-regulated kinases (Erk-1 and Erk-2) which phosphorylate ADAM 17 increasing membrane expression which promotes L-selectin proteolysis. $PI(3,4,5)P_3$ levels can be regulated by the phosphatase and tensin homolog (PTEN) which removes a phosphate group forming $PI(4,5)P_2$ and consequently reduces activation of mTOR and MAP kinases and blocks L-selectin downregulation (Sinclair*, et al.* 2008). PMA activates PKC which also induces ERK mediated phosphorylation of Thr-735 in the cytoplasmic tail of ADAM 17 increasing membrane expression and proteolysis of substrates (Diaz-Rodriguez, *et al.* 2002; Soond, *et al.* 2005).

1.5 Cell surface L-selectin expression levels regulate leucocyte recruitment to lymph nodes and inflamed tissues

1.5.1 Mutated L-selectin constructs and metalloproteinase inhibitors

In mouse models of inflammatory tissue injury, blockage of L-selectin function using cross-linking L-selectin using mAbs (Ma*, et al.* 1993), non-specific soluble oligosaccharides or sulfatides (Nelson*, et al.* 1993) or chimeric Igs (Mulligan*, et al.* 1993) decreased leucocyte emigration to inflamed tissues and prevented damage. Potentially, decreased L-selectin expression by ADAM 17 proteolysis attenuates the immune response in both acute and chronic inflammation.

To analyse the immunological relevance of L-selectin proteolysis *in vivo*, mice have been injected with matrix metalloproteinase (MMP) (KD-IX-73-4) or ADAM (Ro 31-9790) inhibitors. Also, different mutations of L-selectin have been generated where the membrane proximal region (MPR) has been truncated or replaced with shorter homologous domains of E- or P-selectin (Migaki, *et al.* 1995; Stoddart, *et al.* 1996; Zhao, *et al.* 2001) (Fig 1.7 A) and expressed in gene targeted mice resisting both basal and activation-induced proteolysis of L-selectin (Venturi, *et al.* 2003; Galkina, *et al.* 2003; Wirth, *et al.* 2009). Human L-selectin has also been truncated at the MPR (ΔM-N) (Chen, *et al.* 1995) (Fig 1.7 B), which has been used to inhibit proteolysis in transduced monocytes (Rzeniewicz, *et al.* 2015).

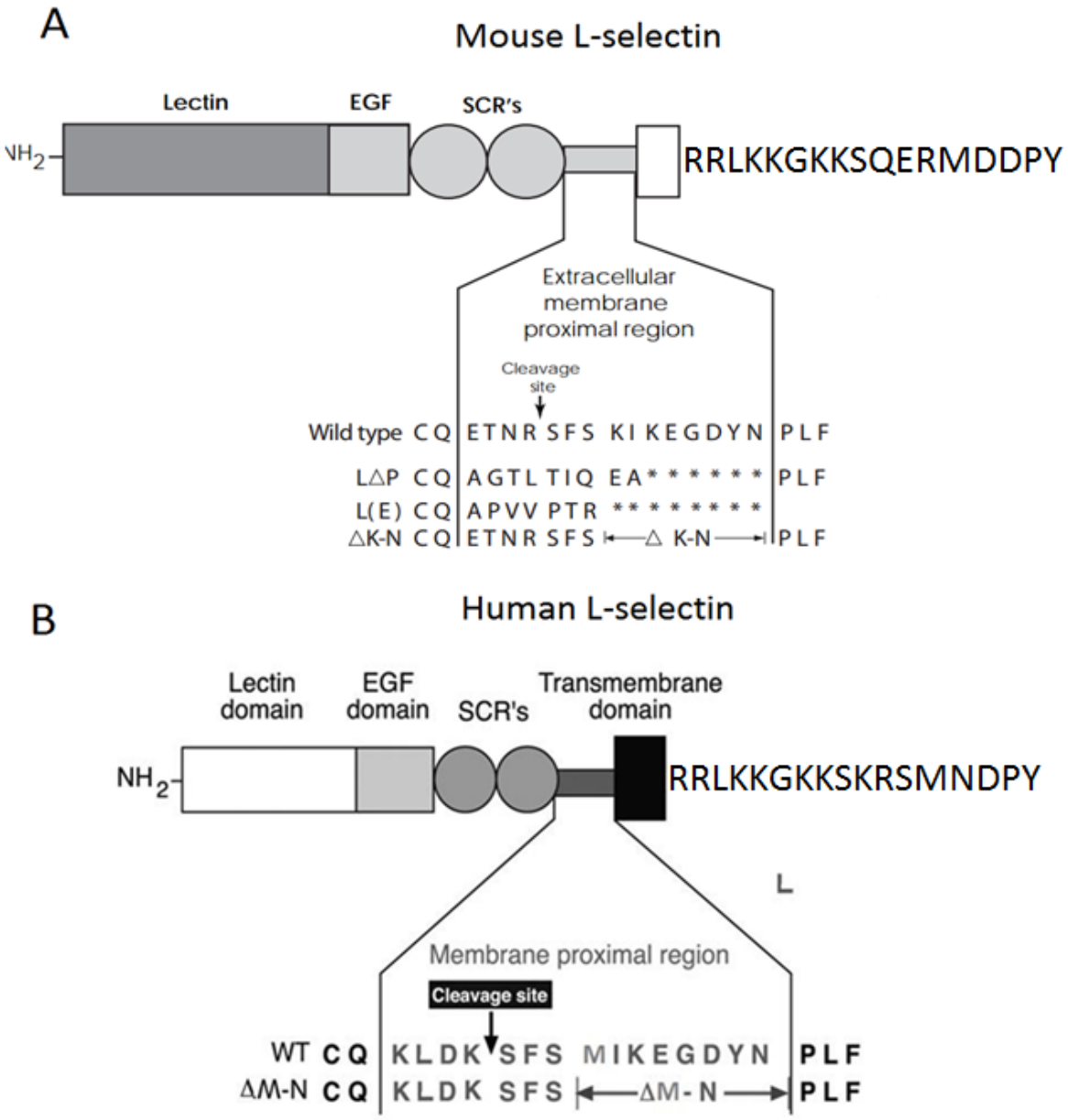

Figure 1.7: Various L-selectin MPR mutants resistant to ADAM proteolysis. The amino acid sequence of the MPR of mouse (A) and human (B) L-selectin are shown alongside the primary cleavage site. (A) For mouse L-selectin, three non-shedding mutants have been generated where the MPR has been replaced with shorter regions from E-selectin (L(E)) or P-selectin (LΔP) or truncated at 8-amino acids (KIKEGDYN) (ΔK-N). (B) A human form of the ΔK-N mutation has been generated in human L-selectin where 8-amino acids (MIKEGDYN) have been truncated from the MPR.

1.5.2 L-selectin expression levels regulate the velocity of cell rolling along the endothelium

Studies have shown that L-selectin expression levels affect the efficiency of leucocyte rolling. *In vitro* studies showed KD-IX-73-4 increased cell surface L-selectin expression, causing neutrophils to roll at a slower velocity under hydrodynamic flow (Walcheck, *et al.* 1996). Leucocytes from mice injected with KD-IX-73-4 also showed reduced rolling velocity on exteriorised postcapillary venules that express non-identified L-selectin ligands (Hafezi-Moghadam and Ley, 1999). Hafezi-Moghadam *et al* later found that inhibition of L-selectin proteolysis prevents leucocytes from microjumping during rolling. Instead, leucocytes adopted a new form of rolling, where contact with cytokine activated blood vessels was more constant (Hafezi-Moghadam, *et al.* 2001). They argued that increased contact periods between leucocytes and cytokine stimulated endothelium accelerates activation of the integrin, CD18 which binds to ICAM-1, leading to cell arrest and decelerated rolling (Hafezi-Moghadam*, et al.* 2001; Hafezi-Moghadam*, et al.* 1999). Galkina *et al* used a hydrodynamic flow assay to show that increasing cell surface L-selectin to supraphysiological levels did not reduce T cell rolling velocity, potentially due to the limited amounts of PNAd ligand presented. However, T cells from L-selectin (+/-) increased rolling velocity and thus lymphocytes failed to effectively monitor endothelial chemokine levels required for integrin activation and cell arrest (Galkina*, et al.* 2007).

1.5.3 L-selectin proteolysis regulates transmigration of leucocytes across the endothelium

Studies have also shown that L-selectin expression decreases while leucocytes transmigrate across the endothelium to enter lymphoid organs or inflamed tissue. For instance, Evans *et al* demonstrated that human monocytes lose cell surface expression of L-selectin after transmigration into skin blisters (Evans, *et al.* 2006). T cells also showed a 70 % reduction of cell surface L-selectin after transmigration across HEVs entering lymph nodes and spleen (Klinger, *et al.* 2009).

Further studies using gene targeted mice expressing MPD mutants or complete deficiency of L-selectin have shown that shedding-resistant or complete deficiency of L-selectin impairs transmigration across the vessel wall and entry to inflamed tissues or lymphoid organs, which suggests that L-selectin proteolysis is important for leucocyte transmigration across endothelium (Venturi, *et al.* 2003; Galkina, *et al.* 2000; Hickey, *et al.* 2000). Hickey *et al* firstly showed that L-selectin deficient and WT leucocytes adhered equally to the endothelium of PAF or keratinocyte chemoattractant (KC) activated cremaster muscle. However, chemokine dependent extravasation and leucocyte migration away from the vessel into the interstitium was impaired in L-selectin deficient mice (Hickey, *et al.* 2000). In later studies, Venturi *et al* showed that greater numbers of neutrophils expressing L(E) L-selectin migrated to the inflamed peritoneum than WT L-selectin. Although the rate of migration of neutrophils expressing WT or L(E) L-selectin were similar, recruitment of neutrophils expressing L(E) L-selectin persisted longer than WT L-selectin 24 h after thioglycolate challenge (Venturi*, et al.* 2003). Galkina *et al* then demonstrated that the number of T lymphocytes that entered PLNs from the bloodstream were similar regardless

of WT or LΔP L-selectin expression. However, lymphocytes expressing LΔP L-selectin transmigrated across HEVs more slowly than WT (Galkina, *et al.* 2003). Also, lymphocytes failed to complete diapedesis and accumulated within the endothelial cell lining of HEVs after mice were injected with Ro 31-9790 (Faveeuw, *et al.* 2001).

Rzeniewicz *et al* found that L-selectin proteolysis promotes cell polarity, which enhances chemotaxis of monocytes across HUVECs during transmigration *in vitro*. Monocytes expressing wild type L-selectin showed reduced numbers of pseudopods than cells treated with MMP inhibitor TAPI-O or those expressing shedding resistant (ΔM-N) L-selectin after 15 min perfusion over HUVECs. It was argued that L-selectin/ERM protein complexes induce Rho-GTPase signalling which causes actin polymerization and protrusion of membranes forming pseudopods. Hence, proteolysis would reduce L-selectin/ERM complexes and consequently pseudopod formation. This would polarize the cell and promote transmigration (Rzeniewicz, *et al.* 2015).

1.5.4 Released sL-selectin controls leucocyte recruitment to HEVs and inflamed tissue

The cleaved soluble L-selectin ECD (sL-selectin) acts as an adhesion buffer limiting excess lymphocyte recruitment to inflamed tissues during ongoing inflammation. During constitutive proteolysis, sL-selectin is present in the plasma at concentrations of 1.6 ± 0.8 μg/mL in healthy blood donors and retains its lectin, EGF-like and SCR domains allowing interaction with the luminal surface of endothelial cells on both inflamed tissues and HEVs. sL-selectin concentrations of at least 1.5 μg/mL inhibited leucocyte-endothelial interactions by competing with membrane bound L-selectin for available ligands which arguably attenuate immune diseases (Schleiffenbaum*, et al.* 1992). In later studies, plasma sL-selectin

levels in patients with adult respiratory distress syndrome (ARDS) and connective tissue disorders such as sclerosis and vasculitis were reduced in comparison to healthy individuals and potentially cause increased leucocyte-endothelial interactions on inflamed tissue amplifying the immune response (Donnelly, *et al.* 1994; Blann, *et al.* 1996). Proteolysis of L-selectin by ADAM 17 therefore attenuates acute and chronic inflammation by preventing T cell recruitment and activation in lymphoid organs and infiltration in inflamed tissue by decreasing cell surface expression of L-selectin and increasing sL-selectin levels in the plasma.

1.6 A disintegrin and metalloproteinases

1.6.1 The structure of A disintegrin and metalloproteinases

A Disintegrin And Metalloproteinase (ADAM) enzymes are Zn^{2+}dependent, complex multidomain proteins that are members of the adamalysin protein family. ADAMs contain an ectodomain with an N terminal signal sequence (1-17 aa), a prodomain (18-214 aa), a metalloproteinase (MP) domain (215-473 aa), a disintegrin domain (474-572 aa), a cysteine-rich domain (603-671 aa) followed by a transmembrane region (672-694 aa) and lastly a cytoplasmic tail (695-824 aa) (Edwards*, et al.* 2008; Hartmann*, et al.* 2013) (Fig 1.8).

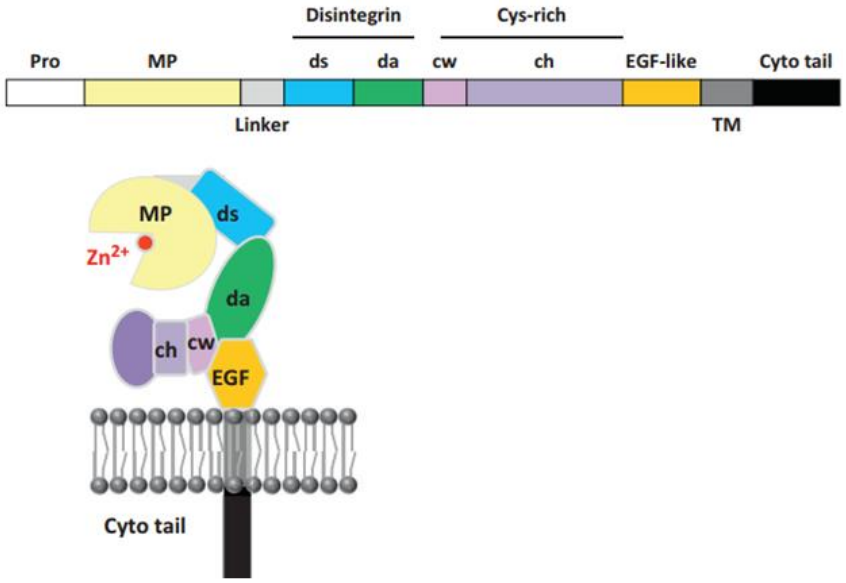

Figure 1.8: The structure of mature ADAMs. Mature ADAMs contain an MP domain with bound Zn^{2+} to allow ectodomain proteolysis of substrates. Following the MP domain is a disintegrin domain split by the shoulder (ds) and arm (da) regions. The ds and da domains of ADAMs bind to integrins for adhesive functions. The cysteine rich domain contains hand (ch) and wrist (cw) regions that contain disulphide bridges vital for structural stability of the MP domain. The ectodomain also contains an epidermal growth factor like (EGF) domain. Following the ectodomain of ADAMs is a transmembrane region trailed by a cytoplasmic tail that anchors the protein to the membrane (Modified from Hartmann, *et al.* 2013).

1.6.2 The metalloproteinase domain of ADAMs

The metalloproteinase (MP) domain is classified as a globular structure which is divided into two subdomains (Fig 1.9). Between the two subdomains lies the active site cleft composed of the sequence HEXXHXXGXXH termed the Zn^{2+} binding region (Gomis-Ruth, 2003). The upper subdomain is composed of 5 β-pleated sheets lying parallel to one another and also to the substrate. In this configuration, the upper subdomain binds the substrate in an extended manner. The upper domain also contains several α-helices (labelled as A in Fig 1.9); the lower α helix (labelled as B in Fig 1.9) includes the catalytic zinc binding site HEXXHXXGXXH followed by a conserved methionine residue that induces a 1,4-β-turn (Met-turn) essential for orientating the lower subunit to complete the catalytic cleft. The lower subdomain only contains one α-helix (labelled as C in Fig 1.9) located at the C terminus. The essential catalytic zinc atom is situated between the two subdomains at the bottom of the groove (Edward, *et al.* 2008).

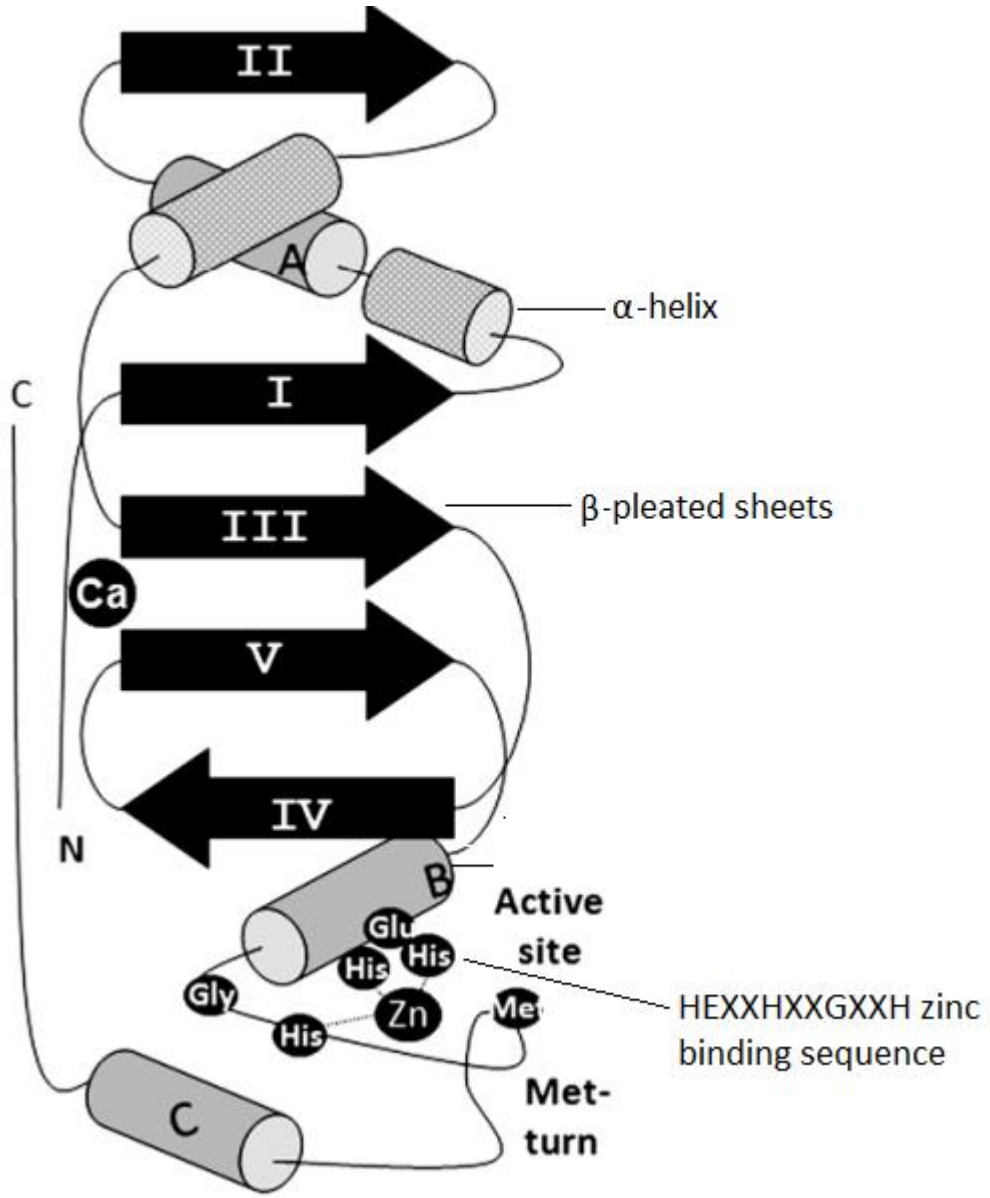

Figure 1.9: Structure of the MP domain of ADAM 17. The MP domain of ADAM 17 contains two subdomains called the upper and lower subdomains. The upper subdomain contains 5 β-pleated sheets and several α-helices (labelled as A). The lower α helix (labelled as B) contains the conserved HEXXHXXGXXH region that binds zinc allowing catalytic activity of ADAM 17. A 1, 4 ß-turn (Met-turn) is found after the αβ helix that orientates the lower subdomain (comprising of one α helix (labelled as C)) to be within the correct position. Between the two subdomains lies the active site (Modified from Edwards, *et al.* 2008).

1.6.3 Catalytically active and inactive ADAMs

ADAMs possess both catalytic and adhesive functions which serve as important mediators of cell signalling events (Edwards, *et al.* 2008). These distinct functions of ADAMs are correlated with their role in disease processes such as cancer, asthma and Alzheimer's disease (Deuss, *et al*; 2008; Holgate, *et al.* 2006; Garton, *et al.* 2006). The human genome contains 21 different ADAMs, where ADAMs 1-7, 22, 23, 29, 31 and 32 are catalytically inactive and are deficient in either an MP domain or the essential Zn^{2+} binding sequence (HEXXHXXGXXH) at the catalytic domain. These catalytically inactive ADAMs are involved in intercellular communication due to their adhesive interactions with integrins (Edwards, *et al.* 2008). The remaining 13 ADAMs regulate ectodomain proteolysis of various type I and II transmembrane proteins such as growth factors, cytokines, receptors and adhesion molecules. In 1997, ADAM 17 was the first ADAM identified with catalytic function and it was shown to cleave TNF-α, causing release of the soluble active cytokine (Black, *et al.* 1997; Moss, *et al.* 1997b) (Fig 1.10). ADAM 17 expression is tissue specific and is found mainly in the heart, kidney, skeletal muscle and brain (Black, *et al.* 1997). ADAM 17 has a unique sequence with negligible similarities to other ADAMs. Its closest relative is ADAM 10 however; the homology is less than 30 % (Gooz, *et al.* 2010).

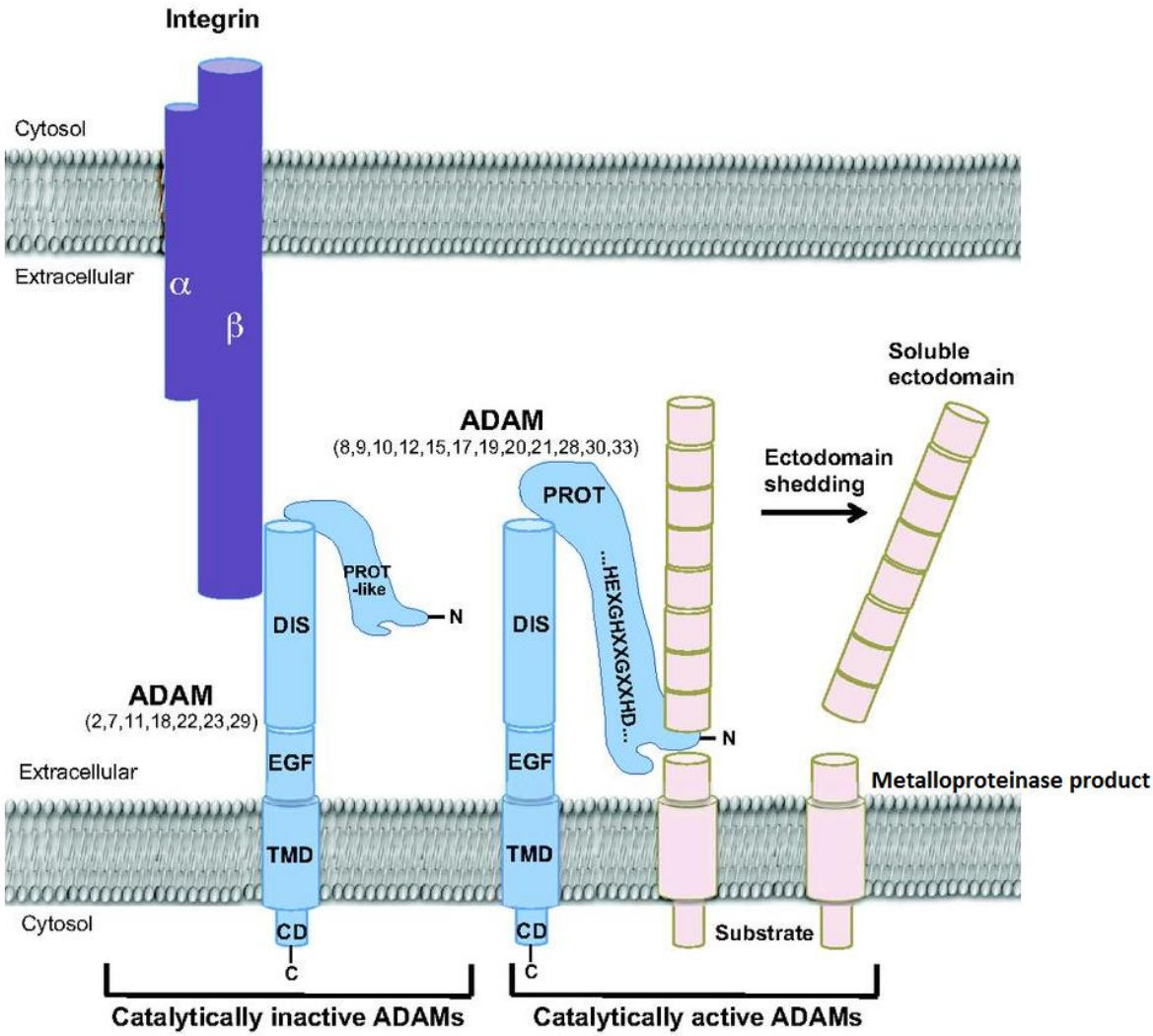

Figure 1.10: Catalytically active ADAM 17 regulates ectodomain proteolysis of type I and II transmembrane proteins. Both catalytically inactive and active ADAMs have a disintegrin domain (DIS), epidermal growth factor like (EGF) domain, transmembrane domain (TMD) and cytoplasmic domain (CD). Both forms of ADAM 17 also contain the metalloproteinase domain (PROT). Unlike non-catalytic ADAMs, catalytic ADAMs contain the zinc binding region HEXGHXXGXXHD required for proteolysis of substrates. Catalytically inactive ADAMs function to bind integrins. Catalytically active ADAMs cleave type I and II transmembrane proteins at the ectodomain generating an MP product. The cleaved soluble ectodomain of type I and II transmembrane proteins are released and can act by binding cognate receptors on interacting cells initiating downstream signalling (Weber and Saftig, 2012).

1.6.4 ADAM 17 proteolysis regulates biochemical pathways

ADAM 17 proteolysis of substrates either stimulates or inhibits specific biochemical pathways. Firstly, ectodomain release of inactive growth factor substrates allow binding to cognate receptor initiating downstream signalling. For instance, ADAM 17 cleaves heparin-binding EGF-like growth factor (HB-EGF) and releases soluble HB-EGF which can bind its cognate epidermal growth factor receptor (EGFR) causing proliferation of the cell (Gooz, *et al.* 2006). ADAM 17 proteolysis also downregulates membrane expression of receptors, which abolishes interactions with cognate ligands such as the macrophage colony stimulating factor receptor, which attenuates macrophage activation (Rovida, *et al.* 2001). The importance of ADAM 17 proteolysis of receptors is correlated with diseases such as TNF-α receptor associated periodic febrile syndrome (TRAPS). Here, the TNF-α receptor has a mutation at the cleavage site which abrogates ADAM 17 proteolysis and consequently accumulates at the membrane elevating interactions with soluble TNF-α leading to inflammatory responses (McDermott, *et al.* 1999). Elevated ADAM 17 proteolysis is also correlated with diseases such as breast cancer. Overexpression of human epidermal growth factor -2 (Her-2) in breast cancer cells causes high levels of soluble Her-2 due to proteolysis. As a consequence, therapeutic antibodies targeting Her-2 signalling in breast cancer interacting with high levels of the soluble receptor result in inefficient blockade of cell surface EGFR and cancer recurrence (Brodowicz, *et al.* 1997).

1.7 Regulation of ADAM 17 catalytic activity

1.7.1 Maturation of ADAM 17

Newly synthesised immature ADAM 17 is catalytically inactive and is termed a zymogen. Immature ADAM 17 contains a pro-domain at the N terminus which inhibits its catalytic function (Gonzales, *et al.* 2004). Amino acids Phe^{72}, Asp^{134}, Asp^{135} Val^{136} IIe^{137} and a 19-amino acid leucine rich sequence in the pro-domain interacts with the catalytic site of ADAM 17 rendering the enzyme inactive (Buckley*, et al.* 2005). The pro-domain also acts as a chaperone preventing degradation of immature ADAM 17 during trafficking (Anders, *et al.* 2001; Milla, *et al.* 2006). Initially, at the endoplasmic reticulum (ER), immature ADAM 17 is N-glycosylated, where endoglycosidase-H (endo-H) sensitive glycans are added to ADAM 17. At the medial Golgi, more N-linked sugars are conjugated to immature ADAM 17 before entering the trans-Golgi network. Glycans are then modified to become resistant to endo-H (Schlöndorff, *et al.* 2000), allowing cleavage at amino acids RVKR between the pro-domain and catalytic domain of ADAM 17 by Golgi resident enzyme furin. This proteolytic event removes the pro-domain generating mature ADAM 17 with catalytic potential (Adrain, *et al.* 2012; Schlöndorff, *et al.* 2000). Phosphofurin acidic cluster sorting protein 2 (PACS-2) then binds the cytoplasmic tail of mature ADAM 17 and facilitates trafficking to the membrane (Dombernowsky, *et al.* 2015) (Fig 1.11). ADAM 17 also traffics from the ER to the cell surface after Thr^{735} in the cytoplasmic tail is phosphorylated by MAP kinase extracellular signal-regulated kinase (Erk) (Soond, *et al.* 2005).

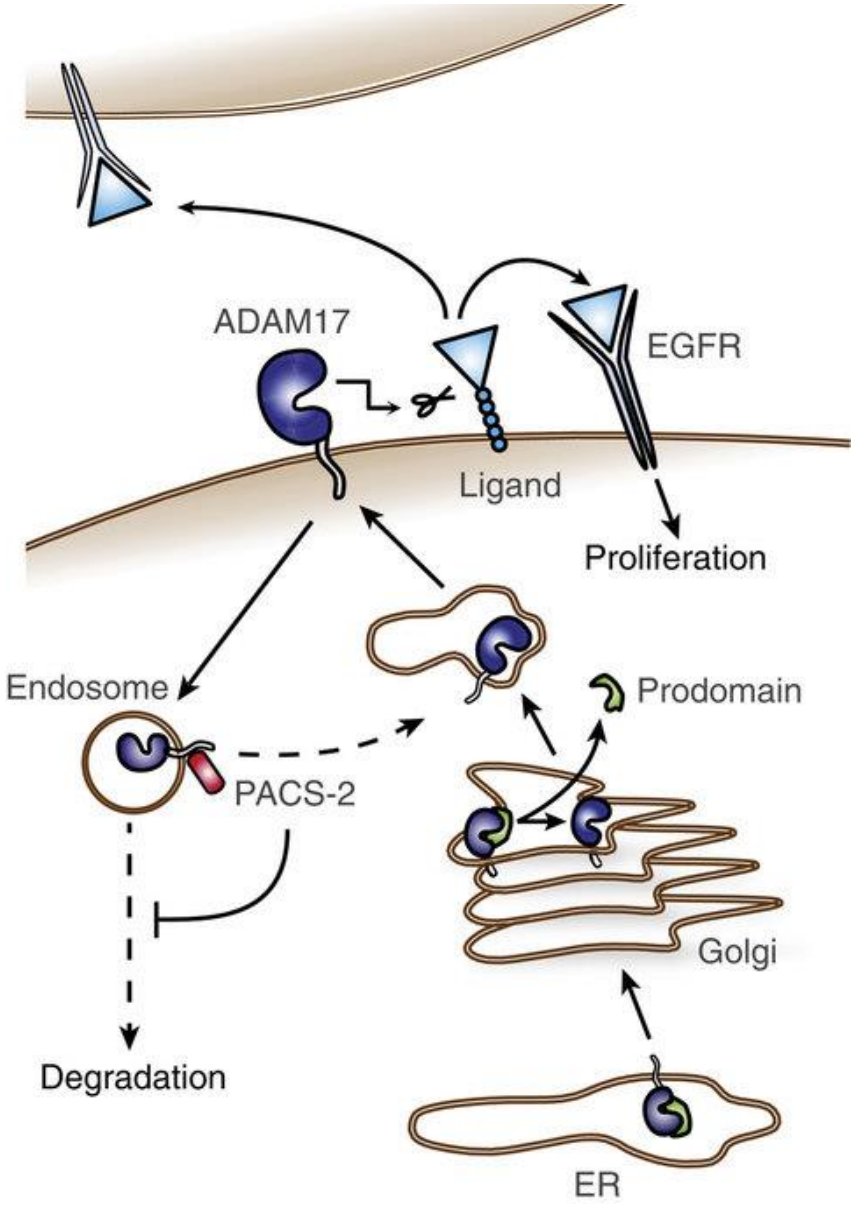

Figure 1.11: Maturation of ADAM 17. Immature ADAM 17 contains a prodomain at the N terminus and is catalytically inactivate. Immature ADAM 17 is first located at the ER where it is N-glycosylated and later trafficked to the trans-Golgi network. Immature ADAM 17 is processed at the trans-Golgi where the prodomain is cleaved by furin. Mature and catalytically active ADAM 17 is generated and enters the secretory pathway to traffic to the membrane to cleave substrates. PACS-2 binds to the cytoplasmic tail of mature ADAM 17 and promotes trafficking to the membrane preventing intracellular degradation (Dombernowsky, *et al.* 2015).

Mature ADAM 17 localizes in cholesterol rich lipid rafts at the Golgi apparatus separating this enzyme from substrates. Moreover, lipid raft depletion using cyclodextrin caused excessive ADAM 17 mediated proteolysis of substrates. Lipid raft localization of ADAM 17 during the maturation process therefore acts to protect the host against unnecessary shedding of cell surface proteins which would activate/inhibit biochemical pathways causing potentially harmful effects (Tellier, *et al.* 2006).

1.7.2 IRhoms facilitates maturation and substrate specify of ADAM 17

IRhoms are non-catalytic members of the rhomboid intramembrane protease family and are deficient of the catalytic residues Ser^{201} and His^{254} (Lemberg and Freeman, 2007; Wang, *et al.* 2006) (Fig 1.12 A). Adrian *et al* showed that ADAM 17 is not expressed in iRhom-2 deficient macrophages and remains in an endo-H non-resistant state in the ER, which cannot be cleaved by furin. IRhom-2 binds to both mature and immature ADAM 17; however, the interaction is reduced after furin cleavage. It has therefore been suggested that IRhom-2 binds ADAM 17 in the ER and migrates to the Golgi apparatus. Furin cleavage of ADAM 17 would then remove IRhom-2 allowing mature ADAM 17 to reside in the trans-Golgi network (Adrian*, et al.* 2012) (Fig 1.12 B). However, in their later studies, they showed that loss of iRhom-1 or iRhom-2 in mouse embryonic fibroblasts (MEFs) partially reduces maturation of ADAM 17 and subsequent trafficking to the cell surface, whereas loss of both iRhoms show complete inhibition. They argued that IRhom-2 expression is high in macrophages explaining why IRhom-2 deficient macrophages from their earlier studies showed complete deficiency of ADAM 17 maturation. However, IRhom-1 expression is

abundant in other cell types such as MEFs where it would regulate ADAM 17 maturation (Christova, *et al.* 2013).

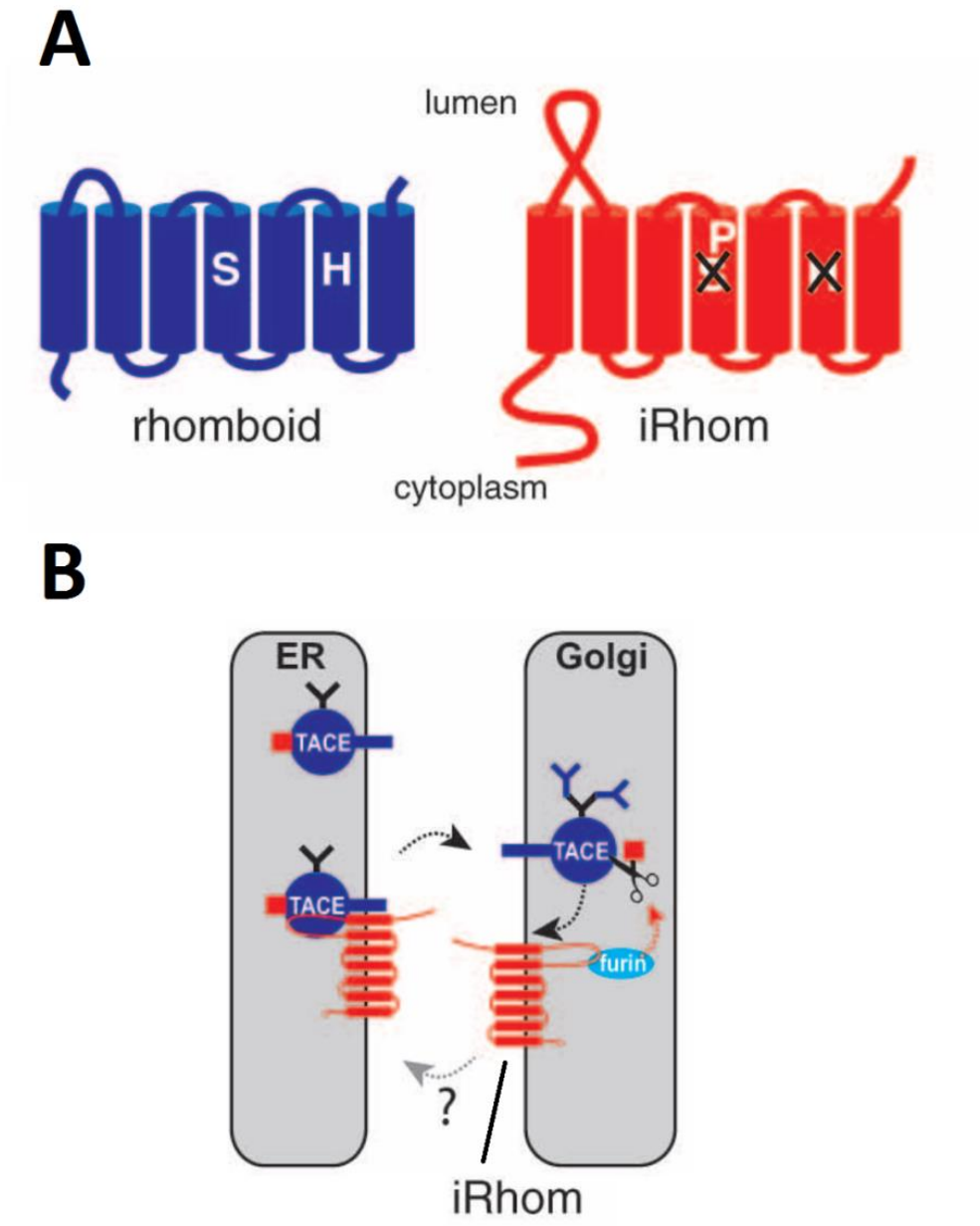

Figure 1.12: IRhom structure and function during ADAM 17 maturation. (A) The structure of iRhoms. IRhoms (red) have a similar sequence and structure as the catalytically active rhomboids (blue). However, iRhoms lack the catalytic residues Ser^{201} and His^{254} and are catalytically inactive. (B) IRhoms function during ADAM 17 maturation. IRhoms and immature ADAM 17 are both abundantly expressed at the ER where they initially interact. IRhoms then traffics immature ADAM 17 to the Golgi apparatus. At the Golgi apparatus, the prodomain of immature ADAM 17 is cleaved by furin which removes iRhoms (Adrian, *et al.* 2012).

ADAM 17/iRhom-1 and ADAM 17/iRhom-2 complexes act as two different molecular scissors which proteolyze different substrates with distinct stimuli (Matthews, *et al.* 2016). For instance, PMA-stimulation did not induce ADAM 17 proteolysis of some substrates such as Eph receptor B4 (EphB4), kit ligand 2 (KitL2) and tyrosine kinase with immunoglobulin-like and EGF-like domains-2 (Tie-2) in iRhom-2 deficient MEF cells yet proteolysis for other substrates such as transforming growth factor-α (TGF-α) was elevated. Furthermore, siRNA against iRhom-1 in iRhom-2 deficient MEF cells abolished ADAM 17-proteolysis of TGF-α after PMA stimulation. However, ADAM 17 substrate specificity based on the bound isoform of iRhom also depends on cell type. For example, IRhom-2 deficiency in brain leucocytes attenuated L-selectin proteolysis after PMA-stimulation (Li, *et al.* 2015); yet shedding was unaffected in iRhom-2 deficient MEF cells (Maretzky, *et al.* 2013). In MEFs, the N terminal cytoplasmic domain of iRhoms regulate PMA induced ADAM 17 proteolysis as shown in iRhom-2 deficient MEF cells where complementation of iRhom-2, but not iRhom-2 lacking its N-terminal cytoplasmic domain rescued proteolysis of KitL2 (Le Gall*, et al.* 2010, Maretzky*, et al.* 2013).

1.7.3 Extracellular stimuli activates ADAM 17 and induces proteolysis

Ectodomain proteolysis of substrates is stimulated by extracellular stimuli such as thrombin, growth factors, pathogen-activated molecular patters (PAMPs) and cytokines (Arribas and Massague, 1995; Fan and Derynck, 1999; Horiuchi, *et al*. 2007b; Le Gall, *et al*. 2009; Prenzel, *et al*. 1999; Sahin, *et al*. 2004; Swendeman, *et al.* 2008; Chanthaphavong*, et al.* 2012). These extracellular stimuli initiate intracellular signalling pathways which activate ADAM 17 inducing proteolysis of substrates. For instance, thrombin binds to the G-protein coupled

receptor called protease activated receptor-1 (PAR-1) and initiates nitric oxide (NO) production which activates ADAM 17 and induces proteolysis of endothelial protein C receptor (EPCR) (Gur-Cohen, *et al.* 2015). Also, stimulation of the Toll-like receptor 4 (TLR-4) by PAMPs such as LPS causes expression of nitric oxide synthase (iNOS) in hepatocytes, which induces production of NO. NO activates cyclic guanosine monophosphate (cGMP) and protein kinase G (PKG). Activated PKG phosphorylates serine and threonine residues in the cytoplasmic tail of ADAM 17 alongside iRhom-2 facilitating increased membrane expression and activation of ADAM 17 causing elevated proteolysis of tumour necrosis factor-α receptor-1 (TNFR-1) in hepatocytes (Chanthaphavong*, et al.* 2012). LPS also upregulates ROS by flavoprotein oxidoreductases which rapidly activate ADAM 17 using p38 MAP kinase. Activation is redox sensitive as exogenous H_2O_2 phosphorylates MAP kinase, while scavenging ROS attenuates LPS-activation of ADAM 17 (Scott, *et al.* 2011). Additionally, the inflammatory peptide N-Formylmethionine-leucyl-phenylalanine (fMLP) initiates both p38 and Erk MAP kinase pathways, which triggers L-selectin proteolysis in neutrophils (Fan and Derynck, 1999).

Cytokines such as IL-6 and IFN-γ stimulates Erk, causing activation of ADAM 17 and proteolysis of neuregulin (Kalinowski, *et al.* 2010). The proinflammatory cytokine IL-1β increases ADAM 17 mRNA levels by threefold and consequently elevates amyloid precursor protein (APP) proteolysis in human neuroblastoma cells (Tachida, *et al.* 2008). Later studies showed that IL-1β elevates expression of ADAM 17 by p38 MAPK, PI3K and nuclear factor kappa-light-chain-enhancer of activated B cells (NF-kB) and substrate amphiregulin using NF-kB, c-Jun N-terminal kinases (JNK), ERK 1/2 and p38 MAPK signalling pathways which increases proteolysis of amphiregulin (Liu*, et al.* 2014).

Additionally, mitogenic growth factors such as fibroblast growth factor (FGF) and platelet-derived growth factor (PDGF) bind to cognate tyrosine kinase receptors FGFR and PDGFR and induce Erk MAP kinase signalling which triggers proteolysis of TNF-α. Additionally, inhibition of PKC using mutational or pharmacological approaches does not abrogate TNF-α proteolysis by FGF or PDGF showing growth factors do not upregulate PKC for proteolysis (Fan and Derynck, 1999).

1.7.4 Protein disulphide isomerase inactivates ADAM 17 and regulates substrate interaction

Bennett *et al* showed that ADAM 17-proteolysis of substrates was potentiated in the presence of thiol isomerase inhibitor bacitracin (Bennett, *et al.* 2000). In later studies, Willems *et al* demonstrated that protein disulphide isomerase (PDI) was the thiol isomerase which regulates ADAM 17 activity. Blocking antibodies against PDI or siRNA silencing elevated ADAM 17-dependent proteolysis of HB-EGF after PMA treatment. Furthermore, addition of exogenous PDI reduced proteolysis of HB-EGF in PMA-stimulated, but not resting HeLa cells (Willems, *et al.* 2010). Wang *et al* found that catalytic activity of ADAM 17 lacking both a pro-domain and cytoplasmic tail was lowered after reduction by dithiothreitol and potentiated after oxidation with H_2O_2 showing that thioldisulfide conversion occurs in the extracellular domain. Furthermore, they also mutated two conserved CXXC motifs ($C^{522}XXC$ and $C^{600}XXC$) in the disintegrin/cysteine rich region to ADAM 17 to alanines which abrogated L-selectin proteolysis which potentially showed that redox modifications of these cysteinyl sulfhydryl groups regulate catalytic activity (Wang, *et al.* 2009). Antibodies were used to bind the MP domain (A9) and the disintegrin/cysteine rich region (A7 and D3) of recombinant ADAM 17, treatment with PDI prevented A7 and D3 from interacting the

disintegrin/cysteine rich region, yet A9 still bound the MP domain which was correlated with reduced proteolysis of TNF-α and a myelin basic protein. These results illustrated that PDI isomerizes disulphide bonds in the disintegrin/cysteine rich region of ADAM 17 which causes a conformational change in the catalytic site interfering with proteolysis (Willems, *et al.* 2010).

However, Düsterhöft *et al* showed that PDI interacts directly to the MPR of ADAM 17. The MPR of ADAM 17 possesses two disulphide bonds one between Cys^{600} and Cys^{630} (Cys 600-630) and the other between Cys^{635} and Cys^{641} (Cys 635-641). PDI isomerizes these disulphide bonds causing both the Cys 600-635 and Cys 630-641 disulphide bonds overlap. This change in structure causes the MPR to convert from an open and elongated conformation to a closed, rigid and compact structure which suggestively prevents substrate recognition (Düsterhöft*, et al.* 2013) (Fig 1.13). In later studies, Düsterhöft *et al* researched how PDI isomerization of the MPR prevents substrate recognition of ADAM 17. They found that ADAM 17 contains a small α-helical juxtamembrane segment termed a small stalk region between the MPR and transmembrane region. This stalk region contains 14-amino acids termed the conserved ADAM seventeen dynamic interaction sequence that binds substrates (CANDIS) which was shown to bind amino acids 317-ESRSPPAENEVSTPMQ-332 in the ectodomain of the ADAM 17 substrate, interleukin 6 receptor (IL-6R). PDI isomerization of the MPR to a closed structure consequently blocked CANDIS from binding IL-6R which attenuated proteolysis (Düsterhöft, *et al.* 2014).

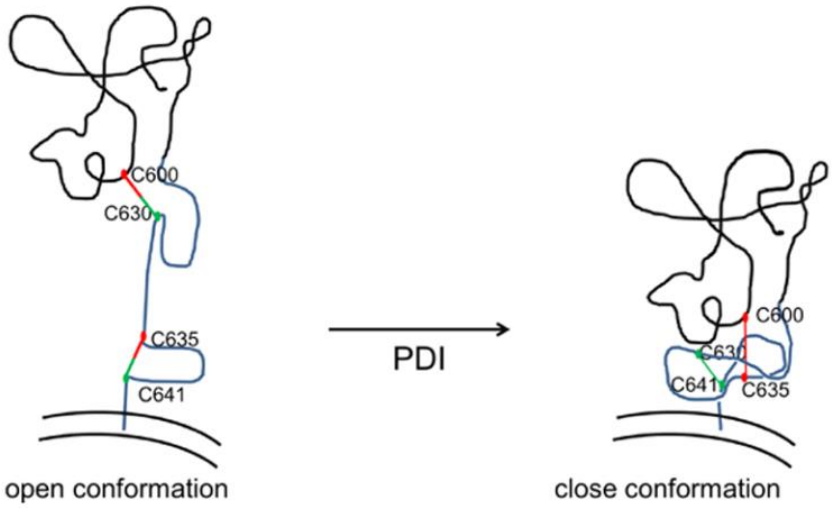

Figure 1.13: Structural consequences of PDI-mediated disulphide isomerization of the ADAM 17 MPR. In the open conformation two disulphide bonds between Cys 600-635 and Cys 630-641 in the MPR of ADAM 17 are positioned away from one another. PDI causes overlap between Cys 600-635 and Cys 630-641 which causes a structural change of the MPR converting from an open to closed structure (Düsterhöft, *et al.* 2013).

1.7.5 Phosphatidylserine lipids in the plasma membrane regulate ADAM 17 activity

Cationic amino acid residue region (RK_K) in the MPR of ADAM 17 binds to phosphatidylserine (Ptd-L-Ser) lipids at the plasma membrane (Düsterhöft, *et al.* 2015; Sommer, *et al.* 2016). In a resting cell, Ptd-L-Ser is located at the inner leaflet of the plasma membrane and does not interact with the MPR of ADAM 17. Consequently, the MPR of ADAM 17 is freely structured causing the catalytic site to be at a distance from type I and II transmembrane proteins. After cell stimulation, Ptd-L-Ser translocates from the inner to outer plasma membrane leaflet and interacts with the MPR of ADAM 17 which orientates the catalytic site towards the substrate facilitating proteolysis (Sommer*, et al.* 2016) (Fig 1.14).

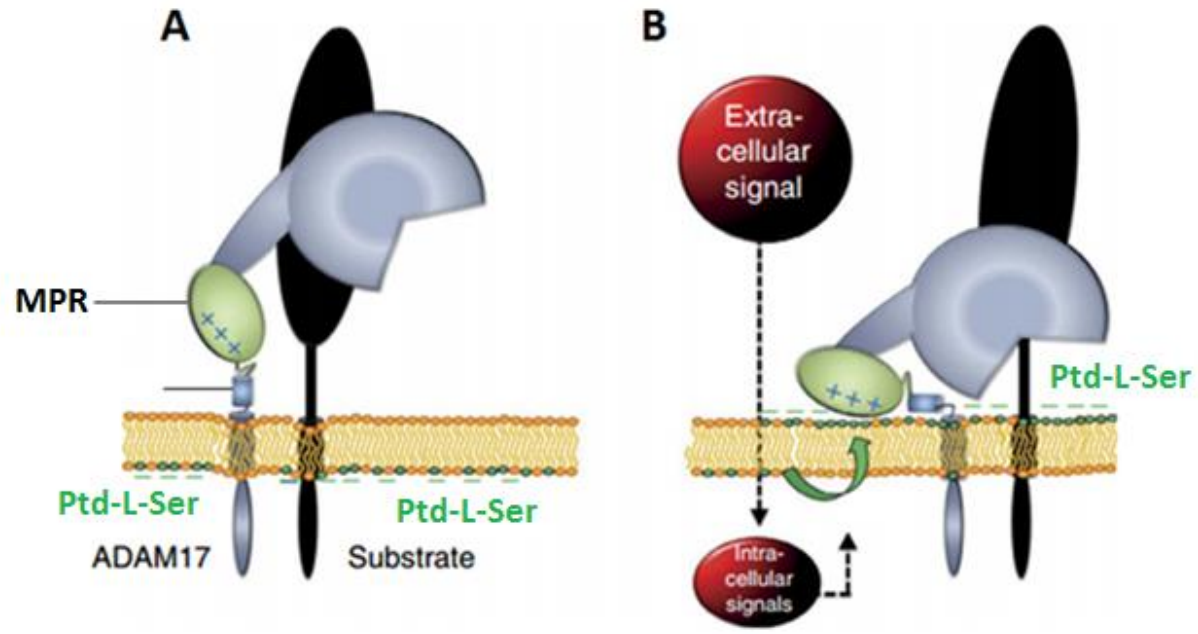

Figure 1.14: Interaction of the MPR and stalk regions of ADAM 17 to Ptd-L-Ser promotes ectodomain proteolysis. (A) Under basal conditions, Ptd-L-Ser is located at the inner leaflet of the plasma membrane. The catalytic site of ADAM 17 is located at a distance from its substrate reducing ectodomain proteolysis. (B) After cell activation, Ptd-L-Ser is translocated from the inner to outer plasma membrane leaflet. The MPR of ADAM 17 use cationic residues (indicated as +) to bind exposed Ptd-L-Ser. This causes structural reorientation of ADAM 17 allowing the catalytic site to be within a closer region to the substrate allowing ectodomain proteolysis (Sommer, *et al.* 2016).

1.7.6 ADAM 17 binding partners modulate proteolysis

ADAM 17 interacts with various extracellular and intracellular binding partners which either augment or diminish its catalytic activity. Tissue metalloproteinase inhibitor 3 (TIMP-3) naturally inhibits the catalytic function of ADAM 17 after directly interacting with the extracellular catalytic site (Amour, *et al.* 1998). Also, the synapse associated protein-9 (SAP-9) uses its PDZ3 region to bind the extreme intracellular C-terminus of the ADAM 17 cytoplasmic domain, but SAP-9 regulation of ADAM 17 activity remains controversial. Peiretti *et al* firstly showed that overexpression of SAP-9 inhibited ADAM 17 proteolysis of TNF-α and TNFR1 and TNFR2 (Peiretti, *et al.* 2003b). However, Surena *et al* challenged these

findings by showing that SAP-9 interacts with the cytoplasmic tails of the ADAM 17 substrate pro-TGF-α as well as ADAM 17, which potentially enhances substrate presentation for proteolysis (Surena, *et al.* 2009; Gooz, *et al.* 2010). Likewise, nardilysin binds to the intracellular domains of ADAM 17 and HB-EGF enhancing ectodomain shedding (Nishi, *et al.* 2006). Also, intracellular Four and Half LIM domain 2 protein (FHL2) bridges ADAM 17 to the actin cytoskeleton to be at near membrane bound substrates (Canault, *et al.* 2006b).

1.7.7 Tetraspanin CD9 binds to ADAM 17 and regulates activity

Tetraspanins (TSPANs) (Fig 1.15) such as CD9 organizes cell surface microdomains after interaction with additional tetraspanins and transmembrane proteins (Yanez-Mo, *et al.* 2009; Hemler, *et al.* 2003; Barreiro, *et al.* 2008). In these microdomains, TSPANs regulate functions of transmembrane proteins for instance, CD9 forms complexes with several β_1 integrins and regulate cell adhesion, signalling, proliferation and migration (Ovalle, *et al.* 2007; Berditchevski, 2001).

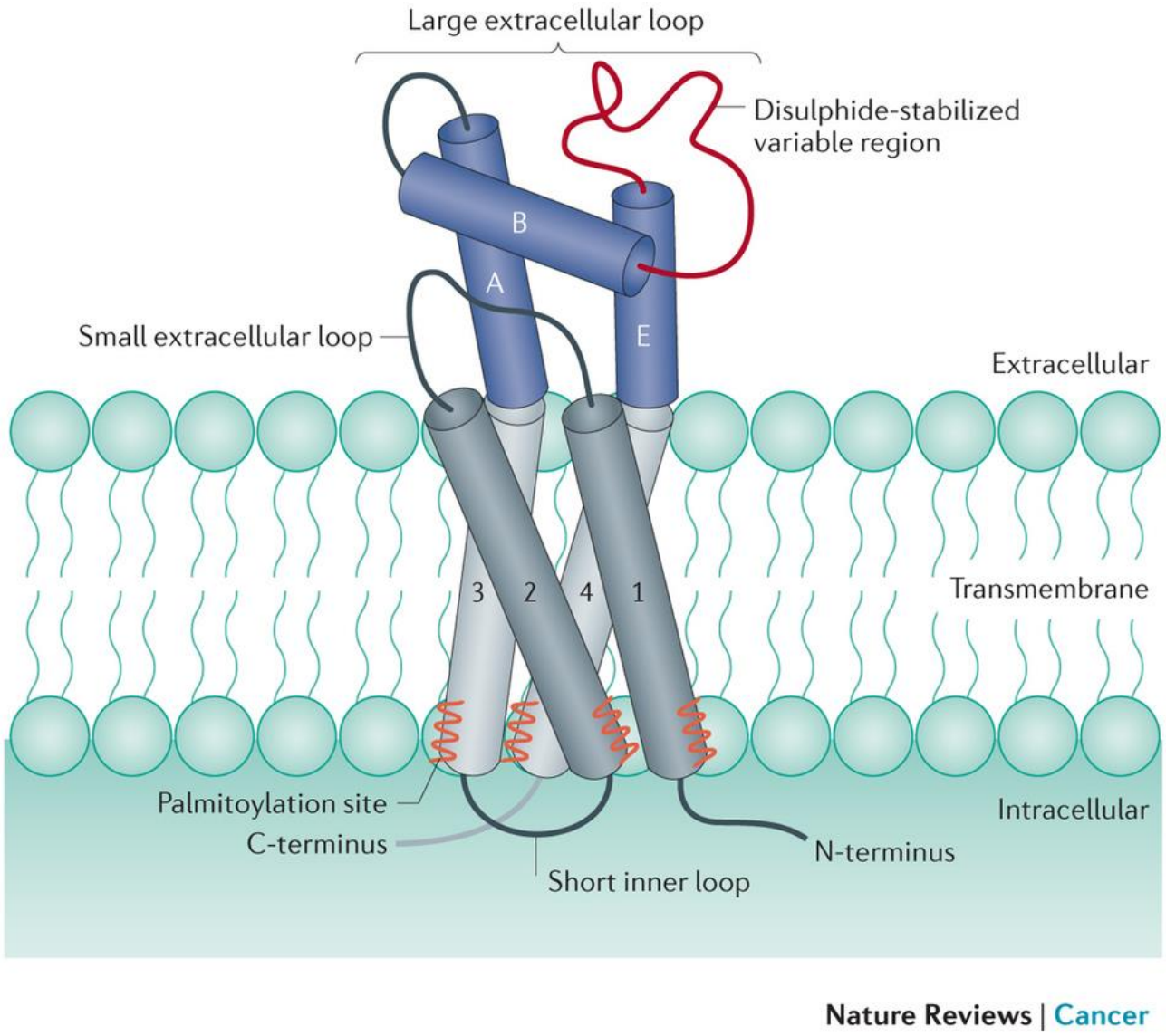

Figure 1.15: Diagram of typical TSPAN structure. TSPANs have four transmembrane helices (light and dark grey; labelled as 1-4). A large extracellular loop (between 70 to 130 amino acids) link transmembrane domains (TMD) 3 and 4 and contains three helices labelled as A, B and E in blue and also a variable region (red) in between helices B and E which allow interactions with binding partners. TSPANs also contain a small extracellular loop (between 13 to 30 amino acids) between TM domains 1 and 2 alongside short N- and C- terminal cytoplasmic tails (6 to 19 amino acids) and a small inner loop (of 4 amino acids). TSPANs exist as homodimers, or associate with other TSPANs which is regulated by palmitoylation of multiple membrane proximal cysteines (orange zigzags) (Hemler, 2014).

Gutiérrez-López *et al* found that ADAM 17 directly interacts with the large extracellular loop (LEL) of CD9 at the plasma membrane. Furthermore, overexpression of CD9 reduced ADAM 17 proteolysis of both TNF-α and ICAM-1, whereas CD9 silencing decreased ICAM-1 expression on stimulated HUVECs due to elevated ADAM 17 proteolysis. Additionally, PMA dissociated ADAM 17 from CD9 enhancing its catalytic function (Gutiérrez-López, *et al.* 2011). CD9 also interacts with ADAM 17 substrates pro-HGF, pro-TGF-α, pro-epiregulin and pro-amphiregulin (Shi, *et al.* 2000; Higashiyama, *et al.* 1995; Inui, *et al.* 1997; Hemler, 2003). Tsukamoto *et al* further showed in Jurkat T cells that cell surface expression of ADAM 17 substrate, sortilin-related receptor (LR11) is regulated by its interaction with CD9. After CD9 silencing, LR11 was localized in the intracellular compartment and did not proteolyze after PMA treatment (Tsukamoto, *et al.* 2014). CD9 therefore potentially forms cell surface substrate-enzyme complexes in resting cells where rapid ADAM 17 proteolysis occurs after CD9 dissociation by PMA (Gutiérrez-López, *et al.* 2011; Tsukamoto, *et al.* 2014).

1.7.8 The cytoplasmic tail and transmembrane region of ADAM 17

It remains disputed whether the cytoplasmic domain of ADAM 17 regulates catalytic activity and proteolytic cleavage of substrates. Several studies have demonstrated ADAM 17 activation after phosphorylation of the cytoplasmic domain (Diaz-Rodriguez, *et al.* 2002; Fan and Derynck, 1999; Fan, *et al.* 2003; Soond, *et al.* 2005; Xu and Derynck, 2010). Diaz-Rodriguez *et al* showed that Thr^{735} in the cytoplasmic domain of ADAM 17 is phosphorylated by the Erk MAPK signaling pathway after PMA treatment and later proposed that Thr^{735} phosphorylation activates ADAM 17 and induces proteolysis (Diaz-Rodriguez, *et al.* 2002).

In later studies, Xu *et al* showed that ADAM 17 forms dimers which are predominantly expressed in the plasma membrane of resting cells while TIMP-3 binds directly to both ECDs

of the ADAM 17 dimer silencing its catalytic activity. After cell activation, ERK and p38 MAPK signalling pathways shifts cell surface ADAM 17 dimers to monomers causing dissociation of TIMP-3 which then generates a catalytically active ADAM 17 that proteolyzes TNF-α. The biochemical mechanisms by ERK and p38 MAPK signalling that increase levels of cell surface ADAM 17 monomers are currently unknown. Xu *et al* suggested that ERK/p38 MAPK phosphorylation of the ADAM 17 cytoplasmic domain at Thr^{735} disrupts intermolecular interactions between ADAM 17 dimers. Also, ERK/p38 MAPK phosphorylation of Thr^{735} in the cytoplasmic domain of ADAM 17 would cause increased trafficking of intracellular ADAM 17 monomers to the plasma membrane (Xu*, et al.* 2012) (Fig 1.16).

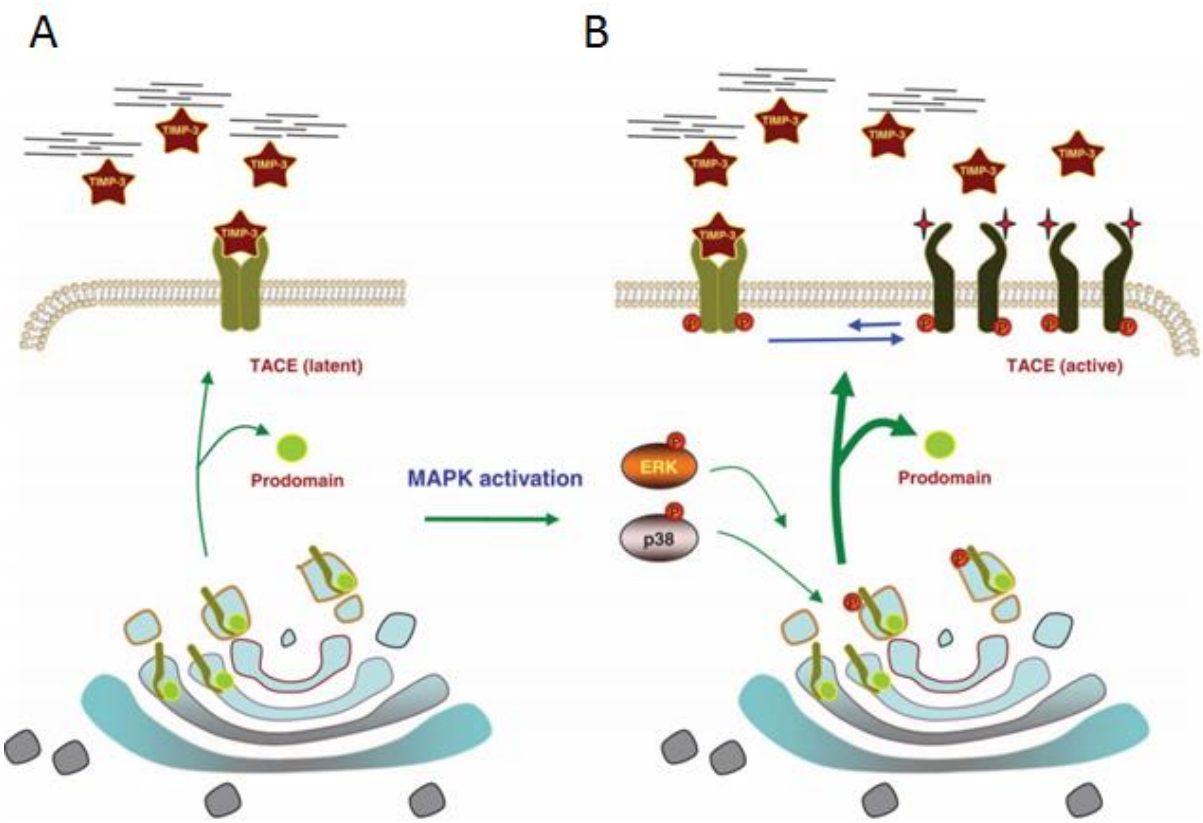

Figure 1.16: MAP kinase signalling pathway regulates cell surface expression of activated ADAM 17. (A) In the absence of MAP kinase signalling, inactive ADAM 17 is present at the membrane as a dimer while associated with TIMP-3. (B) After cell activation, the MAP kinase ERK phosphorylates the cytoplasmic domain of ADAM 17 causing dissociation of dimers and disrupting TIMP-3 interaction which increases cell surface presentation of active ADAM 17 monomers. Intracellular monomers of ADAM 17 are also phosphorylated by MAP kinase ERK facilitating trafficking to the cell surface (Xu, *et al.* 2012).

However, other studies have shown that the cytoplasmic domain of ADAM 17 is not required for its activation after cell stimulation (Horiuchi, *et al.* 2007; Le Gall, *et al.* 2010; Reddy, *et al.* 2000; Hall, *et al.* 2012). Le Gall *et al* found that phosphorylation of threonine, serine and tyrosine residues in the cytoplasmic domain of ADAM 17 was not required for catalytic activity as ADAM 17 truncated of its cytoplasmic domain was still activated by thrombin, LPA, TNF-α and the growth factor EGF. They suggested that Thr^{735} acts as an

inhibitory residue and allows ADAM 17 activation after phosphorylation (Le Gall, *et al.* 2010).

Hall and Blobel challenged this hypothesis by generating two forms of ADAM 17 where the Thr^{735} residue was mutated to a non-phosphorylatable (T735A) or phospho-mimicking (T735D) state alongside a truncated version where the cytoplasmic domain was removed and showed that all three constructs of ADAM 17 were activated IL-1β or MAP kinase. They also revealed that the MAP kinase inhibitor SB203590 attenuated activation of ADAM 17 lacking its cytoplasmic domain, displaying that activation of ADAM 17 is not reliant on the cytoplasmic domain or Thr^{735} phosphorylation (Hall and Blobel, 2012). Fan *et al* did not observe phosphorylation of Thr^{735} after cellular activation, also Thr^{735} mutation to non-phosphorylatable alanine (T735A) did not abolish growth factor phosphorylation of ADAM 17 (Fan, *et al.* 2003). Instead, they showed phosphorylation at Ser^{819} in the cytoplasmic domain of ADAM 17 by the Erk MAPK signalling pathway after cell activation by growth factors EGF and FGF. Neither mutation of Ser^{819} to non-phosphorylatable alanine (S819A) nor truncation of the cytoplasmic domain attenuated ADAM 17 proteolysis of TGF-α (Fan, *et al.* 2003). Ser^{819} is adjacent to a motif which interacts to the PDZ domain-containing protein (PTPH1) which suggestively down-regulates ADAM 17 expression (Zheng, *et al.* 2002). Fan *et al* suggested that Ser^{819} phosphorylation regulates ADAM 17 processing (Fan, *et al.* 2003).

Other studies have reported that the transmembrane region of ADAM 17 regulates activity (Horiuchi, *et al.* 2007; Le Gall, *et al.* 2010; Reddy, *et al.* 2000; Hall, *et al.* 2012; Xu, *et al.* 2012). Reddy *et al* demonstrated that overexpression of the soluble ECD of ADAM 17 did not induce proteolysis of TNF-α, however catalytic activity was restored after anchorage to the plasma membrane with the transmembrane, which was further shown for ADAM 17

lacking its cytoplasmic domain (Reddy*, et al.* 2000). Also, replacement of the transmembrane domain (TMD) of ADAM 17 with L-selectin or the ADAM 10 substrate betacellulin (BTC) attenuated activation after PMA treatment (Le Gall, *et al.* 2010).

1.8 L-selectin ICD binding partners regulate ADAM 17 proteolysis

Truncation of the 17-amino acid L-selectin ICD lowers PMA induced shedding of L-selectin from 88 % to 44 %, highlighting that this domain is important in regulating ectodomain proteolysis (Zhao*, et al.* 2001). Kahn *et al* found that calmodulin (CaM) binds to the MPR of the L-selectin ICD. This interaction is disrupted in response to CaM inhibitors such as trifluroperazine and calmidazolium and this correlated with downregulated L-selectin expression, which was rescued using broad-spectrum metalloprotease inhibitors. This CaM/L-selectin ICD complex therefore protects L-selectin from ectodomain proteolysis (Kahn, *et al.* 1998; Matala, *et al.* 2001).

Gifford *et al* monitored interactions between CaM and a synthetic L-selectin peptide comprising of a transmembrane region and ICD in aqueous solution. The N- and C- lobes of CaM bind to hydrophobic residues Ile^{352} and Leu^{354} in the transmembrane region of L-selectin and Leu^{358} in the L-selectin ICD. A two-step model was proposed, where CaM firstly binds to positively charged residues in L-selectin ICD and then to Ile^{352}/Leu^{354}, consequently pulling the transmembrane region of L-selectin downwards and/or perturbing the lipid bilayer, burying the ADAM 17 cleavage site in the extracellular region (Gifford*, et al.* 2012) (Fig 1.17).

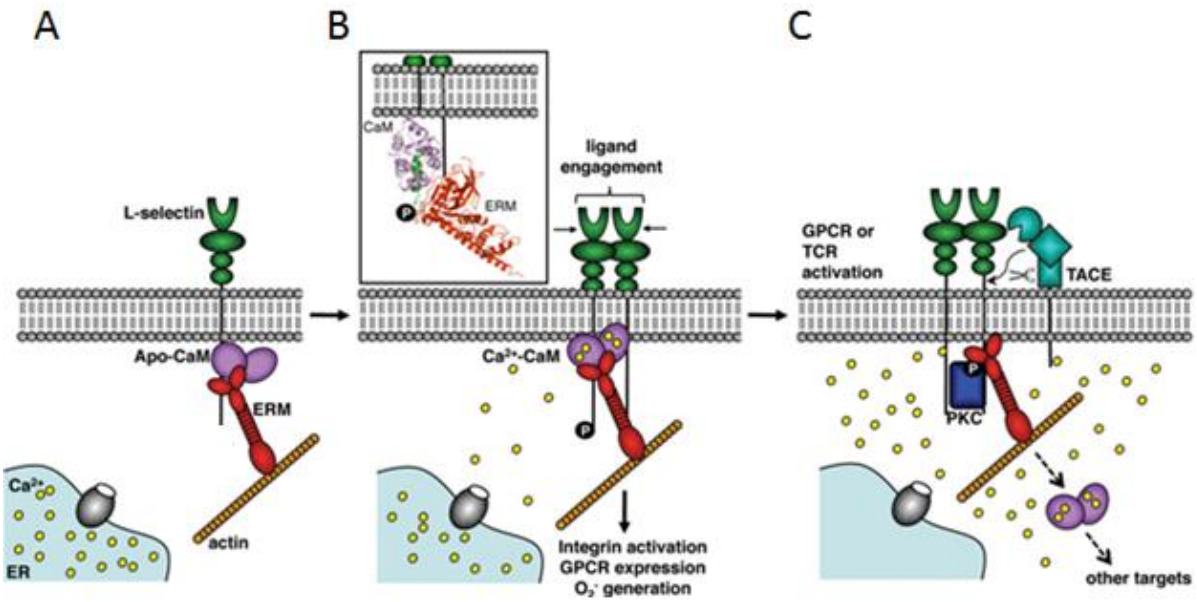

Figure 1.17: CaM binds to both the transmembrane and ICD of L-selectin inducing structural changes. (A) In a resting cell, CaM interacts with positively charged residues in the juxtamembrane region of the L-selectin ICD. The L-selectin ICD also binds ERM family proteins which connect to actin. (B) Clustering of L-selectin by ligand causes release of Ca^{2+} from the endoplasmic reticulum (ER) allowing CaM to bind hydrophobic residues in the ICD (Leu^{358}) and transmembrane region (Ile^{352} and Leu^{354}). CaM pulls the transmembrane region downwards, inducing a conformational change at the extracellular side of L-selectin burying the cleavage site from ADAM 17. (C) After cell activation, cytoplasmic Ca^{2+} increases causing dissociation of CaM from L-selectin. This exposes the ADAM 17 cleavage site in the ectodomain of L-selectin promoting proteolysis. ERM proteins continue to interact with L-selectin allowing an indirect linkage to the actin cytoskeleton which potentially allows co-localization with ADAM 17. The L-selectin ICD is also phosphorylated by PKC isozymes which may modulate interactions with other protein binding partners (Modified, Gifford, *et al.* 2012).

However, Deng *et al* argued that a downward shift of L-selectin would cause polar residues in the extracellular region to be inserted in the hydrophobic lipid bilayer, costing free energy (Fig 1.18 A). It was disputed that the L-selectin/CaM interactions could be studied in aqueous solution as the transmembrane region adopts a helical structure in a lipid bilayer, which potentially buries Ile^{352} and Leu^{354} from CaM. Therefore, Deng *et al* embedded a synthetic L-selectin peptide (CLS) in a liposome and monitored interactions with CaM. CaM adopted an extended conformation while bound to basic residues in the juxtamembrane

region of L-selectin ICD. They showed that CaM cannot interact with the transmembrane region of L-selectin when CLS was presented in liposomes (Deng, *et al.* 2013) (Fig 1.18 B).

They also showed that CaM/L-selectin ICD interactions were abolished when liposomes were enriched with Ptd-L-Ser. Positively charged L-selectin ICD formed electrostatic interactions with negatively charged Ptd-L-Ser sequestering C-terminal L-selectin away from CaM. CaM alone does not disrupt interactions between Ptd-L-Ser and L-selectin ICD and fails to interact (Fig 1.18 C). However, CaM, L-selectin ICD and moesin formed a complex in Ptd-L-Ser enriched liposomes suggesting that CaM and moesin together interrupt electrostatic interactions between L-selectin ICD and Ptd-L-Ser allowing this heterotrimeric complex to form (Deng*, et al.* 2011; Deng*, et al.* 2013) (Fig 1.18 D). This finding agreed with molecular modelling by Killock *et al* displaying a 1:1:1 heterotrimeric complex of CaM, L-selectin and ERM proteins (Killock, *et al.* 2009).

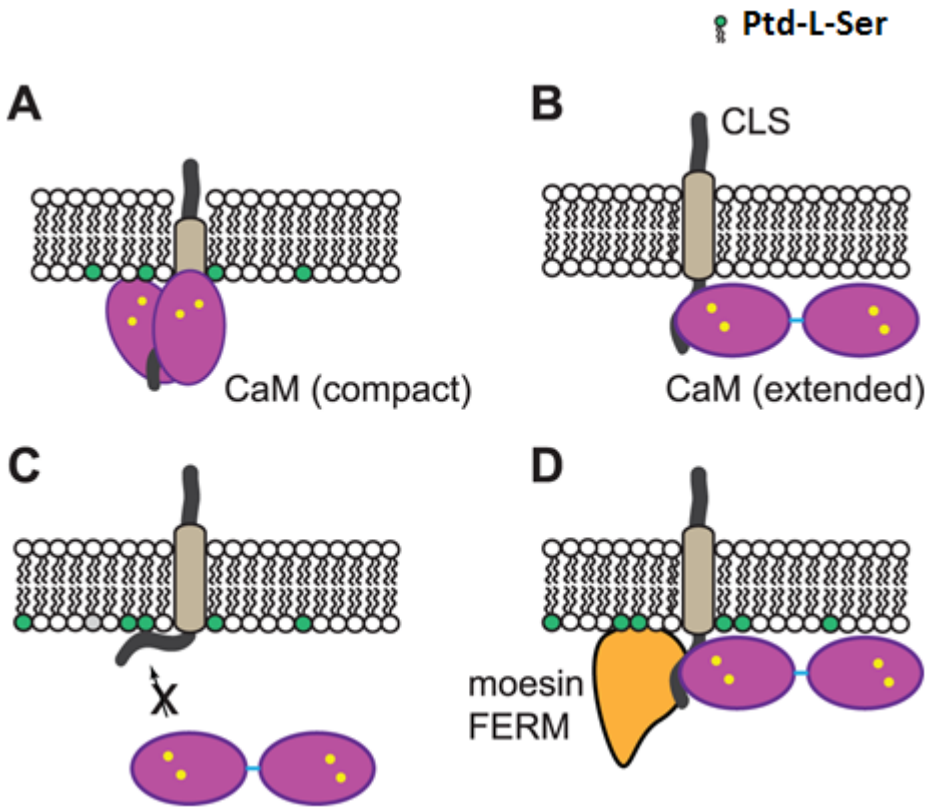

Figure 1.18: Complex L-selectin CaM/ERM interactions. (A) Proposed model by Gifford *et al* (Fig 1.17), CaM adopts a compact structure while bound to the transmembrane and L-selectin ICD of L-selectin in aqueous solution. (B) Deng *et al* showed that CaM is found in an extended conformation while bound to L-selectin ICD of a synthetic peptide corresponding to L-selectin (CLS) in liposomes deficient in Ptd-L-Ser. (C) Interaction between L-selectin ICD and CaM is interrupted when liposomes contain Ptd-L-Ser in the bilayer. Positively charged L-selectin ICD instead forms electrostatic interactions with negatively charged Ptd-L-Ser. (D) Moesin and CaM together disrupt these electrostatic interactions and bind the L-selectin ICD (Modified, Deng, *et al.* 2013).

Affinity chromatography studies by Ivetic *et al* showed that moesin from extracts of PMA-treated lymphocytes associates with the L-selectin ICD; this interaction was disrupted following PKC inhibitor treatment. In contrast, ezrin constitutively bound to L-selectin ICD irrespective of PKC activation status (Ivetic, *et al.* 2002). Furthermore, the disruption of an interaction between the L-selectin ICD and ERM proteins attenuated PMA induced proteolysis (Ivetic, *et al.* 2004). It was argued that post-translational modification such as PKC phosphorylation of the L-selectin ICD may regulate interaction between CaM, ERM

proteins and subsequently ectodomain proteolysis. For instance, Kilian *et al* showed that during PMA treatment, PKC isozymes Θ and ι bind to L-selectin to phosphorylate Ser^{364} and Ser^{367} in the L-selectin ICD (Kilian, *et al.* 2004). Mutating S367 to phospho-mimicking D367 leads to constitutive proteolysis in the absence of PKC stimulation; whilst A367 could not be cleaved by ADAM 17 (Killock, *et al.* 2010) showing that phosphorylation of serine residues regulates proteolysis. Gifford *et al* also showed that the side chains of both Ser^{364} and Ser^{367} are orientated towards the N-terminal F for 4.1 protein, E for ezrin, R for radixin and M for moesin (FERM) domain of bound ERM proteins. They argued that introduction of one or two negatively charged phosphate groups due to PKC phosphorylation may induce or disrupt intra/intermolecular interactions and consequently exchange ezrin for moesin. Such a conformational change in the L-selectin ICD would also cause CaM to dissociate, rendering L-selectin susceptible to ectodomain proteolysis (Gifford, *et al.* 2012).

1.9 ADAM 17 independent proteolysis of L-selectin

L-selectin proteolysis has been documented in ADAM 17-deficient fibroblasts generating a 6 kDa transmembrane fragment. ADAM-17 dependent proteolysis was not observed after cell stimulation with PMA; however, sL-selectin was released under basal conditions and was blocked using a hydroxymate metalloproteinase inhibitor (Walcheck, *et al.* 2003). Le Gall *et al* demonstrated that ADAM 10 compensates for ADAM 17 activity after long-periods of inhibition and sheds L-selectin. For instance, ADAM 10 only proteolyzed L-selectin in transfected WT MEFs when ADAM 17 was inhibited with SP26 for 2 days, but not at earlier time points of 30 min to 2 h. Upregulating intracellular Ca^{2+} with ADAM 10-activator ionomycin in ADAM 17 deficient mouse B cells caused slight proteolysis of L-selectin, however complementation of ADAM 17 induced complete loss of L-selectin expression.

Also, in ADAM 10 and ADAM 17 doubly deficient B cells, complementation of ADAM 17 causes higher levels of released sL-selectin than ADAM 10. These results illustrated that ADAM 10 can compensate for ADAM 17 activity, but does not act as a principal enzyme, where proteolysis is markedly reduced (Le Gall, *et al.* 2009).

Gómez-Gaviro *et al* showed that after neutrophil activation, ADAM 8 mobilized from intracellular granules to the plasma membrane and is proteolyzed by metalloproteinases releasing a soluble, catalytic active form (sADAM 8) to circulation. Levels of released sL-selectin increased in lymphoblastic cells co-transfected with ADAM 8 in comparison to catalytically inactive ADAM 8 or empty vector, which was inhibited by MMP inhibitor KD-IX-73-4. Also, s-L-selectin was released from ADAM 17-deficient cells after incubation with catalytically active, sADAM 8 (Gómez-Gaviro *et al* 2007).

1.9.1 sL-selectin release during homeostatic proteolysis and apoptosis is ADAM 17 independent

Li *et al* studied constitutive and homeostatic L-selectin proteolysis in mice that contained a catalytically inactive ADAM 17 lacking a Zn^{2+} binding domain (ADAM 17^{Zn-}) and found that levels of sL-selectin were similar to WT mice. However, L-selectin expression on ADAM 17 deficient neutrophils was not reduced after PMA treatment or transmigration into the inflamed peritoneal cavity. These results showed that ADAM 17 regulates the density of L-selectin on the surface of neutrophils and their migration to inflamed tissues, but not required for sL-selectin release during homeostatic proteolysis (Li, *et al.* 2006). Further studies by Wang *et al* showed that ADAM 17 proteolysis was required for release of sL-selectin at early time points of Fas signalling during apoptosis. However, at later time points of apoptosis, sL-selectin release was independent of ADAM 17 activity and not inhibited by

the wide spectrum metalloproteinase inhibitor TAPI, broad spectrum serine, aspartic and cysteine protease inhibitors or ADAM 8 knockout mice (Wang, *et al.* 2010). Apoptosis occurs to neutrophils shortly after entry to inflamed tissues to resolve acute inflammation (Serhan and Savill; 2005; Kennedy and DeLeo, 2009) and these studies have therefore shown a correlation with sL-selectin release by an unknown protease(s) which prevents further infiltration of neutrophils (Wang, *et al.* 2010).

1.9.2 ADAM 17 independent proteolysis of L-selectin by MDSCs suppress immune surveillance during tumour escape

Myeloid-derived suppressor cells (MDSCs) accumulate during tumour progression causing poor clinical outcomes (Liu, *et al.* 2010) while attenuating anti-tumour adaptive immunity (Gabrilovich, *et al.* 2012) and causes resistance to chemotherapy, immunotherapy and radiation in murine tumour models (Acharyya, *et al.* 2012; Alizadeh, *et al.* 2014). Expansion of MDSCs in tumour bearing mice was correlated with reduced cell surface L-selectin expression on T and B cells and a 2-fold increase of sL-selectin in circulation (Ku*, et al.* 2016). Furthermore, MDSCs cause downregulated L-selectin expression on CD4+ and CD8+ naïve T cells by proteolysis in the spleen which increases leucocyte rolling along HEVs and destabilizes cell arrest leading to reduced transmigration across HEVs and antigen driven expansion of effector T cells which suppresses immune surveillance during early phases of tumour escape. MDSCs also caused L-selectin proteolysis in ADAM 17-deficient lymphocytes. Additionally, ADAM 17 on the surface of MDSCs do not proteolyze L-selectin on the lymphocytes in *trans* as L-selectin downregulation was observed in the presence of specific ADAM 17 inhibitor PF-5480090 or lymphocytes expressing L(E) L-selectin (Ku*, et al.* 2016; Oh*, et al.* 2013; Parker*, et al.* 2014). sL-selectin is elevated in patients with bladder

and thyroid cancer (Choudhary*, et al.* 2015; Kobawala*, et al.* 2016), which Ku *et al* suggest is caused by these protease(s) expressed on MDSCs which initiate L-selectin proteolysis (Ku*, et al.* 2016).

1.10 Microbes induce proteolysis of L-selectin modulating T cell chemotaxis

Some pathogens have been shown to directly interact with L-selectin and induce L-selectin proteolysis in the absence of TCR activation. This will reduce T cell entry into lymph nodes thereby avoiding immune surveillance and leading to rapid spread of infection. L-selectin directly interacts with pathogens such as *Cryptococcus Neoformans* (Ellerbroek, *et al.* 2004) and *Trypanosoma Cruzi* (Alcaide, *et al.* 2010; de Diego, *et al.* 1997). *Trypanosoma Cruzi* contains a mucin-like cell surface protein named AgC10. During an infection, AgC10 is released from the membrane of *Trypansoma Cruzi* and interacts directly with L-selectin on the surface of human monocytes and T cells disrupting interactions with PNAd on the surface of HEVs affecting tethering. Furthermore, the MMP inhibitor Ro 31-9790 restored the ability of monocytes to adhere to HEVs confirming that AgC10 induces proteolysis of L-selectin (Alcaide, *et al.* 2010; de Diego, *et al.* 1997). AgC10 is a highly sialylated O glycoprotein similar to GlyCAM-1 and has therefore been suggested to interact with the carbohydrate structures of L-selectin (Alcaide, *et al.* 2010). Other microorganisms are able to regulate L-selectin expression at the transcriptional level. For example, mycolactone, a macrolide secreted by *Mycobacterium ulcerans* reduces levels of let-7b, a regulatory component for L-selectin transcription in T and B cells. Mice injected with mycolactone

showed reduced homing of B cells to peripheral lymph nodes (Guenin-Mace, *et al.* 2011; Tang, *et al.* 1998).

Various studies have shown that HIV-1 modulates cell surface L-selectin expression on infected T cells downregulating the immune response. For instance, HIV-1 patients have increased L-selectin ECD in their plasma (Spertini, *et al.* 1992; Kourtis, *et al.* 2000) competing with membrane bound L-selectin on leucocytes for endothelial ligands on HEVs (Tu, *et al.* 2002). HIV-1 viral proteins Nef and Vpu associate with and sequester newly synthesised L-selectin in the trans-Golgi network and ER reducing cell surface L-selectin expression (Vassena, *et al.* 2015). Nef and another HIV-1 viral protein Tat, activate the PI3K/Akt pathway. Activated protein kinase B (Akt) phosphorylates and inactivates forkhead box protein O1 (FOXO1), which decreases expression of KLF-2, lowering transcription of L-selectin. HIV infected T cells have reduced cell surface L-selectin expression and do not migrate to peripheral lymph nodes, explaining their impaired function (Trinité, *et al.* 2014).

1.11 The ϒ-secretase complex

ϒ-secretase is a multi-subunit protease responsible for intramembrane proteolysis of 60 identified type I transmembrane proteins (Fig 1.19) (Beel and Saunders, 2008).

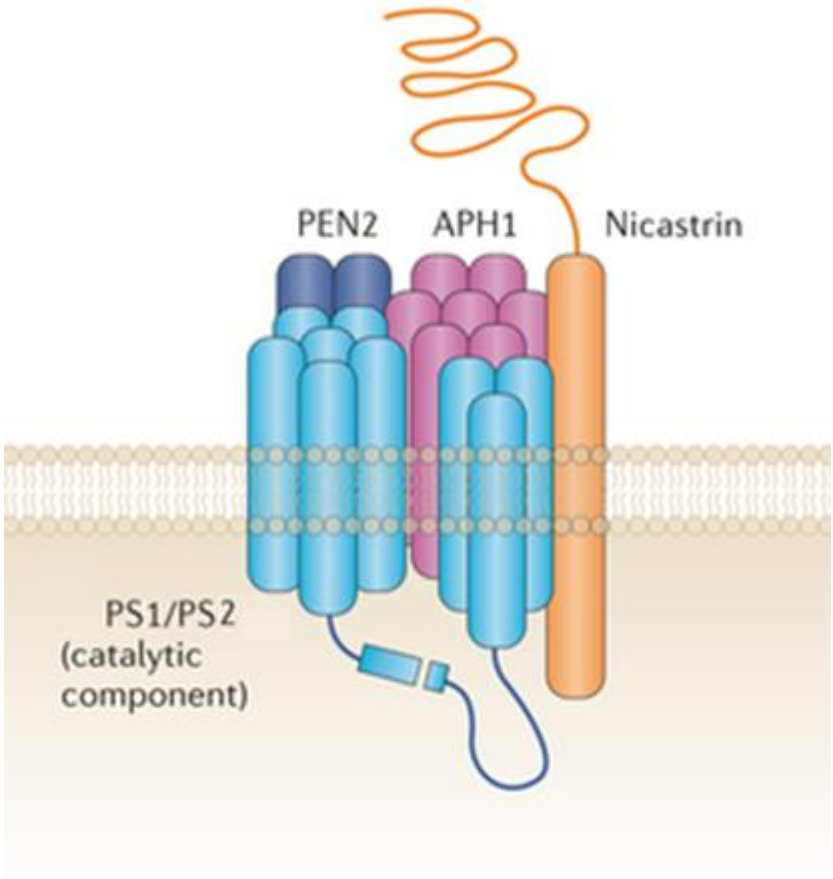

Figure 1.19: Structure of the γ-secretase complex. The γ-secretase complex is a multi-subunit protease consisting of PS 1/2 (PS 1/2), nicastrin, PS enhancer-2 (Pen-2) and anterior pharynx defective-1 (Aph-1) (Andersson and Lendahl, 2014).

Presenilin (PS) is an integral membrane protein spanning the membrane nine times, with the N-terminus facing the cytoplasmic side and C-terminus orientated towards the lumen or outside of the cell (Laudon, *et al.* 2005). Nicastrin is a heavily glycosylated type I transmembrane protein with a large extracellular domain (Shirotani, *et al.* 2003). Anterior

pharynx defective-1 (Aph-1) contains seven TMDs, the N-terminus faces the lumen side and C-terminus is situated in the cytoplasm (Fortna, *et al.* 2004). PS enhancer-2 (Pen-2) spans the membrane twice; both the N- and C-termini face the luminal side (Crystal, *et al.* 2003).

Syndecan-3, E-cadherin, APP and Notch are type I transmembrane proteins that are substrates of γ-secretase (Schulz*, et al.* 2003; Marambaud*, et al.* 2002; De Strooper*, et al.* 1998; De Strooper*, et al.* 1999). Intramembrane proteolysis by γ-secretase releases the ICD and these regulate specific signalling pathways that modulate cell behaviour.

1.12 Nicastrin and Aph-1 form the substrate recognition site of γ-secretase

The N terminus of full length type I transmembrane proteins binds His^{171} and His^{197} of TMDs 5 and 6, respectively of Aph-1 (Chen, *et al.* 2010). After ectodomain proteolysis, the exposed N-terminus of the MP product interacts with a DIYGs and peptidase homologous region (DAPs) in nicastrin. A carboxylate side chain of glutamate acid (Glu^{333}) in the DAPs region interacts with the N terminus of the MP product via a salt bridge interaction (Shah, *et al.* 2005; Dries, *et al.* 2009). The DAPs domain also contains a tetratricopeptide repeat (TPR) region with a conserved leucine (Leu^{571}) at the C-terminus which recognizes substrates (Fig 1.20) (Zhang, *et al.* 2012).

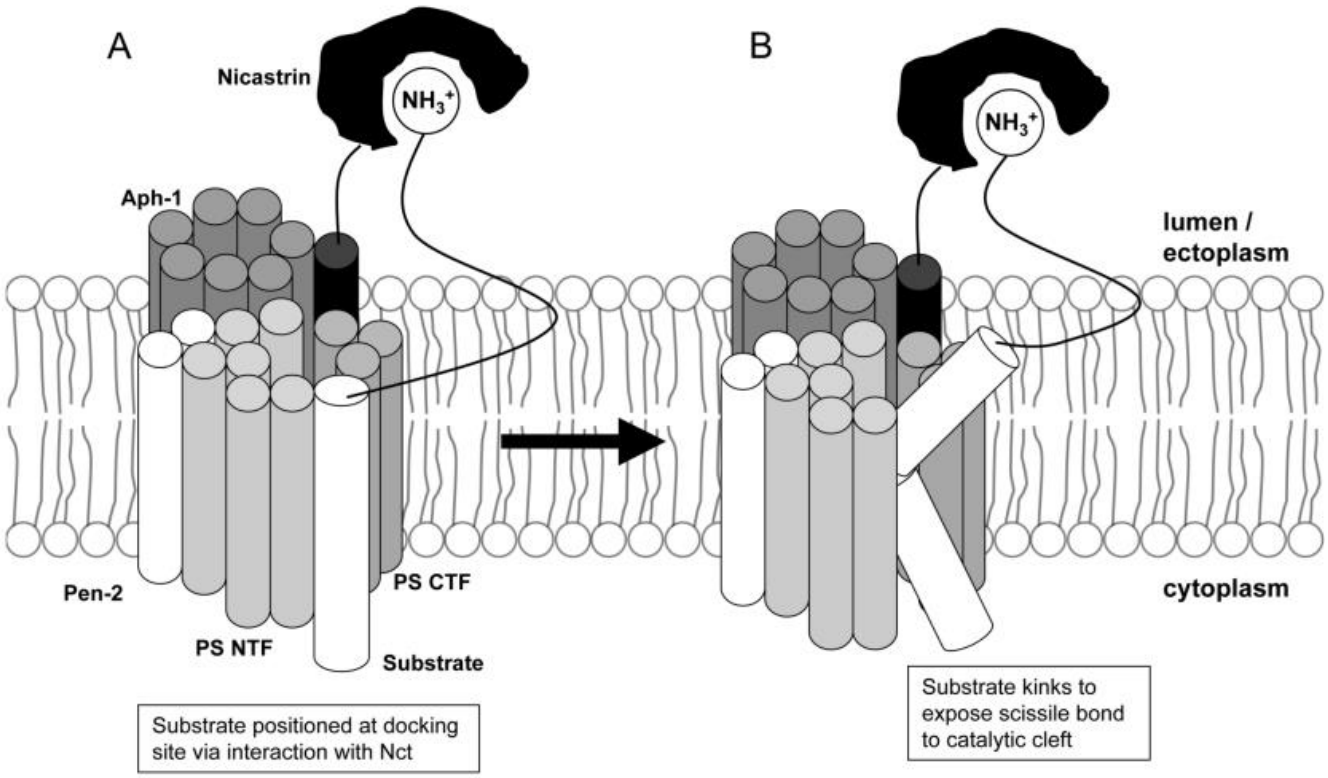

Figure 1.20: Nicastrin and Aph-1 compose the substrate binding site for γ-secretase. After ectodomain proteolysis, the type I transmembrane protein binds to nicastrin (Nct) using its exposed extreme N-terminus. This allows substrate recognition by γ-secretase before PS induced intramembrane proteolysis (Beel and Saunders, 2008).

1.13 Intramembrane proteolysis by PS

1.13.1 Identification of PS's catalytic activity

ϒ-secretase was firstly named as the protease that cleaves APP at the transmembrane region leading to the pathogenesis of Alzheimer's disease (AD) (Haass and Selkoe 1993; Selkoe, 1994). However, family members who inherited AD all contained mutations in both isoforms of PS-1 (PS1) and PS-2 (PS2) at chromosomes 14q24.3 and 1q42.2 respectively (Sherrington, *et al.* 1995; Levy-Lahad, *et al.* 1995; Rogaev, *et al.* 1995). PS was therefore implicated in the pathogenesis of AD and was suggested to act as a receptor, channel or transporter protein (De Strooper, *et al.* 2012). Further studies using PS1-deficient mice

showed ectodomain cleavage of APP in neuronal cells, however intramembrane proteolysis was attenuated causing carboxyl-terminal fragments (CTFs) to accumulate (De Strooper, *et al.* 1998). Additionally, site directed mutagenesis of two conserved aspartates (Asp^{257} in TMD6 and Asp^{385} in TMD7) of PS to alanines abolished intramembrane proteolysis of APP (Wolfe*, et al.* 1999b) yet this mutant was assembled into the γ-secretase complex (Nyabi*, et al.* 2003). ϒ-secretase inhibitors L-685 and DAPT bind directly to PS which inhibits intramembrane proteolysis of substrates (Shearman, *et al.* 2000; Morohashi, *et al.* 2006) (Fig 1.21). Absence of other γ-secretase subunits such as nicastrin, Pen-2 and Aph-1 abolished activation of PS (Edbauer, *et al.* 2003; Kimberly, *et al.* 2003; Takasugi, *et al.* 2003). These findings showed that PS is the catalytic subunit of γ-secretase but its catalytic activity depends on correct assembly of the γ secretase complex.

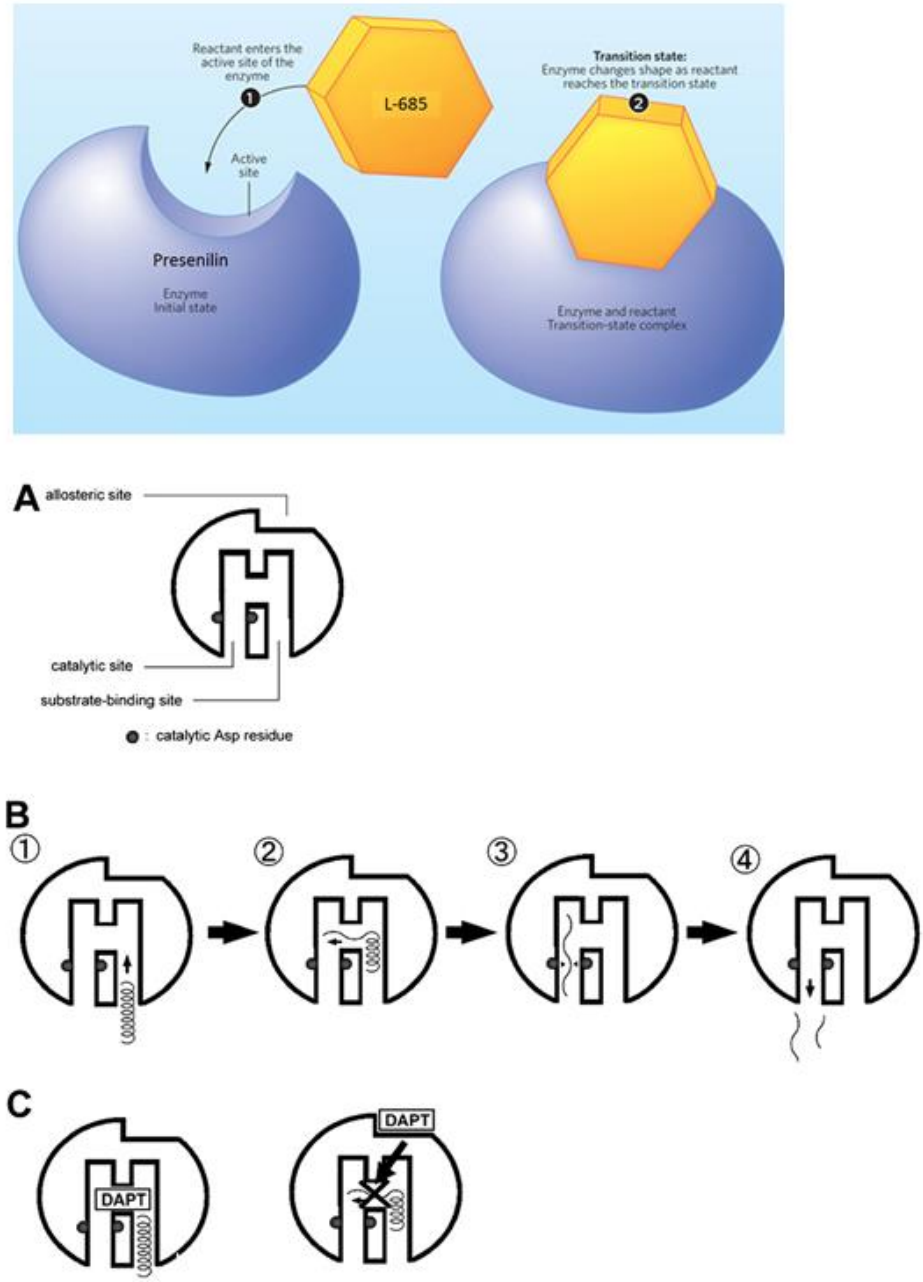

Figure 1.21: L-685 and DAPT inhibit PS proteolysis using different mechanisms. (1) L-685 is a transitional state analog inhibitor and possesses a similar structure to PS substrates. L-685 binds directly to the active site of PS and blocks entry of substrates. (2) (A) The structure of PS. (B) (1) The substrate (indicated as a helix) initially enters the substrate binding site. (2) Upon translocation to the catalytic site, the substrate starts to unwind. (3) The unwound substrate then exposes the scissile bond to catalytic aspartates in the catalytic site of PS. (4) PS then induces intramembrane proteolysis of the substrate releasing the cleaved fragments. (C) DAPT binds to the C terminal region of TMD7 in PS which blocks substrate entry. (D) Consequently, the substrate cannot enter the catalytic site and is not unwound preventing proteolysis (Morohashi, *et al.* 2006).

1.13.2 Lateral diffusion of substrates to the catalytic core of PS

PS is the catalytic component of γ-secretase and contains 9 TMDs. The catalytic core of PS is formed by TMD 6 and 7 which are connected by a hydrophobic domain VII (HDVII). HDVII blocks the catalytic pore in the inactive PS 1/2 zymogen thereby blocking substrate entry (Fukumori, *et al.* 2010). After cell activation, PS auto-proteolyzes between residues Thr^{291} and Ala^{299} (Podlisny*, et al.* 1997), this biochemical event called endoproteolysis results in a 28 kDa N-terminal fragment consisting of TMD6 and a 17 kDa C-terminal fragment including TMD7 (Fig 1.22) (Thinakaran*, et al.* 1996).

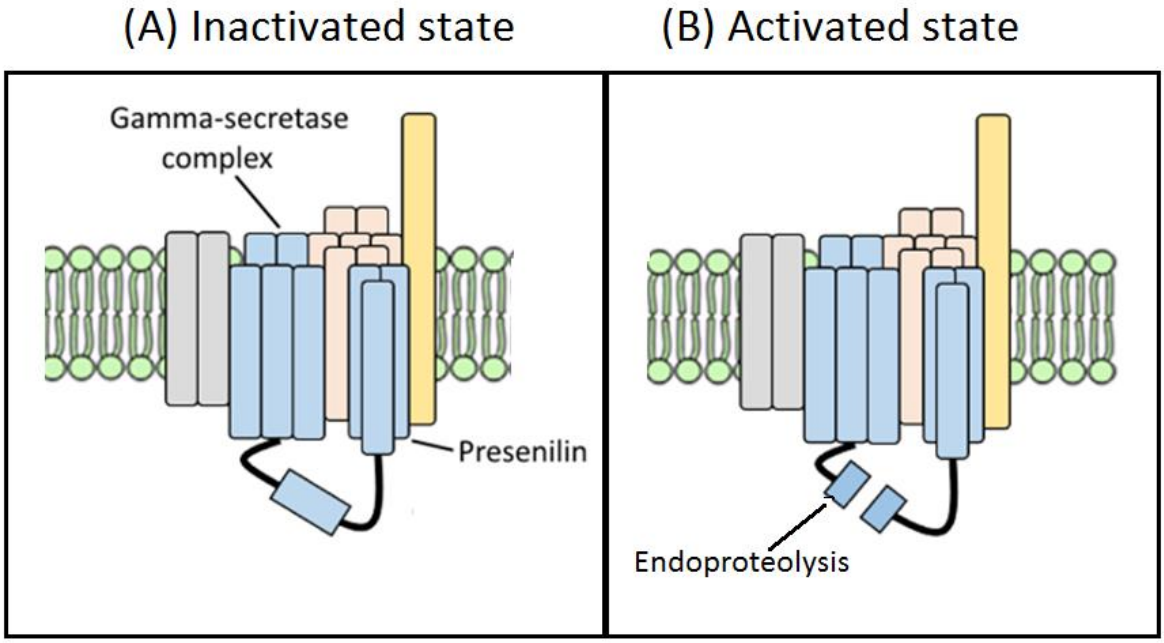

Figure 1.22: Endoproteolysis of PS. PS contains 9 TMDs, between TMD 6 and 7 lies the catalytic core allowing intramembrane proteolysis of type I transmembrane proteins. (A) The zymogen of PS. In this resting state, hydrophobic domain VII (HDVII) is whole and is blocks the catalytic pore preventing substrate entry. (B) Endoproteolysis of PS occurs leading to cleaved HDVII. Cleaved HDVII is removed from the catalytic core allowing substrate entry.

The substrate binding site of γ-secretase consisting of nicastrin and Aph-1 associates with the C-terminus of Pen-2 (Prokop, *et al.* 2004; Mao, *et al.* 2012); this interaction is dependent on PS (LaVoie, *et al.* 2003). It is proposed that substrate recognition by nicastrin and Aph-1 induces Pen-2 binding to transmembrane 4 of PS to promote cleavage of HDVII (Hun-Kim and Sisodia, 2005). Cleavage of HDVII frees the catalytic pore of PS allowing the substrate to enter in a process called lateral diffusion (Fig 1.23) (Fukumori, *et al.* 2010).

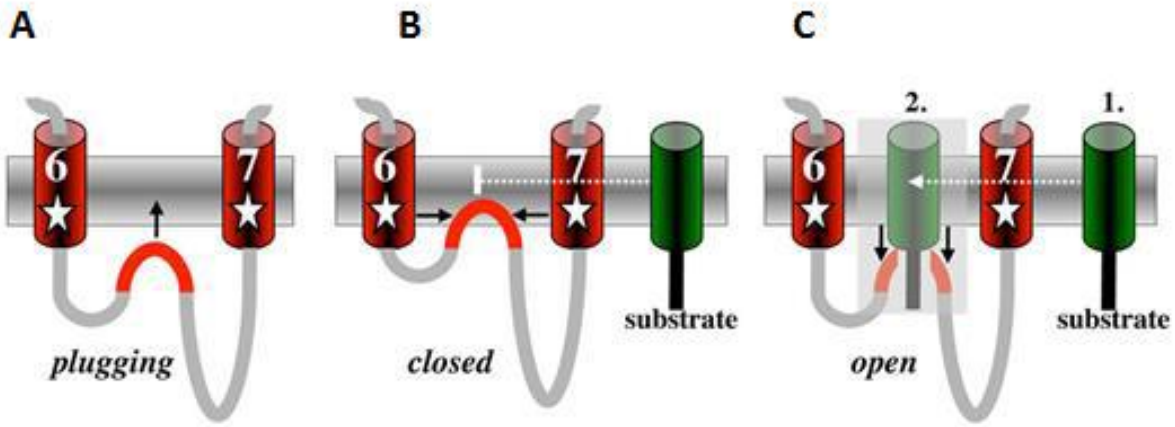

Figure 1.23: Substrates enter the catalytic site of PS by lateral diffusion. (A) Inactivated PS is in closed conformation with the HDVII localized between TMD6 and 7. (B) In the closed conformation, HDVII blocks entry of the type I transmembrane protein substrate. (C) Endoproteolysis causes removal of HDVII from the catalytic site. The substrate laterally migrates across the membrane to enter the catalytic site between TMD6 and TMD7 leading to intramembrane proteolysis (Fukumori, *et al.* 2010).

1.13.3 TMD 9 of PS acts as a lateral gate to the active site

TMD 9 of PS acts as a lateral gate to the active site. Tolia *et al* hypothesise that the γ-secretase substrate uses a specific region of its hydrophobic TMD to interact with an unknown sequence of the intramembrane of TMD9. After substrate recognition, a proline-alanine-leucine (PAL) motif causes TMD9 to shift to one side allowing lateral migration of the substrate to the active site (Fig 1.24) (Sato, 2008; Tolia, *et al.* 2008).

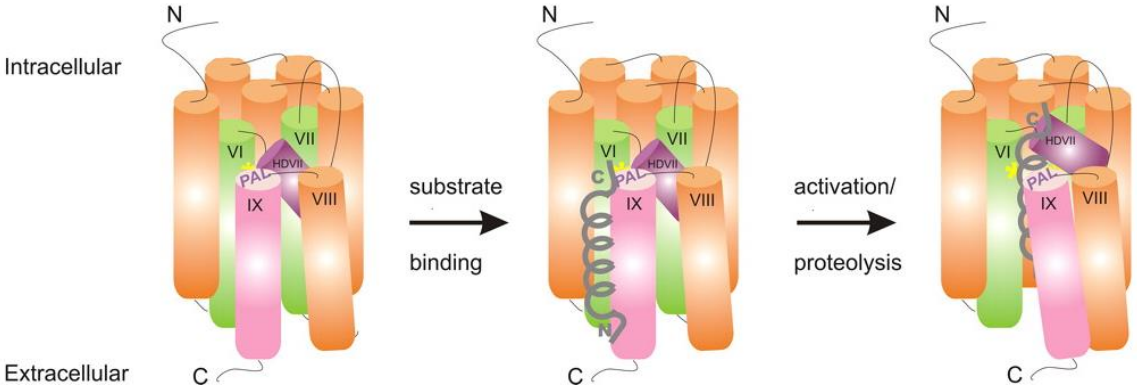

Figure 1.24: TMD9 of PS shifts after interaction with substrate. TMD9 acts as a lateral gate for the catalytic core of PS blocking entry of substrates (grey helix) preventing lateral diffusion. Substrates use their TMDs to bind TMD9. After substrate recognition, TMD9 shifts to one side allowing access to the active site, which is regulated by a proline-alanine-leucine (PAL) motif (Tolia, *et al.* 2008).

1.14 The biochemical pathways induced by PS mediated intramembrane proteolysis

The type I transmembrane protein Notch binds to cognate ligands Delta and Jagged and stimulates ectodomain proteolysis and successive PS induced intramembrane proteolysis causing release of the cytoplasmic tail (NICD) to the nucleus and altered gene transcription. Notch modulates biochemical pathways that regulate cell division. Overexpression of this protein causes increased cell division allowing progression of cancer. Truncated Notch can signal without interacting with its' ligands Delta and Jagged. T cell acute lymphoblastic leukaemia (T-ALL) is triggered due to this truncated form of Notch. Here, increased NICD traffics to the nucleus causing increased cell division (Ellisen, *et al.* 1991; Grabher, *et al.* 2006). Likewise, non-small cell lung cancer and ovarian cancer are characterized by increased cell surface expression of Notch (Dang, *et al.* 2000; Park, *et al.* 2006). Increased Notch signalling has also been demonstrated in breast cancer (Stylianou, *et al.* 2006). Future studies for anticancer treatment could be aimed at blocking PS mediated cleavage of Notch preventing nuclear signalling of NICD (Tammam, *et al.* 2009). However, limitations of this approach are shown in some cancers where only the NICD is transcribed leading to PS independent nuclear signalling (Pear and Aster, 2004). Notably, PS dependent proteolysis of Notch will have diverse effects on cancer depending on the tissue studied. Demehri *et al* showed that NICD dependent nuclear signalling suppresses tumour development (Demehri, *et al.* 2009). Also, nuclear localized NICD causes transcription of the hairy and enhancer of split (HES) resulting in the progression and development of melanoma (Pinnix, *et al.* 2007). Huynh *et al* further showed that mice injected with the γ-secretase inhibitor RO4929097 had less melanoma cell derived tumour development (Huynh, *et al.* 2011). NICD generation

by PS has also been linked with the generation of ischemic stroke. Arumugam *et al* found that ischemia-reperfusion increases PS catalytic activity causing increased expression of NICD in neuroblastoma cells. NICD overexpression caused increased levels of the apoptotic protease caspase-3 in neuroblastoma cells. NICD also elevated leucocyte and platelet membrane expression of CD11b and ICAM-1 causing increased cell adhesion to cerebral vasculature. Hence, NICD promotes the progression of ischemia-reperfusion by causing ischemic induced death of neurons and allow homing of lymphocytes to ischemic injury after stroke (Arumugam, *et al.* 2006).

ErbB4 interacts with growth factors such as neuregulins. There are two isoforms of ErbB4 named JM-a CYT-2 and JM-b CYT-2 (Ni, *et al.* 2001). Isoform JM-a CYT-2 is a substrate for PS and intramembrane proteolysis causes release of an ICD that migrates to the nucleus. In contrast, isoform JM-b CYT-2 cannot generate an ICD. JM-a CYT-2 derived ICD associates with adaptor complex (AP-2) in the cytoplasm and this complex enters the nucleus, activating promoter activity of platelet-derived growth factor receptor-alpha (PDGFRA). JM-a CYT-2 stably transfected mouse NR6 fibroblasts showed stimulation of cell growth, conversely, JM-b CYT-2 triggered apoptosis. PS mediated intramembrane proteolysis of ErbB4 isoform JM-a CYT-2 therefore triggers cell proliferation which could highlight ErbB4's role in cancer progression shown from other studies (Sundvall, *et al.* 2010).

1.15 Aims and hypothesis

For this study, it is hypothesised that after ADAM 17 proteolysis of L-selectin stimulated by TCR engagement, the generated MP product is further cleaved at the transmembrane region by PS, the catalytic component of γ-secretase. This would release the cleaved L-selectin ICD into the intracellular compartment to induce biochemical events that can either benefit or harm the host (Fig 1.25).

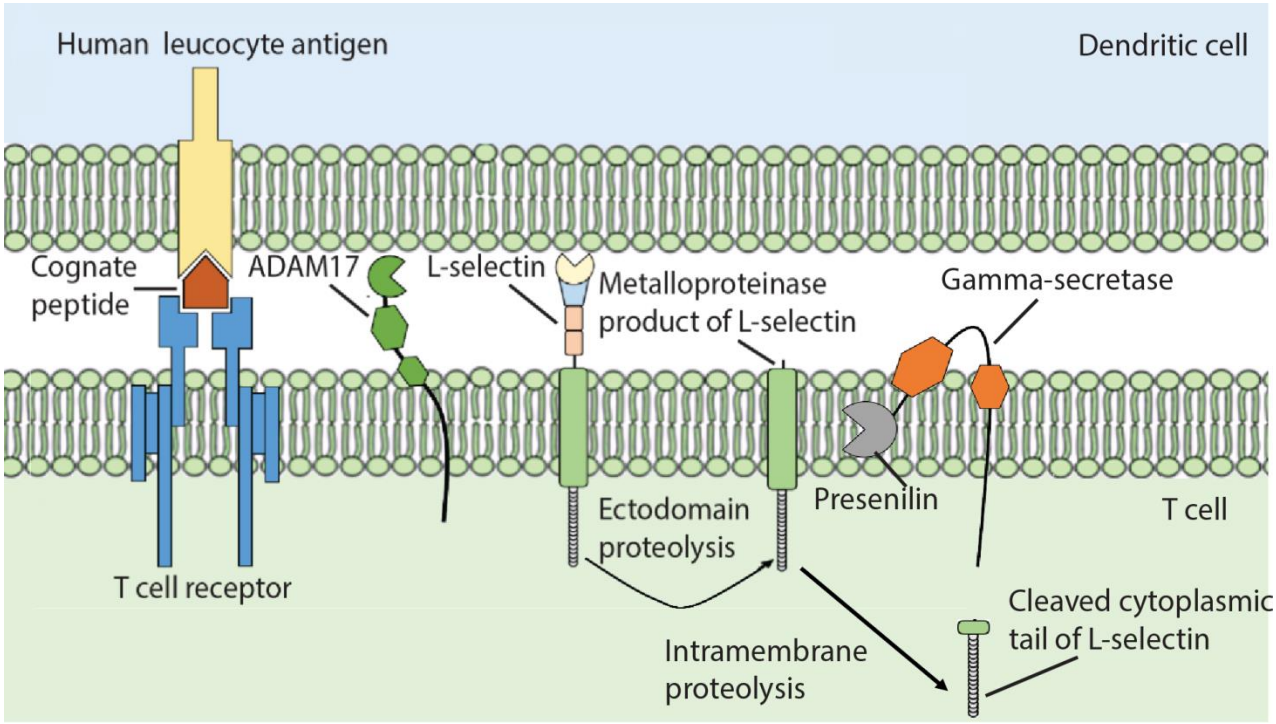

Figure 1.25: The hypothetical model for TCR-induced L-selectin proteolysis. TCR stimulation activates ADAM 17 and causes ectodomain proteolysis of L-selectin. The generated MP product is further shed by PS, the catalytic component of γ-secretase causing release of the cleaved L-selectin ICD into the intracellular compartment.

Work in this thesis is based on four main hypotheses:

(1) The first hypothesis is that TCR induced shedding of L-selectin is ADAM17 dependent.

To test this hypothesis, the main aims were to:

- Express V5 His C terminal tagged L-selectin in pSxW plasmid and produce a pLentivirus.
- Stably transduce human T cells with V5 His tagged L-selectin and stimulate the TCR using cognate peptide and monitor ectodomain proteolysis using both flow cytometry and western blot analysis and determine the role of ADAM17.

(2) The metalloproteinase product of L-selectin is further cleaved by PS, the catalytic component of γ-secretase.

To test this hypothesis, the main aims were to:

- Transiently transfect MEF cells deficient or non-deficient in PS with L-selectin V5 His in a pcDNA5 plasmid.
- Using western blot analysis, quantitate the level of detection of the MP product after 1 h incubation with the γ-secretase inhibitor L-685 or vehicle control DMSO.

(3) TCR stimulation causes endoproteolysis of PS causing intramembrane proteolysis of the MP product of L-selectin

To test this hypothesis, the main aims were to:

- Stimulate the TCR of L-selectin transduced human T cells after pre-incubation with L-685 to monitor intramembrane proteolysis of the MP product in the first instance to determine if γ-secretase cleaves L-selectin in T cells.
- In a time-course experiment of 0 min, 5 min, 15 min, 30 min and 60 min, stimulate the TCR T cells and monitor detection of full length or the C-terminal cleaved fragment of PS to determine if TCR stimulation causes endoproteolysis.

(4) Mutational analysis of the TMD of L-selectin to generate γ-secretase resistant mutants.

To test this hypothesis, the main aims were to:

- Use molecular modelling to predict mutations for testing
- Induce single point mutations of L-selectin in a pSxW plasmid and stably transduce human T cells
- Monitor TCR induced proteolysis of mutant in comparison to wild type L-selectin to determine whether these mutants resist PS proteolysis.

2 Materials and Methods

The formulations of solutions and buffers are shown in Appendix I, used chemicals are listed in Appendix II, laboratory equipment alongside consumables in Appendix III, primers in Appendix IV and the plasmid maps in Appendix V.

2.1 Molecular biology

2.1.1 Polymerase chain reaction (PCR)

All L-selectin constructs used in this thesis had a C terminal V5 His tag. Site directed mutagenesis was performed to mutate isoleucine (Ile^{351}) in the transmembrane region of L-selectin to tryptophan (I351W) or lysine (I351K). Primers (Appendix IV) were designed using CLC DNA Workbench Software and purchased from Eurofins (Manchester, UK). Mutagenic primers 1 and 2 generated I351K L-selectin and primers 3 and 4 produced I351W L-selectin. Wild type, I351W and I351K L-selectin in pcDNA5 were amplified using primers 5 and 6, to allow insertion into the pSxW plasmid (table A1) to allow production of lentiviral particles described later. PCR cycling conditions are shown in table 2.2 using a Peltier DNA Engine Dyad Thermal Cycler.

Reagent	Volume	Final concentration
dH_2O	Up to 50 µL	/
Pfu ultra II Fus Buffer (X 10) (Agilent, Cheshire)	5 µL	X 1
dNTPs (100 mM for each nucleotide) (New England Biolabs, Hitchin)	1 µL	100 µM
Forward primer (10 pmol/µL)	1 µL	0.20 µM
Reverse primer (10 pmol/µL)	1 µL	0.20 µM
Template DNA	X µL (corresponding to 5 ng)	0.1 ng/µL
PfuUltra II Fusion HS DNA Polymerase (Agilent) (2U/µL)	1 µL	0.04 U/µL

Table 2.1: Reagents used for a standard PCR or site-directed mutagenesis reaction.

Cycle step	Number of cycles	Cycle name	Temperature	Time
1	1	Initial denaturation	95 °C	30 sec
2	29	Denaturation	95 °C	10 sec
		Annealing	72 °C	20 sec
		Extension	72 °C	25-30 sec
3	1	Final extension	72 °C	6 min
4	-	Pause	4 °C	hold

Table 2.2: Cycling conditions for a standard PCR.

2.1.2 Restriction digest

The pcDNA5 or pSxW plasmids were digested using NEB reagents in table 2.3. The reaction mixture was incubated at 37 °C for 1 h.

Reagent	pcDNA5 plasmid	pSxW plasmid
DNA	2 µg	2 µg
BamHI (20 U/µL)	1 µL	1 µL
XhoI (20 U/µL)	1 µL	-
Buffer 3 (X 10)	5 µL	5 µL
BSA (X 100)	1 µL	1 µL
dH_2O	Up to 50 µL	Up to 50 µL

Table 2.3: Reagents used to digest pcDNA5 and pSxW plasmids

2.1.3 Agarose gel electrophoresis

DNA mixed with 6 X Orange G loading buffer was loaded onto a 1 % (w/v) agarose gel containing 0.5 µg/mL ethidium bromide (Sigma-Aldrich) in 1x TBE buffer. 1 kb plus DNA marker (Thermo Fisher) was used to estimate the size of each DNA fragment. DNA fragments were separated at 120 V for 60 min and visualized using an UV transilluminator (UVP, Upland, USA).

2.1.4 Purification of DNA from agarose gels

PureLink Quick PCR purification kit (Invitrogen) was used to purify PCR products. Linearized plasmids were isolated from agarose gels using the QIAquick gel purification kit (Qiagen, Manchester, UK) using manufacturer's protocol.

2.1.5 In-fusion reactions

The purified PCR L-selectin mutant products were inserted into linearized plasmids using an In-fusion cloning kit (Clontech, Saint-Germain-en-Laye, France) (Fig 2.1). Reagents used for In-fusion are shown in table 2.4. The reaction was incubated at 50 °C for 15 min and then placed on ice.

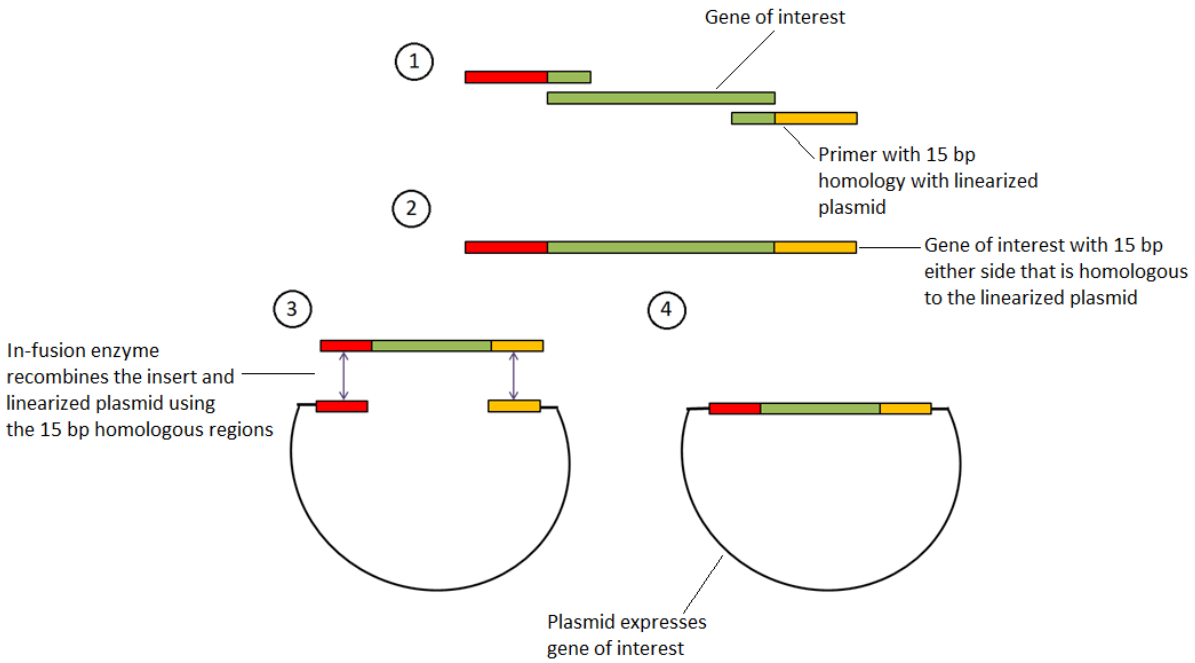

Figure 2.1: The In-fusion cloning technique. (1) Gene of interest (green) is amplified by PCR using primers with a 15 bp overhang (red and yellow) with the linearized plasmid. (2) The amplified DNA insert contains 15 bp overhangs either side to the linearized plasmid. (3) The In-fusion enzyme disrupts hydrogen bonds at 15 bp either side of the digested restriction site of the linearized plasmid. The In-fusion enzyme causes hydrogen bonds to form between single stranded 15 bp overhang of the insert and linearized plasmid. (4) The insert has now recombined into the plasmid.

Reagent	Volume
5 X In-Fusion HD enzyme premix (Clontech)	2.0 µL
Linearized plasmid	3.0 µL
Insert (PCR product)	1.0 µL
dH_2O	4.0 µL

Table 3: Reagents used for In-fusion.

2.1.6 Transformation

Plasmid DNA (1-10 ng) was added to 50 µL of DH5α competent *Escherichia coli* (Thermo Scientific) and left on ice for 30 min. Heat shock transformation was performed at 42 °C for 30 sec. Cells were then placed on ice for 2 min. Bacteria were plated on an agar plate containing 50 µg/mL carbenicillin (Sigma-Aldrich) and incubated at 37 °C overnight.

2.1.7 Identification of positive clones

Antibiotic resistant colonies were picked using a sterile pipette tip and transferred to 5 mL LB broth containing 50 µg/mL carbenicillin. Bacteria were incubated in an orbital shaker at 37 °C and 220 rpm overnight. Bacterial culture (4 mL) was centrifuged at 10,000 rpm for 1 min and plasmid DNA was isolated from pellets using the PureLink Quick plasmid miniprep kit (Thermo Fisher) according to manufacturer's instructions. Restriction enzyme digest (2.1.2) was used to release the L-selectin fragment and agarose gel electrophoresis (2.1.3) was performed to screen for a DNA insert of the right size from positive clones.

2.1.8 DNA sequencing

Positive clones were sent to Eurofins using the Smart Seq service to confirm DNA sequences of L-selectin inserts and that mutations have been introduced. Sequencing primers were purchased from Eurofins and shown in table A2 in Appendix IV.

2.1.9 Plasmid DNA maxiprep

A positive clone was cultured in 400 mL LB Broth containing 50 µg/mL carbenicillin at 37 °C and 220 rpm overnight. Bacterial culture was centrifuged at 6,000 rpm for 10 min using the SLA-3000 rotor (Thermo Fisher). Plasmid DNA was purified from bacterial pellets using PureLink Quick plasmid maxiprep kit (Thermo Fisher) according to manufacturer's instructions. DNA purity (A260/280 ratio >1.8) and concentration were determined using the ND-1000 NanoDrop ™ spectrophotometer (Thermo Scientific).

2.2 Cell culture

Dulbecco modified Eagle's minimal essential media (DMEM), Roswell Park Memorial Institute medium 1640 (RPMI 1640), OPTI-MEM medium, Penicillin/Streptomycin, sodium pyruvate and trypsin/EDTA were purchased from Gibco, Thermo Scientific. Fetal calf serum (FCS) was obtained from Sigma-Aldrich. Cells were grown at 37 °C in a humidified atmosphere containing 5 % CO_2 in an incubator.

2.2.1 Cell lines

Wild type (WT) and presenilin deficient (PSdKO) MEF cells were provided by Professor Bart de Strooper. A PS gene in C57BL/6 mice was inactivated using homologous recombination where exon 5 was replaced by a hygromycin cassette. Resulting PS +/- mice were bred to

produce the homologous wild type (PS +/+) and embryonic lethal (PS -/-) strains. The resulting PSdKO MEF cells were stably transduced with a retroviral vector containing cDNA for either PS1 or PS2 to generate PSdKO + PS1 or PSdKO + PS2 MEF cell lines (Herreman, *et al*. 1999; De Strooper, *et al*. 1998; De Strooper, *et al*. 1999; Schulz, *et al*. 2003). ADAM 17 deficient MEF cells were obtained from Professor Carl Blobel where C57BL/6 mice containing a floxed ADAM 17 allele was crossed with a germline Cre-deleter stain to generate ADAM 17+/- mice which bred to produce ADAM 17-/- mice (Horiuchi, *et al*. 2007). The L-selectin deficient, acute lymphoblastic leukemic Molt3 T cell line and C1R B-cell lymphoblastoid line were both obtained from Dr John Bridgeman.

2.2.2 Cultivating adherent cells

MEF cells were cultured in D10 medium (table 2.5) and passaged every 3-4 days upon confluency. Cells were washed once with PBS (without Ca^{2+} and Mg^{2+}) and subsequently, incubated with 5 mL trypsin/EDTA per 75 cm^2 tissue culture flask for 1 min at 37 °C. Trypsination of cells was stopped with of 5 mL D10 medium. The cell suspension was centrifuged using a Heraeus Megafuge 4R (Thermo Scientific) for 5 min at 1,200 rpm. Cells were diluted in a ratio of 1:5 in fresh D10 medium and cultured.

2.2.3 Cultivating suspension cells

Molt3 T cells and C1R cells were cultured in R10 medium (table 2.5) and passaged every 3 days maintaining a density of 1.5 x 10^6 cells/mL. Cells were counted using a Neubauer cell counting chamber.

Medium	Composition	Use
R10 (Complete RPMI)	RPMI 1640 (4.5 g/L glucose), 10 % FCS, 2mM L-Glutamine, 100 IU penicillin, 100 µg/mL streptomycin and 1 mM sodium pyruvate	Cultivating Molt3 T cells
R1	RPMI 1640, 1 % FCS and 10 mM HEPES	L-selectin shedding experiments
D10 (Complete DMEM)	DMEM (4.5 g/L glucose and 4 mM L-glutamine), 10 % FC, 100 IU penicillin, 100 µg/mL streptomycin and 1 mM sodium pyruvate	Cultivating MEF cells and HEK293 T cells
D1	DMEM, 1 % FCS and 10 mM HEPES	L-selectin shedding experiments
Freezing medium	R10 or D10 medium with 10 % DMSO	Freezing cells

Table 4: Composition of cell culture media.

2.2.4 Thawing and freezing cell lines

Cells stored in liquid nitrogen were thawed in a water bath at 37 °C and washed with serum free medium. Cells were cultured with D10 or R10 medium (table 2.5) and incubated at 37 °C.

For long term storage, adherent cells were grown to confluency of 80 % in a T-175 flask and trypsinized. Suspension cells were grown at a density of 7 x 10^6 cells/mL in a T-75 flask. Cells were centrifuged at 1,200 rpm and resuspended in 10 mL freezing medium (table 2.5). The cell suspension was distributed into seven cryo vials, placed in a freezing container at -80 °C for 24 h. Frozen cells were then transferred to a liquid nitrogen Dewar.

2.2.5 Transient transfection of MEF cells

In preparation for transfection, 2.5 x 10^5 MEF cells/well were seeded in a 24 well plate and cultured in 1 mL D10 medium at 37 °C for 24 h. Transfection of MEF cells was performed using the transfection agent FuGENE 6 (Promega, Southampton). A total of 8 µL FuGENE 6 and 2 µg plasmid DNA (1:4 ratio DNA:FuGENE 6) were diluted in 100 µL optiMEM medium, incubated for 35 min at room temperature and added to cells. Cells were incubated at 37 °C for 24 h.

2.2.6 Generation of stably transfected Molt3 T cells

2.2.6.1 $CaCl_2$ transfection of HEK293 T cells producing lentivirus

Lentivirus was produced after $CaCl_2$ transfection of HEK293T packaging cells with 2nd generation transfer vector pSxW which contain L-selectin inserts in combination with pMD29 and pCMVΔ8.91 to produce integrase sufficient lentivirus (Demaison*, et al.* 2002; Yanez-Munoz*, et al.* 2006).

A total of 20 x 10^6 HEK293 T cells were plated in a T-175 flask in 20 mL D10 medium. After 24 h, a pLentivirus transfection mix was made containing 3 mL pH 7.1 medium (Serum free DMEM, 25 mM HEPES at pH 7.1), 30 µg pSxW, 30 µg pCMVΔ8.91 and 15 µg pMD29, which was incubated at room temperature for 35 min. D10 medium was removed from cultured HEK293 T cells and replaced with 12 mL pH 7.9 medium (D10, 25 mM HEPES at pH 7.9) and the pLentivirus transfection mixture which was then incubated at 37 °C. After 24 h, medium replaced with 20 mL fresh D10 medium. After 48 h and 72 h, collected medium containing lentiviral particles was passed through a 0.45 µM filter and stored at 4 °C. The viral supernatant was transferred to a 38.5 mL thin wall, ultra-clear centrifugation tube (Beckman

Coulter, High Wycombe), placed into a Beckman Coulter SW28.1 rotor and centrifuged in a Beckman Coulter Optima L-100 XP ultracentrifuge at 26,000 rpm for 2 h at 4 °C. The viral pellet was resuspended in 0.5 mL R10 medium, snap-frozen on dry ice and stored at -80 °C.

2.2.6.2 Lentiviral transduction of Molt3 T cells

A total of 0.5 x 10^6 Molt3 T cells were plated into a 96 well plate with 0.5 mL R10 medium containing L-selectin Lentivirus and 4 µg/mL polybrene (Sigma-Aldrich) which was then incubated at 37 °C. After 24 h, cells were transferred to a 48 well plate with 1 mL fresh R10 medium and incubated at 37 °C. Cells were analysed for transgene expression 48 h post transduction using flow cytometry (section 2.5).

2.3 Protein analysis by western blotting

2.3.1 Production of cell lysates

2.3.1.1 Cell lysis buffer

Cell lysis buffer containing 25 mM HEPES (pH 7.5), 150 mM NaCl, 10 mM $MgCl_2$, 1 mM EDTA, 2 % glycerol (v/v), 1 % Triton X-100 (v/v)) was prepared. For production of cell lysates, one Roche complete proteinase ULTRA Tablet (Basel, Switzerland) alongside 1.8 mg/mL 1,10 Phenanthroline (Sigma-Aldrich) and 1 mM sodium orthovanadate (Sigma-Aldrich) were added to 10 mL cell lysis buffer.

Medium was removed from adherent MEF cells or pelleted 1 x 10^6 Molt3 T cells. Cells were lysed in 35 µL of cell lysis buffer and incubated on ice for 35 min. Cell lysates were centrifuged at 13,000 rpm for 5 min to remove cell debris. Supernatant was collected and stored at -80 °C prior to analysis.

2.3.1.2 Laemmli buffer

A total of 1 x 10^6 pelleted Molt3 T cells were directly lysed in 35 µL Laemmli buffer containing 660 mM Tris-HCl (pH 6.8), 26 % glycerol (v/v), 4 % SDS (w/v), 0.01 % bromophenol blue (w/v), 5 % β2-meracaptoethanol (v/v). Cell lysates were sonicated on ice for 15 sec using a Sonic Dismembrator model-120 (Thermo Scientific) and centrifuged at 13,000 rpm. Collected supernatants were immediately used for SDS-PAGE and western blot analysis.

2.3.2 Protein concentration assay (DC assay)

The colorimetric DC-assay (Bio-Rad) was used to determine protein concentrations from MEF cells lysates. A protein standard curve was generated after analysing BSA concentrations from 0.2 to 1.5 mg/mL. In a 96 well plate, 5 µL of each BSA standard or sample was pipetted alongside 25 µL of Reagent A' (20 µL Reagent S in 1 mL Reagent A) and 200 µL of Reagent B. The plate was gently rocked for 20 min at room temperature and subsequently, absorbance was measured at 570 nm using a microplate reader (FLUOstar OPTIMA microplate reader, BMG Labtech, Aylesbury, UK). A DC-assay was not needed for Molt3 T cells as a cell count was performed prior to lysis to ensure equal protein concentration

2.3.3 SDS polyacrylamide gel electrophoresis (SDS-PAGE)

MEF cell lysates (50 µg) were diluted 1:2 in 2X SDS reducing sample buffer. A larger number of 1 x 10^6 Molt3 T cells were lysed due to low expression of L-selectin. Consequently, 15 µL of the lysate was diluted 1:2 in 4X SDS reducing sample buffer to allow efficient running during gel electrophoresis. Mixtures were incubated at 95 °C for 2 min to denature proteins.

Samples were resolved alongside 7 µL SeeBlue Plus 2 pre-stained protein standard (Thermo Fisher) using either NuPAGE Novex 4-12 % Bis-Tris gels and 1 X MES SDS running buffer (Thermo Fisher) or NuPAGE Novex 16 % Tris-glycine gels and 1 X Tris-glycine SDS running buffer (Thermo Fisher) in a SureLock Mini Cell system (Thermo Fisher). Bis-Tris gels were run at 200 V for 35 min, whereas Tris-glycine gels were run at 196 V for 90 min.

2.3.4 Western blotting

Immobilon-PSQ 0.2 µM polyvinyliden-difluorid (PVDF) membrane was activated for 30 sec in methanol, followed by equilibration in transfer buffer (1X NuPAGE transfer buffer or 1X Novex Tris-glycine transfer buffer). Proteins were transferred onto a PVDF membrane at 30 V for 1 h in an XCell II™ Blot Module (Thermo Fisher). The PVDF membrane was incubated for 1 h in 5 % milk (w/v) dissolved in TBS-T. The membrane was then incubated with 5 % milk (w/v) in TBS-T containing diluted primary antibody (table 2.6) on a rotator plate overnight at 4 °C. Membranes were washed 5X for 5 min in 1X TBS-T and incubated for 1 h with 5 % milk (w/v) in TBS-T containing diluted secondary antibody (table 2.6) on a rotator plate for 1 h at room temperature. The PVDF membrane was washed 5X and further incubated at room temperature for 1 h with 1 X TBS-T. The membrane was covered with SuperSignal West Pico Chemiluminescence developing solution (1:1 of peroxide and Luminol/enhance, Thermo Scientific) and incubated for 1 min before exposure (30 sec to 5 min) in myECL imager (Thermo Scientific).

During chemiluminescence detection, luminol is oxidized by peroxide in the presence of the HRP-enzyme causing release of a photon. The myECL imager contains a high performance cooled- charge-coupled device (CCD) camera which includes a light-sensitive silicon chip that

converts photons into digital signals. The silicon chip kept at sub-zero temperatures lowering the dark current preventing background noise.

Primary antibodies		
Antibody	**Working dilution**	**Manufacturer**
Mouse anti-GAPDH	1:3000	Sigma-Aldrich
Mouse anti-V5	1:2500	Thermo Fisher
Rabbit anti-PS-1	1:2500	Sigma-Aldrich
Rabbit anti-PS-2	1:2500	NEB
Rabbit anti-Nicastrin	1:2500	NEB
Rabbit anti-ADAM 17	1:2500	Sigma-Aldrich
Sheep anti-CD62L	1:1000	R & D systems (Oxford, UK)
Secondary antibodies		
Antibody	**Working dilution**	**Manufacturer**
Secondary HRP-conjugated anti-rabbit IgG (H +L)	1:2500	Bio-Rad
Secondary HRP-conjugated anti-mouse IgG (H +L)	1:2500	Bio-Rad
Secondary HRP-conjugated anti-sheep IgG (H +L)	1:2500	Bio-Rad

Table 5: Antibodies used for western blotting.

2.3.5 Densitometry

Image J software was used to quantify each band intensity. Gel pictures were opened with Image J and the *rectangular selection tool* was used to mark bands (Fig 2.2, A). Using the *analyse tool*, bands were selected for quantification using *gels*, *select first lane* (Fig 2.2, B) and then *plot lanes* (Fig 2.2, C). Peaks were then shown representing the relative density of each band. The *straight-line tool* was used to draw lines both between and at the base of the peaks (Fig 2.2, D). After selection of the *wand tool*, each peak was selected to obtain values representing the intensities of protein bands with the GAPDH loading control (Fig 2.2, E and F). For analysis, blots were quantified from three independent experiments (n=3).

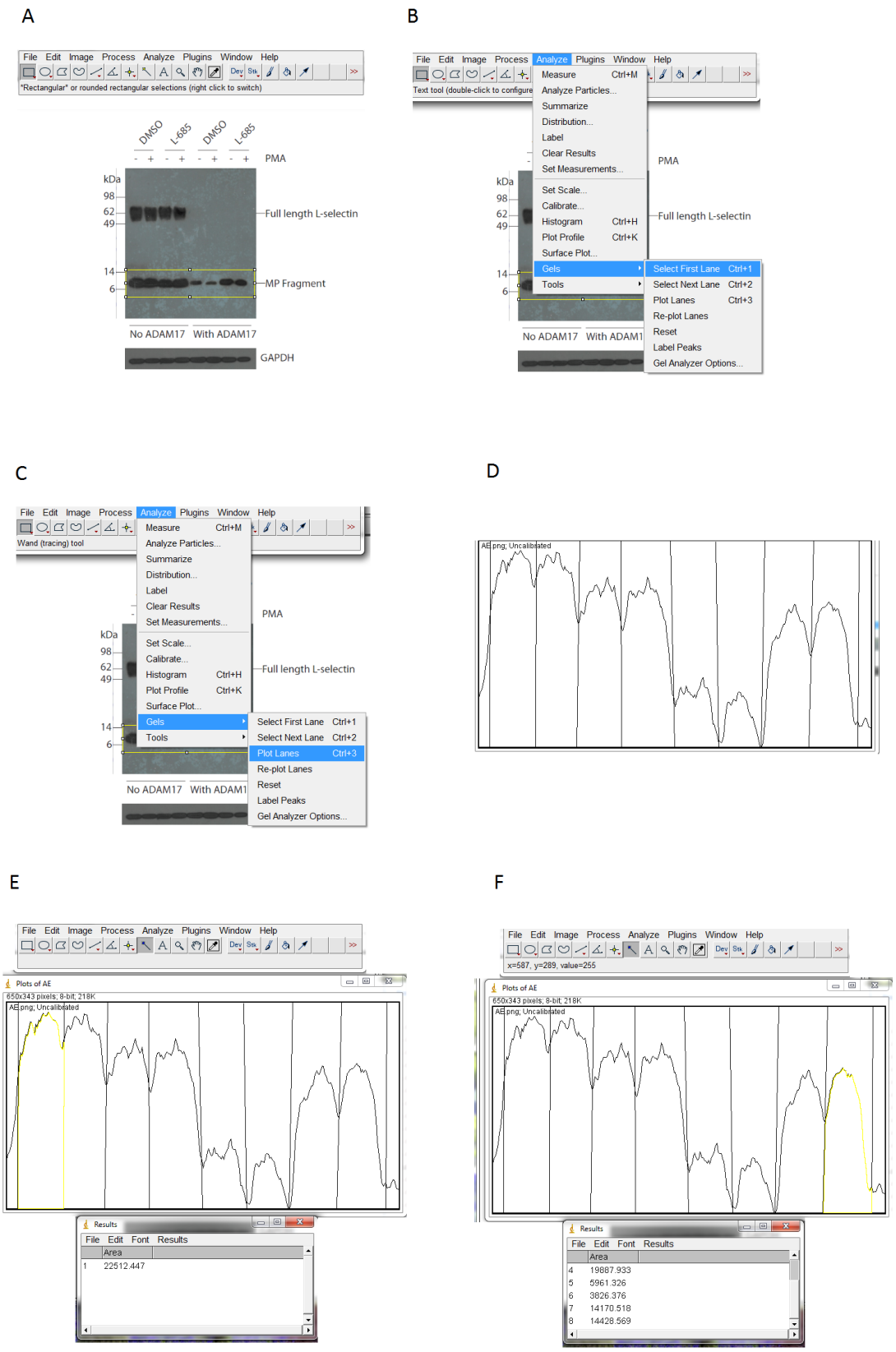

Figure 2.2: Quantification of the intensity of each band using Image J.

2.3.6 Medium concentration

Culture medium was removed from previously transiently transfected MEF cells which were washed once in serum-free Opti-MEM medium. Cells were incubated for 1 h in 1 mL serum-free Opti-MEM medium under various conditions. Conditioned medium was collected and centrifuged at 13,000 rpm for 5 min to remove cell debris. Centrifugal concentration tubes (Amicon Ultra-4, Millipore) with a 3 kDa cut-off were used to concentrate the medium to 100 µL by centrifugation at 4,000 rpm for 90 min. Concentrated medium (20 µL) was diluted 1:2 with 2x SDS reducing sample buffer, heated at 95 °C for 2 min and analysed using western blotting.

2.4 Pulldown

Pelleted 6 x 10^6 Molt3 T cells were lysed in 140 µL cell lysis buffer for 35 min on ice. After lysis, 80 µg of lysate was stored in -80 °C until further analysis. The remaining lysate was diluted in 700 µL of 1X binding/wash buffer and added to 50 µL His tag isolation and pulldown dynabeads (Thermo Fisher) and incubated on a roller for 10 min at 4 °C. Dynabeads were magnetically collected using a DynaMag-5 magnet (Thermo Fisher) and washed 4X in binding/wash buffer (100 mM sodium phosphate (pH 8.0), 600 mM sodium chloride, 0.02 % Tween 20 (v/v)). L-selectin was released from dynabeads by incubation in 100 µL His-elution buffer at room temperature for 10 min. Dynabeads were magnetically pelleted and the collected sample was stored at -80 °C until further analysis.

2.5 Flow cytometry

A total of 2.5 x 10^5 Molt3 T cells were resuspended in 100 µL PBS containing 1:1000 diluted AmCyan live/dead fixable stain (Thermo Fisher) and incubated at 4 °C for 30 min. After 5 min centrifugation at 1,200 rpm, cells were stained with diluted antibody in 25 µL FACs buffer (PBS and 1 % FCS (v/v)) (table 2.7) and incubated at 4 °C for 30 min. Pelleted cells were washed three times in FACs buffer before being fixed in 100 µL of 4 % paraformaldehyde (v/v) (Thermo Scientific) at room temperature for 15 min. Fixed cells were resuspended in 200 µL PBS and analysed on a BD FACs Canto II.

Abc anti-mouse compensation beads (Thermo Fisher) were labelled with 0.5 µL of the fluorochrome conjugated antibodies used during flow cytometry (table 2.7). ArC reactive beads were labelled with 2 µL of AmCyan live/dead stain solution. Beads were incubated for 30 min at 4 °C, centrifuged at 1,200 rpm and washed in PBS before final re-suspension in 200 µL FACs buffer. A drop of negative beads was added before electronic compensation was performed using the BD Diva software.

Specificity	Conjugate	Clone (isotype)	Company name and product code (#)	Dilution
CD62L/ L-selectin (human)	PE	Dreg56 (IgG, k)	eBioscience, #12-062942	1:50
Isotype control	PE	p3.6.2.8.1 (IgG1, k)	eBioscience, #12-471482	1:50
CD19 (human)	APC	HIB19 (IgG1, k)	BD Pharmigen, #555415	1:25
Isotype control	APC	11711 (IgG1, k)	R&D Systems, #IC002A	1:25

Table 6: Antibodies used for flow cytometry.

2.6 ELISA

Human L-selectin/CD62L DuoSet ELISA (R & D systems) was used to measure the concentration of soluble L-selectin using the reagents and protocols provided. A standard curve for human L-selectin standard was generated after seven serial 2-fold dilutions in Reagent Diluent allowing detection of protein concentrations to range from 78 to 5000 pg/mL. A total of 100 µL diluted standard or sample (1:2 ratio of sample: Reagent Diluent) were pipetted in triplicates into a 96-well plate previously coated with capture antibody. Absorbance was measured at 570 nM using a microplate reader and protein concentrations were derived from the shape of the human L-selectin standard curve.

2.7 T cell activation

2.7.1 T cell receptor activation using Anti-CD3/CD28 dynabeads

A total of 80 µL Dynabeads Human T-Activator CD3/CD28 (Thermo Fisher) were washed in PBS, magnetically pelleted and incubated with 1.3 x 10^6 Molt3 T cells in 100 µL R1 medium. After TCR-activation, 2.5 x 10^5 Molt3 T cells were prepared for flow cytometry (section 2.5). Remaining Molt3 T cells at 1.0 x 10^6 cells/mL were centrifuged at 1,200 rpm for 5 min and lysed in cell lysis or Laemmli buffer as described in section 2.3.1.

2.7.2 T cell receptor activation using SLY peptide pulsed C1R antigen presenting cells

Proteolysis of L-selectin in response to cognate peptide stimulation was studied using SLYNTVATL (SLY) peptide (Eurofins, Manchester) to activate gag+ TCR expressing Molt3 T cells. C1R cells were resuspended in 1 mL R1 medium and incubated in the presence or absence of SLY peptide for 1 h at 37 °C. After, Molt3 T cells at 6 x 10^6 cells/mL were added to the C1R cells (in a 1:3 ratio of C1R cells : Molt3 T cells) and incubated for 1 h at 37 °C. For flow cytometry, Molt3 T cells were used at 1.5 x 10^5 cells/mL and C1R cells at 0.5 x 10^5 cells/mL. For pulldown assays, Molt3 T cells were used at 6.0 x 10^6 cells/mL and C1R cells at 2.0 x 10^6 cells/mL.

2.8 MEF cell activation using PMA

Transiently transfected MEF cells were prepared as described in section 2.24. After 24 h transfection, conditioned medium was replaced with fresh D1 medium containing 100 ng/mL PMA or the vehicle control DMSO. Cells were incubated at 37 °C for 1 h and subsequently lysed (section 2.3.1) producing lysates for western blot analysis (section 2.3.4).

2.9 Inhibition of ADAM 17 and PS

The D1(A12) ADAM 17 antibody was obtained from Professor Gillian Murphy (Cambridge University) and used at a concentration of 100 nM. The wide spectrum metalloproteinase inhibitor Ro 31-9790 was obtained from Roche (Hertfordshire) at used at a final concentration of 30 µM. The γ-secretase inhibitors L-685 (Sigma Aldrich) and DAPT (N-[N-(3,5-difluoro-phenacetyl)-L-alanyl]-S-phenylglycine t-butyl ester, ALX-270-416) (Enzo, Life Sciences, Exeter, UK) were both used at 10 µM.

MEF cells in D1 medium or Molt3 T cells in R1 medium were incubated for 1 h at 37 °C with the inhibitors or DMSO solvent control at the specified concentrations. Cells were then stimulated (sections 2.7 and 2.8) in the presence of the inhibitors or DMSO control.

2.10 Statistical analysis

GraphPad Prism was used to analyse the data using a One-way Anova with Tukey post-test. P-values below 0.05 (95 % confidence interval) were termed significant. Each experiment contains data from 3 independent experiments (n=3).

For flow cytometry analysis, the % of cell surface L-selectin expression on Molt3 T cells was calculated relative to non-TCR stimulated cells, after subtracting the isotype control mean fluorescence intensity (MFI) from all samples:

$$\% \text{ Cell surface L-selectin} = 100 \times \frac{\text{MFI of TCR activated T cells - MFI of Isotype control}}{\text{MFI of control cells - MFI of Isotype control}}$$

3. ADAM 17 mediated ectodomain proteolysis of L-selectin induced by TCR

3.1 Introduction

Data from Ann Ager's laboratory has shown that stimulation of the TCR causes activation of ADAM 17. Activated ADAM 17 then cleaves L-selectin at the ectodomain generating an MP product comprising a transmembrane region and a 17-amino acid L-selectin ICD (Fig 3.1).

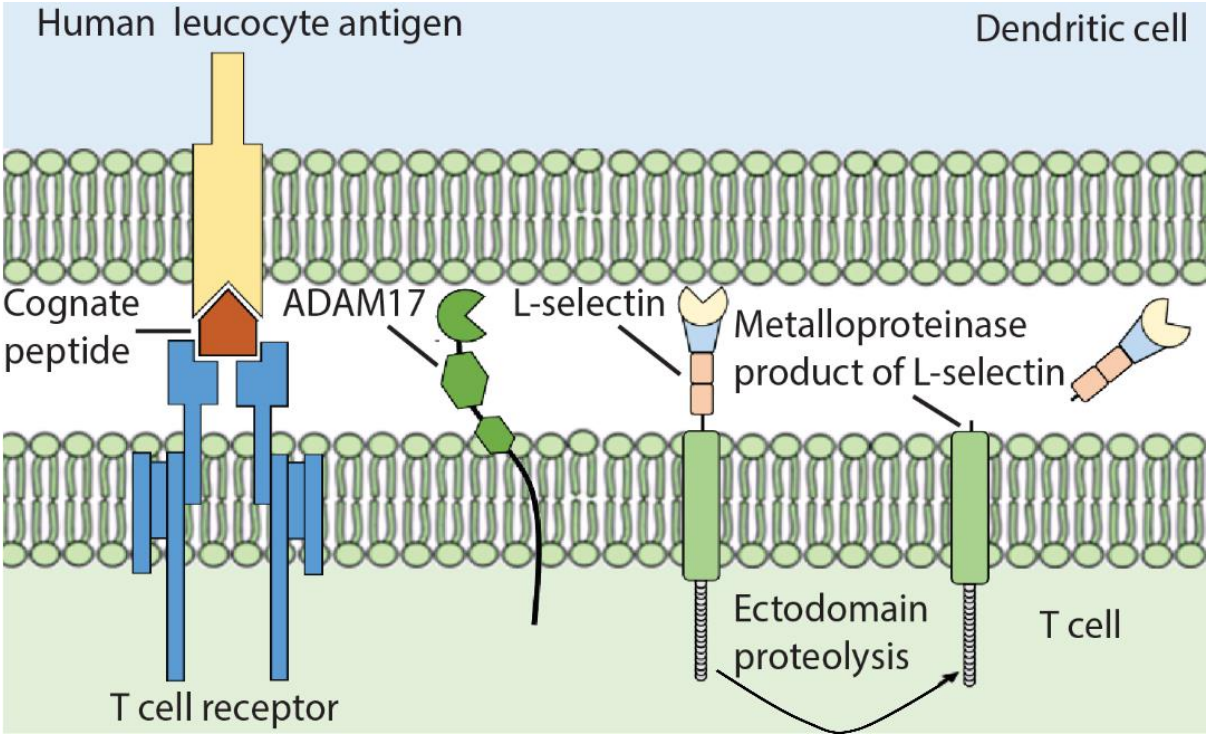

Figure 3.1: ADAM 17 proteolysis of L-selectin induced after TCR stimulation. (A) Human leucocyte antigens present a cognate peptide which binds to and stimulates the TCR causing ADAM 17 activation and L-selectin proteolysis.

In this study, I used leukemic, L-selectin negative Molt3 T cells which expressed a HIV based gag TCR. A pSxW plasmid expressing C terminally V5 His tagged L-selectin was used to stably transduce Molt3 T cells (Fig 3.2 A). Initially, experiments were performed to confirm that the C terminal V5 His tag of L-selectin did not interfere with ADAM 17 proteolysis after TCR stimulation. Two different approaches were used for T cell activation; firstly, Molt3 T cells were incubated with APCs (C1R cells) pulsed with the gag TCR cognate peptide SLYNTVATL (SLY) (Fig 3.2 B). Secondly, Molt3 T cells were treated with anti-human CD3/CD28 conjugated dynabeads (Fig 3.2 C).

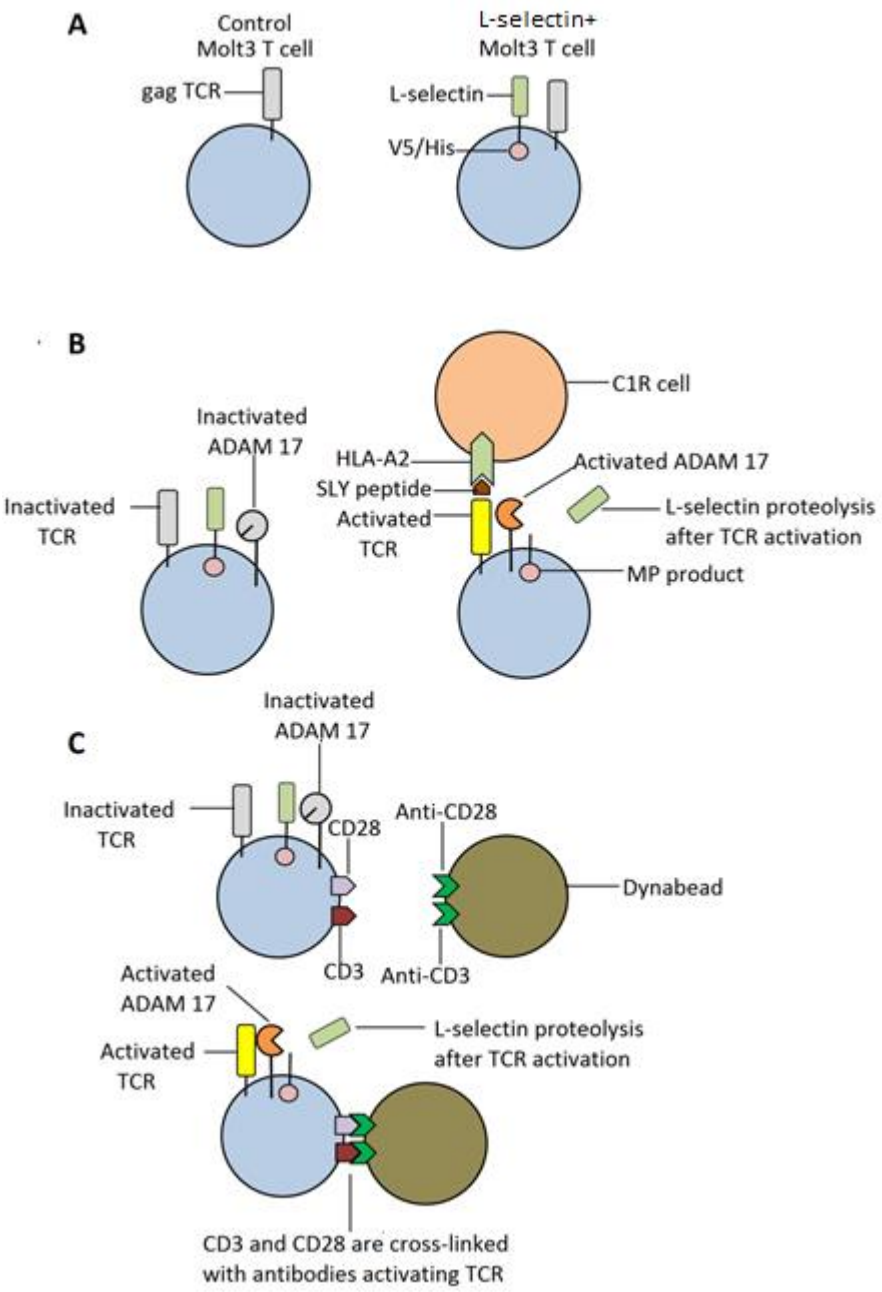

Figure 3.2: A representation of the two different approaches of TCR stimulation. (A) L-selectin negative Molt3 T cells expressing a gag TCR are termed control Molt3 T cells. Control Molt3 T cells were stably transduced with L-selectin V5 His are named as L-selectin+ Molt3 T cells. (B) TCR activation using SLY peptide pulsed C1R cells. C1R cells present a cognate (SLY) peptide to gag TCR on the surface of Molt3 T cells. After TCR stimulation, ADAM 17 becomes activated and cleaves L-selectin. (C) TCR activation using anti-human CD3/CD28 conjugated dynabeads. Dynabeads coated with antibodies against CD3 and CD28 are incubated with Molt3 T cells. Anti-CD3 and Anti-CD28 presented on the surface of dynabeads bind directly to CD3 and CD28 on the surface of Molt3 T cells stimulating the TCR which activates ADAM 17 causing L-selectin proteolysis.

Pull down assays were also performed to determine whether WT or non-sheddable ΔM-N L-selectin directly interacts with ADAM 17 in both resting and TCR stimulated conditions. I hypothesised that TCR stimulation encourages interaction between L-selectin and ADAM 17 which would induce proteolysis. Cobalt coated dynabeads were used to bind to the His tag of L-selectin to extract potential L-selectin/ADAM 17 complexes from the original cell lysate (Fig 3.3).

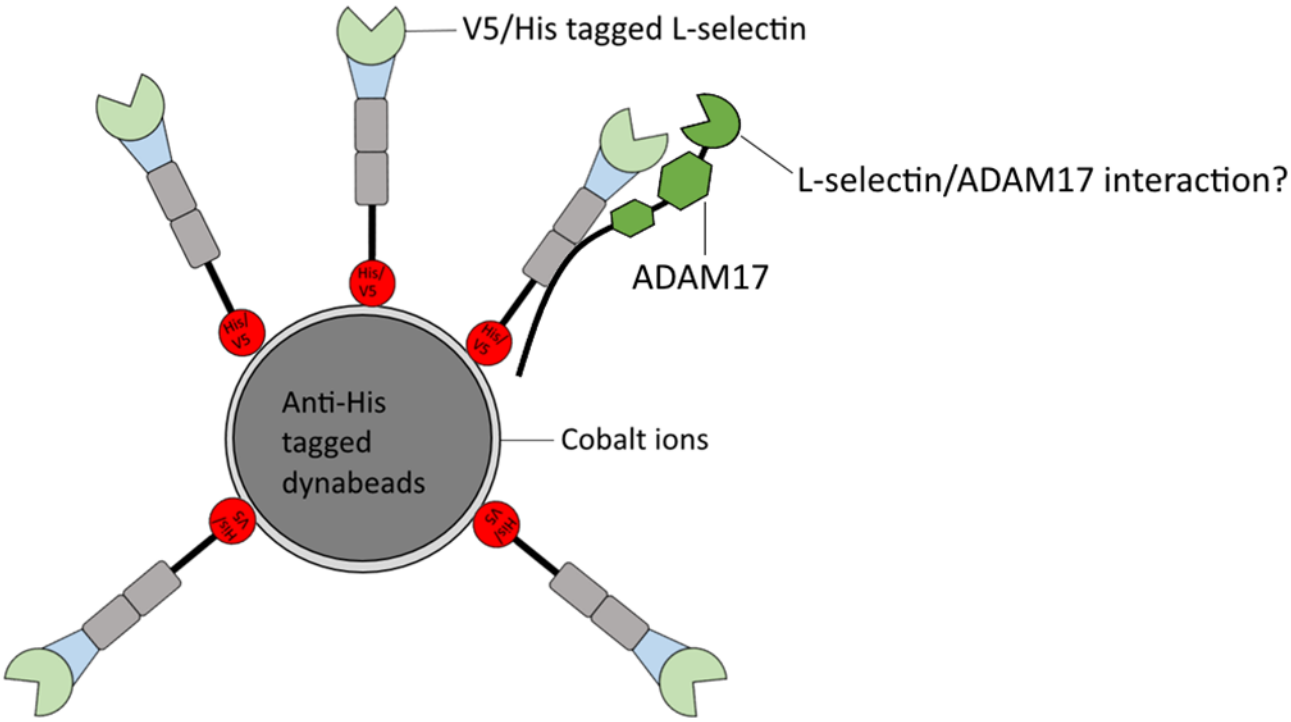

Figure 3.3: Pulldown of L-selectin V5 His using cobalt ion covered dynabeads. The His tag region of L-selectin binds to cobalt ions presented on the surface dynabeads. This allows the isolation and pulldown of potential L-selectin/ADAM 17 complexes.

3.1.1 Aims of the chapter

- To confirm that the C terminal V5 His tag of L-selectin does not interfere with ADAM 17 proteolysis after TCR stimulation.

- To determine if ADAM 17 interacts with L-selectin in both resting and TCR-activated T cells.

3.2 Generation of Molt3 T cells expressing V5 His tagged WT or ΔM-N L-selectin

3.2.1 Generation of a pSxW plasmid expressing WT or ΔM-N L-selectin V5 His

In this study, I stably transduced Molt3 T cells with WT and ΔM-N L-selectin V5 His using a pLentivirus. ΔM-N L-selectin has an 8-amino acid truncation (MIKEGDYN), which causes resistance to ADAM 17-proteolysis (Chen, *et al*. 1995) (Fig 1.7). Molt3 T cells were stably transduced with WT or ΔM-N L-selectin V5 His using a pLentivirus. PcDNA5 plasmids containing WT or ΔM-N L-selectin were provided by Dr Aleksander Ivetic (King's College London) and Prof Tom Tedder (University of Alabama) respectively. Dr Vera Knäuper (Cardiff University) later conjugated WT and ΔM-N L-selectin to V5 and His tags. A HIV based lentiviral transfer plasmid, pSxW, expressing zinc finger nuclease-1 (ZFN-1) and rat cluster of differentiation 2 (rCD2) obtained by fellow PhD student Sophie Wehenkel was digested with BamHI. BamHI digest caused release of ZFN-1 and rCD2 forming a linearized pSxW plasmid. WT or ΔM-N L-selectin V5 His inserts were then introduced into the BamHI linearized pSxW plasmid using the In-fusion cloning technique (Fig 3.4).

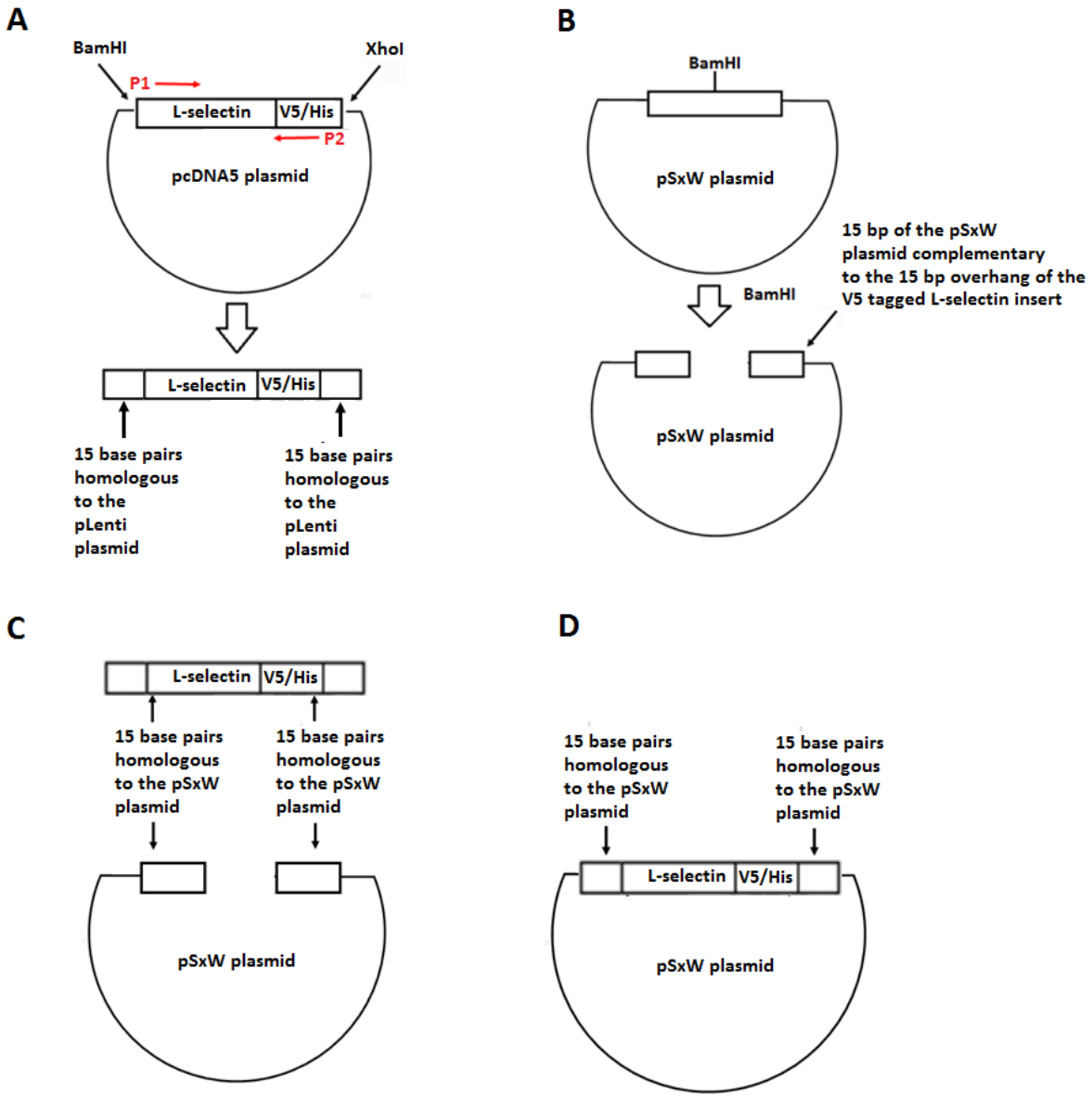

Figure 3.4: Cloning strategy to generate the pSxW plasmid expressing L-selectin V5 His. (A) The L-selectin V5 His insert was amplified from the pcDNA5 plasmid using PCR. The amplified L-selectin V5 His insert contained 15 base pairs (bp) either side that were homologous to a pSxW plasmid. (B) The original pSxW plasmid was digested with BamHI to generate a linearized form with 15 bp either side that were homologous to the sequences at the end of the L-selectin V5 His insert. (C) The BamHI linearized pSxW plasmid and amplified L-selectin V5 His insert were recombined using In-fusion. Here, In-fusion causes denaturation of double strands at the end of the linearized plasmid and insert at around 15 bp. These 15 bp homologous single stranded nucleotides either end of the linearized plasmid and insert form hydrogen bonds regenerating double stranded DNA. This allows the L-selectin V5 His to be inserted into the pSxW plasmid. (D) The pSxW plasmid now encodes L-selectin V5 His.

A BamHI digest was performed to determine if WT or ΔM-N L-selectin V5 His was present in the pSxW plasmid. The original pSxW plasmid was also digested with BamHI as a control to determine the efficiency of in-fusion. Bands appeared at around 1281 bp and 1273 bp which were not present in the control. This showed that the pSxW plasmids contained WT and ΔM-N L-selectin V5 His respectively (Fig 3.5).

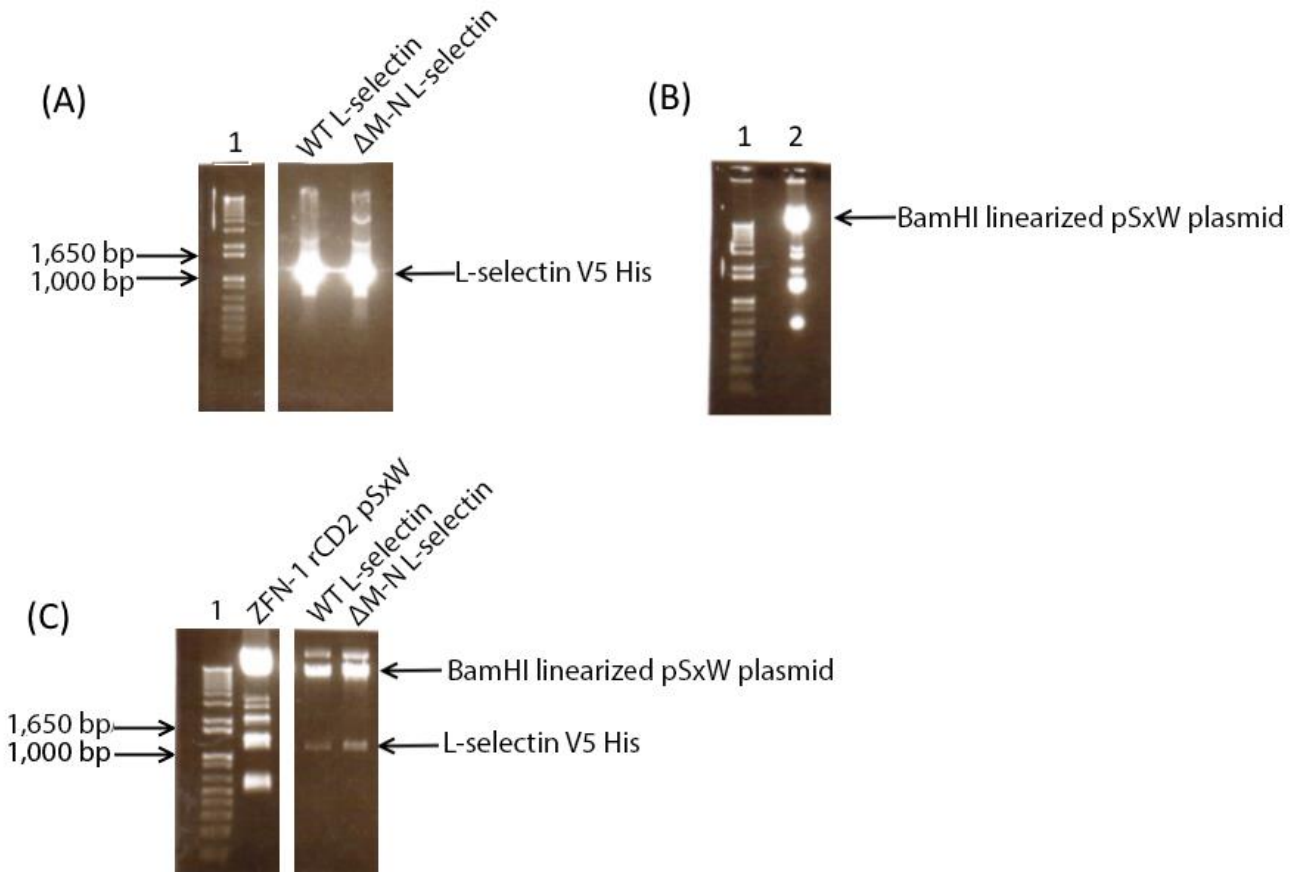

Figure 3.5: Cloning of L-selectin V5 His in pSxW plasmid. Lane 1 of all the images represents the 1 kb plus DNA ladder (A) PCR amplification of V5 His WT and ΔM-N L-selectin V5 His. Lanes 2 and 3 illustrate PCR amplified WT (1281 bp) and ΔM-N L-selectin V5 His (1273 bp) respectively. (B) BamHI digest of pSxW plasmid. Lane 2 shows BamHI digest of the pSxW plasmid originally expressing ZFN-1 and rCD2. BamHI linearized the pSxW plasmid removing ZFN-1 and rCD2. This generated a linearized pSxW plasmid. (C) Miniprep DNA isolated from carbenicillin selected DH5 α colonies. After In-fusion, minipreps were digested with BamHI to confirm expression of the WT and ΔM-N L-selectin V5 His inserts. Lane 2 represents the original pSxW plasmid digested with BamHI. Lanes 3 and 4 display in-fused pSxW plasmid expressing WT or ΔM-N L-selectin. Bands seen at 1281 bp and 1273 bp represent WT and ΔM-N L-selectin V5 His respectively.

The plasmids were sent for sequencing, which confirmed the DNA sequences of WT and ΔM-N L-selectin V5 His.

3.2.2 Lentiviral transduction of Molt3 T cells using pSxW plasmid expressing WT or ΔM-N L-selectin

Molt3 T cells were transduced with pLentivirus containing either WT or ΔM-N L-selectin. After 48 h, flow cytometry analysis showed enrichment of a high subpopulation of Molt3 T cells expressing WT L-selectin (Fig 3.6 A). However, only a small subset of the Molt3 T cell population expressed ΔM-N L-selectin (Fig 3.6 B). Magnetic activated cells sorting (MACS) separation was used to isolate the subset of Molt3 T cells that expressed high levels of ΔM-N L-selectin which were grown for one week. This subpopulation showed high levels of ΔM-N L-selectin expression showing that the MACS separation enriched high expressing Molt3 T cells (Fig 3.6 C).

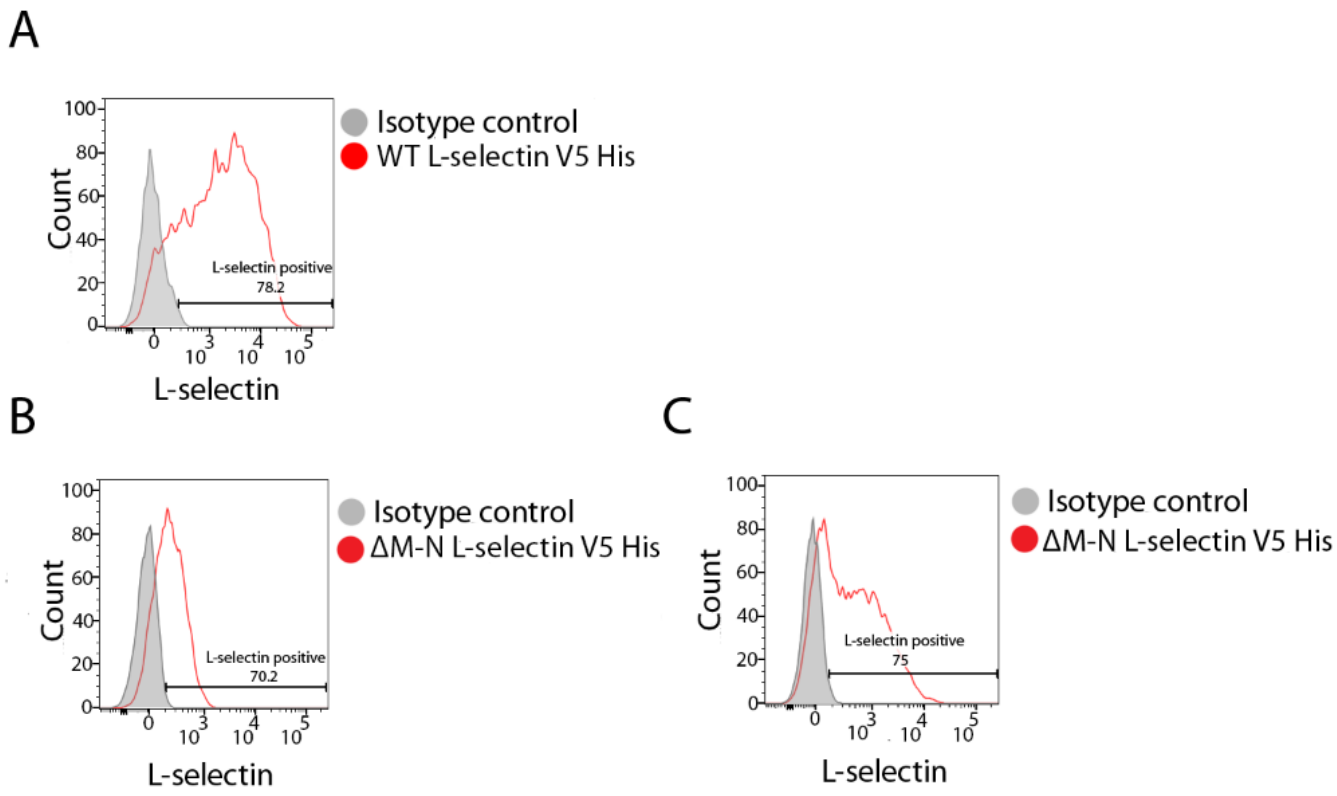

Figure 3.6: Lentiviral transduction of Molt3 T cells with WT or ΔM-N L-selectin. (A) Molt3 T cells were lentivirally transduced with pLentivirus containing WT L-selectin. Cells were stained with PE conjugated anti-CD62L (L-selectin) antibody (red peak) or mouse IgG1 PE isotype control (grey peak). Transduced cells show sufficient expression of WT L-selectin expression indicating successful lentiviral transduction. (B) Molt3 T cells were lentivirally transduced with pLentivirus containing ΔM-N L-selectin. A subpopulation of Molt3 T cells did not show expression of ΔM-N L-selectin after transduction due to an overlap with the isotype control. (C) Molt3 T cells were subjected to MACS separation and the isolated high ΔM-N L-selectin expressing Molt3 T cells were grown for 1 week and later analysed for L-selectin expression. After MACS separation, the isolated subset of Molt3 T cells showed enrichment of high ΔM-N L-selectin expressing Molt3 T cells.

3.3 Monitoring metalloproteinase dependent proteolysis of L-selectin after TCR activation

Initially, I wanted to show that the C terminal V5 His tag of L-selectin did not attenuate metalloproteinase dependent proteolysis after TCR-activation. Molt3 T cells were pre-treated with the wide spectrum metalloproteinase inhibitor (Ro 31-9790) or DMSO solvent control and then incubated for 1 h with C1R cells previously pulsed with increasing concentrations (10^{-8} to 10^{-4} M) of SLY peptide. To show that the C terminal V5 His tag of L-selectin did not interfere with proteolysis, previous data performed on non-tagged L-selectin from fellow PhD student Sophie Wehenkel was compared (Fig 3.7 A, B and C). Molt3 T cells were also stimulated with increasing volumes of R2 medium containing suspended anti-human CD3/CD28 coated dynabeads while L-selectin expression was analysed using flow cytometry (Fig 3.8 A, B and C).

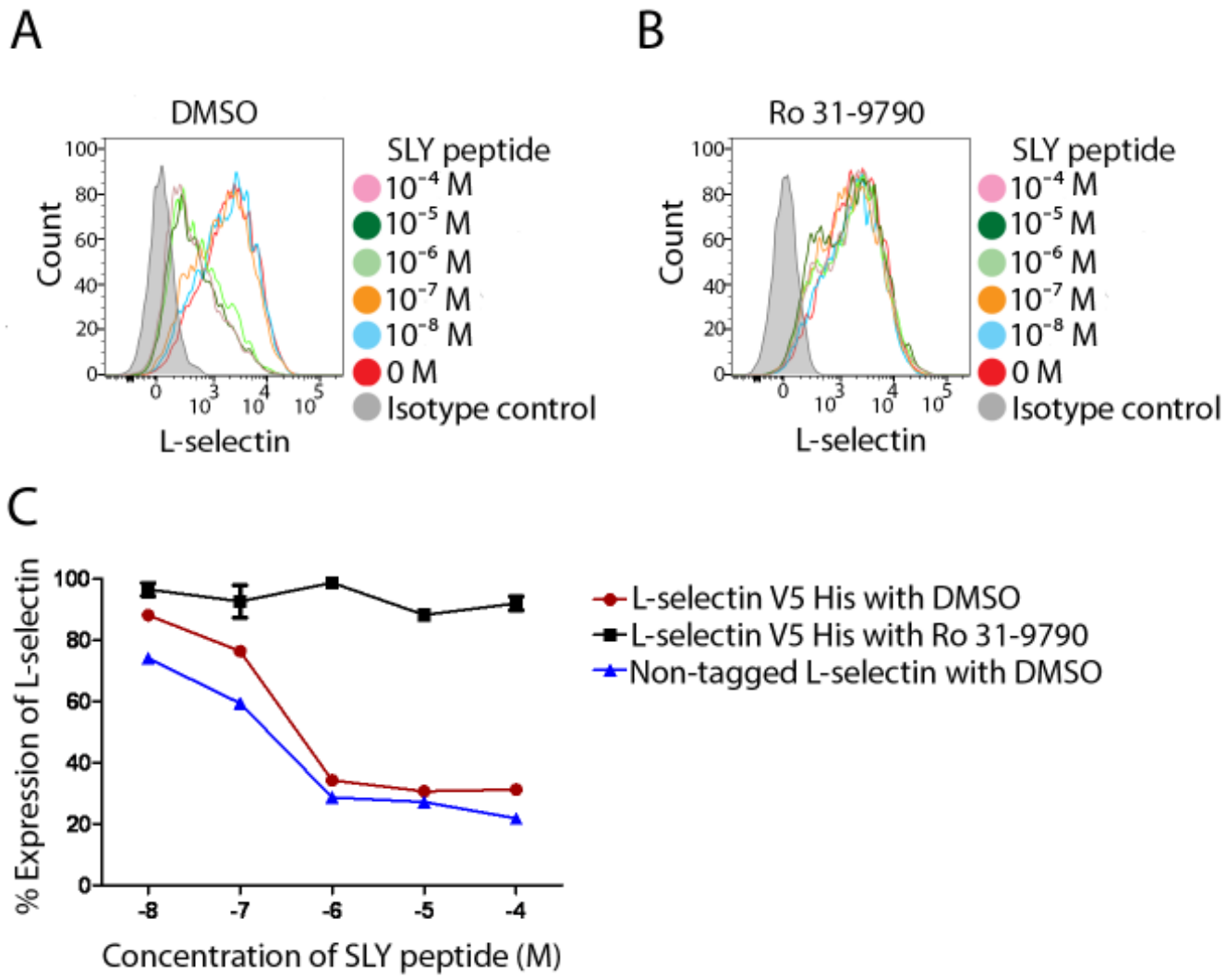

Figure 3.7: Stimulation of the TCR using cognate SLY peptide causes proteolysis of L-selectin. WT L-selectin Molt3 T cells were pre-treated with (A) DMSO or (B) Ro 31-9790 and later incubated with C1R cells pulsed with SLY peptide concentrations of 10^{-8} M to 10^{-4} M. As a negative control, Molt3 T cells were incubated with C1R cell that were not pulsed with SLY peptide. (C) The percentage expression of cell surface L-selectin was calculated from three independent experiments (n=3).

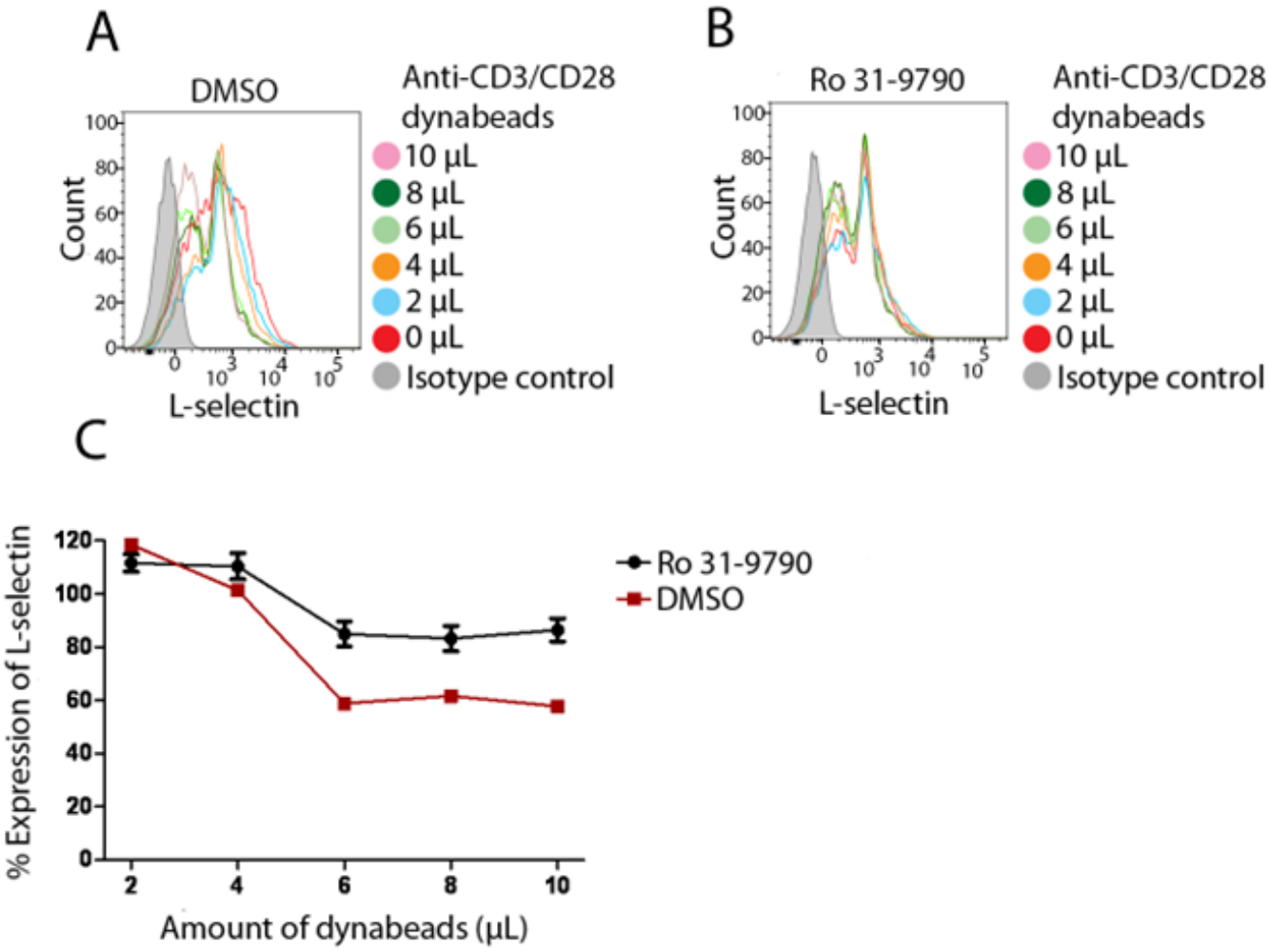

Figure 3.8: Stimulation of TCR by anti-CD3/CD28 coated dynabeads induces proteolysis of L-selectin. WT L-selectin Molt3 T cells were pre-treated with (A) DMSO or (B) Ro 31-9790 and later incubated with increasing volumes of anti-CD3/CD28 dynabeads resuspended in R2 medium. (C) The percentage expression of cell surface L-selectin was calculated from three independent experiments (n=3).

Cell surface expression of both V5 His and non-tagged L-selectin decreased significantly after Molt3 T cells were incubated with C1R cells pulsed with 10^{-6} M SLY peptide. L-selectin expression stabilized at lower levels at higher peptide concentrations of 10^{-5} M and 10^{-4} M. Ro 31-9790 maintained L-selectin expression levels regardless of SLY peptide concentration. (Fig 3.7 A, B and C). Cell surface L-selectin expression was also reduced to 41 % after DMSO control Molt3 T cells were incubated with 6 µL anti-CD3/CD28 dynabeads. Lower L-selectin expression levels trailed after Molt3 T cells were incubated with higher volumes of anti-CD3/CD28 dynabeads. Molt3 T cells pre-incubated with Ro 31-9790 maintained L-selectin levels at 85 % after incubation with 6 µL anti-CD3/CD28 dynabeads (Fig 3.8 A, B and C). These results show that TCR-activation by cognate SLY peptide or anti-CD3/CD28 dynabeads induces metalloproteinase dependent proteolysis of L-selectin which is not attenuated by the C terminal V5 His tag.

3.4 Analysing ADAM 17 mediated ectodomain proteolysis of L-selectin induced after TCR stimulation using western blot analysis

ADAM 17 has already been shown to proteolyze L-selectin (Preschon*, et al.* 1998). To confirm that ADAM 17 proteolyzes L-selectin after TCR stimulation, Molt3 T cells stably transduced with WT or ΔM-N L-selectin were pre-incubated with a known specific inhibitor of human ADAM 17 called D1(A12) (Richards*, et al.* 2012) (referred as Anti-ADAM 17 in this thesis). As a negative control, cells were also incubated with the isotype control IgG D1(A12) which does not inhibit ADAM 17. After pre-treatment, Molt3 T cells were further incubated with anti-CD3/CD28 coated dynabeads and as a negative control, Molt3 T cells were treated with mouse anti-sheep IgG dynabeads (referred to as IgG control dynabeads in this thesis) which would not stimulate the TCR (Fig 3.9).

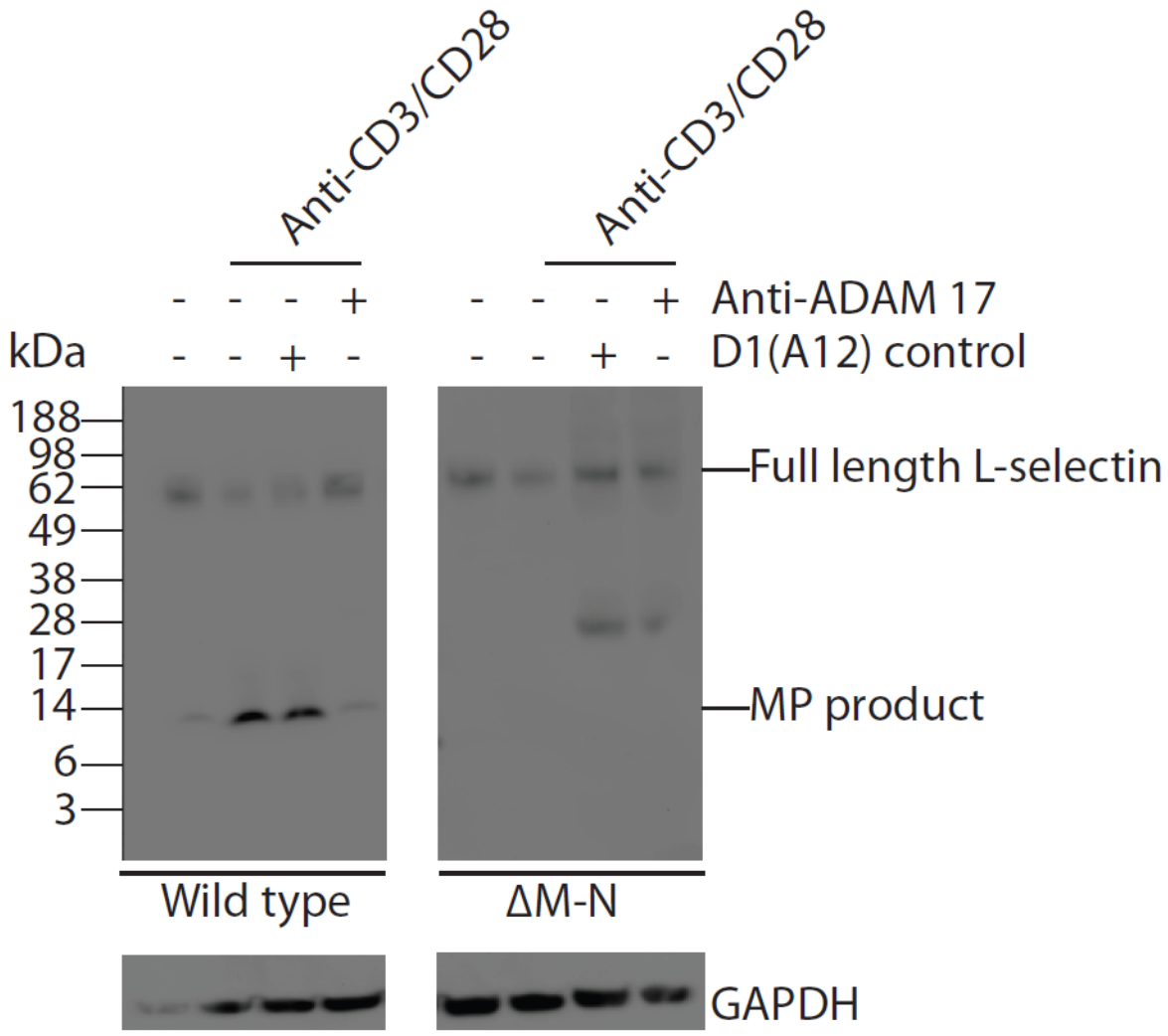

Figure 3.9: Western blot analysis confirming ADAM 17 proteolysis of L-selectin induced after TCR-activation. Molt3 T cells stably expressing WT (A) or ΔM-N (B) L-selectin were incubated with D1(A12) (Anti-ADAM 17 antibody) or the isotype control (D1(A12) control) and later treated with anti-CD3/CD28 dynabeads to stimulate the TCR or incubated in resting conditions with IgG control dynabeads. Blots were stained with anti-V5 antibody to detect L-selectin and GAPDH as a loading control. This result was from a single observation (n=1).

Only WT L-selectin could be visualized after short exposure of 30 sec. After longer exposure of 5 min, detection of the ΔM-N L-selectin was shown. Variance in detection between WT and ΔM-N L-selectin likely reveals differences in transduction efficiency between the two constructs as already shown by flow cytometry (Fig 3.6). Bands at around 56 kDa and 8 kDa

were detected which represent full length and the MP product respectively. TCR stimulation using anti-CD3/CD28 dynabeads caused loss of full length WT L-selectin and accumulation of the MP product. However, pre-treatment with anti-ADAM 17 antibody prevented downregulation of full length L-selectin. These findings were not shown after incubation with the isotype control for anti-ADAM 17 (IgG D1 (A12)). These results agree with data generated from Richards *et al* showing that the anti-ADAM 17 (D1(A12)) antibody is specific to ADAM 17 (Richards*, et al.* 2012). These results display that TCR stimulation mediates ADAM 17 proteolysis of L-selectin generating an MP product.

Only full length ΔM-N L-selectin was detected after TCR stimulation. There was no detection of an MP product confirming that this mutant is resistant to ADAM 17-proteolysis. A band at 28 kDa was detected for ΔM-N L-selectin after Molt3 T cells were incubated with antibodies anti-ADAM 17 and isotype control IgG D1(A12). This band could represent dissociation of the light and heavy chains of these antibodies after lysates have been incubated in 4 X SDS sample reducing buffer. However, the 28 kDa band could be specific to ΔM-N L-selectin as it was not detected from lysed Molt3 T cells expressing WT L-selectin. This blot would need to be repeated to determine whether the 28 kDa band was reproducible for ΔM-N L-selectin only. Subsequently, the detected band would be excised and sequenced by mass spectroscopy for characterization.

3.5 Studying the interactions between L-selectin and ADAM 17 in resting and TCR-activated Molt3 T cells

3.5.1 ADAM 17 interacts with L-selectin in resting T cells, but dissociates after TCR-activation

To determine whether ADAM 17 and L-selectin interaction requires prior TCR activation, experiments were performed in the presence of metalloproteinase inhibitors to capture enzyme substrate complexes as previously shown for CD44 (Hartmann*, et al.* 2015). Molt3 T cells were incubated overnight with Ro 31-9790 and cells were then either incubated with C1R cells pulsed with 10^{-4} M or no SLY peptide and incubated with cobalt coated dynabeads which bound to the His tag of L-selectin (Fig 3.3). As a negative control, control Molt3 T cells were also used to prove that eluted proteins were specific to L-selectin and ADAM 17 (Fig 3.10).

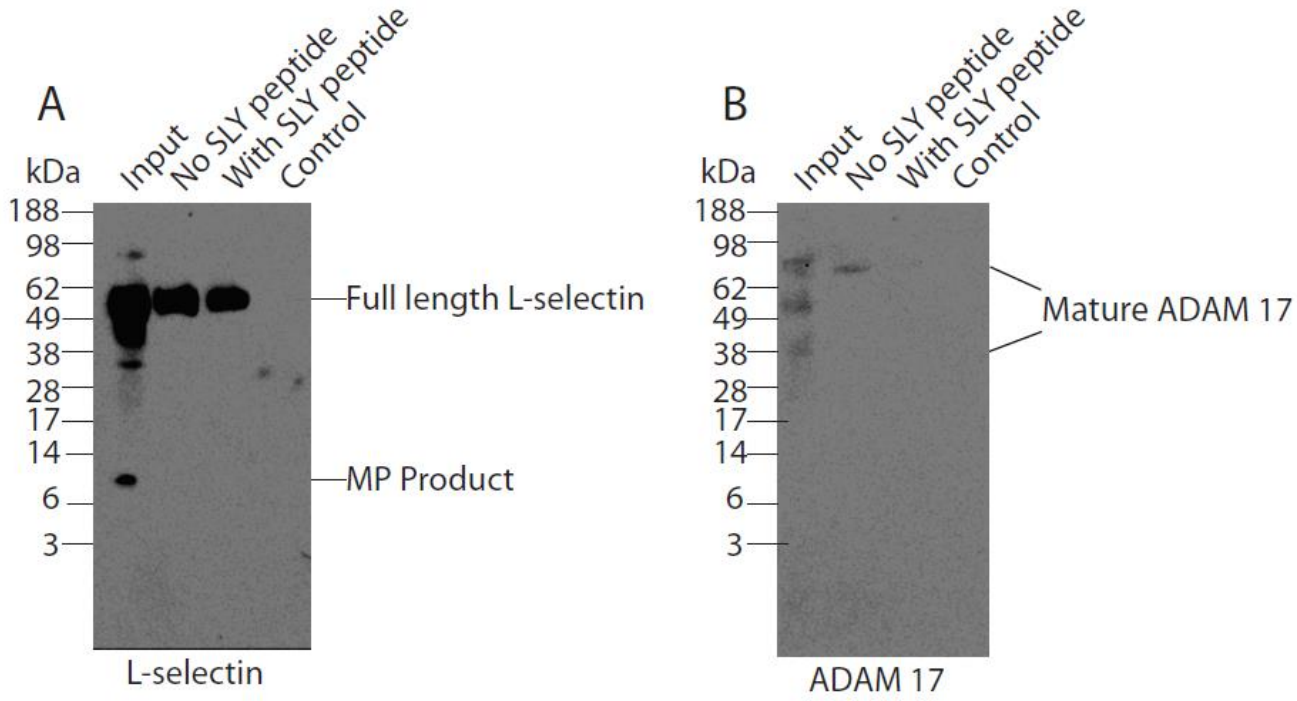

Figure 3.10: L-selectin interacts with ADAM 17 only in resting T cells. Lysates from cell lysis buffer lysed L-selectin+ Molt3 T cells or control Molt3 T cells were incubated with cobalt covered dynabeads. Lysates were used for western blot analysis and stained for L-selectin (A) or ADAM 17 (B). Anti-V5 antibody was used to detect L-selectin and a C terminal antibody for ADAM 17. This pull down is one representation of three repeats (n=3) which have shown reproducible results.

Pulldowns from L-selectin+ Molt3 T cells incubated with C1R cells either pulsed with or without 10^{-4}M SLY peptide only showed full length L-selectin. This indicates that Ro 31-9790 allowed efficient accumulation of full length L-selectin causing more to bind cobalt ions presented on the surface of dynabeads in comparison to the MP product. Lysates from control Molt3 T cells did not show any bands indicating that detection obtained from the pulldown was specific to L-selectin. For ADAM 17, a band of 80 kDa was detected from resting T cells, but was lost after TCR-activation. Together, these results indicate that L-selectin and ADAM 17 form complexes in resting T cells which is disrupted by unknown biochemical pathways after TCR-activation.

3.5.2 ΔM-N L-selectin binds to ADAM 17 under both resting and TCR-activated T cells

ADAM 17 contains a small stalk region between the MP domain and transmembrane region. This stalk region contains a short α-helical juxtamembrane region containing 14 amino acids termed CANDIS. The CANDIS region of ADAM 17 acts as a substrate binding domain and has been reported to interact with IL-6 (Düsterhoft*, et al.* 2014). It was hypothesised that amino acids (MIKEGDYN) at the MPR of L-selectin bind to the CANDIS region of ADAM 17. The MIKEGDYN sequence has been truncated from ΔM-N L-selectin (Chen*, et al.* 1995) which potentially removes the CANDIS binding region. Consequently, ΔM-N may not interact with ADAM 17 explaining why this mutant resists ectodomain proteolysis.

This hypothesis was tested to determine if loss of ADAM 17 interaction to ΔM-N L-selectin defines its resistance to ectodomain proteolysis. L-selectin+ Molt3 T cells or control Molt3 T cells were pre-incubated with Ro 31-9790 overnight. These cells were then further

incubated with C1R cells pulsed with 10^{-4} M or no SLY peptide. Resulting lysates were incubated with cobalt ion covered dynabeads (Fig 3.11).

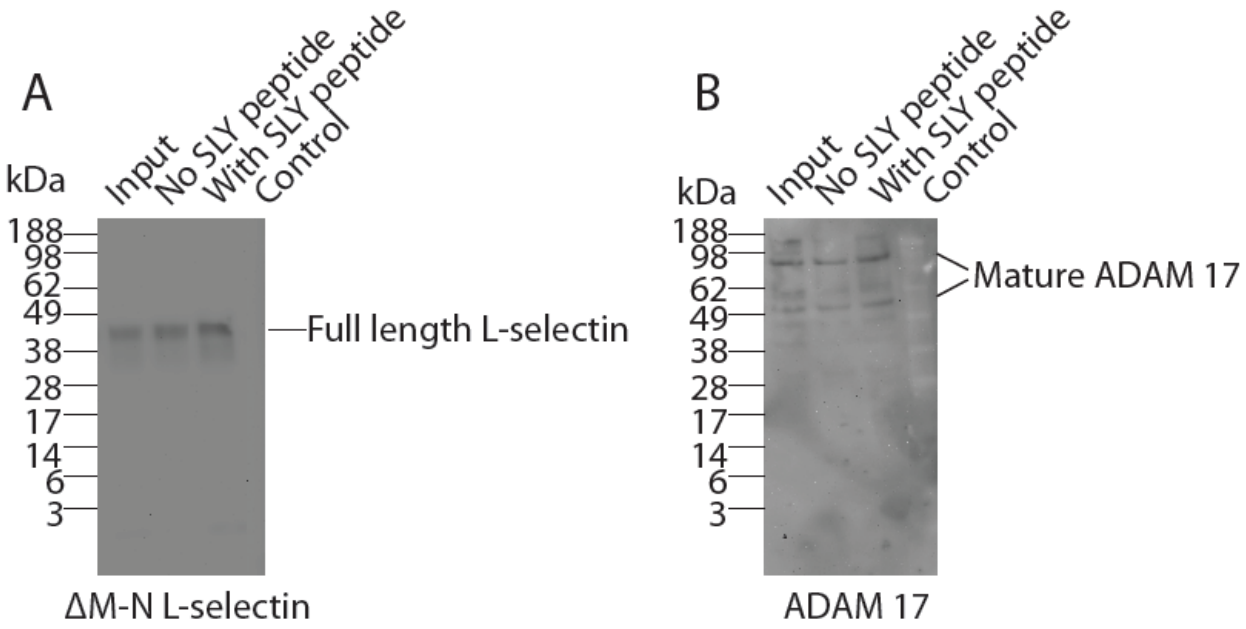

Figure 3.11: ΔM-N L-selectin binds to ADAM 17 in both resting and TCR-activated T cells. Lysates from cell lysis buffer lysed L-selectin+ Molt3 T cells or control Molt3 T cells were incubated with cobalt covered dynabeads. Lysates were used for western blot analysis and stained for L-selectin (A) or ADAM 17 (B). Anti-V5 antibody was used to detect L-selectin and a C terminal antibody for ADAM 17. This result is from a single observation (n=1).

After pull-down assay, bands were obtained from 40 kDa to around 80 kDa representing the active form of ADAM 17 in both resting and TCR-activated L-selectin+ Molt3 T cells, which were not present in control Molt3 T cells. These results therefore conclude that the MIKEGDYN truncation from the MPR of L-selectin does not prevent interaction with ADAM 17. Additionally, unlike WT L-selectin, the ΔM-N mutant does not dissociate from ADAM 17 after TCR stimulation.

3.6 Discussion

In this chapter, I generated Molt3 T cells which stably expressed WT or ΔM-N L-selectin V5 His using lentiviral transduction. After stimulating the TCR using cognate SLY peptide (Fig 3.7 A-C) or anti-CD3/CD28 dynabeads (Fig 3.8 A-C) I showed metalloproteinase dependent proteolysis of both non-tagged and V5/His tagged L-selectin. These results confirmed that the C terminal V5 His tag of L-selectin did not interfere with proteolysis after TCR-activation. Western blot analysis then showed that ADAM 17 was the metalloproteinase responsible for ectodomain proteolysis of L-selectin which generated an 8 kDa MP product (Fig 3.9). In later studies, pull down assays showed for the first time that L-selectin forms complexes with ADAM 17 in resting T cells, but dissociates after TCR-activation (Fig 3.10). Unexpectedly, although ΔM-N L-selectin showed resistance to ADAM 17 proteolysis (Fig 3.9, B), an interaction was observed in both resting and TCR-activated T cells (Fig 3.11). These results conclude that the 8-amino acid truncation in the MPR of ΔM-N does not disrupt interactions with ADAM 17 as previously suggested by Chen *et al* (Chen, *et al*. 1995).

In this study, the extreme C terminus at the L-selectin ICD was fused to a V5 His tag. This V5 His tag could potentially hinder interaction with protein binding partners that regulate metalloproteinase dependent ectodomain proteolysis. For instance, Arg^{357} and Lys^{362} in the L-selectin ICD binds ezrin and moesin allowing L-selectin to be positioned in the microvilli. Disruption of this interaction causes L-selectin to be resistant to PMA induced shedding (Ivetic*, et al.* 2002; Ivetic*, et al.* 2004). Also, calmodulin binds to hydrophobic residues Ile^{352} and Ile^{354} in the transmembrane region and Leu^{358} in the L-selectin ICD (Gifford*, et al.* 2012; Chakravarthy*, et al.* 1999). Calmodulin inhibitors such as trifluroperazine induce metalloproteinase dependent shedding of L-selectin (Kahn*, et al.* 1998). Flow cytometry

analysis was done to compare proteolysis of V5 His tagged and non-tagged L-selectin after Molt3 T cells were incubated with SLY peptide pulsed C1R antigen presenting cells. Data from section 3.3 showed that both V5 His tagged and non-tagged L-selectin decreased membrane expression after incubation with C1R antigen presenting cells pulsed with 10^{-6} M SLY peptide. Pre-incubation of Molt3 T cells with the wide metalloproteinase inhibitor Ro 31-9790 prevented loss of L-selectin expression at the membrane. Furthermore, western blot analysis from section 3.4 showed loss of detection for full length WT L-selectin V5 His and an accumulation of a MP product after Molt3 T cells were incubated with anti-CD3/CD28 coated dynabeads. Additionally, pre-incubation of cells with the anti-ADAM 17 antibody (D1(A12)) caused loss of detection for the MP product. Together, these results confirmed that insertion of the V5 His tag to the C terminus of L-selectin did not interfere with ADAM 17-dependent ectodomain proteolysis after TCR-stimulation.

Western blot analysis (Fig 3.9) and pull-down assays (Figs 3.10 and 3.11) showed detection of full length L-selectin at around 56 kDa which was initially suggested as the membrane bound form. However, studies performed by Rzeniewicz showed two bands for full length L-selectin at 80 kDa and 110 kDa. They suggested that the higher molecular weight band was a glycosylated, membrane bound form of L-selectin and the lower molecular weight band as a non-glycosylated intracellular form (Rzeniewicz, *et al*. 2015). It is therefore possible that full length L-selectin at 56 kDa shown in these studies represents an intracellular form and future experiments will need to be completed to determine whether ADAM 17 interaction with L-selectin (Fig 3.10) and subsequent proteolysis (Fig 3.9) shown in this study occurs at the membrane or intracellular region. Surface biotinylation experiments could be performed to determine whether full length L-selectin at 56 kDa is at the membrane or intracellular compartment. After biotinylation of Molt3 T cells, labelled cell surface L-selectin would be

harvested using streptavidin and later detected using western blot analysis with anti-V5 antibody. Additionally, a subcellular fractionation could be performed after TCR-stimulation to isolate the membrane fraction containing glycosylated full-length L-selectin V5 His. Membrane fractions could either be directly blotted using anti-V5 to monitor ADAM 17-proteolysis after TCR activation, or pulled down using cobalt coated dynabeads to visualize interactions with ADAM 17.

Flow cytometry analysis showed that cell surface expression of ΔM-N L-selectin was lower than WT (Fig 3.6). Additionally, western blot analysis showed that WT L-selectin was detected after 30 sec exposure to chemiluminescence substrate, whereas ΔM-N L-selectin took longer at 5 min (Fig 3.9). Unequal expression of WT and ΔM-N L-selectin in transduced Molt3 T cells is likely caused by a variance in the multiplicity of infection (MOI). The MOI is defined at the number of lentiviral particles used to infect each cell. For my study, the concentration of pLentivirus was not quantified and therefore induced variance for the MOI of each cell line causing a difference in the efficiency of lentiviral transduction and cell surface expression of WT and ΔM-N L-selectin. In future work, equal amounts of quantified pLentivirus will need to be used when generating stably transduced Molt3 T cells to ensure equal expression of WT and ΔM-N. Equal expression of WT and ΔM-N L-selectin would allow the same exposure time after addition of chemiluminescence substrate for similar detection levels in resting T-cells and more accurate analysis for the levels of proteolysis after TCR-activation.

Pull down assays from section 3.5 showed that WT L-selectin binds to ADAM 17 in a resting T cell and dissociated after TCR-activation. It is not currently known whether ADAM 17 interacts with the ECD or ICD of L-selectin. Understanding this would provide an insight

behind the biochemical mechanisms that occur causing ADAM 17 to dissociate from L-selectin after TCR stimulation. Like ADAM 17, CaM dissociates from L-selectin after T cell activation (Kahn*, et al.* 1998). Proteins such as adducin, Igloo protein and neurogranin have overlapping CaM and PKC binding regions (Matsuoka*, et al.* 1996; Neel and Young, 1994; Gerendasy and Sutcliffe, 1997). Protein kinases phosphorylate binding sites for CaM causing dissociation (Chakravarthy*, et al.* 1999). Specifically, phosphorylation of Ser^{364} at the L-selectin ICD causes dissociation of calmodulin (Rzeniewicz*, et al.* 2015). If ADAM 17 does bind to the L-selectin ICD, it is likely that protein kinases modulate this interaction. For instance, Kilian *et al* have shown that TCR stimulation causes PKC θ and PKC α to bind and phosphorylate serine residues in the L-selectin ICD (Kilian*, et al.* 2004). Based on the findings from section 3.5.1 it is tempting to speculate that after TCR stimulation, intramolecular interactions at the L-selectin ICD are modulated due to the introduction of two negative charges of bound PKC α and PKC θ causing dissociation of ADAM 17.

The L-selectin ICD may also act as an anchoring protein for PKC isozymes allowing them to be at close-proximity to phosphorylate substrates. For instance, PKC θ phosphorylates the actin binding domain at the C terminus of moesin disrupting the intramolecular interactions between both N and C termini (Pietromonaco*, et al.* 1998). Moesin interacts with the L-selectin ICD after treatment with the PKC upregulator PMA (Ivetic*, et al.* 2002). Hypothetically, after TCR stimulation, PKC θ bound to the L-selectin ICD may phosphorylate moesin. Moesin would then be in an open conformation allowing interaction with the L-selectin ICD competing with ADAM 17 for binding sites. It is likely that moesin causes dissociation of ADAM 17 after cell activation.

However, TCR stimulation also causes recruitment of tyrosine kinases such as Lck to the intracellular CD3 chains of the TCR complex. Lck then phosphorylates tyrosine residues at the immunoreceptor tyrosine based activation motifs (ITAMs) in the CD3 chains of the TCR (Weiss, 1993). Lck has also been shown to interact directly and phosphorylate the L-selectin ICD (Xu*, et al.* 2008). It therefore cannot be ruled out that phosphorylation of tyrosine as well as serine residues at the L-selectin ICD regulate interaction with ADAM 17.

Studies done by Chen *et al* showed that ΔM-N L-selectin, bearing an 8-amino acid deletion (MIKEGDYN) at the MPR can no longer be shed by ADAM 17. Chen *et al* hypothesised that ΔM-N L-selectin may prevent metalloproteinase mediated ectodomain proteolysis because this mutant is shorter than its precursor. Consequently, the metalloproteinase cleavage site of L-selectin would be closer to the membrane and would not be able to reach the catalytic site of ADAM 17 (Chen*, et al.* 1995). It was initially hypothesised that the MIKEGDYN region at the MPR of L-selectin either acts to bind the CANDIS domain of ADAM 17. Or, the MIKEGDYN region optimizes the length of the MPR of L-selectin allowing the metalloproteinase cleavage site (Lys^{321} and Ser^{322}) to reach the catalytic site of ADAM 17. It was therefore initially anticipated that truncation of MIKEGDYN would abolish interactions between L-selectin and ADAM 17. However, pull down assays from section 3.5.2 did not support our initial hypothesis as ΔM-N L-selectin was shown to interact with ADAM 17 despite being resistant to ectodomain proteolysis (shown in section 3.4). Interestingly, unlike the WT precursor, ΔM-N L-selectin still interacted with ADAM 17 after TCR stimulation. Possibly, the MIKEGDYN region at the MPR of L-selectin is regulating dissociation from ADAM 17 after TCR stimulation. However, this experiment would need to be repeated using a positive control for TCR stimulation to solidify this suggestion.

Hypothetically, the slightly shorter ectodomain of ΔM-N L-selectin may position residues to interact with regions at the MP domain of ADAM 17 that would not occur with bound WT L-selectin. These compromised interactions between ΔM-N L-selectin and ADAM 17 could potentially be more stable after TCR activation. It is also conceivable that the MIKEGDYN region induces structural conformational changes at the ECD of L-selectin allowing this protein to shift from an ADAM 17 interacting to non-interacting state. It has already been suggested that CaM binds to the L-selectin ICD and consequently, "pulls" the ectodomain close to the outer membrane concealing the metalloproteinase cleavage site from ADAM 17 (Gifford*, et al.* 2012). After cell activation, release of CaM may cause the ectodomain of L-selectin to slightly shift away from the outer membrane which could disrupt interactions with bound ADAM 17. Theoretically, this outward shift may be dependent on the hydrophobic rich MIKEGDYN region at the MPR of L-selectin. Theoretically, release of CaM would allow the hydrophobic MIKEGDYN to migrate away from polar phospholipids such as Ptd-L-Ser at the outer membrane potentially disrupting the interaction between L-selectin and ADAM 17. Truncation of MIKEGDYN in ΔM-N L-selectin allows the upstream polar residues QKLDKS to be close to the outer membrane after CaM interacts with the ICD of L-selectin. These polar residues could interact with phospholipids at the outer membrane which potentially would not be disrupted after CaM dissociates from the cytoplasmic tail of L-selectin. Consequently, the ectodomain may not shift upwards after CaM release preventing L-selectin and ADAM 17 from dissociating after cell activation. If correct, CaM release would also not allow the metalloproteinase cleavage site of L-selectin (Lys^{321} and Ser^{322}) to reach the active site of ADAM 17. This hypothesis would explain how ΔM-N L-selectin can interact with ADAM 17 yet resists proteolysis.

Understanding that L-selectin and ADAM 17 interact in a resting leucocyte may shed some insight on how ectodomain proteolysis is governed after TCR stimulation. PDI modulates disulphide bridges at the MP domain of ADAM 17 changing its conformation from an elongated, flexible and open structure to a compact, rigid and closed one. Thus, PDI converts ADAM 17 from an active to inactive enzyme. (Dusterhoft*, et al.* 2013). Furthermore, these conformational structure changes induced by PDI prevented the CANDIS region of ADAM 17 binding its substrate IL-6 abolishing ectodomain proteolysis (Dusterhoft*, et al.* 2014). PMA stimulation has been shown to generate ROS that inactivates PDI causing ADAM 17 to maintain its open conformation (Bass and Edwards, 2010). Currently, it is not known if TCR stimulation also inactivates PDI. Nonetheless, based on the findings from section 3.5.2, it would be enticing to suggest that in a resting leucocyte, the MP domain region of ADAM 17 is at a closed conformation whilst bound to L-selectin. TCR stimulation may then inactive PDI causing the MP domain of ADAM 17 to adopt an open conformation exposing the metalloproteinase catalytic site to Lys^{321} and Ser^{322} in the MPR of bound L-selectin inducing ectodomain proteolysis. If correct, then L-selectin may not bind to the CANDIS region at the ectodomain of ADAM 17. Otherwise, these two proteins would not be able to interact in the resting leucocyte where hypothetically, the MP domain of ADAM 17 would be at a closed conformation concealing the CANDIS region from L-selectin. TNF-α, does not depend on the CANDIS region of ADAM 17 for interaction (Dusterhoft*, et al.* 2014). Unlike IL-6, TNF-α and L-selectin may interact to ADAM 17 independently of the CANDIS region.

4. Intramembrane proteolysis of L-selectin by presenilin

4.1 Introduction

After ectodomain proteolysis, PS, the catalytic component of the γ-secretase complex is responsible for intramembrane proteolysis of type I transmembrane proteins such as APP, notch and ErbB4 causing release of the ICD (De Strooper*, et al.* 1998; De Strooper*, et al.* 1999; Hoeing*, et al.* 2011). In this chapter, I hypothesised that after ADAM 17-mediated ectodomain proteolysis, the generated MP product of L-selectin is cleaved in the intramembrane region by PS (Fig 4.1).

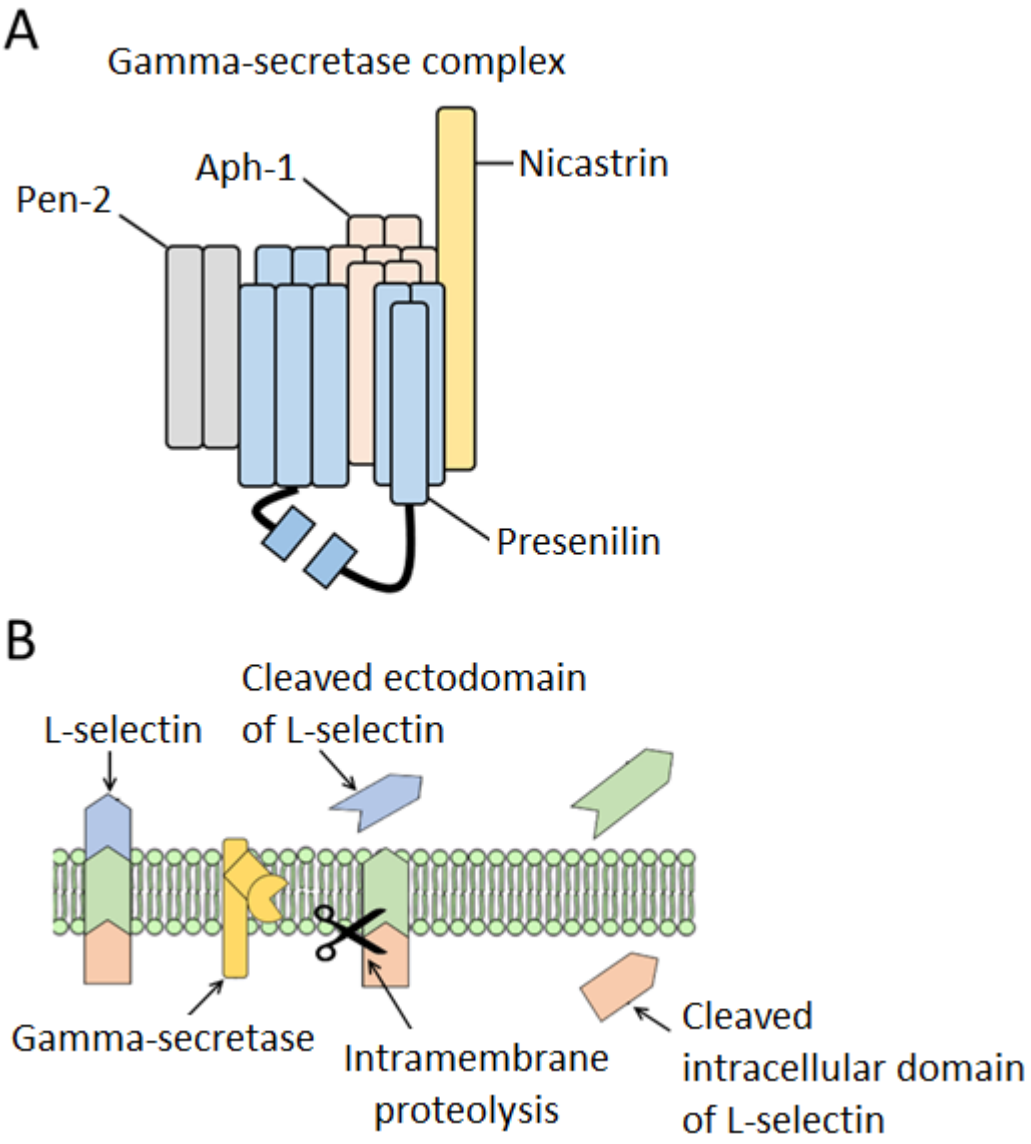

Figure 4.1: Model of intramembrane proteolysis of L-selectin by PS. (A) ϒ-secretase is a multi-subunit protease comprising of nicastrin, anterior pharynx-1 (Aph-1), presenilin enhancer-2 (Pen-2) and presenilin (PS). PS is the catalytic subunit of γ-secretase. (B) After ADAM 17 mediated ectodomain proteolysis of full length L-selectin, γ-secretase uses its subunit PS to cleave the MP product in the intramembrane region releasing the ICD.

Two PS isoforms have been discovered named PS1 and PS2 (Sherrington*, et al.* 1995; Levy-Lahad*, et al.* 1995; Rogaev*, et al.* 1995). Studies were performed to determine whether the MP product of L-selectin was a substrate for PS1 and/or PS2. To achieve this, L-selectin V5 His was transiently transfected in MEF cells that were deficient in PS1 and/or PS2.

Other type I transmembrane proteins such as Notch and APP are proteolyzed by both ADAM 10 and ADAM 17 (Bozkulak*, et al.* 2009; Qian*, et al.* 2016; Tousseyn*, et al.* 2009). In this chapter, I was also interested to learn whether L-selectin was proteolyzed by another metalloproteinase(s) other than ADAM 17.

4.1.1 Aims of the chapter

- Determine if the MP product of L-selectin is proteolyzed by PS1 and/or PS2, the catalytic component of γ-secretase
- To learn whether L-selectin is proteolyzed by metalloproteinase(s) other than ADAM 17

4.2 Validation of γ-secretase inhibitors L-685 and DAPT

To show whether the MP product of L-selectin is cleaved in the intramembrane region by PS, WT MEF cells were transiently transfected with L-selectin V5 His and incubated with the γ-secretase inhibitors L-685 (Barthet*, et al.* 2011; Gasparini*, et al.* 2004) and DAPT (Micchelli*, et al.* 2003; Dovey*, et al.* 2001). After 1 h incubation, cells were further treated with PMA to stimulate proteolysis for 45 min (Fig 4.2).

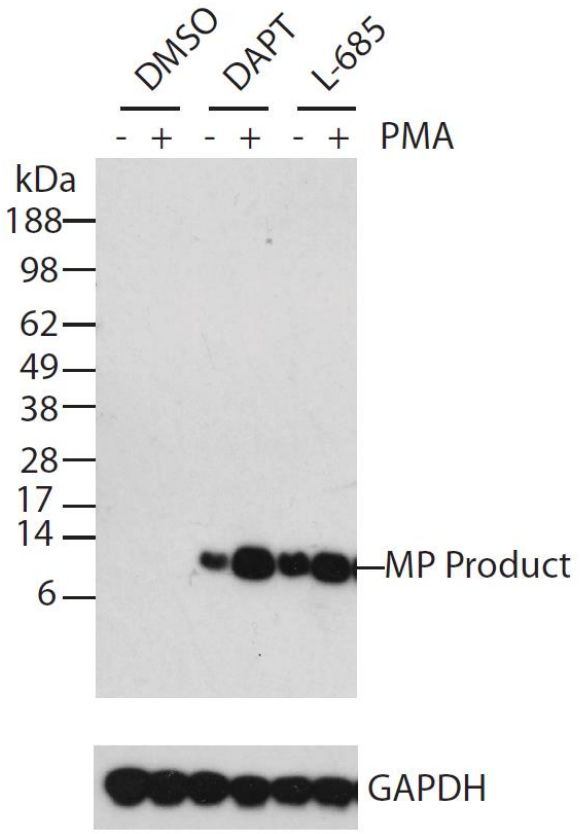

Figure 4.2: L-685 and DAPT both cause accumulation of the 8 kDa L-selectin MP product. WT MEF cells were transiently transfected with L-selectin V5 His and incubated in the presence or absence of γ-secretase inhibitors L-685 and DAPT. Cells were further treated with PMA to induce proteolysis. DMSO was used as a solvent control.

Full length L-selectin was not detected and incubation with L-685 and DAPT enriched a cleaved fragment of L-selectin at 8 kDa which corresponds to the MP cleavage product described in chapter 3. This data indicates that these MEF cells were highly active and proteolyzed L-selectin rapidly. Furthermore, the 8 kDa MP product was shown to be a substrate for PS. Due to the high proteolytic activity of these MEF cells, PMA was not essential to stimulate proteolysis and was thus excluded from future experiments.

4.3 Analysing L-selectin proteolysis in PS deficient MEF cells

Studies were performed to address whether the MP product of L-selectin is cleaved by PS1 and/or PS2. L-selectin V5 His was transiently transfected in MEF cells deficient in PS1 and/or PS2, obtained from Professor Bart de Strooper (Bart de Strooper*, et al.* 1999). To characterize the 8 kDa fragment as an MP product, MEF cells were incubated with Ro 31-9790 alongside transfection and incubated overnight to accumulate full length L-selectin (Fig 4.3).

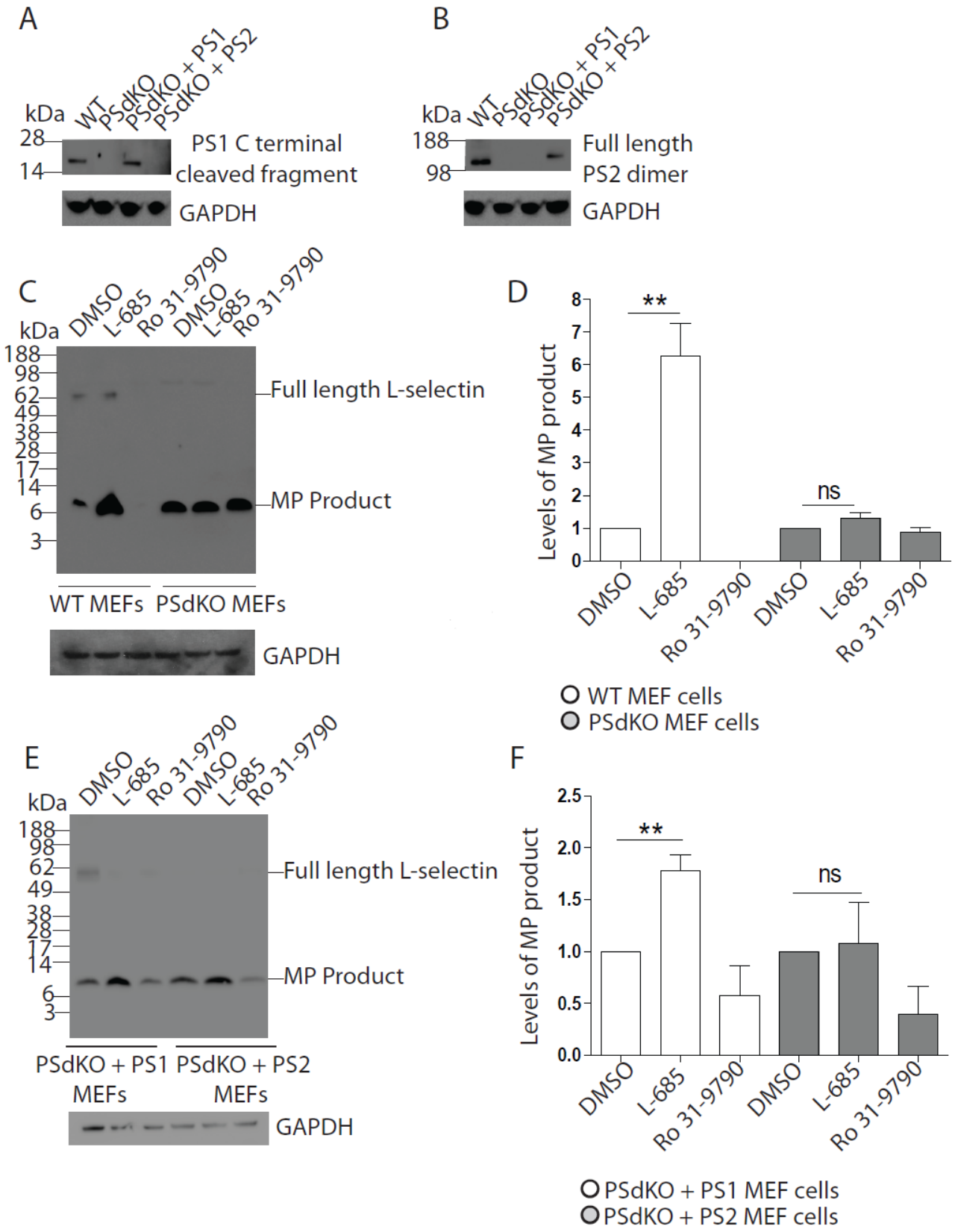
A
kDa
WT
PSdKO
PSdKO + PS1
PSdKO + PS2
28
14
PS1 C terminal
cleaved fragment
GAPDH
B
kDa
188
98
Full length
PS2 dimer
GAPDH
C
kDa
DMSO
L-685
Ro 31-9790
188
98
62
49
38
28
17
14
6
3
Full length L-selectin
MP Product
WT MEFs
PSdKO MEFs
GAPDH
D
Levels of MP product
**
ns
WT MEF cells
PSdKO MEF cells
E
kDa
PSdKO + PS1
MEFs
PSdKO + PS2
MEFs
Full length L-selectin
MP Product
GAPDH
F
Levels of MP product
PSdKO + PS1 MEF cells
PSdKO + PS2 MEF cells

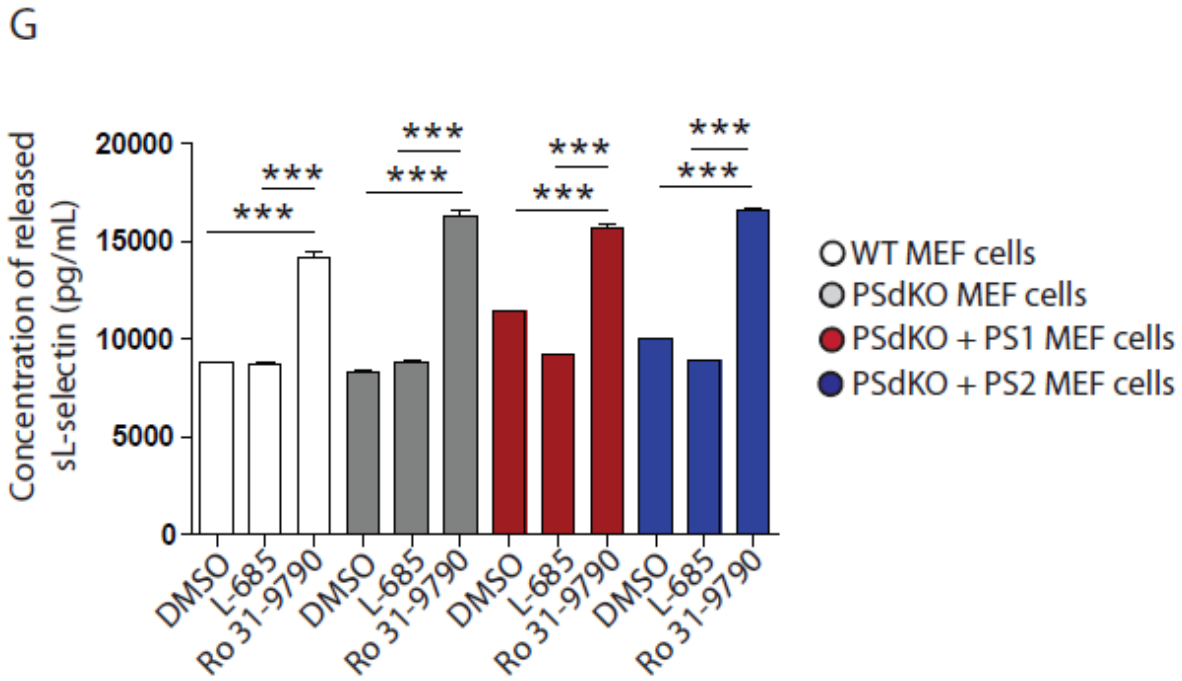

Figure 4.3: PS1 mediates intramembrane proteolysis of the MP product of L-selectin. C terminal antibodies against PS-1 (PS1) (A) and PS-2 (PS2) (B) were used to characterize wild type (WT) and PS deficient MEF cell lines. (C) WT or PS knockout (PSdKO) MEF cells were transiently transfected with L-selectin V5 His and incubated with DMSO, L-685 or Ro 31-9790. (D) Histograms shows levels of MP product in DMSO, L-685 and Ro 31-9790 treated cells based on the mean value of three independent experiments n=3, ± SD, **P<0.05. (E) PSdKO MEF cells complimented with PS1 (PSdKO + PS1) or PS2 (PSdKO + PS2) were transiently transfected with L-selectin V5 His and incubated with DMSO, L-685 or Ro 31-9790. (F) Histograms shows levels of MP product in DMSO, L-685 and Ro 31-9790 treated cells based on the mean value of three independent experiments n =3, ± SD, *P<0.05 (G) Histograms show release of soluble (sL-selectin) based on the mean value of three independent experiments, ± SD ***P<0.05. A one-way ANOVA with post-hoc Tukey test was used for all statistical analysis.

Immunoblotting with C terminal antibodies of PS1 and PS2 confirmed that PS deficient (PSdKO) MEF cells were true knockout cells. Also, that PSdKO MEF cells were singly complemented with PS1 (PSdKO + PS1) and PS2 (PSdKO + PS2). WT MEF cells expressed both PS1 and PS2 (Fig 4.3 A and B). Due to transient transfection efficiency differences between experiments, full length L-selectin was often below the detection limit. However, bands at 62 kDa correspond to full length L-selectin (Fig 4.3 C and E).

In WT MEF cells, L-685 treatment caused a 6-fold increase in the MP product of L-selectin in comparison to DMSO. However, in PSdKO MEF cells there was no statistical difference in detection irrespective of treatment (Fig 4.3 C and D). Furthermore, in PSdKO + PS1 MEF cells, the MP product increased detection 1.7-fold after treatment with L-685 when compared to DMSO. However, in PSdKO + PS2 MEF cells, there was no significant change in MP product levels between DMSO and L-685 treatment (Fig 4.3 E and F). These results illustrate that PS1 is responsible for intramembrane proteolysis of the MP product of L-selectin.

Unexpectedly, Ro 31-9790 did not accumulate full length L-selectin in these MEF cell lines, however MP product levels decreased in WT and PSdKO + PS1/PS2 MEF cells (Fig 4.3 C, D, E and F). Ro 31-9790 treatment also increased release of sL-selectin in WT and PS deficient MEF cells (Fig 4.3 G). This data may indicate that Ro 31-9790 treatment stabilizes a protease in MEF cells that is capable of releasing L-selectin into the medium. An alternative route of release would equate to exosomal release as described for other ADAM 17 substrates such as Tumor-associated calcium signal transducer 2 (Trop-2) (Wagner*, et al.* 2015).

4.4 Monitoring L-selectin proteolysis in ADAM 17 deficient MEF cells

Proteolysis of L-selectin has been reported in ADAM 17 deficient leucocytes and fibroblasts (Evans*, et al.* 2016; Walcheck*, et al.* 2003) and ADAM 8 and ADAM 10 have been testified to proteolyze L-selectin (Gomez-Gaviro*, et al.* 2007; Le Gall*, et al.* 2009). Additionally, my data shows that the wide spectrum metalloproteinase inhibitor Ro 31-9790 does not increase detection for full length L-selectin in cell lysates (Fig 4.3 C and E), but instead elevates levels of released sL-selectin in the medium (Fig 4.3). I argued that L-selectin is proteolyzed by another protease(s) in these MEF cells which is regulated by ADAM 17 activity. In the presence of Ro 31-9790, ADAM 17 is inhibited preventing proteolysis of this unknown protease(s) allowing it to accumulate at the membrane and proteolyze L-selectin (Fig 4.4).

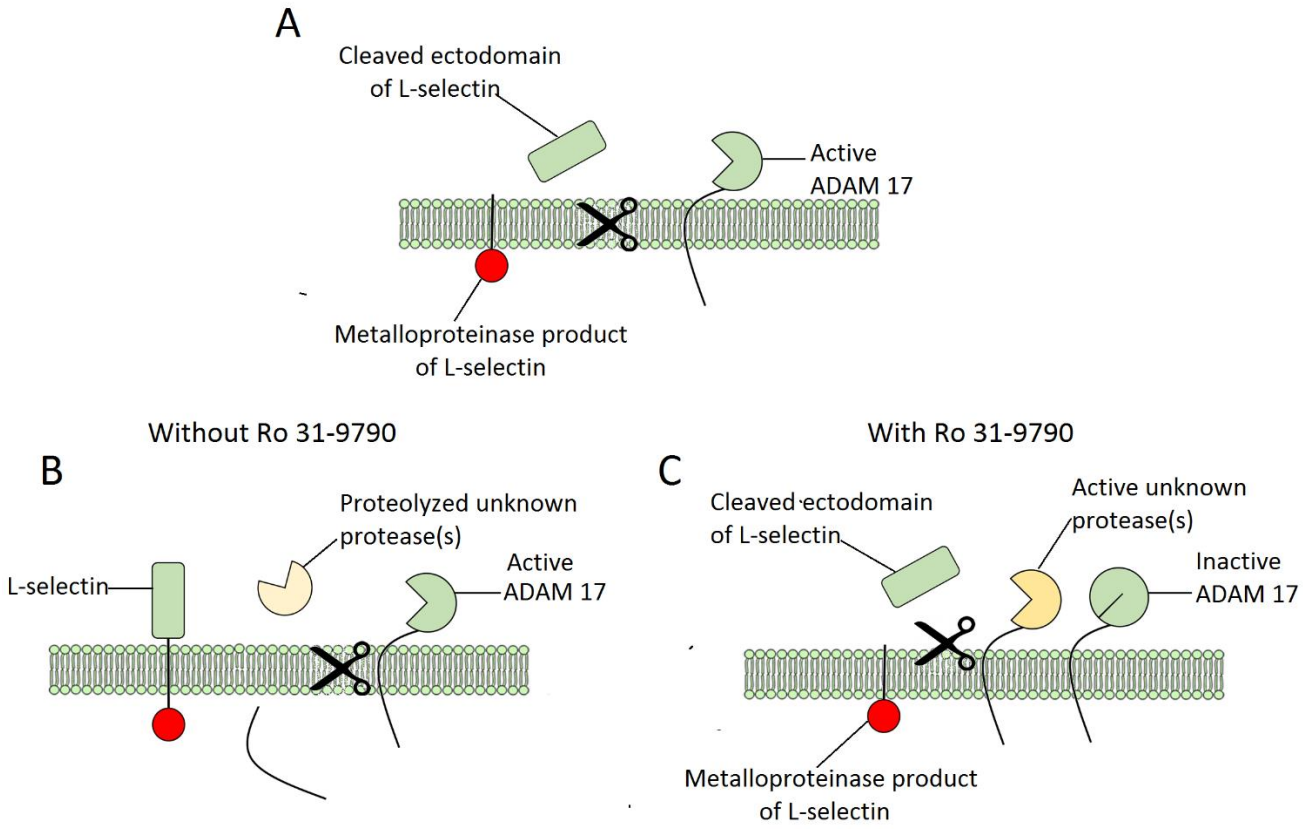

Figure 4.4: An unknown protease proteolyzes L-selectin which is potentially regulated by ADAM 17. (A) ADAM 17 cleaves L-selectin at the ectodomain generating an MP product comprising a transmembrane region and ICD. (B) L-selectin is also proteolyzed by unknown protease(s). ADAM 17 proteolyzes this unknown protease decreasing membrane expression. This prevents this unknown protease cleaving L-selectin. (C) Inhibition of ADAM 17 activity using Ro 31-9790 averts proteolysis of this unknown protease(s). Increased cell surface levels of this unknown protease(s) elevates ectodomain proteolysis of L-selectin.

I wanted to determine whether L-selectin is proteolyzed in ADAM 17 deficient MEF cells, generating an MP product that acts as a substrate for PS1. ADAM 17-/- MEF cells generated by Carl Blobel (Sahin*, et al.* 2004) were transiently transfected with L-selectin V5 His alone, or in combination with FLAG tagged ADAM 17. Cells were incubated with Ro 31-9790 alongside transfection and incubated overnight. Cells were then treated with L-685 for 1 h and then ADAM 17 was activated using the PKC activator PMA (Hahn*, et al.* 2003) to induce proteolysis of L-selectin.

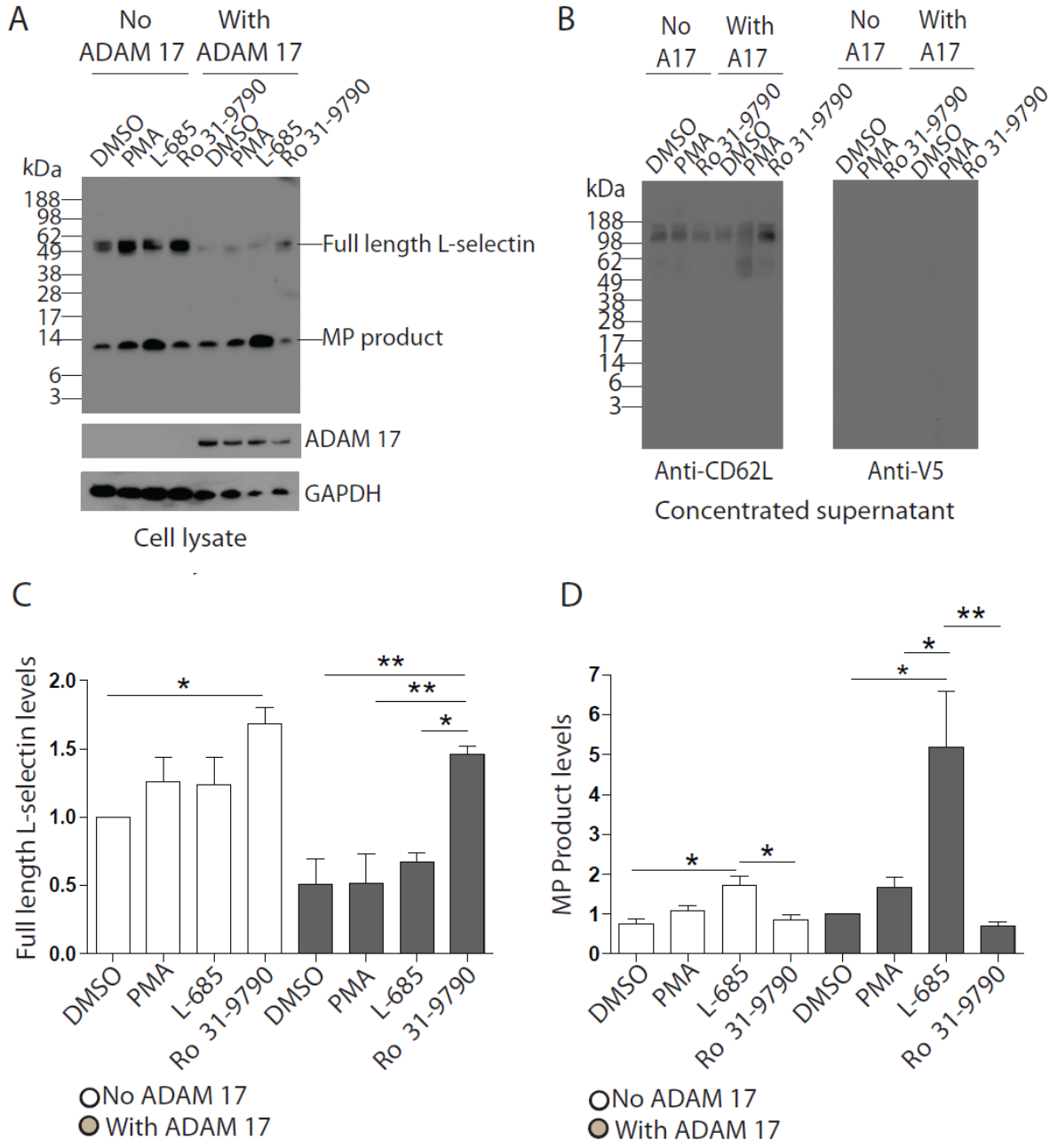

Figure 4.5: Analysis of L-selectin proteolysis in ADAM 17-deficient MEF cells. ADAM17-/- MEF cells were transiently transfected with L-selectin V5 His alone, or in combination with FLAG tagged ADAM 17. Cells were incubated with DMSO, PMA, L-685 and Ro 31-9790. A C terminal antibody of ADAM 17 was used to confirm expression. (B) Supernatants from ADAM 17-/- MEF cells were concentrated and immunoblotted. The cleaved ECD of L-selectin was detected using an N terminal antibody (Anti-CD62L) and the anti-V5 antibody was used to bind the C terminal V5/His tag of both full length or the cleaved fragments of L-selectin. Histograms shows levels of full length L-selectin (C) or metalloproteinase (MP) product (D) from lysates of ADAM 17-/- MEF cells with or without ADAM 17 expression based on the mean of three independent experiments (n=3), ± SD, *P<0.05, **P<0.05. A one-way ANOVA with post-hoc Tukey test was used for statistical analysis.

Full length L-selectin at 56 kDa was detected in ADAM 17-/- MEF cells, which decreased significantly after complementation of ADAM 17. Incubation with Ro 31-9790 increased full length L-selectin levels in both the absence and presence of ADAM 17 (Fig 4.5 A and C). Furthermore, the MP product of L-selectin was detected regardless of ADAM 17 expression, but was enriched after incubation with L-685 (Fig 4.5 A and D). These results illustrate that L-selectin is cleaved at the ectodomain by ADAM 17 and another metalloproteinase(s) generating an 8 kDa membrane tethered MP product which is further proteolyzed by PS.

PMA did not modulate levels of full length L-selectin or the MP product, irrespective of ADAM 17 expression (Fig 4.5 A and C) indicating that the second protease does not respond to PKC activation. Arguably, PMA does not further stimulate metalloproteinase activity in these highly active MEF cell lines as shown in section 4.3.

Concentrated supernatants from ADAM 17-/- MEF cells were immunoblotted and stained with an anti-V5 antibody to detect full length L-selectin or an N terminal anti-CD62L antibody to detect the cleaved ectodomain. Only the cleaved ectodomain of L-selectin was detected (Fig 4.5 B left panel). The calculated molecular weight of the soluble L-selectin ectodomain is approximately 54 kDa and was detected in PMA treated ADAM 17 expressing MEF cells. Additionally, in ADAM 17 deficient and DMSO or Ro 31-9790 treated ADAM 17 positive MEF cells, the medium showed an additional band for L-selectin which ran at 100 kDa (Fig 4.5 B left panel). Since it is known from the literature that ADAM-substrates can form dimers at the membrane (Wagner*, et al.* 2015; Hartmann*, et al.* 2015) it is possible that the 100 kDa band represents two cleaved L-selectin ECDs bound as a dimer. However, the protein loading buffer contains β-mercaptoethanol, which is a reducing agent and should disrupt non-covalent interactions in dimers. Rzeniewicz *et al* showed detection of a higher

molecular weight band representing glycosylated, full length L-selectin at the membrane at 110 kDa (Rzeniewicz, *et al*. 2015). It is therefore likely that the 100 kDa band detected from the concentrated supernatant is the cleaved ECD from glycosylated full-length L-selectin at the membrane. Additionally, Ro 31-9790 increased detection of this band (Fig 4.5 B), which correlates with increased release of sL-selectin from my previous ELISA data (Fig 4.3 G). These results likely show that these unknown protease(s) cleave L-selectin at the membrane. If correct, then full length L-selectin at 56 kDa from MEF cell lysates (Fig 5.A) could represent the non-glycosylated, intracellular form, which would correlate with the equally described, lower 70 kDa molecular weight band found from Rzeniewicz *et al*'s studies (Rzeniewicz, *et al*. 2015). Interestingly, the released soluble ECD of L-selectin at 56 kDa was only detected from concentrated supernatants when ADAM 17-/- MEF cells were complemented with ADAM 17 and later treated with PMA (Fig 4.5 B). This result illustrates that ADAM 17 cleaves potential intracellular L-selectin after activation by PMA.

4.5 Discussion

In this chapter, I showed that L-selectin is proteolyzed by ADAM 17 and additional metalloproteinase(s) which generate a MP product at 8 kDa. Activity of these unknown metalloproteinase(s) increased in the presence of Ro 31-9790 which elevated levels of the released soluble L-selectin ECD (Fig 4.3 G and Fig 4.5 B). Using PS deficient MEF cells, I later displayed that PS1 further proteolyzes the generated MP product, however the released ICD was below the detection threshold likely due to rapid degradation.

PS deficient MEF cells showed that the MP product of L-selectin is shed by PS1, but not PS2. This finding correlates with other studies showing that PS1 principally cleaves amyloid precursor protein (APP) (De Strooper*, et al.* 1998), Notch (De Strooper*, et al.* 1999), ErbB4 (Hoeing*, et al.* 2011; Fiaturi*, et al.* 2014) and E-cadherin (Marambaud*, et al.* 2002). Although PS2 exhibited a redundant role for L-selectin proteolysis in this chapter, studies have illustrated that this isoform of PS is also important for intramembrane proteolysis of type I transmembrane proteins. For instance, Steiner *et al* showed that mutating aspartic acid to alanine at residue 366 (D366A) in PS2 causes loss of catalytic activity. Consequently, intramembrane processing of Notch1 and APP was suppressed (Steiner*, et al.* 1999). These findings exemplify that γ-secretase substrates are differentially processed by either PS1 and/or PS2.

Although these PS deficient MEF cells showed accumulation of the L-selectin MP product in comparison to WT MEFs, detection for full length L-selectin was often below the threshold and did not increase in the presence of Ro 31-9790 (Fig 4.3 A and C). Western blots obtained from these PS deficient MEF cells therefore did not display our complete hypothesis for L-selectin proteolysis shown as ADAM 17-dependent ectodomain shedding followed by

intramembrane cleavage by PS (Fig 3.1). In contrast to MEFs, Molt3 T cells reproducibly show detection for full length L-selectin, which accumulates after inhibition of ADAM 17 (Fig 3.9). In future experiments, PS1 and/or PS2 could be gene silenced in Molt3 T cells expressing L-selectin. WT and PS deficient Molt3 T cells could then be incubated with Anti-ADAM 17 or control (ADAM 17 D1(A12)) antibody in both resting and TCR-activated conditions to display both ADAM 17 and PS dependent proteolysis.

Many type I transmembrane proteins are processed by multiple metalloproteinases. For instance, Notch, APP and T cell immunoglobulin and mucin domain 3 (Tim-3) are cleaved by ADAM 17 and ADAM 10 (Bozkulak*, et al.* 2009; Möller-Hackbarth*, et al.* 2013; Qian*, et al.* 2016; Tousseyn*, et al.* 2009). Our data in chapter 3 solidly shows that ADAM 17 proteolyzes L-selectin. However, L-selectin has also been shown to be proteolyzed by ADAM 10 and ADAM 8 (Le Gall*, et al.* 2009; Gomez-Gaviro*, et al.* 2007). Furthermore, L-selectin proteolyzes in ADAM 17 deficient fibroblasts and lymphocytes (Evans*, et al.* 2016; Walcheck*, et al.* 2003). To determine if L-selectin is proteolyzed by multiple metalloproteinase(s), L-selectin V5 His was transiently transfected in ADAM 17-/- MEF cells (Fig 4.5). Full length L-selectin was detected in ADAM 17-/- MEF cells, however levels decreased significantly after complementation of ADAM 17. Full length L-selectin increased after incubation with Ro 31-9790 regardless of ADAM 17 expression. Furthermore, an MP product was detected in the presence or absence of ADAM 17, which enriched after incubation with L-685. Our data demonstrate that L-selectin is proteolyzed by ADAM 17 and another metalloproteinase(s) which generate an MP product that acts as a substrate for PS1.

Soluble L-selectin was detected in the media at 100 kDa (Fig 4.5 B). As full-length L-selectin was detected at around 56 kDa in MEF cell lysates (Fig 4.5 A), I suggested that after cleavage

from the 8 kDa MP product, the resulting cleaved ECD would have an approximate molecular weight of 48 kDa. I later hypothesised that L-selectin was present at the membrane as a dimer like other ADAM-substrates such as Notch, cadherin and CD40 (Troyanovsky*, et al.* 2005; Liu*, et al.* 2010; Reyes-Moreno*, et al.* 2004) causing release of two bound ECDs at around 100 kDa. However, the protein loading buffer contains the reducing agent β-mercaptoethanol, which would have disrupted non-covalent bonds between dimers. Rzeniewicz *et al* showed detection of glycosylated, membrane bound full length L-selectin at 110 kDa and a non-glycosylated, intracellular form at 70 kDa (Rzeniewicz *et al*, 2015). In agreement to Rzeniewicz *et al*'s data, it is conceivable that the released ECD at 100 kDa was proteolyzed from glycosylated membrane bound L-selectin (Fig 4.5 B). Full length L-selectin at 56 kDa obtained from MEF cell lysates (Fig 4.5 A) therefore likely represents the non-glycosylated intracellular form and illustrates that the components in my lysis buffer do not allow efficient solubilization of membrane bound L-selectin.

Interestingly, the PKC activator PMA caused release of the soluble ECD of L-selectin at 54 kDa, which was dependent on ADAM 17 expression. In contrast, PMA did not elevate release of the soluble ECD at 100 kDa in both the presence or absence of ADAM 17 (Fig 4.5 B). However, Ro 31-9790 did increased release of this 100 kDa band (Fig 4.3 G, Fig 4.5 B) which could suggest that ADAM 17 proteolyzes this unknown metalloproteinase(s). In the presence of Ro 31-9790, ADAM 17 activity would be inhibited allowing these metalloproteinase(s) to accumulate. Increased expression of these metalloproteinase(s) would elevate proteolysis of L-selectin (Fig 4.4). These results possibly indicate that ADAM 17 cleaves non-glycosylated intracellular L-selectin releasing a 54 kDa ECD which is upregulated after PMA-activation. In contrast, the unknown metalloproteinase(s) likely proteolyzes glycosylated L-selectin at the membrane releasing the 100 kDa ECD and is not

activated by the same biochemical pathways as ADAM 17. However, levels of expression of this unknown metalloproteinase(s) is regulated by ADAM 17-proteolysis.

Future experiments will need to be completed to determine whether the detected band from cell lysates at 56 kDa (Fig 4.5 A) or concentrated supernatant at 100 kDa (Fig 4.5 B) represents membrane localized L-selectin. For instance, biotinylated ADAM 17-/- MEF cells would firstly be incubated with DMSO, L-685, PMA or Ro 31-9790, with or without complemented ADAM 17 and labelled L-selectin could be harvested from both the cell lysate and collected supernatant. Additionally, Rzeniewicz *et al* used the membrane solubilization agent Nonidet X-100 in their lysis buffer to achieve detection of both the 110 kDa and 70 kDa bands of full length L-selectin (Rzeniewicz, *et al*. 2015). In future studies, I could also use Nonidet X-100 instead of Triton-X which is the current membrane solubilizing agent in my lysis buffer.

5. Intramembrane proteolysis of L-selectin by γ-secretase induced after TCR stimulation

5.1 Introduction

Data from chapter 4 showed that PS1 cleaves the MP product of L-selectin when expressed in MEF cells. However, as L-selectin is found only in leucocytes, it was unclear whether the MP product is cleaved by γ-secretase in Molt3 T cells. TCR stimulation activates ADAM 17 causing ectodomain proteolysis of L-selectin generating the MP product (Fig 3.7, 3.8 and 3.9). Experiments were designed to establish if TCR stimulation also causes intramembrane proteolysis of the MP product by PS1. During endoproteolysis, an intramolecular cleavage in PS1 occurs between TMDs 6 and 7 of PS forming the catalytically active enzyme (Ahn*, et al.* 2010; Brunkan*, et al.* 2005). In this study, the hypothesis that TCR stimulation induces endoproteolysis of PS1 will be addressed (Fig 5.1 A). Activated PS1 would then cleave the MP product of L-selectin releasing the intracellular domain (ICD) into the cytoplasm (Fig 5.1 B).

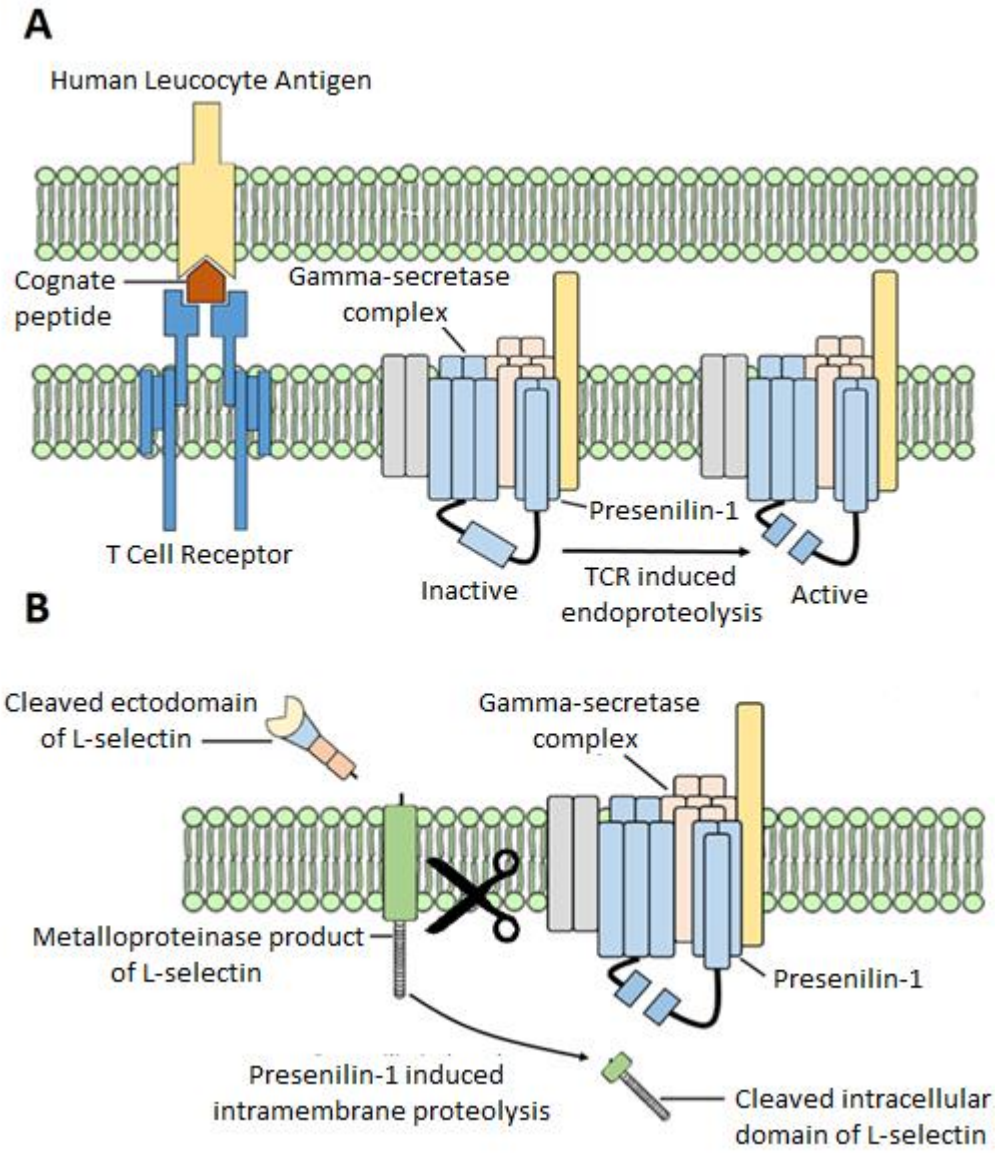

Figure 5.1: TCR stimulation hypothetically induces endoproteolysis and activation of PS1 inducing intramembrane proteolysis of L-selectin. (A) After presentation of cognate peptide, the TCR becomes stimulated and induces endoproteolysis of PS. During endoproteolysis, an intramolecular cleavage occurs between TMDs 6 and 7 generating a catalytically active C terminal fragment of PS. (B) After endoproteolysis; PS becomes activated and cleaves the MP product of L-selectin at the transmembrane region releasing the ICD.

Data from chapter 4 also showed that a cleaved L-selectin ICD generated by γ-secretase was unstable and rapidly degraded. Other ICDs such as ErbB4 (EICD) and notch (NICD) are rapidly degraded by the proteasome (Oberg*, et al.* 2001; Gupta-Rossi*, et al.* 2001; Fryer*, et al.* 2004; Zeng*, et al.* 2009). In this chapter, Molt3 T cells were directly lysed in Laemmli buffer to prevent rapid degradation of the L-selectin ICD.

Nicastrin, termed the substrate binding domain of γ-secretase, has been shown to bind both full length and cleaved fragments of type I transmembrane proteins (Shah*, et al.* 2005; Dries*, et al.* 2009; Yu*, et al.* 2000). PS also directly interacts with full length APP facilitating proteolysis (Xia*, et al.* 1997). It was hypothesised that after TCR stimulation and ADAM 17 mediated ectodomain proteolysis of L-selectin, the MP product would bind nicastrin and PS1 in a complex. In this study, pull down assays were performed to learn whether full length or the MP product of L-selectin binds to nicastrin and/or PS under resting or TCR stimulated conditions.

5.1.1 Aims of this chapter

- To determine if TCR stimulation induces intramembrane proteolysis of the MP product of L-selectin by γ-secretase
- To determine if TCR stimulation causes endoproteolysis and activation of PS1
- To monitor interactions between L-selectin and nicastrin/PS1 under both resting and TCR stimulated conditions
- To determine if the PS1 generated L-selectin ICD is degraded

5.2 Time course of ectodomain and intramembrane proteolysis of L-selectin in Molt3 T cells after TCR stimulation

5.2.1 Ectodomain proteolysis of L-selectin occurs at early time points after TCR stimulation

Type I transmembrane proteins are shed at the ectodomain before γ-secretase induces intramembrane proteolysis (Lichtenthaler*, et al.* 2011; Struhl and Adachi, 2000). To test whether L-selectin is sequentially proteolyzed by ADAM 17 and then γ-secretase, L-685 or DMSO treated Molt3 T cells were stimulated with 8 µL of R2 medium containing resuspended anti-CD3/CD28 dynabeads for 0 min, 5 min, 15 min, 30 min and 60 min and analysed by flow cytometry to determine the kinetics of ectodomain proteolysis. Cells were also incubated with 8 µL R2 medium containing resuspended IgG control dynabeads (Fig 5.2 A-D). Supernatants were collected and analysed for release of sL-selectin (Fig 5.2 E).

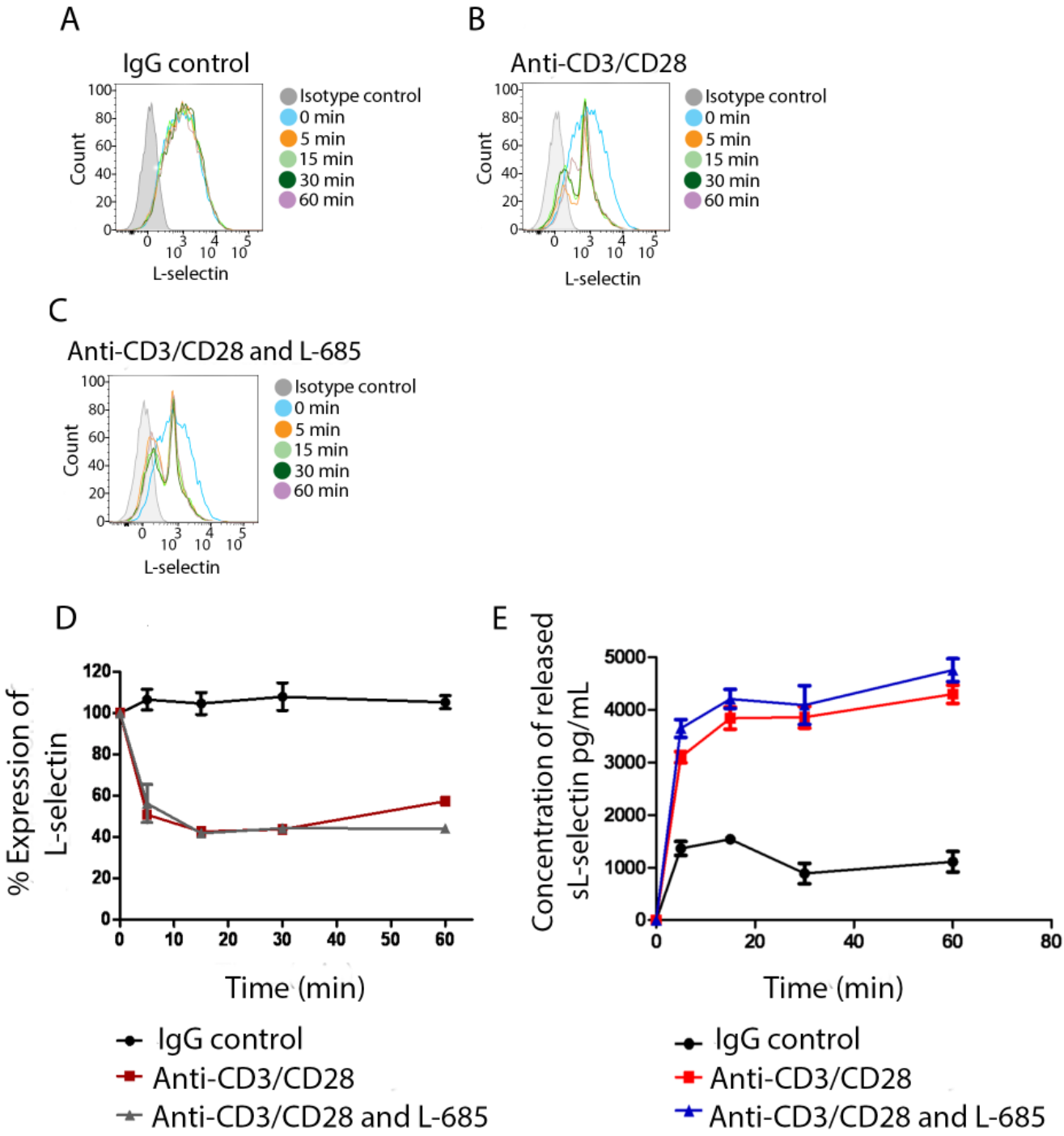

Figure 5.2: TCR stimulation induces rapid metalloproteinase dependent proteolysis of L-selectin. Molt3 T cells expressing L-selectin V5 His were incubated with IgG control (A), anti-human CD3/CD28 (B) and anti-human CD3/CD28 dynabeads with L-685 for 0 min, 5 min, 15 min, 30 min and 60 min and analysed using flow cytometry. (D) The percentage expression of cell surface L-selectin was calculated from three independent experiments (n=3). (E) Histograms show release of soluble (sL-selectin) based on the mean value of three independent experiments.

Cell surface levels of L-selectin did not change during 60 min incubation with IgG control dynabeads (Fig 5.2 A and D). Following TCR activation, cell surface L-selectin decreased rapidly to 50% of control levels within the first 5 min and stabilised at 40% of control levels between 15 and 60 min (Fig 5.2 B, C and D). Changes in membrane expression were accompanied by a 5-fold increase in sL-selectin by 5 min which increased to 6-fold and stabilised after 15 min. Although sL-selectin levels in IgG control treated cells were found to increase within the first 5 min, they were 3.3-fold lower than in TCR activated cells (Fig 5.2 E). The γ-secretase inhibitor L-685 had no effect on membrane turnover or release of L-selectin following TCR activation. These results show TCR stimulation activates ADAM 17 at early time points causing rapid proteolysis of L-selectin. Also, inhibition of γ-secretase does not interfere with ADAM 17 dependent ectodomain proteolysis.

5.2.2 TCR stimulation induces intramembrane proteolysis of L-selectin by γ-secretase

Our earlier findings show that TCR stimulation induces ectodomain proteolysis of L-selectin by ADAM 17 (sections 3.3 and 3.4) and that the generated MP product is susceptible to cleavage by PS1 (section 4.3). I now wanted to determine whether TCR stimulation initiates PS dependent intramembrane proteolysis. Molt3 T cells from section 5.2.1 were analysed by western blotting (Fig 5.3).

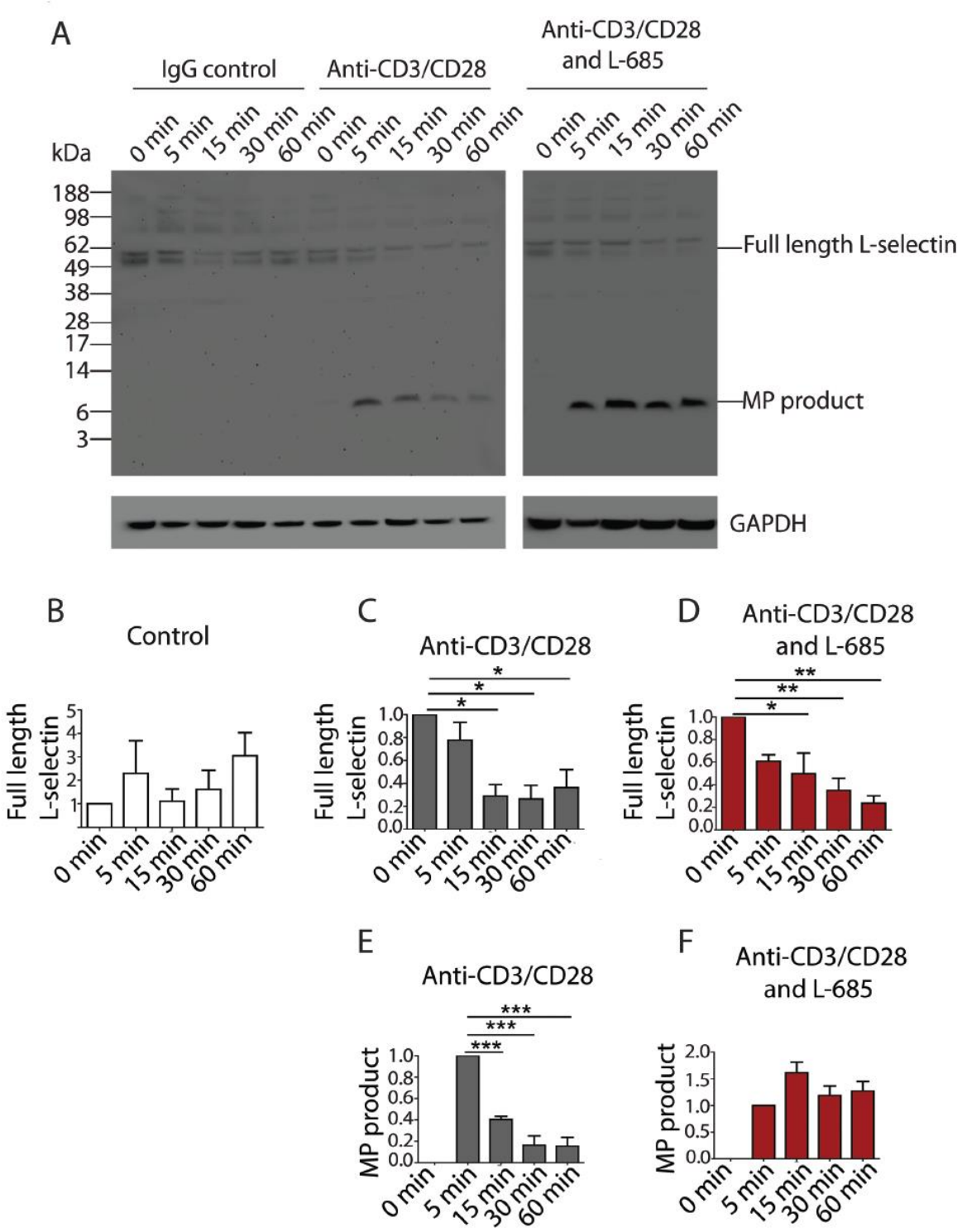

Figure 5.3: Stimulation of the TCR induces intramembrane proteolysis by PS. (A) Molt3 T cells expressing L-selectin V5 His from section 5.2.1 were analysed by western blotting. (B-F) Histograms show fold induction compared to Molt3 T cells incubated at 0 min (full length L-selectin) or 5 min (MP product) with the various treatments based on the mean values of three independent experiments n=3, SD ±, *P <0.05, **P <0.05, ***P<0.05. A one-way ANOVA with post-hoc Tukey test was used for statistical analysis.

There were two bands of similar molecular weight around 52 to 56 kDa representing different forms of full length L-selectin. In resting T cells, both forms of full length L-selectin remained unchanged during the 60-min time course and importantly lacked the MP product in the lysate (Fig 5.3 A and B). These results demonstrate clearly that L-selectin does not undergo ectodomain proteolysis in the absence of TCR stimulation.

In TCR-activated T cells, only the lower 52 kDa band decreased between 0 min to 60 min. Detection of the upper 56 kDa band did not change showing that this form of L-selectin did not undergo ectodomain proteolysis. Statistical analysis was therefore calculated using only the lower L-selectin band at 52 kDa.

Following TCR-activation, the level of full length L-selectin was reduced by 20% after 5 min, which coincided with the detection of the MP product. In the presence of L-685, the reduction in full length L-selectin was higher at 40%. Full length L-selectin continued to decrease to 20% of start levels between 15 min and 30 min (Fig 5.3 A, C and D).

The level of MP product detected after 5 min decreased between 15 and 30 min in DMSO treated TCR-activated cells (Fig 5.3 A, E). The γ-secretase inhibitor L-685 stabilized the MP product (Fig 5.3 A, E and F). These results show that TCR stimulation initiates intramembrane proteolysis of the MP product by PS. However, the PS generated ICD of L-selectin was not detected which likely illustrates that the ICD is rapidly degraded.

5.3 Approaches to detect the L-selectin ICD

All western blots generated so far lacked detection of the cleaved L-selectin ICD. Intracellular domains of other substrates such as amyloid precursor protein (AICD) and Notch (NICD) have been difficult to detect due to rapid degradation by the ubiquitin-proteasome pathway (De Strooper*, et al.* 1999; Schweisguth, 2004; Selkoe and Kopan, 2003). Additionally, AICD is also a substrate for the insulin degrading enzyme, which is a metalloproteinase known to degrade short polypeptides (Edbauer*, et al.* 2002). My data suggested that the ICD of L-selectin is also rapidly degraded preventing detection.

Cleaved AICD and NICD enter the nucleus and act as gene transcriptional factors (von Rotz*, et al.* 2004; Schroeter*, et al.* 1998). Studies performed so far have extracted soluble proteins from the cytoplasm and plasma membrane using cell lysis buffer. My cell lysis buffer does not contain reagents such as sodium deoxycholate or SDS that solubilize cytoskeleton or nuclear membranes. Potentially, the ICD of L-selectin is either rapidly degraded or localized in a subcellular organelle, such as the nucleus, which is not been solubilized by cell lysis buffer.

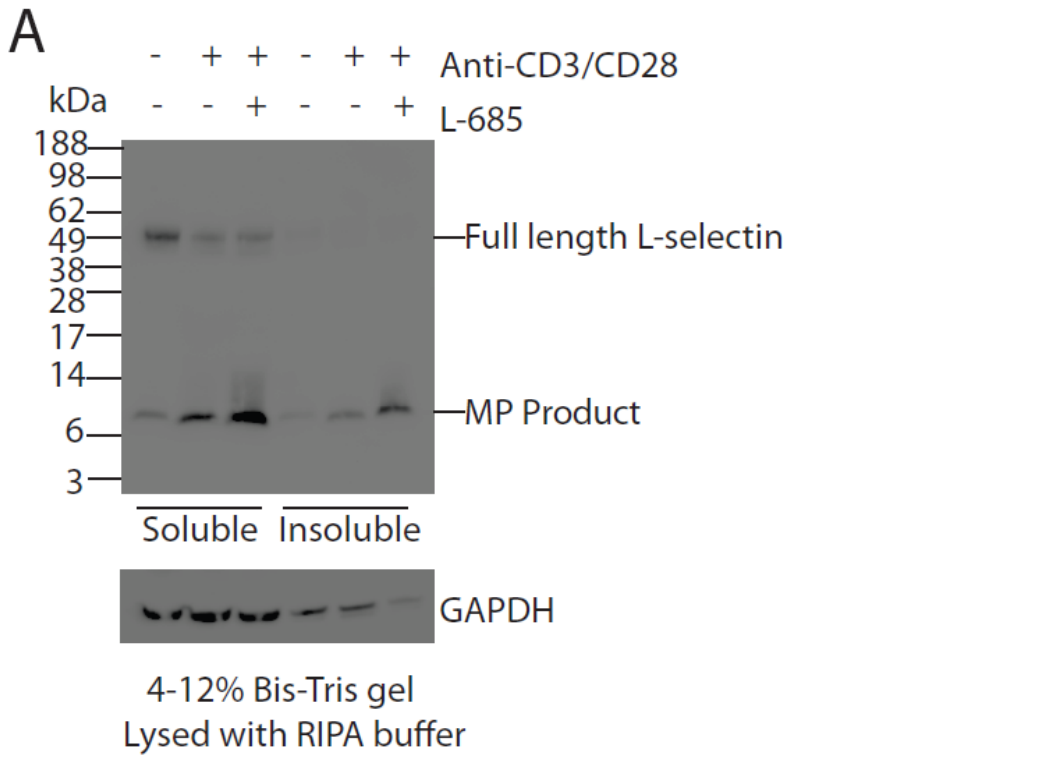
A
- + + - + + Anti-CD3/CD28
kDa - - + - - + L-685
188
98
62
49
38
28
17
14
6
3
Full length L-selectin
MP Product
Soluble
Insoluble
GAPDH
4-12% Bis-Tris gel
Lysed with RIPA buffer

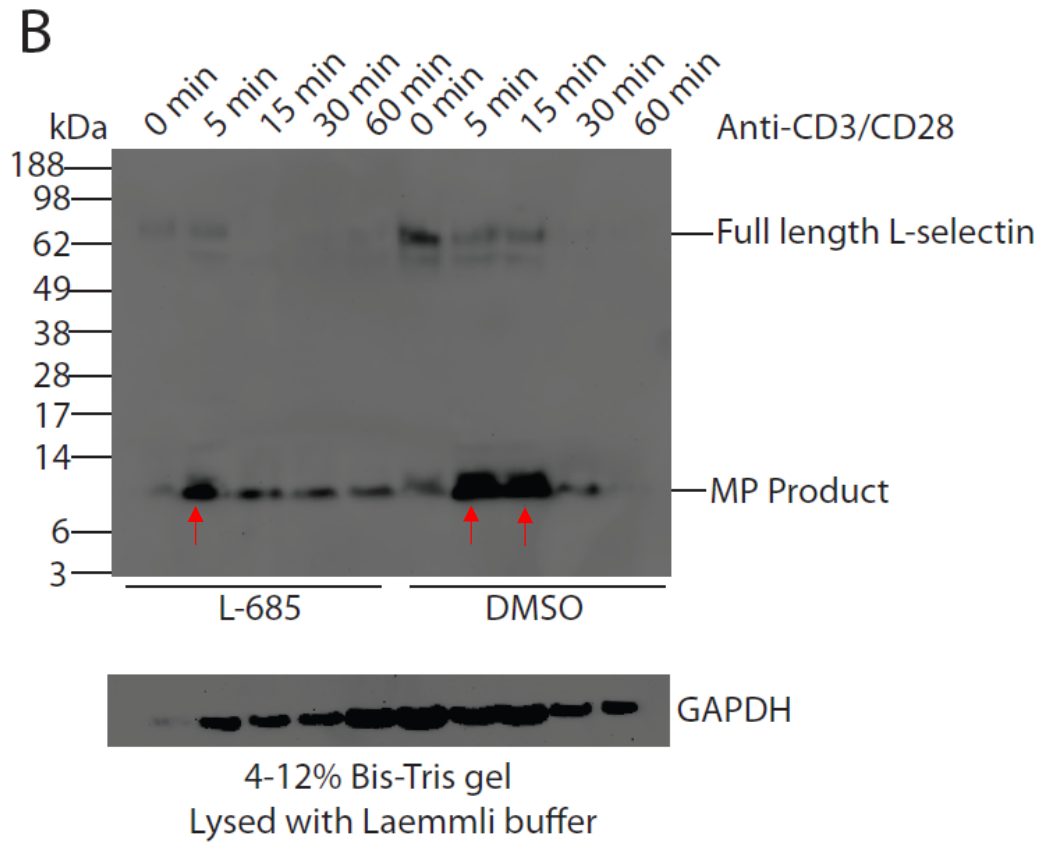
B
kDa
0 min
5 min
15 min
30 min
60 min
0 min
5 min
15 min
30 min
60 min
Anti-CD3/CD28
188
98
62
49
38
28
17
14
6
3
Full length L-selectin
MP Product
L-685
DMSO
GAPDH
4-12% Bis-Tris gel
Lysed with Laemmli buffer

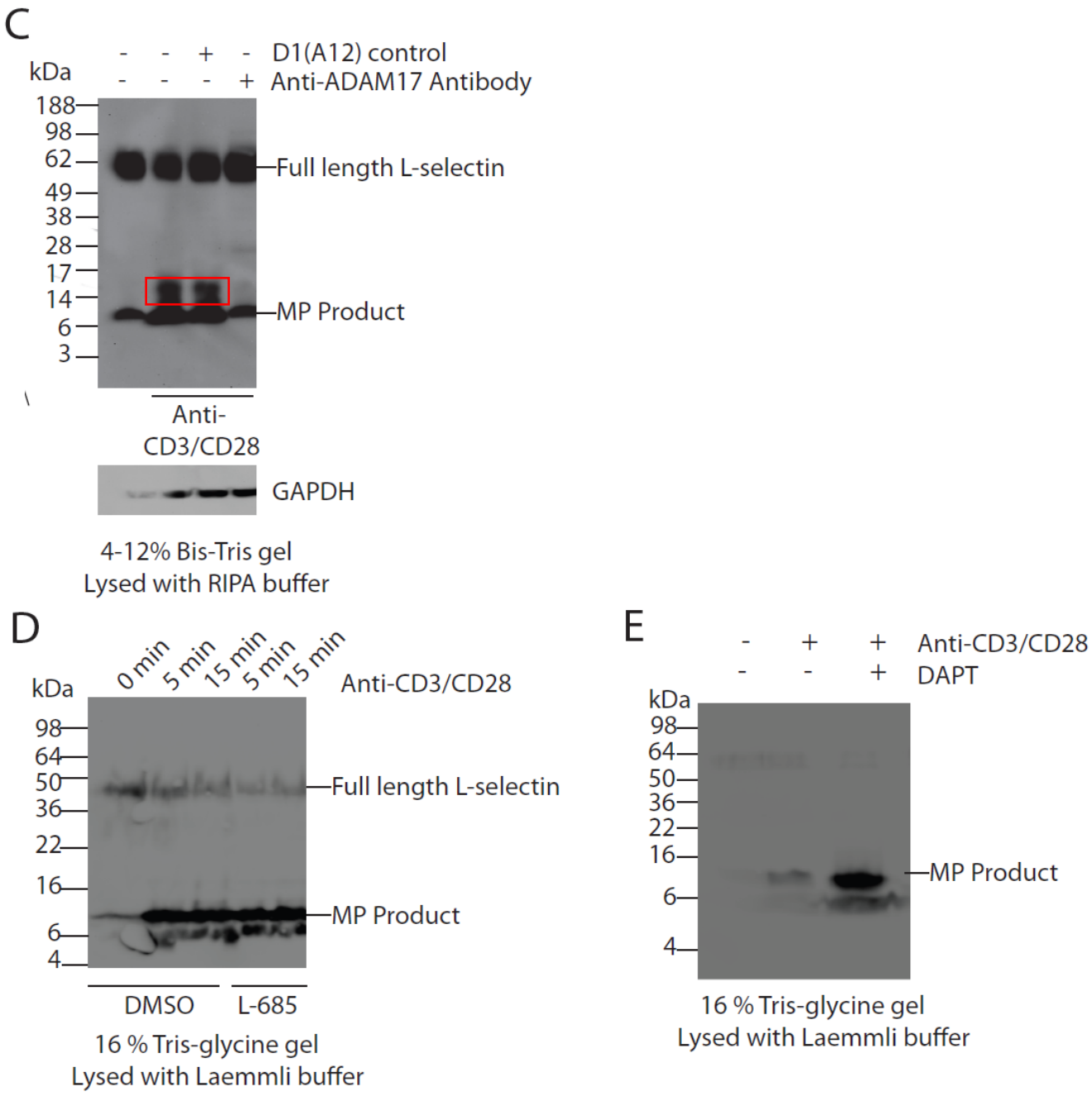

Figure 5.4: Optimisation to detect the PS generated intracellular domain of L-selectin. (A) Molt3 T cells expressing L-selectin V5 His were lysed in cell lysis buffer to extract proteins from the soluble fraction. The insoluble pellet was further lysed in cell lysis buffer supplemented with 0.5 % SDS and 1 % sodium deoxycholate to obtain proteins from insoluble fractions. (B) Molt3 T cells were incubated with anti-human CD3/CD28 dynabeads and directly lysed in Laemmli buffer. Lysates were run on a 4-16 % Bis-Tris gradient gel. A doublet at 8 to 13 kDa (red arrows) is detected in DMSO treated T cells. (C) TCR-activated Molt3 T cells were incubated with Anti-ADAM 17 (D1 (A12)) antibody or the D1 (A12) control. The 13 kDa fragment of L-selectin was detected (in red box only in the presence of ADAM 17 activity. (E and F) Molt3 T cells were directly lysed in Laemmli buffer and run on a 16 % Tris-glycine gel. A 5 kDa band was detected which was not cleared after incubation with DMSO, DAPT (E) or L-685 (F). These results are from single observations (n=1).

L-685 or DMSO treated Molt3 T cells were firstly lysed in cell lysis buffer to extract membrane and cytosolic proteins and the remaining insoluble pellet was re-suspended in cell lysis buffer containing 0.5 % sodium deoxycholate (w/v) and 0.1 % SDS (w/v) followed by sonication. There was no detection of the L-selectin ICD in the soluble or insoluble fractions of non or TCR-activated T cells (Fig 5.4 A).

These Molt3 T cells were incubated for 60 min with anti-CD3/CD28 dynabeads and 35 min lysis in cell lysis buffer. I anticipated that pro-longed incubation allowed degradation of the L-selectin ICD by intracellular proteases. Detection of other ICDs such as AICD has been achieved by directly lysing cells in Laemmli buffer (Suh*, et al.* 2011). Molt3 T cells were activated with anti-CD3/CD28 dynabeads and incubated with DMSO or L-685 prior to lysis Laemmli buffer and western blot analysis. In DMSO controls, a doublet of bands at 8 and 13 kDa were detected at 5 and 15 min (Fig 5.4 B DMSO) which was absent in T cells treated with the γ-secretase inhibitor L-685 (Fig 5.4 B L-685). This band at 13 kDa was also cleared after TCR-activated T cells were incubated with Anti-ADAM 17 (D1 (A12)) antibody (Fig 5.4 C). ICDs of notch (NICD) and ErbB4 (EICD) are ubiquitinated leading to degradation (Oberg*, et al.* 2001; Gupta-Rossi*, et al.* 2001; Fryer*, et al.* 2004). Ubiquitin is 8 kDa and suggestively, the L-selectin ICD is 5 kDa. The 13 kDa band could represent a PS1 generated monoubiquitinated ICD of L-selectin. However, proteomic analysis has only shown one ubiquitin site at lysine (K78) in the ectodomain of L-selectin (Mertins, *et al.* 2013) which could suggest that the L-selectin ICD undergoes other post-translational modifications after proteolysis. Ser^{364} and Ser^{367} in the L-selectin ICD are phosphorylated after cell activation (Rzeniewicz *et al*, 2015). The addition of two negatively charged phosphate groups to the cleaved fragments of L-selectin can interfere with protein-SDS interactions and consequently disrupt the mass to charge ratio during electrophoresis which would modulate

the electrophoretic mobility towards the anode (Grosely, *et al*. 2013). The 13 kDa band would need to be excised and analysed by mass spectroscopy to monitor post-translational modifications of these cleaved L-selectin fragments. However, the bands in Fig 5.4 B were situated too close to one another. Consequently, it would be difficult to excise only the 13 kDa fragment.

In Fig 5.4 B, detection for the 13 kDa fragment was lost completely after 30 min and thus 5 and 15 min time points were chosen for future experiments. 16 % Tris-glycine gels were used to separate the bands at 8 and 13 kDa and contrary to Fig 5.4 B, a 13 kDa fragment was not detected (Fig 5.4 E). However, a band at 5 kDa appeared after both 5 and 15 min TCR stimulation. Remarkably, this band was also detected in the presence of L-685 and DAPT (Fig 5.4 D and E). Thus, this band is not a PS generated L-selectin ICD.

5.4 TCR stimulation causes endoproteolysis and activation of PS1

Data from section 5.2.2 shows that stimulation of the TCR induces intramembrane proteolysis of the MP product of L-selectin by PS. I now wanted to determine if TCR stimulation initiates endoproteolysis and activation of PS1. A C terminal antibody of PS1 that binds amino acids 450-467 was used to detect full length (48 kDa) and the cleaved C terminal fragment (CTF) (18 kDa) during western blot analysis. Firstly, Molt3 T cells were incubated with IgG control or anti-CD3/CD28 dynabeads for 60 min to see if TCR stimulation enriches the CTF of PS1. Lysates of WT and PSdKO MEF cells were used to confirm that bands detected were specific to PS1 (Fig 5.5 A). In non-stimulated T cells, a 48 kDa band was detected representing full length PS1 as well as higher molecular weight bands from 62 to

188 kDa which likely represent glycosylated forms of SDS stable complexes of full length PS1. In TCR-activated T cells, full length PS1 was still detected, but an 18 kDa band representing the cleaved CTF of PS1 appeared (Fig 5.5 B). Both full length and CTF of PS1 were detected in WT MEF cells demonstrating their high activity as discussed in Chapter 4. The PS1 antibody detected no bands in PSdKO MEF cells. This confirmed the specificity of the anti-PS1 antibody (Fig 5.5 A).

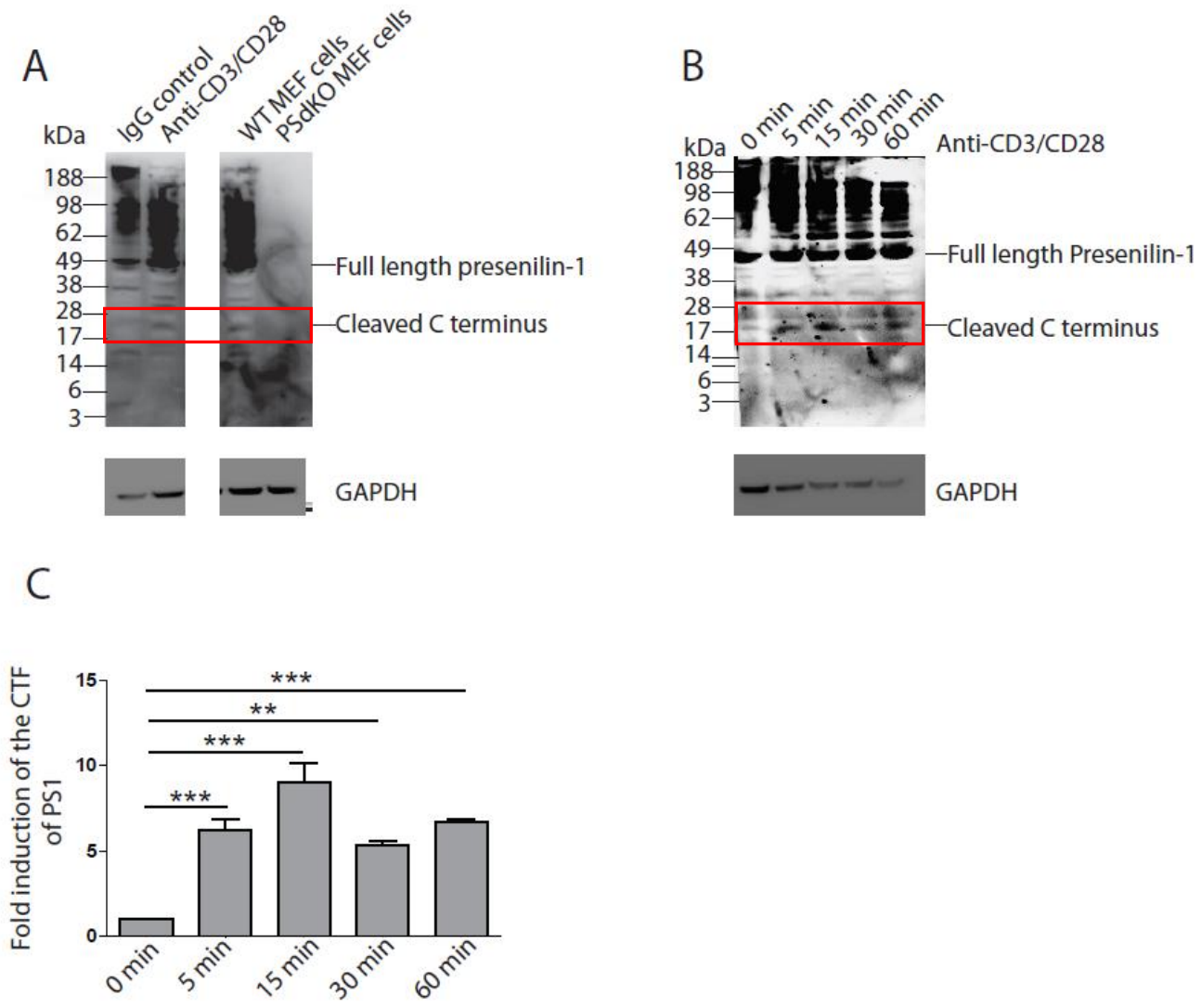

Figure 5.5: TCR stimulation induces endoproteolysis of PS1. A C terminal antibody for PS1 was used to distinguish full length (48 kDa) and the cleaved CTF (18 kDa). (A) Molt3 T cells were incubated with IgG control or anti human CD3/CD28 dynabeads for 1 h. To confirm bands were specific to PS1, lysates from WT and PSdKO MEF cells were also used for western blot analysis. (B) Molt3 T cells were incubated with anti-human CD3/CD28 dynabeads for 0 min, 5 min, 15 min, 30 min and 60 min. (C) Histograms show fold increase in PS1 CTF compared to non-TCR stimulated Molt3 T cells based on the mean of three independent experiments n=3, SD ±, *P <0.05. A one-way ANOVA with post-hoc Tukey test was used for statistical analysis.

The rate of PS1 endoproteolysis in TCR-activated Molt3 T cells was determined after 0 min, 5 min, 15 min, 30 min and 60 min incubation with anti-CD3/CD28 dynabeads. After 5 min stimulation, the PS1 CTF increased by 6-fold. Between 5 and 15 min, the CTF elevated a further 2-fold and decreased thereafter. Potentially, the CTF is degraded by the lysosome or proteasome after pro-longed periods of TCR stimulation regulating the catalytic activity of PS1.

5.5 Monitoring interactions between L-selectin and γ-secretase subunits

5.5.1 L-selectin binds to PS1, but not PS2, under both basal and TCR stimulated conditions

In PS deficient MEF cells, I have shown that PS1 proteolyzes the MP product of L-selectin. In contrast, PS2 does not cleave L-selectin (section 4.3). I therefore hypothesised that L-selectin would interact with PS1, but not PS2, after TCR stimulation triggering L-selectin proteolysis. To monitor these interactions, Molt3 T cells were incubated overnight with 10 μM L-685 to accumulate potential PS1/PS2 L-selectin complexes. After L-685 treatment, Molt3 T cells were further incubated with C1R antigen presenting cells pulsed with or without 10^{-4} M SLY peptide. Molt3 T cells expressing gag TCR but not V5-His tagged L-selectin were used to confirm that L-selectin V5 His was selectively pulled down after incubation with cobalt coated dynabeads (Fig 5.6).

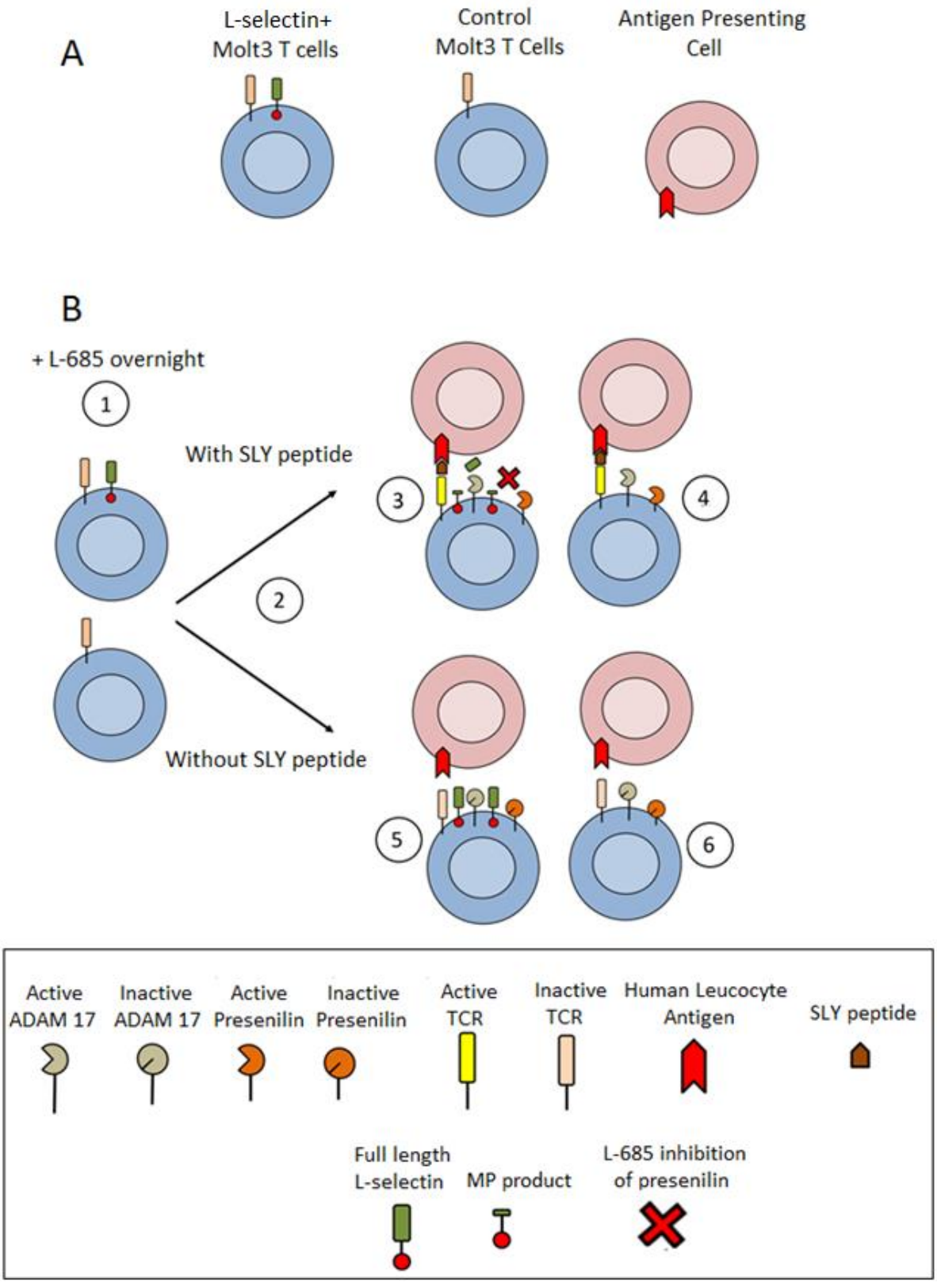
A
L-selectin+
Molt3 T cells
Control
Molt3 T Cells
Antigen Presenting
Cell
B
+ L-685 overnight
1
With SLY peptide
2
3
4
Without SLY peptide
5
6
Active
ADAM 17
Inactive
ADAM 17
Active
Presenilin
Inactive
Presenilin
Active
TCR
Inactive
TCR
Human Leucocyte
Antigen
SLY peptide
Full length
L-selectin
MP product
L-685 inhibition
of presenilin

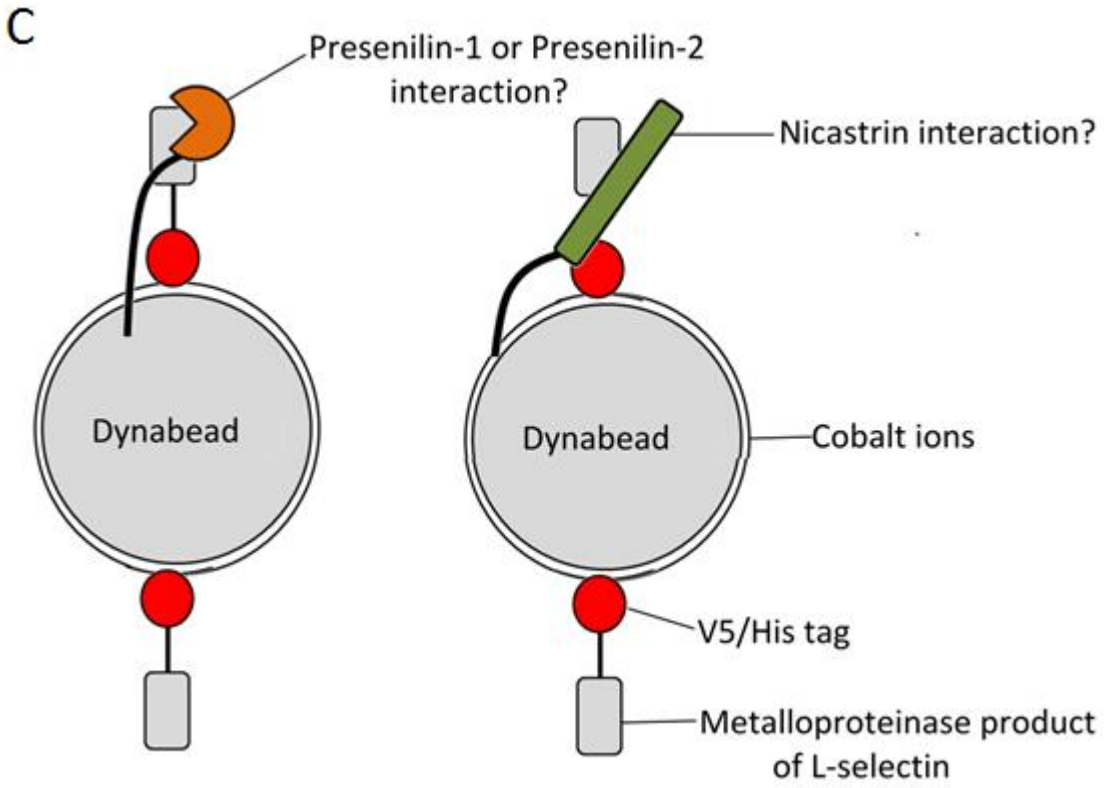

Figure 5.6: Diagrammatic representation of L-selectin V5 His and nicastrin/PS pulldown assays. (A) L-selectin+ Molt3 T cells express L-selectin V5 His. Molt3 T cells not expressing L-selectin V5 His are control Molt3 T cells. (B) (1) Both cell lines are incubated with L-685 overnight. (2) L-685 incubated T cells are then treated with C1R antigen presenting cells pulsed without or with 10^{-4} M SLY peptide. (3) After incubation with peptide pulsed C1R antigen presenting cells, the SLY peptide binds to cognate gag+ TCR presented on L-selectin+ Molt3 T cells and stimulates both ADAM 17 and PS. ADAM 17 cleaves full length L-selectin generating the metalloproteinase (MP) product. In the presence of L-685, PS is inhibited and the MP product accumulates. (4) In control Molt3 T cells, TCR stimulation activates ADAM 17 and PS; however in the absence of L-selectin, no MP product is generated. (5) After incubation with non-peptide pulsed C1R cells, the gag+ TCR is not stimulated in L-selectin+ Molt3 T cells. Consequently, ADAM 17 and PS are not activated and L-selectin is not proteolyzed. This allows full length L-selectin to accumulate on the surface of these T cells. (6) In control Molt3 T cells absence of TCR stimulation also prevents activation of ADAM 17 and PS, however these L-selectin deficient T cells do not accumulate full length protein. (C) Both cell lines are lysed and incubated with cobalt coated dynabeads. The V5 His tag of the accumulated metalloproteinase (MP) product binds to cobalt ions on the surface of the dynabeads only in lysates of Molt3 T cells. Nicastrin and/or PS will also be indirectly attached to these cobalt coated dynabeads if they interact with the MP product of L-selectin**.**

Control Molt3 T cells showed no detection of bands demonstrating clearly that only L-selectin V5 His was pulled down. Both full length and MP product of L-selectin were detected in non-activated as well as TCR-activated T cells. The abundance of full length L-selectin suggests that SLY peptide induces lower levels of ectodomain proteolysis than anti-CD3/28 dynabeads and is, therefore, a weaker stimulus. However, SLY peptide incubated T cells showed increased detection for the MP product confirming that TCR stimulation occurred. It is also possible that the cobalt covered dynabeads bind full length L-selectin more avidly than the MP product. PS1, but not PS2, was detected in both non-activated and TCR activated T cells. This shows that PS1, but not PS2, binds L-selectin (Fig 5.7)

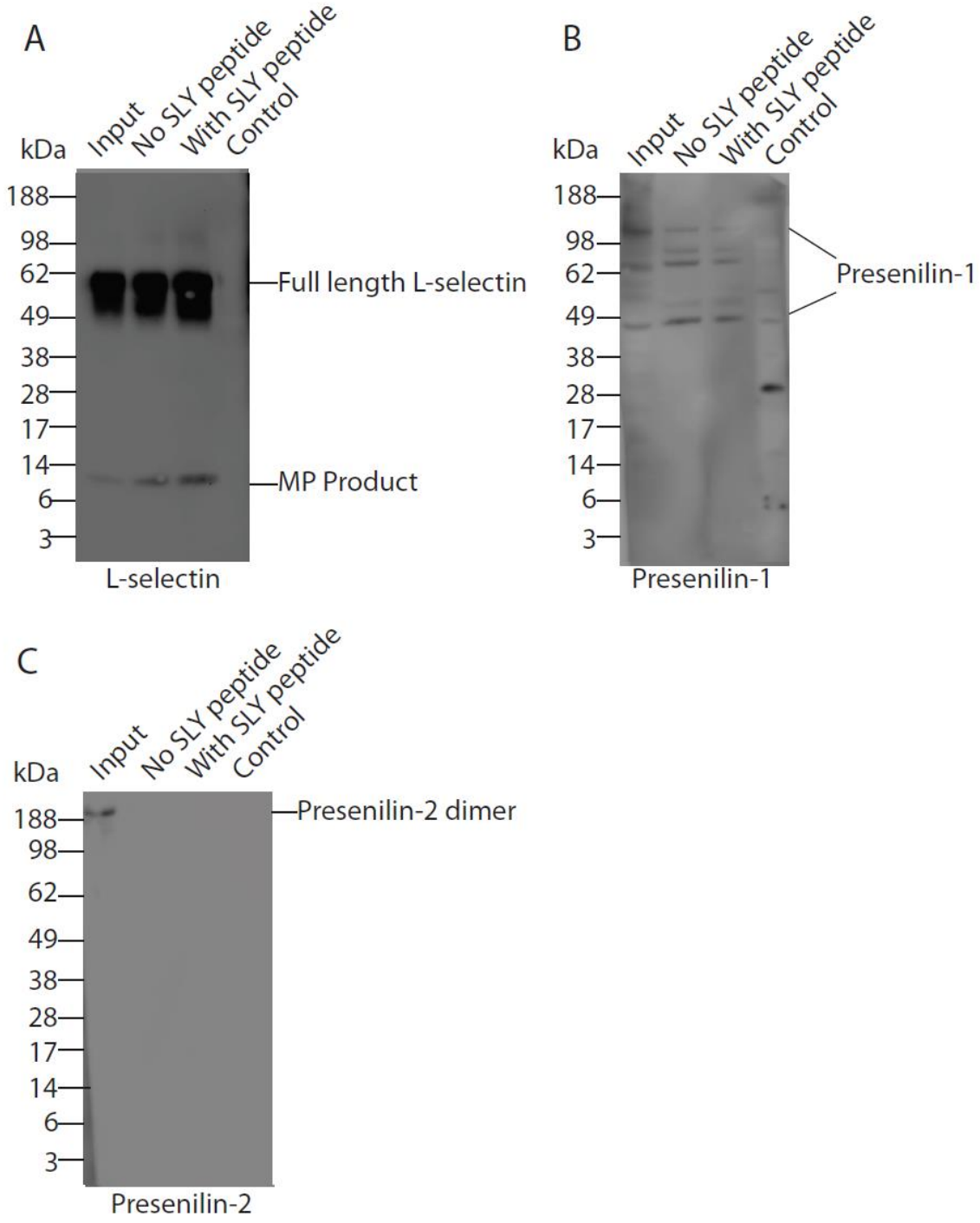

Figure 5.7: PS1 interacts with L-selectin in both resting and TCR-activated T cells. Lysates from cell lysis buffer lysed L-selectin+ or control Molt3 T cells were incubated with cobalt covered dynabeads. Lysates were used for western blot analysis and stained for L-selectin (A), PS-1 (PS1) (B) or PS-2 (PS2) (C). Anti-V5 antibody was used for detection of L-selectin and C terminal antibodies for PS1 and PS2. This result is one representation from three independent experiments which all show reproducible results (n=3).

5.5.2 L-selectin binds to nicastrin in both basal and TCR stimulated conditions

Further pull down experiments were performed as in Fig 5.7 but stained for nicastrin to assess whether it is associated with L-selectin (Fig 5.8).

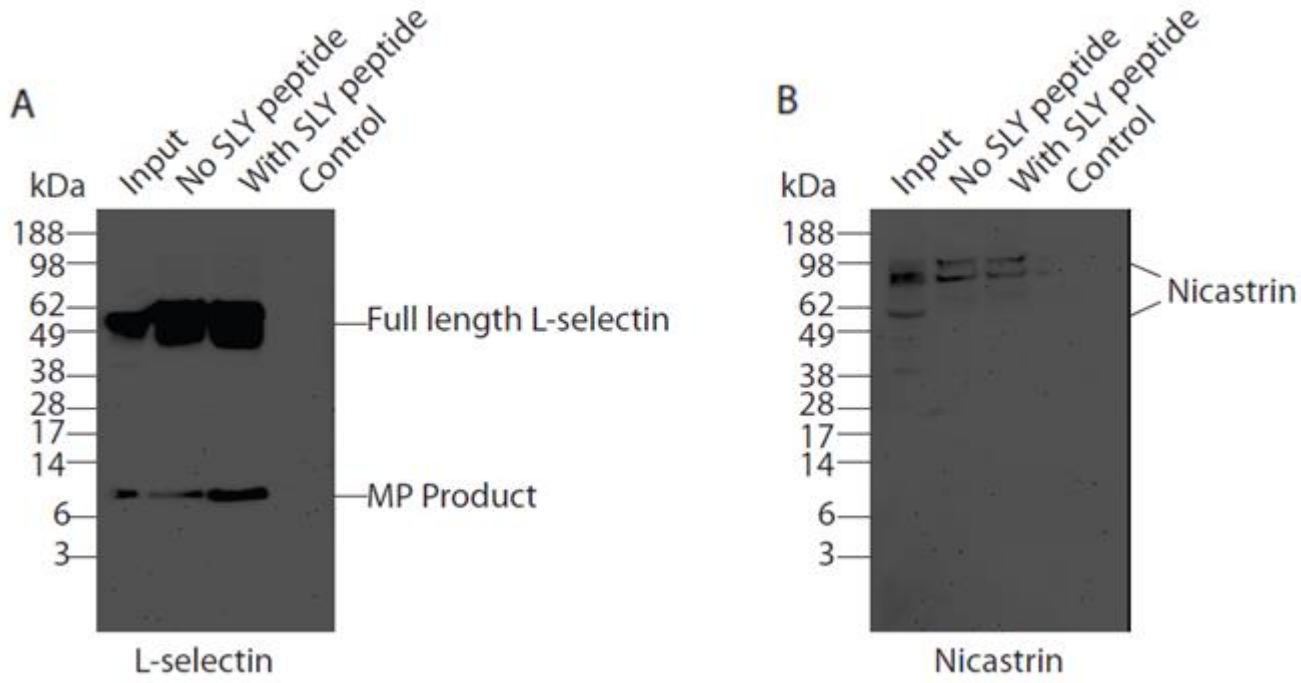

Figure 5.8: L-selectin interacts with nicastrin in both resting and TCR-activated T cells. Lysates from cell lysis buffer lysed L-selectin+ or control Molt3 T cells were incubated with cobalt covered dynabeads. Lysates were used for western blot analysis and stained for L-selectin (A) or nicastrin (B). Anti-V5 antibody was used to detect L-selectin and a C terminal antibody for nicastrin. This result is one observation from three independent experiments which all show reproducible results (n=3).

In the input lysate, nicastrin was detected at 78 kDa representing full length protein (Wolfe, 2016) and 58 kDa, which likely displays a cleaved fragment. After pulldown, Nicastrin at 78 kDa and 98 kDa was detected from lysates derived from non-activated and TCR activated T cells. This 98 kDa band of nicastrin may represent an SDS-stable complex between nicastrin and another subunit of the γ-secretase complex.

5.6 Discussion

In this chapter, I have shown that early time points of TCR-activation induce rapid ADAM 17-dependent proteolysis of L-selectin (Fig 5.2) which generates an 8 kDa MP product (Fig 5.3 A). Furthermore, my data shows that cross-linking the TCR also activates PS by inducing endoproteolysis (Fig 5.5). Activated PS then cleaves the MP product however, the released L-selectin ICD was not detected likely due to rapid degradation (Fig 5.3 A, E and F). Additionally, pull-down assays using cobalt-ion coated dynabeads showed that L-selectin forms complexes with both nicastrin (Fig 5.8) and PS1 (Fig 5.7) in both resting and TCR-activated conditions. Together, my results illustrate that L-selectin already forms a complex with ADAM 17 (Fig 3.10), nicastrin (Fig 5.8) and PS1 (Fig 5.7) in a resting T cell. TCR-activation then activates both ADAM 17 and PS1, which induces rapid proteolysis of bound L-selectin.

PS mediated intramembrane proteolysis of substrates such as APP and notch has been widely published (De Strooper*, et al.* 1999; Palacino*, et al.* 2000). However, it is currently unknown whether TCR stimulation induces PS1 activation. Western blot analysis in section 5.2.2 showed that the MP product of L-selectin was detected 5 min post-TCR stimulation. The MP product decreased from 5 min to 60 min, and this decrease was blocked by the γ secretase inhibitor L-685 (Fig 5.3). In agreement with our initial hypothesis, TCR stimulation induces intramembrane proteolysis of the MP product by γ secretase. I then asked whether TCR stimulation activates PS1 by inducing its endoproteolysis. Western blot analysis from showed that TCR stimulation caused PS1 cleavage (Fig 5.5 A). Additionally, in a time trial study, the PS1 CTF accumulated in TCR-activated T cells between 5 to 15 min, but decreased after 30 min (Fig 5.5 B). Together, these observations show that TCR stimulation initiates

endoproteolysis of PS1 at early time points, generating the catalytically active cleaved CTF. The CTF is potentially degraded after pro-longed periods of TCR stimulation which would limit the catalytic activity of PS1. How TCR signalling regulates endoproteolysis of PS1 is currently unknown. TCR stimulation activates the mitogen and stress activated kinase (MSK). MSK phosphorylates and activates the cAMP response element binding (CREB) protein (Kaiser*, et al.* 2007). CREB binds to the 238 bp region of the promoter for the PS enhancer-2 (Pen-2) gene. After this interaction, Pen-2 expression is increased (Wang*, et al.* 2006). Pen-2 has been shown to interact with PS and induce its' endoproteolysis (Holmes*, et al.* 2014). Disruption of this interaction causes both Pen-2 and PS1 CTF to be degraded at the proteasome (Prokop*, et al.* 2005; Honda*, et al.* 1999). It is possible that signalling pathways induced after TCR stimulation promote interactions between Pen-2 and PS1 initiating endoproteolysis of PS1. After pro-longed periods of TCR stimulation, signalling pathways such as MSK may subside reducing the expression of Pen-2 and abolishing interactions with PS1. Free, unbound PS1 would then be susceptible to degradation by the proteasome.

Notch2 and Notch3 receptors are firstly shed at the ectodomain by ADAM 10 prior to γ-secretase dependent intramembrane proteolysis (Groot*, et al.* 2014). Flow cytometry, ELISA and western blot analysis from sections 5.2.2 and 5.2.3 showed that activation of the TCR using anti human-CD3/CD28 dynabeads caused ectodomain proteolysis of L-selectin independently of γ-secretase activation (Figs 5.2 and 5.3). These results confirmed that after TCR stimulation, metalloproteinases shed L-selectin at the ectodomain before PS can induce intramembrane proteolysis.

Nicastrin binds to newly generated N termini of substrates generated by ectodomain proteolysis via Glu^{333} (Shah*, et al.* 2005; Dries*, et al.* 2009). Furthermore, the cleaved beta fragments of amyloid precursor protein (APP) C99 and C83 bind nicastrin (Yu*, et al.* 2000). However, nicastrin, as well as PS associates with full length APP (Chen*, et al.* 2001; Xia*, et al.* 1997). In this study, pull down assays using cobalt ion-coated dynabeads to bind the His tag of L-selectin (Fig 5.6) were performed to learn whether the full length or the MP product of L-selectin binds to nicastrin and/or PS under resting or TCR stimulated conditions. Pulldown assays from sections 5.5.1 and 5.5.2 showed that nicastrin and PS1 bound to L-selectin under both resting and TCR stimulated conditions. However, I could not determine whether full length or the MP product of L-selectin interacted with nicastrin or PS1. Future studies could be performed where lysates from Molt3 T cells stably expressing V5/His tagged nicastrin or PS and non-tagged L-selectin are lysed and incubated with cobalt covered dynabeads. Blots could then be stained for non-tagged L-selectin using the C terminal CA21 antibody to ascertain whether full length or MP product binds to these γ-secretase subunits.

ICDs for other type I transmembrane proteins such as amyloid precursor protein (AICD) and Notch (NICD) have also been difficult to detect due to rapid degradation. For instance, NICD is ubiquitinated by F-box/WD repeat containing protein 7 (fbxw7). Ubiquitinated NICD is then degraded by the proteasome (Oberg *et al* 2001; Gupta-Rossi*, et al.* 2001, Fryer*, et al.* 2004). The ICD of the related to receptor tyrosine kinase (Ryk) is bound to Cdc37, a subunit for the molecular chaperone heat shock protein 90 (Hsp90). Disruption of this interaction causes proteasome degradation of the ICD of Ryk receptor (Lyu, 2009). CTFs of Met receptor and premelanosome protein (PMEL) generated after γ-secretase activity are stabilized in the presence of lysosomal inhibitors such as leupeptin, pepstatin A and chloroquine (van Niel*, et al.* 2011; Ancot*, et al.* 2012). Contrastingly, degradation of AICD is not inhibited in the

presence of lysosomal (leupeptin and bafilomycin) or protease (Lactacystin) inhibitors (Cupers*, et al.* 2001). Instead, AICD is rapidly cleared by the insulin degrading enzyme, which is a metalloproteinase that proteolyzes small polypeptides (Edbauer*, et al.* 2002). Additionally, other PS generated ICDs localize in subcellular organelles, such as the nucleus, which cell lysis buffer does not solubilize. For instance, AICD binds to Fe65 in the cytoplasm and migrates to the nucleus. In the nucleus, AICD and Fe65 form a complex with Tip-60 that interacts with DNA inducing gene transcription (von Rotz*, et al.* 2004). Comparably, NICD binds to the transcriptional factor CSL in the nucleus and this complex binds to DNA (Schroeter*, et al.* 1998). The 17-amino acid ICD of L-selectin contains 8 positively amino acids. This short, positively charged polypeptide could form electrostatic interactions with the negatively charged phosphate backbone of DNA in the nucleus. Also, the ICD for the L1 cell adhesion molecule (L1CAM) binds to the cytoskeletal proteins actin and ERM proteins (Loers and Schachner, 2007; Herron*, et al.* 2009; Kiefel*, et al.* 2012). The ICD of E-cadherin also binds to the cytoskeleton forming a tertiary complex with α-cadherin and β-catenin (Zaidel-Bar, *et al.* 2013, Han*, et al.* 2012; Van Itallie*, et al.* 2014). It has been established that L-selectin interacts with the ERM proteins ezrin and moesin (Ivetic*, et al.* 2002). Potentially, L-selectin ICD may be associated with these ERM proteins causing retention at the cytoskeleton. I conceptualized that inhibiting degradation of the L-selectin ICD causes accumulation in these subcellular organelles which the cell lysis buffer does not solubilize. Suh *et al* achieved detection of AICD by directly lysing cells in Laemmli buffer (Suh*, et al.* 2011). This approach was beneficial to our studies for two reasons. Firstly, direct lysis would prevent intracellular proteases from degrading the ICD of L-selectin. Secondly, the whole cell lysate would be run and analysed by immunoblotting to determine if the ICD of L-selectin was present in insoluble pellets. TCR stimulation of Molt3 T cells was shortened to 5

min to suppress potential rapid degradation of the ICD of L-selectin. A band at 5 kDa was detected which was initially thought to be the ICD of L-selectin. However, incubation with either L-685 or DAPT (Fig 5.4 E and F) did not affect the band intensity. It needs to be taken into consideration that highly concentrated protein lysates from 1 x 10^6 Molt3 T cells were run on a 16 % tricine gel. Conceivably, the band at 5 kDa could be a smeared band reminiscing from the MP product at 8 kDa due to poor running of the lysate.

We have previously seen a non-reproducible 13 kDa fragment of L-selectin in Molt3 T cells that was cleared after inhibition of ADAM 17 and γ-secretase (Fig 5.4 B and C), we hypothesised that this band represents a post-transnationally modified form of the cleaved L-selectin ICD. I initially hypothesised that the 13 kDa band represents a monoubiquitinated ICD of L-selectin. Monoubiquitination of cytosolic proteins allows entry to the nucleus where they act as gene transcriptional factors (Huang and D'Andrea, 2006). Monoubiquitination of the L-selectin ICD may induce trafficking to the nucleus. However, ubiquitination of L-selectin may initiate degradation proteasome as seen for Notch (Oberg *et al* 2001; Gupta-Rossi*, et al.* 2001, Fryer*, et al.* 2004). Rapid degradation would verify the non-reproducibility of the 13 kDa fragment. However, proteomic analysis has only shown one ubiquitin site at K78 in the ectodomain of L-selectin (Mertins, *et al*. 2013) which could suggest that the ICD is not monoubiquitinated after PS1 proteolysis of the MP product. Further experiments would need to be performed to determine whether the ICD of L-selectin is monoubiquitinated after proteolysis. TCR-activated Molt3 T cells could be co-transfected with non-tagged L-selectin and HA-tagged ubiquitin, directly lysed in Laemmli buffer and then incubated with anti-HA magnetic beads to pull down ubiquitin. Western blot analysis could then be performed to monitor detection of non-tagged L-selectin cleaved

fragments using a C terminal CA21 antibody, which binds the C-terminal 8 amino acids of the ICD.

Rzeniewicz *et al* showed that Ser^{364} and Ser^{367} in the L-selectin ICD are both phosphorylated after cell activation (Rzeniewicz, *et al*. 2015). Potentially, this 13 kDa band could also represent a phosphorylated form of the cleaved L-selectin ICD. SDS in the reducing buffer disrupts the tertiary structure in proteins by breaking disulphide bonds generating linear polypeptides. Subsequently, SDS evenly coats these linear polypeptides with a negative charge allowing all proteins to have similar mass to charge ratios where the rate of migration during electrophoresis is effectively determined by molecular weight. The introduction negatively charged phosphate groups to Ser^{364} and Ser^{367} could interfere with SDS-protein interactions modifying the mass to charge ratio which would affect the rate of migration for the cleaved ICD clarifying why the band is detected at a higher molecular weight of 13 kDa. To determine whether the 13 kDa band represents a phosphorylated form of the cleaved ICD of L-selectin, TCR-activated Molt3 T cells could be lysed in the presence of a serine phosphatase inhibitor such as calyculin A (Harhaj, *et al*. 1997) to enrich this fragment followed by pull down using cobalt-coated dynabeads to bind the His tag of L-selectin. Pulled down L-selectin would then be immunoblotted with an anti-phosphoserine antibody to detect the phosphorylated cleaved fragments of L-selectin.

6. Mutating L-selectin causing resistance to intramembrane proteolysis by PS1

6.1 Introduction

Previous chapters described intramembrane proteolysis of L-selectin and discussed evidence from Ann Ager's laboratory that cleavable L-selectin clears virus infection better than non-cleavable L-selectin, leading to the hypothesis that this may be driven by the short lived γ-secretase product described in this thesis (section 5.3).

In order to be able to address this hypothesis experimentally, I wanted to mutate potential γ-secretase site in the L-selectin transmembrane sequence to generate mutants that resist γ-secretase dependent proteolysis. These mutants can then later be used in virus clearance assays to answer the question above.

Similar mutations have been described for other type I transmembrane proteins such as Trop-2 where valine (Val) 286 to lysine (Lys) (V286K) mutations in the Trop-2 transmembrane sequence cause loss of PS1 dependent cleavage (Stoyanova*, et al.* 2012) and loss of function of Trop-2. Based on this work, a similar point mutation was introduced into the transmembrane region of L-selectin, where isoleucines (Ile) 351 or 352 were mutated to Lys (I351K or I352K L-selectin). I hypothesised that positively charged lysine would induce electrostatic interactions with negatively charged phospholipids at the lipid bilayer (Fig 6.1 A) In collaboration with Pierre Rizkallah (Cardiff University) We also mutated Ile^{351} to tryptophan (Trp). Isoleucine contains a hydrocarbon side chain, in contrast, tryptophan possess a bulky indole ring (Fig 6.1 B). I argued that the indole ring of tryptophan

would sterically hinder the equally bulky benzyl group of neighbouring phenylalanine at residue 350 changing the structure of the transmembrane region of L-selectin (Fig 6.1 C). Change in structure of I351K, I352K or I351W L-selectin potentially hides the PS1 cleavage site or disrupts enzyme substrate complexes. Additionally, this structural conformation change may sterically hinder L-selectin from entering the active site cleft of PS1 preventing intramembrane proteolysis.

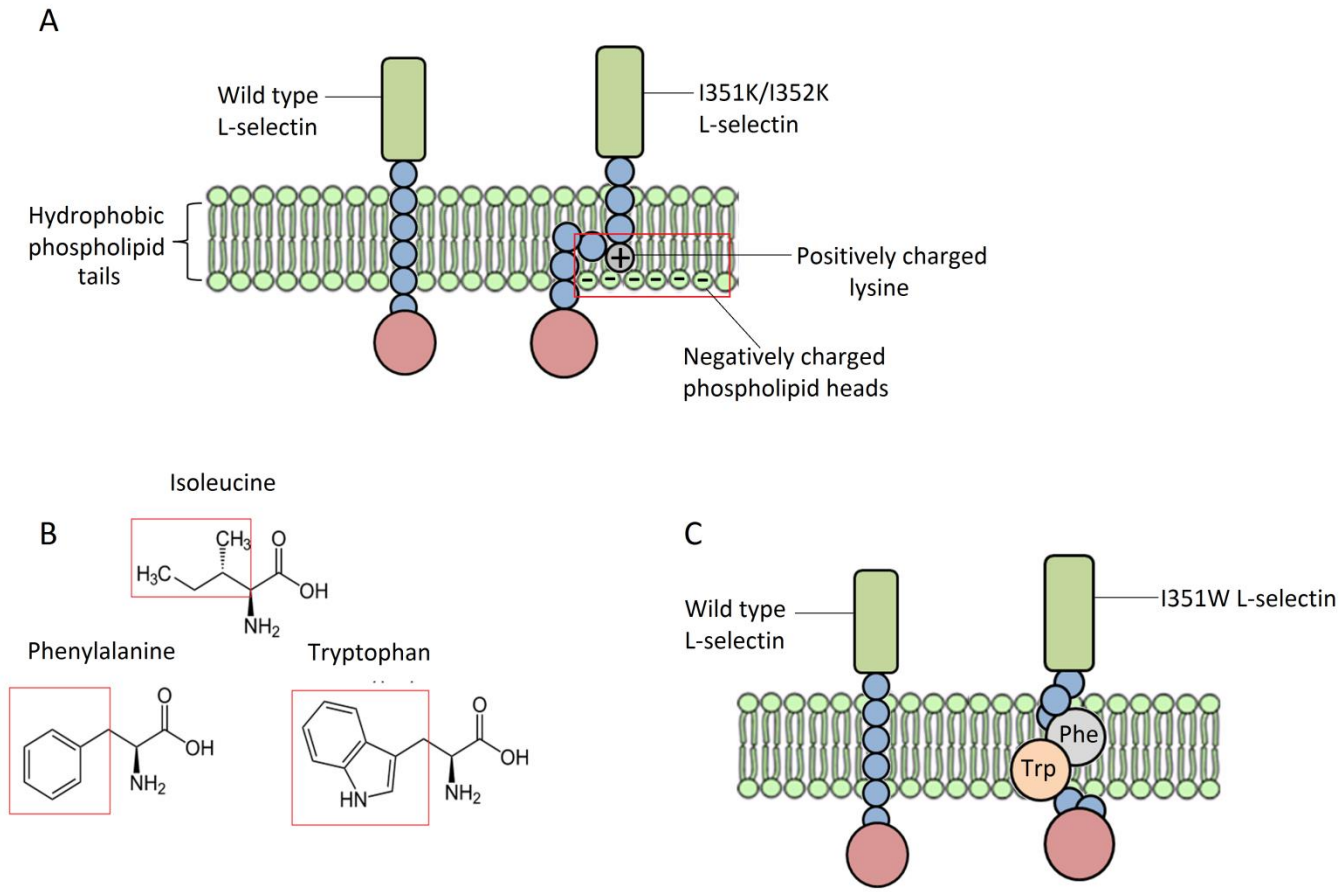

Figure 6.1: Model showing the structural changes of L-selectin mutants. (A) Introduction of positively charged lysine at residue 351 or 352 in the transmembrane region of L-selectin would repel the hydrophobic phospholipid tails of the lipid bilayer and interact with negatively charged phospholipids heads at the surface of the membrane (shown in red box). Consequently, the transmembrane region of L-selectin changes structure burying the PS1 cleavage site causing resistance to intramembrane proteolysis. (B) Isoleucine contains a hydrocarbon side chain. In contrast both tryptophan and phenylalanine contain large bulky side chains. Specifically, phenylalanine possesses an indole ring and tryptophan comprises a benzyl group. Side chains are illustrated in red boxes. (C) The I351W mutation would cause phenylalanine and tryptophan to be positioned adjacent to one another at residues 350 and 351 respectively. The large bulky side chains of phenylalanine and tryptophan would sterically hinder one another causing the structure of the transmembrane of L-selectin to change. Change in structure would disrupt substrate enzyme complexes or prevents L-selectin from entering the active site cleft of PS1 due to steric hindrance.

6.1.1 Aims of the chapter

- To generate a mutant of L-selectin resistant to intramembrane proteolysis by PS1 causing accumulation of the MP product and allowing future analysis of the role of the PS1 product in viral clearance models.

6.2 Generation of Molt3 T cells expressing V5 His I352K mutated L-selectin

I previously generated a pcDNA5 plasmid containing I352K L-selectin V5 His during my MRes studies. A PCR was used to amplify the insert (Fig 6.2 A) which was then cloned into a linearized pSxW plasmid (Fig 6.2 B) using the In-fusion cloning technique (Fig 3.4). A BamHI restriction digest confirmed that the pSxW plasmid contained the insert I352K L-selectin V5 His at 1281 bp which was absent in the original template plasmid (Fig 6.2 C)

The plasmid was sent for sequencing, confirming that the I352K mutation has been introduced.

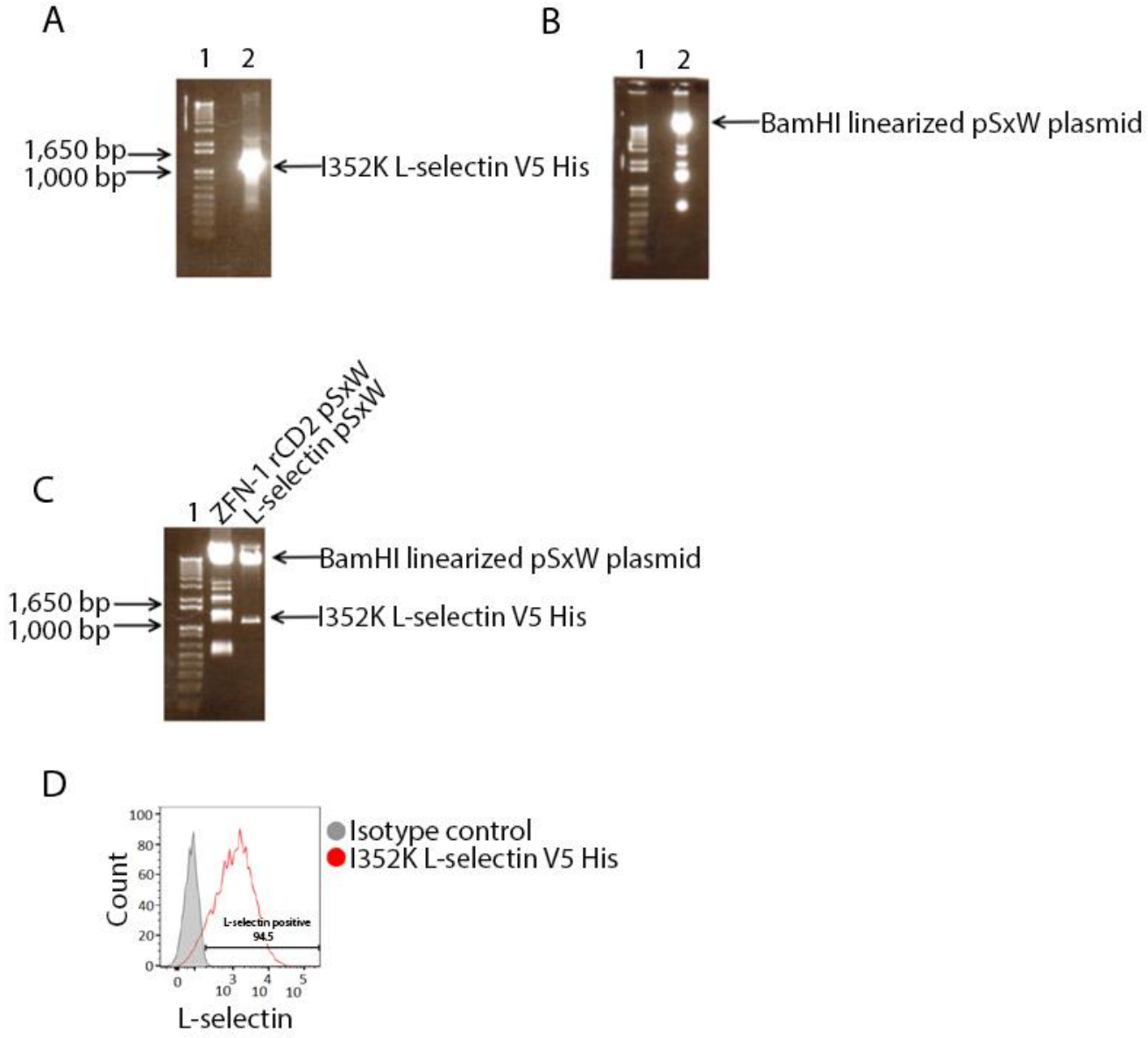

Figure 6.2: Generation of Molt3 T cells stably expressing I352K L-selectin. (A-C) The production of a pSxW plasmid expressing DNA for V5 His I352K L-selectin. Lane 1 of all the images represents the 1 kb plus DNA ladder (A) PCR amplification of V5 His I352K L-selectin. Lane 2 shows PCR amplified V5 His I352K L-selectin (1184 bp). (B) BamHI digest of pSxW plasmid. Lane 2 shows BamHI digest of the pSxW plasmid originally expressing ZFN-1 and rCD2. BamHI linearized the pSxW plasmid removing ZFN-1 and rCD2. This generated a linearized pSxW plasmid at 8942 bp. (C) Miniprep DNA isolated from carbenicillin selected DH5 α colonies transformed with pSxW-I352K L-selectin plasmid were digested with BamHI to confirm expression of the I352K L-selectin insert. Lane 2 represents the original pSxW plasmid digested with BamHI. Lane 3 represents pSxW plasmid containing the I352K L-selectin insert at 1173 bp. (D) Lentivirally transduced Molt3 T cells stably express high levels of I352K L-selectin (red peak); there was no overlap with the isotype control (grey peak).

Molt3 T cells were transduced with a pLentivirus preparation encoding I352K L-selectin. After 48 h post transduction, Molt3 T cells were analysed using flow cytometry analysis which showed high levels of expression for I352K L-selectin (Fig 6.2 D).

6.3 Determining if I352K L-selectin is resistant to PS1 proteolysis

To ensure that I352K L-selectin was expressed at the cell surface and susceptible to ectodomain proteolysis by ADAM 17 following activation of the T cell receptor, flow cytometry and ELISA were used to monitor cell surface expression and soluble L-selectin levels in media. Levels of proteolysis were compared to WT L-selectin and the non-sheddable ΔM-N mutant. L-685 or DMSO treated Molt3 T cells expressing WT, I352K or ΔM-N L-selectin were incubated using anti-CD3/CD28 or IgG control dynabeads (Fig 6.3 A-E).

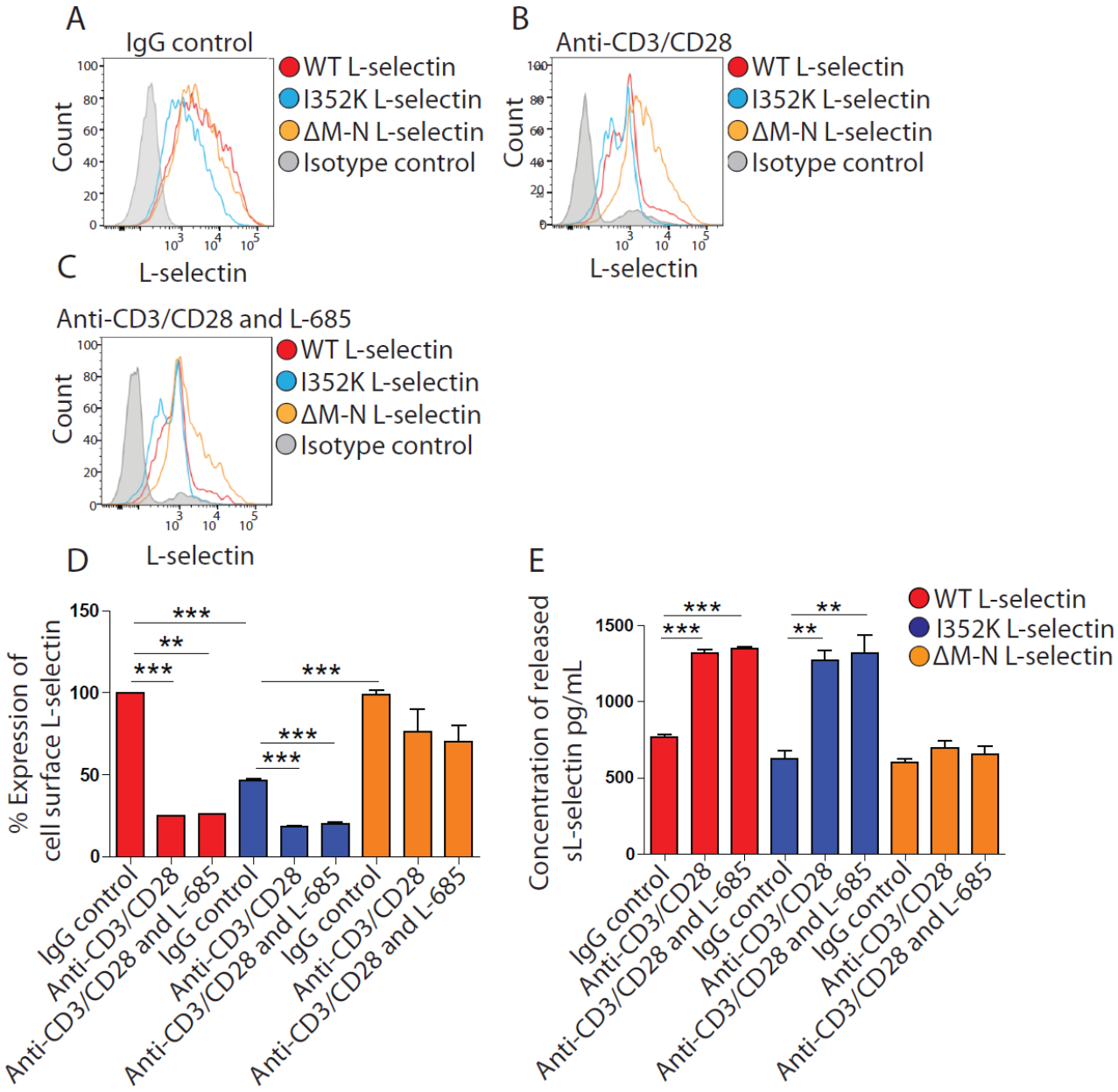
A
IgG control
Count
L-selectin
WT L-selectin
I352K L-selectin
ΔM-N L-selectin
Isotype control
B
Anti-CD3/CD28
C
Anti-CD3/CD28 and L-685
D
% Expression of cell surface L-selectin
E
Concentration of released sL-selectin pg/mL
IgG control
Anti-CD3/CD28
Anti-CD3/CD28 and L-685

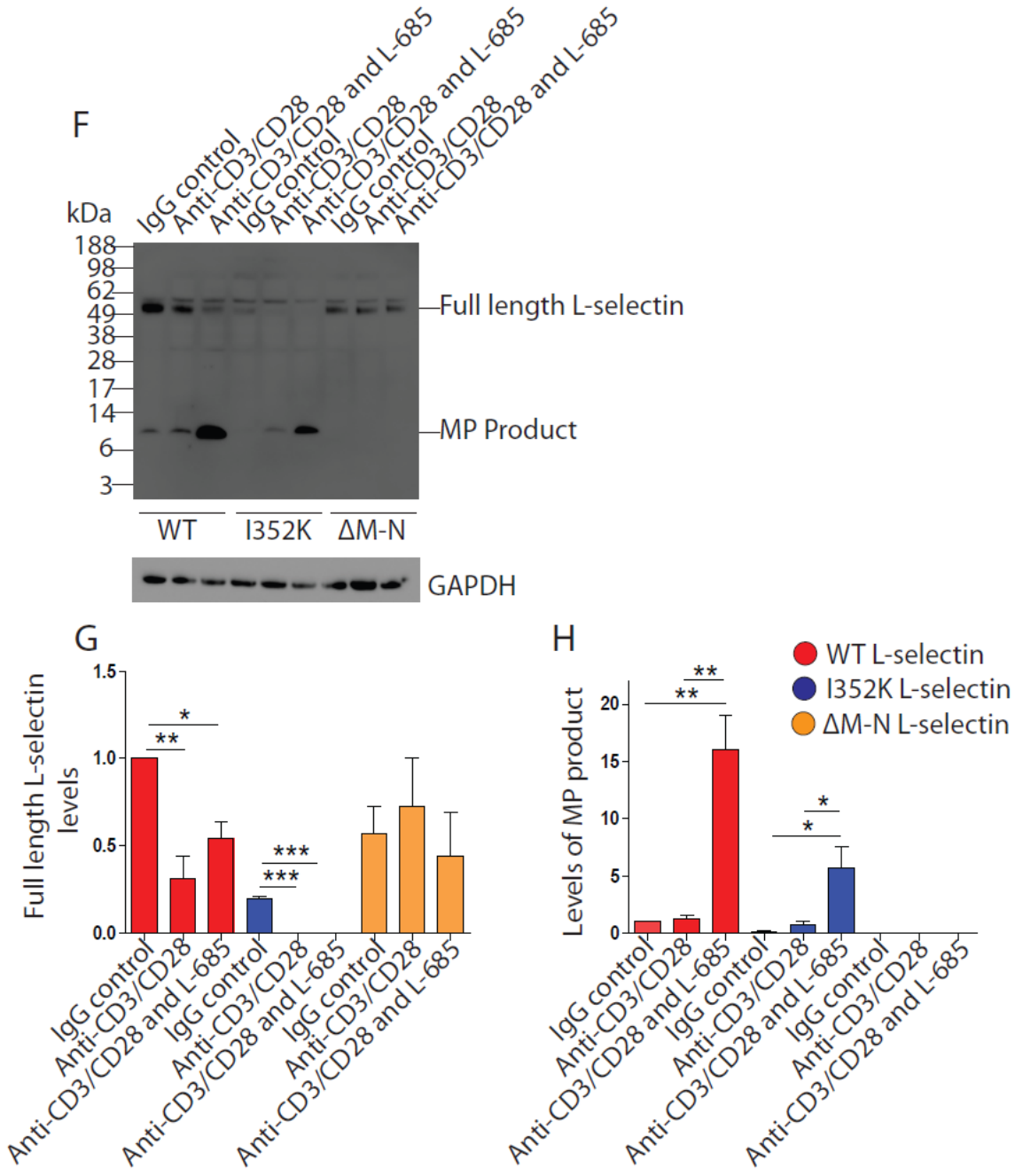

Figure 6.3: I352K L-selectin does not show resistance to PS1 proteolysis. (A-C) L-685 or DMSO treated Molt3 T cells expressing WT, I352K or ΔM-N L-selectin were incubated with anti-CD3/CD28 or IgG control dynabeads for 1 h. (D) The percentage expression of cell surface L-selectin was calculated from three independent experiments (n=3). (E) Histograms show release of soluble (sL-selectin) based on the mean value of three independent experiments, ± SD, ** P <0.05, *** P <0.05. (F) A subset of T cells was used for western blot analysis. (G and H) Histograms show levels of full length (G) or MP product (H) compared to non-TCR stimulated Molt3 T cells based on the mean of three independent experiments n=3, SD ±, *P <0.05, **P <0.05. A one-way ANOVA with post-hoc Tukey test was used for statistical analysis.

Resting T cells showed similar levels of cell surface WT and ΔM-N L-selectin. However, expression of the I352K L-selectin was 50 % lower (Fig 6.3 A and D). Flow cytometry and western blot analysis showed that levels of full length WT and I352K L-selectin decreased after TCR stimulation, regardless of L-685 treatment (Fig 6.3 B, C, D, F, G). TCR-activated T cells also showed a 1.7 fold and 1.8 fold increase of released sL-selectin for WT and I352K L-selectin respectively (Fig 6.3 E). ΔM-N L-selectin was resistant to proteolysis as expected (Fig 6.3 B, C, D, E, F, G). These results showed that I352K L-selectin was present at the cell surface and cleaved by ADAM 17 in response to TCR activation.

To determine the amount of MP product produced western blot analysis was performed. The MP product of WT and I352K L-selectin were detected in resting and TCR-activated T cells. The MP product was not detected in lysates from ΔM-N L-selectin expressing cells confirming its resistance to ectodomain proteolysis (Fig 6.3 F). Incubation of TCR-activated T cells with L-685 caused a 17-fold and 6-fold increase of MP product levels for WT and I352K L-selectin respectively (Fig 6.3 F and H). TCR stimulation therefore caused PS1 dependent proteolysis of I352K L-selectin which was inhibited by L-685 leading to enrichment of the MP product.

6.4 Determining if I351W or I351K mutated L-selectin is resistant to PS1 proteolysis

Based on our data in section 6.3, Pierre Rizkallah (Cardiff University) suggested mutating Ile at residue 351 to Trp (I351W); the bulky side chains of Trp^{351} and neighbouring Phe^{350} would cause a structural change in the L-selectin transmembrane region due to sterical hindrance between these amino acids. We also mutated Ile^{351} to Lys (I351K) to determine if positively charged lysine at this position would show more resistance to PS1 proteolysis (Fig 6.4).

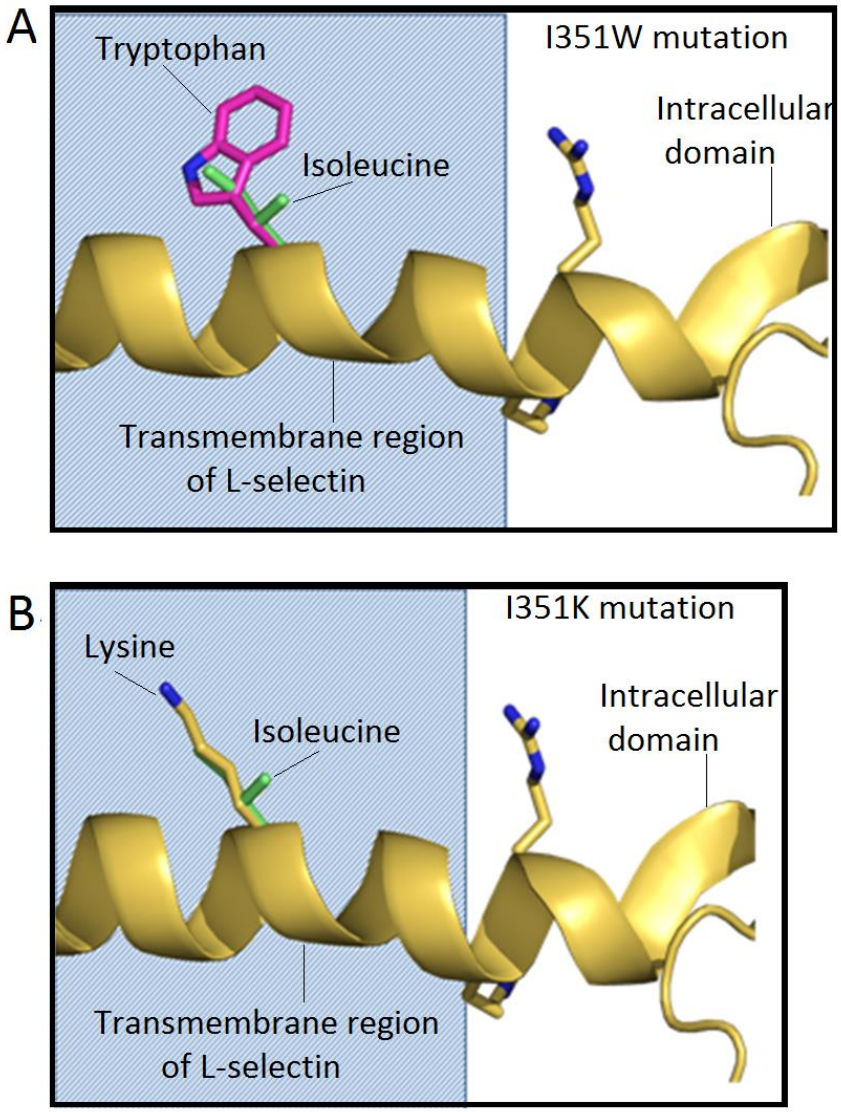

Figure 6.4: Structural models representing I351W and I351K mutated L-selectin. (A) Structural model for I351W L-selectin. Isoleucine (in green) at residue 351 in the transmembrane region of L-selectin is mutated to tryptophan (in pink). The hydrocarbon side group of isoleucine is replaced with a bulky indole ring which hypothetically causes steric hindrance to neighbouring residues. (B) Structural model of I351K L-selectin. Isoleucine (in green) at residue 351 is mutated to lysine (in yellow and blue). Replacement of hydrophobic isoleucine to a positively charged lysine likely repels the other hydrophobic residues in the transmembrane region of L-selectin and also the lipid bilayer (in blue) causing structural changes. Change of structure at the transmembrane region of both I351W and I351K L-selectin likely hides the PS1 cleavage site causing resistance to intramembrane proteolysis. Models were generated by Pierre Rizkallah (Cardiff University).

Rosie Collings (PTY student, Cardiff University) performed site directed mutagenesis to generate pcDNA5 plasmids expressing V5 His I351W and I351K mutated L-selectin. Plasmids were sent for sequencing, which confirmed that mutations were introduced correctly.

PS1 resistance of I351K and I351W L-selectin was tested in WT MEF cells. Transfected WT MEF cells were incubated with DMSO or L-685 (Fig 6.5).

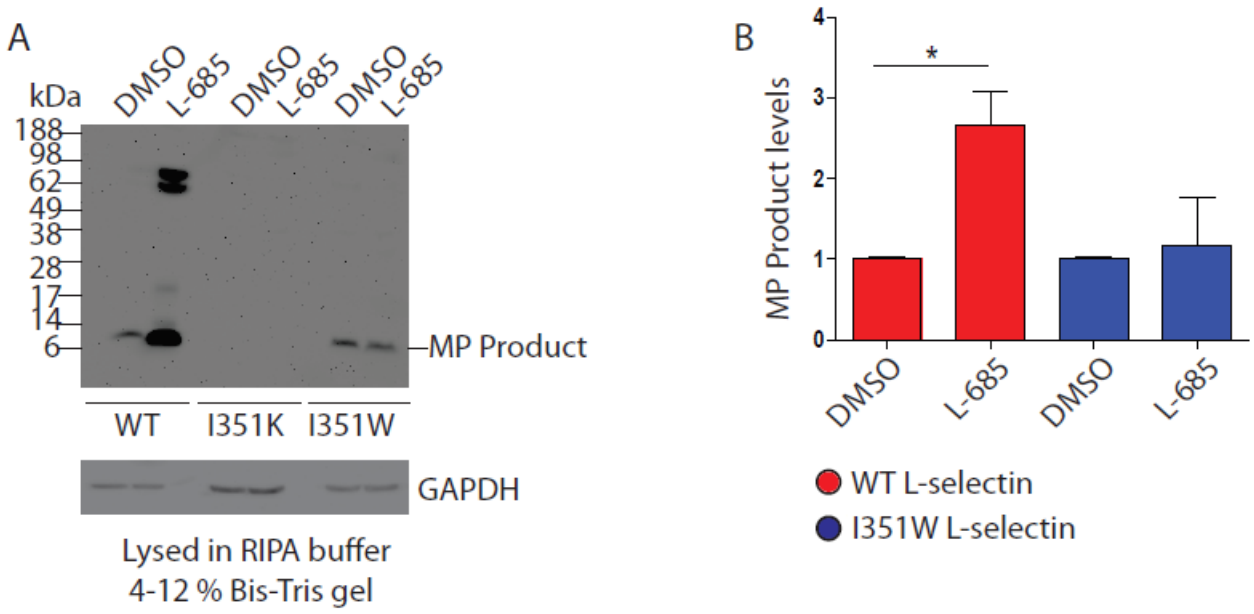

Figure 6.5: I351W L-selectin shows resistance to PS1 proteolysis in MEF cells. (A) WT MEF cells were transiently transfected with WT, I351W or I351K L-selectin V5 His. MEF cells were incubated with DMSO or L-685 for 1 h. (B) Histograms shows levels of MP product in DMSO and L-685 treated MEF cells based on the mean value of three independent experiments n=3, ± SD, *P<0.05. A one-way ANOVA with post-hoc Tukey test was used for statistical analysis.

Studies performed by Rosie Collings firstly showed that I351K L-selectin expression was below the detection limit (Fig 6.5 A). I suggested that the I351K mutation caused structural changes in L-selectin likely resulting in lysosomal/proteasomal degradation. The MP product of both WT and I351W L-selectin were detected in both DMSO and L-685 treated MEF cells. Two bands for full length L-selectin were also detected between 62 and 98 kDa in L-685 treated MEF cells expressing WT L-selectin (Fig 6.5 A).

The MP product of WT L-selectin increased 2.7-fold after L-685 treatment in comparison to the DMSO control. In contrast, the I351W MP product was stable and levels were identical in DMSO or L-685 treated conditions (Fig 6.5 B). Therefore I351W L-selectin was resistant to PS1 proteolysis.

Following transient transfection analysis the I351W mutant was shown to resist γ-secretase dependent proteolysis, thus I351W L-selectin virus was produced and Molt3 T cells was transduced with virus for further analysis. V5 His I351W L-selectin DNA was inserted into a pSxW plasmid using In-fusion (Fig 3.4). Molt3 T cells stably expressing high levels of I351W L-selectin were generated by pLentiviral transduction as seen by flow cytometry (Fig 6.6 A).

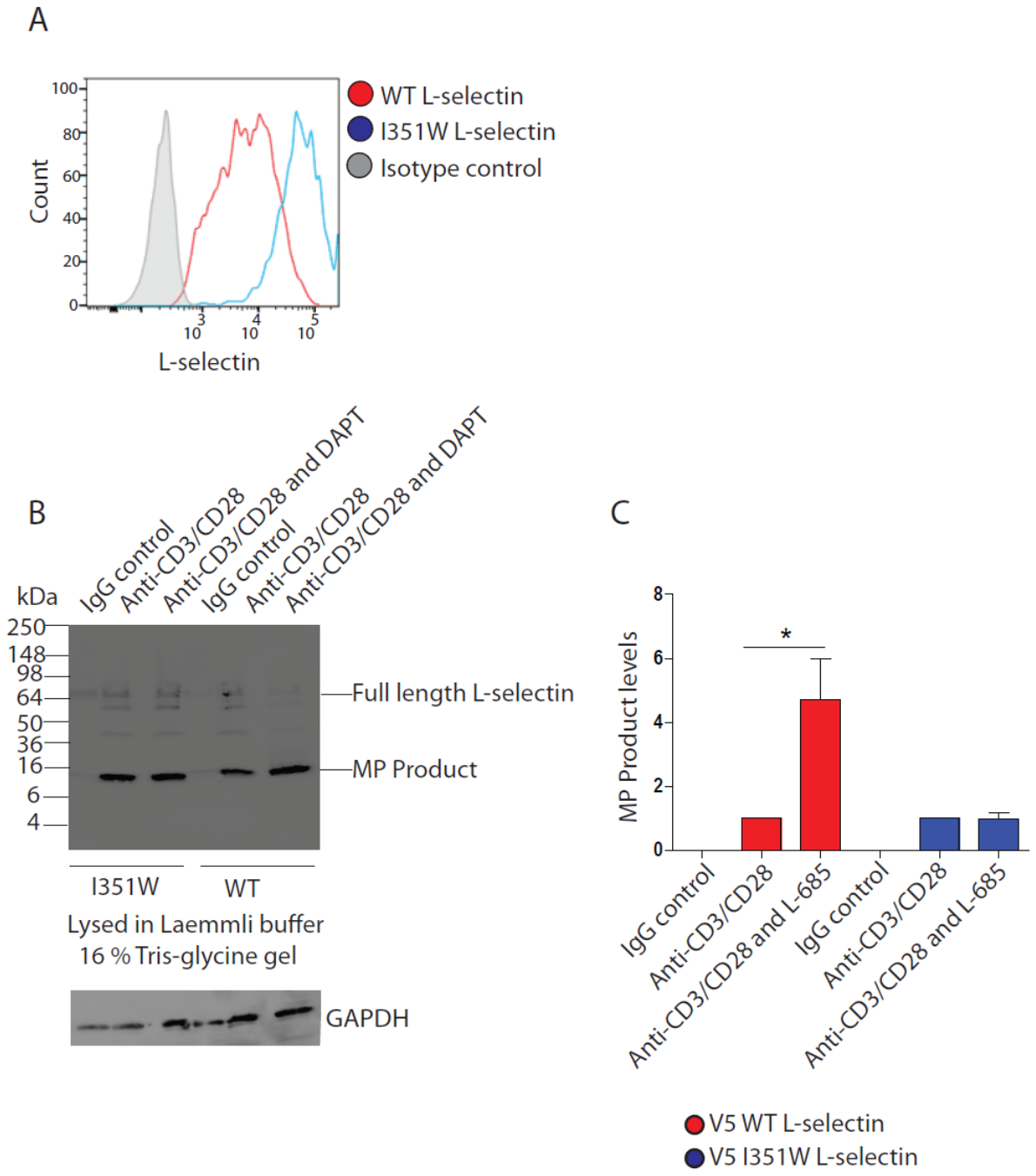

Figure 6.6: I351W L-selectin shows resistance to PS1 proteolysis after TCR-activation. (A) Lentivirally transduced Molt3 T cells shows cell surface expression for both WT (in red) and I351W L-selectin (in blue) which does not overlap with the isotype control (in grey). (B) DMSO or DAPT treated Molt3 T cells stably expressing WT or I351W L-selectin were incubated with anti-CD3/CD28 or IgG control dynabeads for 15 min. (C) Histograms shows levels of MP product in DMSO and L-685 treated MEF cells based on the mean value of three independent experiments n=3, ± SD, *P<0.05. A one-way ANOVA with post-hoc Tukey test was used for statistical analysis.

DMSO or DAPT treated Molt3 T cells expressing WT or I351W L-selectin were incubated with anti-CD3/CD28 or IgG control dynabeads for 15 min and directly lysed in Laemmli buffer and analysed by western blotting. Full length L-selectin at 50 to 64 kDa and the MP product at 8 kDa were detected (Fig 6.6 B). Levels for the MP product of WT L-selectin in TCR-activated T cells increased 4.8-fold after DAPT treatment (Fig 6.6 C). In contrast, the MP product levels of I351W L-selectin were stable. This result illustrated that I351W L-selectin was resistant to PS1 proteolysis following TCR activation.

6.5 Discussion

In this chapter, I aimed to generate a mutant of L-selectin that was expressed at the cell membrane and normally processed by ADAM 17, but resistant to PS1 dependent proteolysis. Using site directed mutagenesis, I mutated Ile^{351} or Ile^{352} in the transmembrane region of L-selectin to Lys (I351K or I352K) and argued that positively charged lysine would bind negatively charged phospholipids in the lipid bilayer burying the PS1 cleavage site (Fig 6.1 A). Ile^{351} was also mutated to Trp (I351W), where I suggested that the bulky side chains of both Trp^{351} and neighbouring Phe^{350} would sterically hinder one another resulting with a structural change in the transmembrane region of L-selectin (Fig 6.1 B). My data showed that only I351W L-selectin generated the same level of resistance to PS1 proteolysis in both transfected MEF (Fig 6.5) and Molt3 T cells (Fig 6.6) as the pharmacological inhibitor L-685. Together, this chapter illustrates that Ile^{351} in the transmembrane region of L-selectin is important for PS1 proteolysis. Furthermore, mutating Ile^{351} to an amino acid with a bulkier side chain interrupts PS1 proteolysis by inducing structural changes in the transmembrane region of L-selectin.

I initially mutated Ile^{352} to Lys (I352K) and argued that a positively charged residue in the hydrophobic transmembrane region of L-selectin would cause structural changes burying the PS1 cleavage site (Fig 6.1 A) and data confirmed that the I352K mutation was expressed at the cell surface and cleaved by ADAM 17 (Fig 6.3 A-E) in response to TCR stimulation (Fig 6.3 F and H). However, MP product levels of I352K L-selectin increased 6-fold in L-685 treated TCR-activated T cells indicating that PS1 proteolysis was occurring (Fig 6.3 F and H). This result showed that the I352K mutation did not cause resistance to PS1 proteolysis.

Expression of I352K L-selectin was 50 % lower in resting T cells when compared to WT and ΔM-N L-selectin (Fig 6.3 A and D). However, amounts of released sL-selectin between WT and I352K L-selectin were similar in both resting and TCR-activated conditions (Fig 6.3 E). Potentially, I352K L-selectin was more susceptible to ADAM 17 proteolysis than WT, because CaM interacts with Ile^{352} and Ile^{354} in the transmembrane region of L-selectin alongside Leu^{358} in the ICD (Gifford*, et al.* 2012). L-selectin/CaM complexes resist ectodomain proteolysis by ADAM 17 (Kahn*, et al.* 1998; Gifford*, et al.* 2012), and thus, mutating Ile^{352} to Lys (I352K) likely disrupts this interaction encouraging ADAM 17 proteolysis. However, the concentration of pLentivirus used to stably transduce Molt3 T cells with WT, I352K or ΔM-N L-selectin was not quantified. It is likely that Molt3 T cells were transduced with lower concentrations of pLentivirus containing I352K L-selectin in comparison to WT and ΔM-N. In future experiments, Molt3 T cells would need to be transduced with equal amounts of quantified pLentivirus to ensure the MOI is normalized. Molt3 T cells expressing equal levels of WT, I352K and ΔM-N L-selectin could then be stimulated with anti-CD3/CD28 dynabeads to solidify our initial argument that the I352K mutation sensitizes L-selectin to ADAM 17-proteolysis. Additionally, WT, I352K and ΔM-N L-selectin could be pulled down using cobalt ion coated dynabeads and immunoblotted for CaM. This would determine whether the I352K mutation elevates ectodomain proteolysis by disrupting interactions with CaM.

Therefore, the mutation of I351K was generated, as the mutation was outside the L-selectin/CaM interaction site. The mutant was analysed in WT MEF cells for ADAM 17 and γ-secretase dependent processing. However, the expression level was below the detection limit of western blot analysis (6.5 A). Membrane proteins use their TMDs as a stop transfer signal sequence to orientate themselves in the plasma membrane (Blobel*, et al.* 1979). Likely, structural changes in the transmembrane region of I351K L-selectin either affects the

stop transfer signal sequence preventing insertion in the plasma membrane or potentially, mis-folded and aggregated L-selectin would be degraded. Mis-folded, aggregated proteins are ubiquitinated and degraded by the autophagy-lysosomal pathway (Eskelinen*, et al.* 2009; Hara*, et al.* 2006; Komatsu*, et al.* 2006). Potentially, I351K and to a lesser extent I352K L-selectin are also degraded after transcription leading to reduced expression in transfected cells.

Pierre Rizkallah (Cardiff University) suggested mutating Ile^{351} to Trp (I351W) to conserve the hydrophobic mature of the transmembrane sequence of L-selectin at this position. The bulky side chains of Trp^{351} and of neighbouring Phe^{350} would sterically hinder one another modulating the structure of the transmembrane region of L-selectin. Our data shows that I351W L-selectin was expressed at the cell membrane, showing increased cell surface expression levels and importantly that the MP-product generated in response to T cell receptor activation showed increased stability (Fig 6.5). Consequently, I have generated a construct of L-selectin which potentially does not release an ICD after TCR stimulation.

Understanding how I351W L-selectin is PS1 resistant would allow us to learn how substrates are proteolyzed by PS1. Hypothetically, a structural change in I351W L-selectin either prevents entry into the PS1 active site, or buries the cleavage site abrogating proteolysis (Fig 6.7).

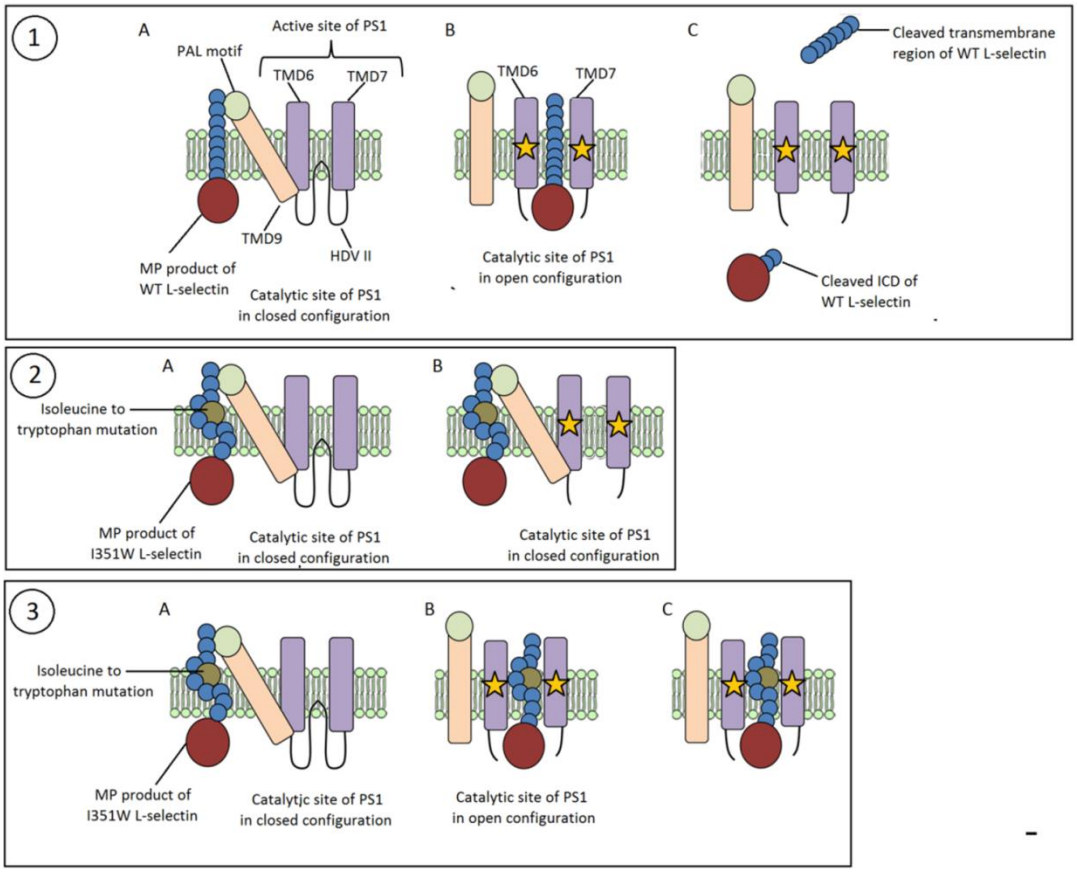

Figure 6.7: Two models illustrating the mechanisms of I351W L-selectin resistance to PS1 proteolysis. (1) (A). TMDs 6 and 7 form the active site of PS-1 (PS1). In resting T cells, the active site of PS1 is in a closed configuration where hydrophobic domain VII (HDVII) is positioned between TMD6 and 7. TMD9 of PS1 acts as a gate of the catalytic site, regulating lateral migration of substrates. (B) After TCR stimulation PS1 induces endoproteolysis removing HDVII from the PS1 active site. TCR stimulation also initiates ectodomain proteolysis of L-selectin, allowing the MP product to bind TMD9 of PS1. TMD9 then rotates, which is governed by a proline-alanine-leucine (PAL) motif, allowing entry of the MP product to the active site. (C) Aspartate ($Asp^{257}$and Asp^{358}) (represented as yellow stars) in TMD6 and 7 respectively cause PS1 proteolysis of the MP product releasing the intracellular domain (ICD) to the cytoplasm. (2) (A) The isoleucine to tryptophan mutation of I351W L-selectin induces a structural conformational change at the transmembrane region of the MP product. Consequently, TMD9 does not recognise the structure of the MP product and does not shift. The MP product of I351W L-selectin does not enter the active site of PS1. (3) (A). Alternatively, the TMD9 does recognise the transmembrane region of I351W L-selectin. (B) The MP product of I351W L-selectin enters the active site by lateral diffusion. (C) However, structural changes due to the I351W mutation buries the PS1 cleavage site in the transmembrane region of the MP product from Asp residues in TMD6 and 7 and intramembrane proteolysis does not occur (Tolia*, et al.* 2008; Sato*, et al.* 2008; Fukumori*, et al.* 2010).

7. General discussion and future work

7.1 Summary of the results

The proteins studied in my thesis (Fig. 7.1A) show that in a resting T cell, L-selectin interacts with ADAM 17, PS1 and nicastrin (Fig 7.1 B). After TCR stimulation, ADAM 17 is activated and rapidly proteolyzes L-selectin at the ectodomain generating an MP product and then dissociates. The MP product remains bound to nicastrin and PS1 (Fig 7.1 C). TCR activation then induces endoproteolysis of PS1 which generates a catalytically active CTF that proteolyzes the MP product in the transmembrane region releasing the L-selectin ICD. The released L-selectin ICD is potentially monoubiquitinated initiating downstream signalling (Fig 7.1 D).

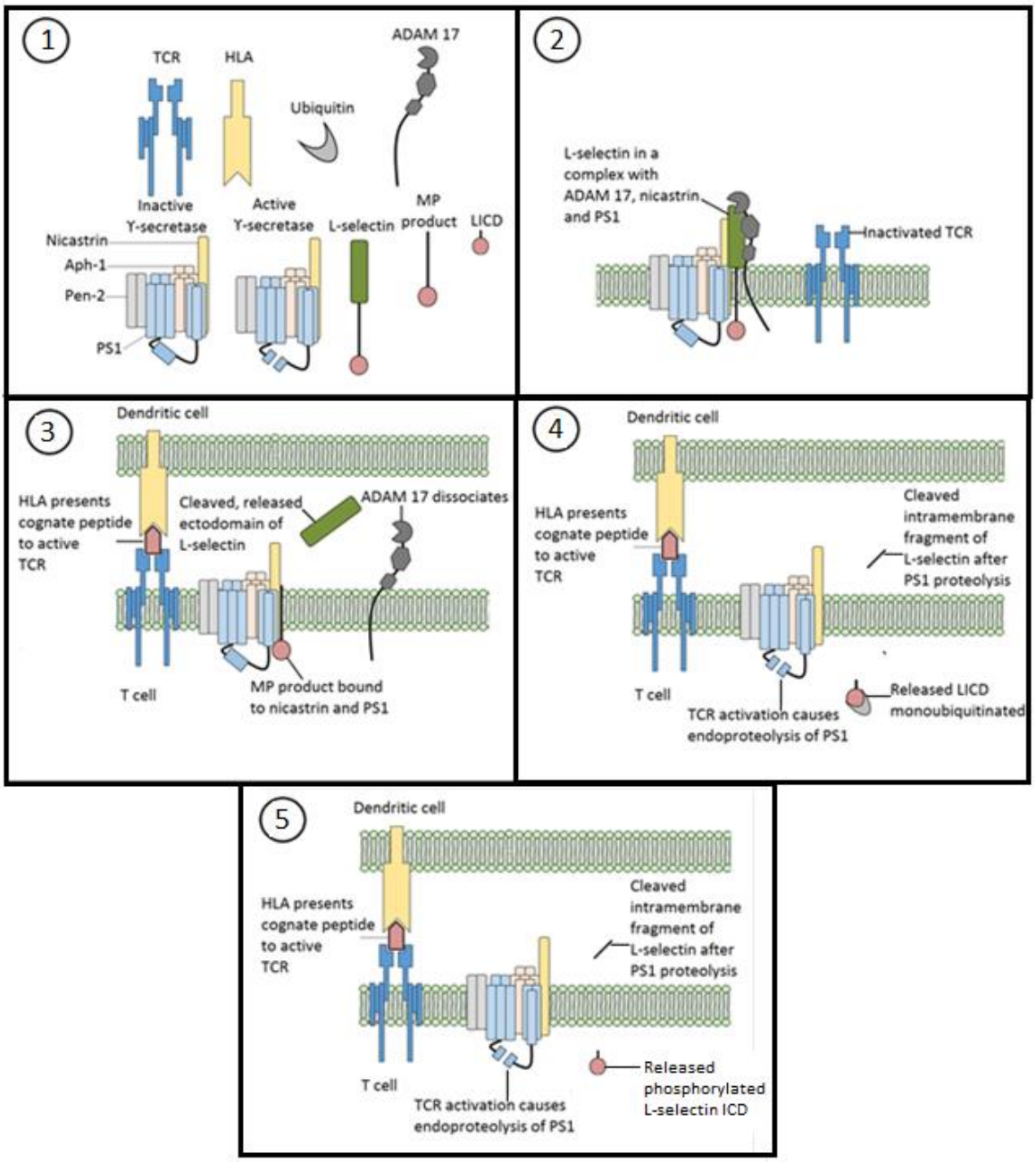

Figure 7.1: Summary of all findings and further hypothesises during my PhD. (1) Labelled proteins as illustrated in summary. (2) In a resting T cell, L-selectin forms a complex with PS1, nicastrin and ADAM 17. All enzymes are inactivated and proteolysis does not occur. (3) Human leucocyte antigen presents cognate peptide to activate the TCR. After TCR activation, ADAM 17 proteolyzes L-selectin at the ectodomain and dissociates. This generates an MP product still bound to nicastrin and PS1. (4) TCR activation also induces endoproteolysis of PS1 causing separation of the N and C termini. Activated PS1 then cleaves the MP product at the transmembrane region releasing the L-selectin ICD. The L-selectin ICD is potentially monoubiquitinated, which regulates further analysis to study the function of this fragment. (5) Alternatively, the cleaved L-selectin ICD is not monoubiquitinated, but instead released in the intracellular compartment after phosphorylation at Ser^{364} and Ser^{367}.

7.2 Limitations

During my studies, I found that ΔM-N L-selectin resisted ADAM 17-proteolysis in comparison WT L-selectin (Fig 3.9). Also, cell surface expression of I352K L-selectin was 50 % lower in resting T cells than WT L-selectin, yet released similar levels of the soluble ECD after TCR-activation (Fig 6.3, D and E). This possibly indicated that the I352K mutation sensitized L-selectin to ADAM 17 dependent proteolysis. Additionally, I351W L-selectin showed resistance to PS1 dependent proteolysis in comparison to WT L-selectin in both MEF cells (Fig 6.5) and TCR-activated Molt3 T cells (Fig 6.6, B and C). However, cell surface expression of WT L-selectin was significantly different to ΔM-N (Fig 3.6, A and C), I352K (Fig 6.3, A) and I351W (Fig 6.6, A) L-selectin after lentiviral transduction, which potentially influenced the outcomes from these studies. Unequal cell surface expression of WT, ΔM-N, I352K and I351W L-selectin is likely caused by a variance in the multiplicity of infection (MOI). The MOI is defined as the number of lentiviral particles used to infect each cell. For my study, the concentration of lentivirus was not quantified which consequently would have induced variance of the MOI of each cell line causing a difference in the efficiency of lentiviral transduction and cell surface expression of WT, ΔM-N, I352K and I351W L-selectin. In future work, Molt3 T cells would need to be infected with equal amounts of quantified lentivirus expressing WT, ΔM-N, I352K or I351W L-selectin. For instance, the Lenti-X p24 rapid titer kit (Takara Bio, USA) could be used to quantify lentivirus concentrations by detecting the capsid protein p24. A microtiter plate would be coated with a capture antibody against p24, where bound lentivirus would be detected using a secondary biotinylated anti-p24 antibody with streptavidin or horseradish peroxidase. The amounts of lentivirus in the sample would then be quantified against a standard curve plotted against the p24 peptide provided in the kit.

During western blot analysis, I detected full length L-selectin at 56-62 kDa, which was initially suggested as the membrane bound form (Fig 3.9, 3.10, 3.11, 4.5 A). However, during my later studies, I detected non-reproducible, higher molecular weight bands of full length L-selectin at 70 kDa to 110 kDa from Molt3 T cell lysates (Fig 5.3, A) alongside the released soluble ECD at 110 kDa from MEF cells (Fig 4.5, B). In relation to my work, Rzeniewicz *et al,* also showed detection for two bands of full length L-selectin at 50 kDa and 80 kDa whey they suggested that the higher molecular weight band was a glycosylated, membrane bound form and the lower molecular weight was a non-glycosylated intracellular form (Rzeniewicz, *et al.* 2015). Based on these findings, it is possible that full length L-selectin detected at 56-62 kDa from my Molt3 T cell and MEF cell lysates represents the non-glycosylated intracellular form and the bands at 70 to 110 kDa represent the glycosylated, membrane bound from. Future studies would need to be performed to determine whether TCR-induced ADAM 17 and PS1-proteolysis of L-selectin (Fig 5.3), alongside ADAM 17 (Fig 3.10), PS1 (Fig 5.7) and nicastrin (Fig 5.8) interactions as displayed during my studies have occurred at the membrane or intracellular region. Rzeniewicz *et al,* used Nonidet P-40 in their cell lysis buffer to solubilize membrane proteins instead of Triton-X, which was used during my studies (Rzeniewicz, *et al.* 2015). In future experiments, Molt3 T cells could be lysed in the presence of Nonidet P-40 to detect reproducible, higher molecular weight bands at 70-110 kDa for full length L-selectin. Subsequently, surface biotinylation experiments would then be performed to determine whether full length L-selectin at 56-62 kDa or 70-110 kDa is membrane bound. After biotinylation of Molt3 T cells, labelled cell surface L-selectin would be immunoprecipitated using streptavidin, followed by immunoblot analysis using anti-V5 to monitor detection for these bands.

Throughout my PhD studies, I aimed to show that ADAM 17 proteolyzes L-selectin generating an MP product which was further cleaved by PS (Fig 1.25). To accomplish this, I transfected L-selectin V5 His into WT and PS deficient MEF cells. These PS deficient MEF cells caused accumulation of the MP product in comparison to WT MEFs which showed that PS induces intramembrane proteolysis. However, detection for full length L-selectin was often below the threshold and did not increase after incubation with the wide-spectrum metalloproteinase inhibitor Ro 31-9790 (Fig 4.3 A and C). Instead, Ro 31-9790 caused increased release of the soluble ECD shown by both ELISA (Fig 4.3 G) and immunoblot analysis (Fig 4.5 B). As Ro 31-9790 only caused increased detection of the soluble ECD in the presence of ADAM 17 (Fig 4.5, B), I reasoned that L-selectin was proteolyzed by an unknown metalloproteinase in the MEF cells which was regulated by ADAM 17 activity (Fig 4.4). Western blots obtained from these PS deficient MEF cells therefore did not display my initial hypothesis for L-selectin proteolysis as ADAM 17-dependent ectodomain shedding followed by intramembrane cleavage by PS (Fig 1.25). However, pre-incubation of Molt3 T cells using Ro 31-9790 (Fig 3.7) and anti-ADAM 17 antibody (Fig 3.9) caused accumulation of full length L-selectin. Additionally, further studies in Molt3 T cells have shown loss of full length L-selectin after TCR-activation followed by PS1 proteolysis of the MP product (Fig 5.3) which correlates with my hypothesis (Fig 1.25). For future work, PS1 and/or PS2 would need to be gene silenced in Molt3 T cells expressing L-selectin V5 His. WT and PS deficient Molt3 T cells would then be incubated with the anti-ADAM 17 antibody or control (ADAM 17 D1(A12)) antibody in both resting and TCR-activated conditions to display both ADAM 17 and PS dependent proteolysis

7.3 Conclusions

7.3.1 TCR activation induces ADAM 17 and PS1 dependent proteolysis of L-selectin

Data generated from Ann Ager's laboratory has shown that TCR activation induces ADAM 17 proteolysis of L-selectin which generates an MP product comprised of a transmembrane region and 17-amino acid L-selectin ICD (Fig 3.1). For my PhD, I wanted to determine whether the MP product was further processed by PS, the catalytic subunit of γ-secretase. APP and Notch are proteolyzed by both PS1 and PS2 (Steiner*, et al.* 1999; De Strooper*, et al.* 1998; De Strooper*, et al.* 1999), whereas ErbB4 and E-cadherin are exclusively shed by PS1 (Marambaud*, et al.* 2002; Hoeing*, et al.* 2011). In this study, I wanted to learn whether the MP product of L-selectin was shed by PS1 and/or PS2. Based on time constraints and costing, I was unable to gene silence PS1 and PS2 in T cells and monitor L-selectin proteolysis after TCR activation. Instead, I used PS deficient MEF cells obtained from Professor Bart De Strooper which were complemented with PS1 and/or PS2. I found that PS1, but not PS2 expression was required for proteolysis of the L-selectin MP product (Fig 4.3 E and F). Subsequently, I wanted to determine whether TCR stimulation induces PS proteolysis of the MP product after ADAM 17 shedding. My data demonstrates for the first time that TCR stimulation induces both ADAM 17 and PS proteolysis of L-selectin. ADAM 17 proteolysis of L-selectin was rapid and occurred after 5 min TCR activation generating the MP product (Fig 5.2 D, Fig 5.3 A and C) which was further processed by PS after 15-60 min (Fig 5.3 A, E and F). I also showed that TCR activation induces endoproteolysis of PS1 generating a catalytically active CTF from 5 min to 15 min. This result illustrated that TCR

stimulation activated PS1, which proteolyzed the MP product of L-selectin. The PS generated L-selectin ICD was below the detection threshold and is outlined in section 7.2.2.

In future research, ADAM 17 and PS proteolysis of non-tagged, endogenous L-selectin could be monitored in human proliferating CD8+ T cells stimulated using anti-human CD3/CD28 dynabeads and immunoblotted using a CA21 C terminal antibody for L-selectin.

7.3.2 The L-selectin ICD is not reproducibly detected during immunoblot analysis

I attempted to optimize conditions to detect a PS1 cleaved L-selectin ICD by western blot analysis. ICDs of other type I transmembrane proteins such as AICD and NICD are also difficult to detect by western blot analysis (Pimplikar*, et al.* 2011), due to their rapid lysosomal/proteasomal degradation. Studies have compromised degradation by overexpressing synthetic peptides of AICD and NICD, which accumulate in the nucleus and act as transcriptional factors (Ellisen*, et al.* 1991; Grabher*, et al.* 2006; Cao and Sudhof, 2001; Sterner and Berger, 2000). Based on these findings, I strongly argued that the L-selectin ICD is either rapidly degraded or trafficked to a subcellular compartment which was not solubilized during cell lysis buffer lysis. A recent study showed that AICD is detectable after direct cell lysis in Laemmli buffer (Boland*, et al.* 2010) as opposed to our protocol of 35 min lysis in cell lysis buffer. I thought that direct lysis in Laemmli buffer would prevent degradation of L-selectin ICD and solubilize all subcellular compartments. TCR-activated T cells lysed under these conditions caused detection of a non-reproducible 13 kDa L-selectin fragment blocked by ADAM 17 (Fig 5.4 C) and PS1 (Fig 5.4 B) inhibition. ICD of L-selectin has an approximate molecular weight of 5 kDa and that of ubiquitin is 8 kDa. The L-selectin ICD could therefore be monoubiquitinated after PS1 proteolysis explaining this 13 kDa band.

Other ICDs such as NICD and ErbB4 (EICD) are ubiquitinated prior to proteasome degradation (Oberg*, et al.* 2001; Gupta-Rossi*, et al.* 2001; Fryer*, et al.* 2004). Additionally, monoubiquitination has also been shown to promote nuclear import of proteins such as phosphatase and tensin homolog (PTEN) (Trotman*, et al.* 2007). The L-selectin ICD contains a conserved C terminal PY motif. Studies have shown that C terminal PY motifs act as nuclear import signals for Hrp-1 and Nab-2 (Lange*, et al.* 2008) so could potentially also regulate nuclear import of L-selectin ICD. The short 17-amino acid L-selectin ICD also contains 8 positively charged residues which likely induce electrostatic interactions with the negatively charged phosphate backbone of DNA. The L-selectin ICD could be monoubiquitinated, regulating intracellular degradation and/or nuclear import. However, proteomics analysis has only shown one ubiquitin site for L-selectin at lysine 78 in the ectodomain which could suggest that the ICD is not monoubiquitinated. However, cell activation has shown to induce phosphorylation of Ser^{364} and Ser^{367} in the L-selectin ICD (Rzeniewicz, *et al*. 2015). The 13 kDa band could therefore alternatively display a phosphorylated form of the cleaved L-selectin ICD.

To facilitate detection of the L-selectin ICD, lysates should be run on 16 % polyacrylamide Tris-Tricine gels used in a longer vertical electrophoresis unit (16.5 cm X 14.5 cm) which has previously been optimized to detect small peptides (Boland*, et al.* 2010). To determine whether the L-selectin ICD is rapidly degraded, T cells should be incubated with lysosomal/proteasomal inhibitors prior to TCR-activation and directly lysed in Laemmli buffer. Additionally, lysosomes could be labelled with dextran conjugated magnetite and T cells incubated with lysosomal inhibitors preceding TCR-activation and analysed for V5 His fragments using immunoblotting to implicate or eliminate degradation of L-selectin ICD. During western blot analysis, 0.2 µM pore size PVDF membranes and 20 % methanol in the

transfer buffer can also be used to optimize transfer of the small L-selectin ICD as used during my PhD studies.

After achieving detection of the L-selectin ICD, further experiments would then be performed to monitor potential ubiquitination or phosphorylation. Firstly, to confirm whether L-selectin ICD is monoubiquitinated, TCR-activated Molt3 T cells co-transfected with HA-tagged ubiquitin and non-tagged L-selectin could be directly lysed in Laemmli buffer and later incubated with anti-HA magnetic beads to pull down ubiquitin. Immunoblot analysis would then be performed to monitor detection of L-selectin cleaved fragments using C terminal CA21 antibody. Additionally, TCR-activated Molt3 T cells could be lysed in the presence of a serine phosphatase such as calyculin A and later incubated with cobalt-ion coated dynabeads to bind the His tag of the enriched cleaved fragments of L-selectin. These cleaved fragments of L-selectin would be immunoblotted using an anti-phosphoserine antibody to monitor detection for the 13 kDa band.

7.3.3 L-selectin and ADAM 17 interaction is disrupted after TCR activation

Hartmann *et al* revealed that ADAM 10 interacts with CD44 where immortalized mouse embryonic fibroblast cells were incubated overnight with the wide spectrum metalloproteinase inhibitor GM-6001 to capture ADAM 10/CD44 complexes (Hartmann*, et al.* 2015). I used these conditions to determine whether ADAM 17 interacts with L-selectin in both resting and TCR-activated T cells. Molt3 T cells were treated overnight with Ro 31-9790 and later incubated with C1R cells pulsed with or without 10^{-4} M SLY peptide. I showed that L-selectin and ADAM 17 interact in a resting T cell and dissociate after TCR-activation (Fig 3.10). It is currently unknown whether ADAM 17 and L-selectin interact with their

ectodomains or ICDs. Understanding this would provide a biochemical insight on how TCR stimulation induces ADAM 17 dissociation from L-selectin.

7.3.3.1 ADAM 17 and L-selectin interact using their ICDs?

PMA induces ADAM 17 proteolysis of L-selectin (Kahn*, et al.* 1996; Peschon*, et al.* 1998) and activates PKC isozymes Θ and α which bind Ser^{364} and Ser^{367} in L-selectin ICD (Killian*, et al.* 2004). Killock mutated Ser^{364} and Ser^{367} to non-phosphorylatable alanine (S364A and S367A) and phospho-mimicking aspartic acid (S364D and S367D). Expectantly, phospho-mimicking S364D and S367D L-selectin would be susceptible to proteolysis, whereas non-phosphorylatable S364A and S367A L-selectin would be resistant. S367A and S367D responded as predicted, however both S364A and S364D were resistant to proteolysis (Killock*, et al.* 2010). Potentially, ADAM 17 could interact with Ser^{364} which is disrupted for both S364A and S364D L-selectin explaining resistance of proteolysis for both mutants. Additionally, Rzeniewicz *et al* later shown that phosphorylation of Ser^{364} regulates the dissociation of CaM (Rzeniewicz*, et al.* 2015). It is possible that after TCR stimulation, PKC isozymes θ and α phosphorylate Ser^{364} in L-selectin ICD regulating interaction with both CaM and ADAM 17. CaM may dissociate firstly, exposing the membrane proximal region for ADAM 17 proteolysis. ADAM 17 would then dissociate after proteolysis freeing phosphorylated Ser^{364} in the L-selectin ICD of the MP product to bind other protein partners for signalling pathways.

We have already generated L-selectin V5 His (S364A and S367A) or (S364D and S367D) double mutants expressed in a pSxW plasmid to transduce Molt3 T cells. For future experiments, mutated L-selectin from both resting and TCR-activated T cells should be pulled-down and immunoblotted for ADAM 17. I would expect only non-phosphorylatable

S364A/S367A L-selectin to interact with ADAM 17. If correct, I could immunoblot singly mutated S364A, S367A, S364D or S367D L-selectin with ADAM 17 to determine whether phosphorylation at Ser-364 or Ser-367 disrupts this interaction after TCR stimulation.

However, other residues in L-selectin and/or ADAM 17 may be phosphorylated that govern interaction such as tyrosine or threonine residues. To monitor this, WT L-selectin V5 His could be pulled down from both resting and TCR-activated T cells and immunoblots stained for anti-phospho-tyrosine and anti-phospho-threonine antibodies. Detected bands would be monitored for molecular weights corresponding to L-selectin and ADAM 17.

7.3.3.2 ADAM 17 and L-selectin interact using their ectodomains?

Recently, it has been emerged that ADAM 17 contains a 14-amino acid sequence between the MP domain and transmembrane region termed CANDIS which interacts with amino acids 317-ESRSPPAENEVSTPMQ-332 in the ectodomain of IL-6R (Düsterhöft*, et al.* 2014). Chen *et al* truncated 8-amino acids (MIKEGDYN) in the membrane proximal region of L-selectin which causes resistance to ADAM 17 proteolysis (Chen*, et al.* 1995) (Fig 1.7). I argued that amino acids MIKEGDYN in the membrane proximal region of L-selectin interact with CANDIS and hypothesised that truncation of MIKEGDYN abolishes interactions between L-selectin and ADAM 17. However, my data did not support this initial hypothesis as ΔM-N L-selectin and ADAM 17 interacted and importantly did not dissociate after TCR-activation as seen for WT L-selectin (Fig 3.10 and Fig 3.11). The MIKEGDYN region of L-selectin could regulate ADAM 17 dissociation after TCR stimulation. However, this result was from a single observation (n=1) and would need to be repeated using a positive control for TCR-activation to solidify this suggestion.

Further studies would need to be completed to determine whether ADAM 17 and L-selectin interact using their ectodomains. Düsterhöft *et al* generated a construct where only the MP domain of ADAM 17 containing CANDIS was linked to a glycosylphosphatidylinositol (GPI) anchor to the plasma membrane (MPD17plusCANDIS-GPI). MPD17plusCANDIS-GPI interacted with IL-6R during immunoprecipitation analysis confirming that enzyme/substrate complexes were formed through ectodomains. The MPD17plusCANDIS-GPI construct would be useful as the ADAM 17 ICD is truncated allowing us to monitor only ectodomain interactions between ADAM 17 and L-selectin. If the MP domain and L-selectin co-immunoprecipitate, I could then compare sequences between IL-6R and L-selectin to monitor any homologous regions which would bind CANDIS. These regions in the ectodomain of L-selectin could be mutated or truncated before monitoring interactions with MPD17plusCANDIS-GPI.

7.3.4 ϒ-secretase subunits nicastrin and PS1 interact with L-selectin in both resting and TCR-activated T cells

Nicastrin and Aph-1 are both termed as substrate binding domains of γ-secretase. Aph-1 interacts with full length γ-secretase substrates, while nicastrin uses Glu-333 to bind the exposed N terminus after ectodomain proteolysis (Chen*, et al.* 2010; Shah*, et al.* 2005; Dries*, et al.* 2009). Additionally, Xia *et al* found that both PS1 and PS2 form complexes with APP in living cells (Xia*, et al.* 1997). I monitored interactions between L-selectin, nicastrin and PS1 and preserved enzyme/substrate complexes after overnight incubation with L-685. I argued that TCR activation and ectodomain proteolysis of L-selectin were required before nicastrin and PS1 interacted with the MP product. However, my data showed that L-selectin interacted with both nicastrin and PS1 in both resting and TCR-activated T cells (Fig 5.7 and

5.8). Also, both full length and MP product were pulled down and I was therefore unable to determine which form of L-selectin interacted with nicastrin and PS1.

In future experiments, nicastrin and PS1 could be pulled-down from resting and TCR-activated T cells and immunoblotted for endogenous L-selectin using the CA21 C terminal antibody. I would then be able to determine whether full length or MP product of L-selectin interacts with nicastrin and PS1 in resting and TCR-activated conditions.

7.3.5 ADAM 17-independent proteolysis of L-selectin

Walcheck *et al* showed metalloproteinase dependent L-selectin proteolysis in ADAM 17-deficient fibroblasts that generated the MP product and release of sL-selectin (Walcheck*, et al.* 2003). In relation to my studies, L-selectin transfected in ADAM 17-deficient MEF cells with or without complemented ADAM 17 was proteolyzed and generated an MP product which was a substrate for PS. Regardless of ADAM 17 expression, full length L-selectin increased after incubation with Ro 31-9790 confirming that proteolysis was regulated by additional metalloproteinase(s) (Fig 4.5 A, C and D). PMA only caused release of a 54 kDa soluble L-selectin ECD in the presence of ADAM 17 (Fig 4.5 B) revealing that the other metalloproteinase(s) are activated by different biochemical pathways than ADAM 17. However, another form of sL-selectin at 100 kDa was released regardless of ADAM 17 expression and/or PMA stimulation.

In my later studies, I also observed ADAM 17 independent proteolysis of L-selectin in resting T cells. Although I demonstrated that ΔM-N L-selectin was resistant to ADAM 17-proteolysis after TCR stimulation (Fig 3.9) and showed high cell surface expression in both resting and TCR-activated T cells, sL-selectin was released in resting T cells which did not elevate after TCR activation (Fig 6.3 A, B, C and E). Also, WT sL-selectin was released at similar levels as

ΔM-N in resting T cells and elevated 2X after TCR-activation (Fig 6.3 E). Additionally, in resting T cells, WT sL-selectin increased around 4X after 5 min which elevated a further 3.3 fold after TCR-stimulation (Fig 5.2 E). In relation to these studies, Li *et al* showed that levels of released sL-selectin from resting neutrophils were similar in WT and ADAM 17-deficient mice illustrating that homeostatic proteolysis of L-selectin was not dependent on ADAM 17 (Li*, et al.* 2006). My data therefore illustrates that in resting T cells and MEFs, L-selectin is proteolyzed by unknown metalloproteinase(s) which is independent of ADAM 17 activity and cell activation by PMA or TCR-activation.

Reduced sL-selectin in the plasma is correlated to immune diseases such as adult respiratory distress syndrome (ARDS), sclerosis and vasculitis (Donnelly*, et al.* 1994; Blann*, et al.* 2001). Homeostatic proteolysis of L-selectin in resting T cells is therefore important to maintain high-levels of sL-selectin in the plasma at around 1.5 μg/mL to prevent these inflammatory diseases (Schleiffenbaum*, et al.* 1992). Future studies will need to be performed to identify the other metalloproteinase(s) which proteolyze L-selectin. In studies done by Gall*, et al.* WT MEF cells were transfected with L-selectin and incubated with ADAM 17-specific inhibitor SP26 for 2 days and showed ADAM 10-dependent proteolysis after cell-activation with ionomycin (Le Gall*, et al.* 2009). Additionally, Gómez-Gaviro *et al* found that cell surface and soluble ADAM 8 proteolyzes L-selectin in ADAM 17-deficient monocytes (Gómez-Gaviro, *et al.* 2007). L-selectin could be transiently transfected in ADAM 17-deficient MEF cells and incubated with ADAM 10-specific inhibitor GI254023X (GI) or ADAM 8-inhibitory peptide BK-1361 and collected supernatants would be immunoblotted and analysed using ELISA to determine if inhibition of ADAM 10 or ADAM 8 causes loss of sL-selectin at 100 kDa. ADAM 10, which unlike ADAM 17 is activated upon increased intracellular Ca_2^+ influx after ATP interacts with and stimulates P2X purinoceptor 7 (P2X7 receptor). L-selectin and P2X7

receptor could be co-transfected in ADAM 17-deficient MEF cells. P2X7 would be activated using ATP and as a positive control cells could also be stimulated using ionomycin. Stimulated cells in the presence of ADAM 10-specific inhibitor GI254023X or solvent control would be lysed and analysed by immunoblot analysis to monitor ectodomain proteolysis of L-selectin for the cleaved C terminal V5 fragments using V5 antibody or 100 kDa sL-selectin using anti-N terminal CD62L antibodies. Additionally, Molt3 T cells expressing ΔM-N L-selectin could be incubated with ionomycin in the presence of GI or DMSO to determine whether ADAM 10-activation increases release of sL-selectin at 100 kDa.

7.4 Future work

7.4.1 Does TSPAN CD9 form a single multiprotease complex consisting of L-selectin, ADAM 17 and PS1?

Chen *et al* showed that γ-secretase subunit Aph-1 immunoprecipitates with ADAM 10 or ADAM 17 in separate complexes in the plasma, where both ectodomain and intramembrane proteolysis of APP occurs by a single multiprotease complex. Furthermore, TSPANs 12 and 17 regulated interactions between ADAM 10, γ-secretase and APP which were crucially required for proteolysis (Chen*, et al.* 2015). Other studies have shown that TSPAN CD9 binds to ADAM 17 and reduces it catalytic activity attenuating proteolysis of TNF-α and ICAM-1. Additionally, CD9 also interacts with ADAM 17 substrates pro-TGF-α, pro-epiregulin and pro-amphiregulin and potentially forms enzyme/substrate complexes at the plasma membrane (Gutiérrez-López*, et al.* 2011; Tsukamoto*, et al.* 2014; Murphy*, et al.* 2009; Hemler*, et al.* 2003). Furthermore, PMA causes dissociation of CD9 from ADAM 17 enhancing proteolysis

of substrates (Gutiérrez-López*, et al.* 2011). Currently, it is unknown whether TCR-activation can also cause dissociation of CD9 from ADAM 17.

We could hypothesize that CD9 binds to ADAM 17, L-selectin and γ-secretase in resting T cells while rendering ADAM 17 inactive abrogating L-selectin proteolysis. Intracellular signalling pathways induced after TCR-activation would dissociate CD9 activating ADAM 17 which would rapidly shed L-selectin allowing the MP product to be proteolyzed by PS1. If correct, then this would explain the ADAM 17/PS1/nicastrin/L-selectin complexes in resting T cells (Fig 3.10, Fig 5.7 and Fig 5.8) and explains how ADAM 17 is able to rapidly proteolyze L-selectin 5 min after TCR-activation (Fig 5.2). Dissociation of CD9 may also disrupt the ADAM 17/L-selectin complex clarifying why ADAM 17 does not pull down with L-selectin in activated T cells (Fig 3.10). To examine this hypothesis, L-selectin could firstly be pulled down from resting and activated-T cells and then immunoblotted for ADAM 17, PS1 and CD9. I could then gene silence or overexpress CD9 in T cells and then monitor ADAM 17/PS1/L-selectin complexes in resting and activated-T cells. I would not expect ADAM 17 or PS1 to pull-down with L-selectin in resting or activated-T cells after CD9-silencing; however overexpressed CD9 may stable ADAM 17/PS1/L-selectin complexes. Additionally, ADAM 17 and PS1-proteolysis of L-selectin could be monitored in TCR-activated CD9 silenced or overexpressed T cells in a time trial study. Expectantly in CD9-silenced T cells, ADAM 17 and PS1 proteolysis of L-selectin should be rapid as seen in Fig 5.2 and Fig 5.3, where TCR-activation potentially dissociated CD9. However, in CD9 overexpressed-T cells I would expect to see reduced ADAM 17 and PS1-proteolysis of L-selectin.

7.4.2 Visualizing L-selectin proteolysis using live cell imaging

During my PhD studies, I generated doubly labelled L-selectin where the N-terminus (ectodomain) was conjugated with a SNAP-tag (green fluorescent substrate) and the C-terminus (L-selectin ICD) with mCherry (red fluorescence) to visualize proteolysis using live cell imaging (Fig 7.2).

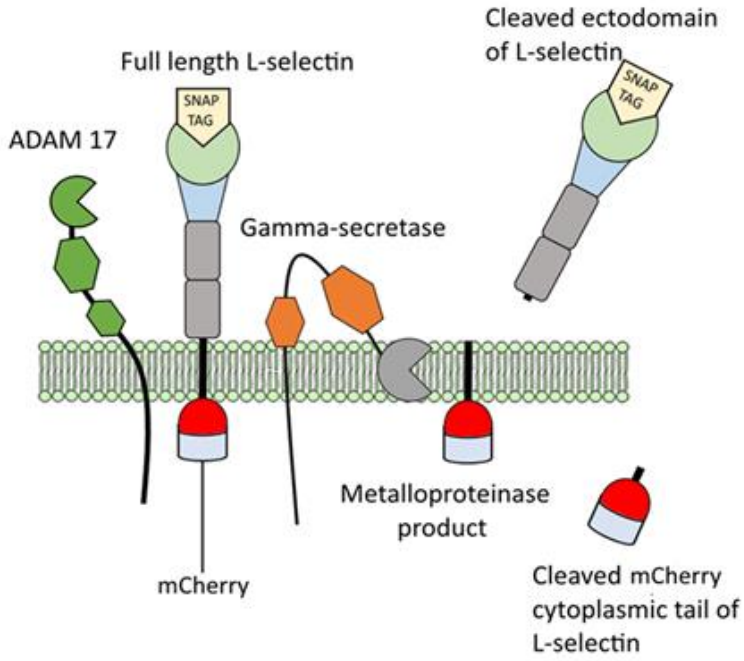

Figure 7.2: A representation of SNAP/mCherry L-selectin. L-selectin was doubly labelled as indicated. Full length L-selectin will be visualized at the membrane as green and red fluorescence. After proteolysis, mCherry cleaved fragments may accumulate in specific subcellular compartments.

In future experiments, SNAP/mCherry L-selectin could be transduced in TCR-activated, proliferating mouse CD8+ T cells using retroviral vectors. Transduced CD8+ T cells would then be stimulated by cognate peptide loaded onto antigen presenting cells (APCs) and live cell imaging would be used to determine if L-selectin proteolysis is restricted to the immunological synapse. Intracellular trafficking of singly mCherry tagged L-selectin

fragments would also be visualized to determine which subcellular compartment the L-selectin ICD migrates to after proteolysis.

7.4.3 L-selectin ICD potentially induces viral clearance by initiating a proliferative response

The biochemical relevance of PS1 mediated intramembrane proteolysis of L-selectin in T lymphocytes is currently not known. Recent data from the Ager laboratory has shown that kinetics of T cell proliferation in mice is regulated by ectodomain proteolysis of L-selectin which correlates with upregulation of the high affinity IL-2 receptor (CD25). Richards *et al* showed that CD8+ T cells expressing LΔP L-selectin showed delayed viral clearance to a recombinant vaccinia virus in comparison to WT L-selectin. Hypothetically, L-selectin ICD enters the nucleus and initiates a proliferative response by upregulating the transcriptional control of CD25 activity which increases the kinetics of viral clearance (Fig 7.5). Due to time constraints, I was unable to measure the transcriptional activity of CD25 during L-selectin proteolysis. In future experiments, a real-time quantitative PCR (q-PCR) could be performed in Molt3 T cells expressing WT and PS-resistant I351W L-selectin to measure the levels of transcribed CD25 mRNA. I would expect the levels of CD25 mRNA to be higher in Molt3 T cells expressing WT L-selectin as the cleaved ICD would enter the nucleus and elevate transcription of CD25. In contrast, PS-resistant I351W L-selectin would not generate a cleaved ICD abolishing increased CD25 transcription.

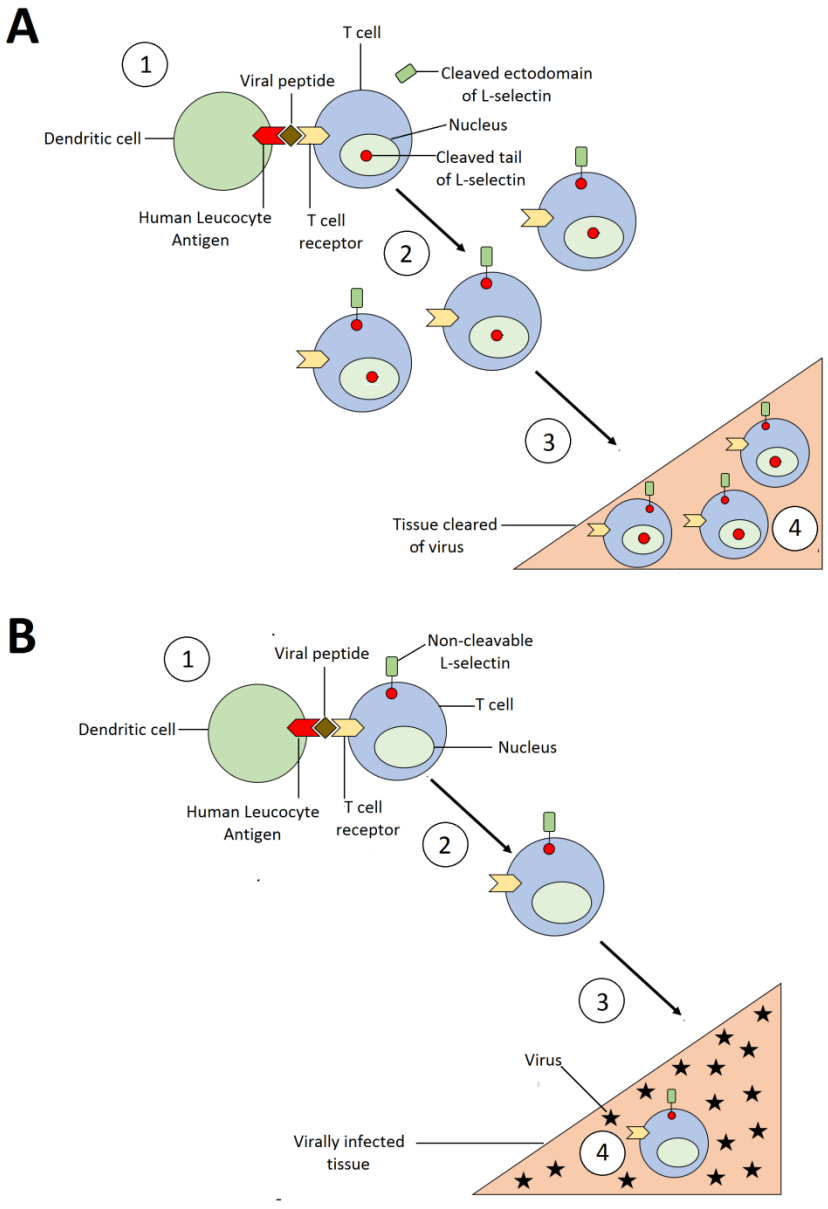

Figure 7.3: L-selectin proteolysis drives rapid viral clearance *in vivo*. (A) (1) Dendritic cells present a viral peptide to the TCR. The TCR is stimulated and causes proteolysis of L-selectin. I hypothesise that the cleaved tail enters the nucleus and acts as a gene transcriptional factor modifying behaviour of T cells. (2) At the nucleus, the cytoplasmic tail induces cell proliferation increasing the number of T cells expressing a TCR that recognises viral peptides. (3) The large number of T cells are recruited to virally infected tissues. (4) In the tissue, these T cells clear the virus. (B) (1) T cells expressing non-cleavable L-selectin do not release the cytoplasmic tail to the nucleus after TCR stimulation. (2) Absence of cytoplasmic tail of L-selectin in the nucleus causes low numbers of T cells. (3) Low levels of T cells expressing a TCR against viral peptide enter virally infected tissue. (4) Low levels of T cells fail to clear virus.

To elucidate the biochemical function of L-selectin ICD, TCR stimulated mouse T cells infected with WT, I351W or ΔM-N L-selectin could be analysed by flow cytometry for CD25 expression. If L-selectin ICD causes expression of CD25, I would expect TCR stimulation to increase CD25 at the membrane of cells expressing WT L-selectin, but not PS1 or ADAM 17 resistant mutants of L-selectin. I could ask whether overexpression of L-selectin ICD helps mice to develop a better immune response. Alternatively, do mice expressing I351W L-selectin take longer to recover from viral infection in comparison to WT L-selectin?

To determine whether L-selectin ICD induces anti-virus immunity, WT, I352K and ΔM-N L-selectin polyclonal mice could be infected with influenza and virally infected organs harvested to define the virus titre using a plaque assay. Alternatively, I could measure the number of infiltrated T cells in virally infected tissue to determine if L-selectin ICD has immunological relevance *in vitro.*

7.4.4 Elucidating the biochemistry of the L-selectin ICD.

If L-selectin ICD does enter the nucleus and act as a gene transcriptional factor, future studies would need to be performed to determine whether such biochemical pathways benefit the host. Detected L-selectin ICD (as outlined in section 7.2.2) would be excised and sent to mass spectroscopy to determine the PS1 cleavage site, allowing us to generate synthetic peptides which can be used for chromatin immunoprecipitation to determine whether L-selectin ICD binds to a specific DNA sequence. If L-selectin ICD binds to DNA, upregulated gene expression such as CD25 could be monitored using DNA microarray analysis using mRNA extracted from TCR-activated T cells expressing WT or I351W L-selectin (Fig 7.4).

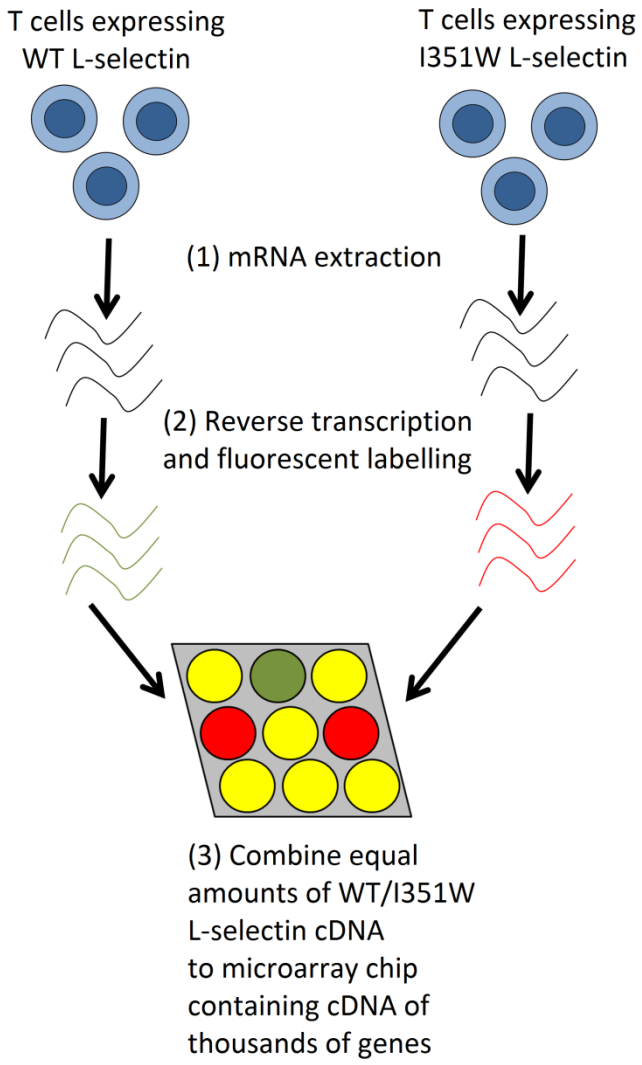

Figure 7.4: Using microarray analysis to determine upregulated gene expression by the L-selectin ICD. For microarray analysis, two subsets of T cells would be used which either expresses wild type L-selectin (releases L-selectin ICD) or PS1 resistant I351W mutated L-selectin (does not release L-selectin ICD). (1) Firstly, mRNA will be extracted from these cells. (2) Reverse transcriptase would be used to generate cDNA which is conjugated to green fluorescent protein (for WT L-selectin T cells) or red fluorescent protein (for I351W L-selectin). (3) A microarray chip is later used, which contains thousands of spots, each expressing cDNA of a specific gene. After, cDNA from both WT and I351W L-selectin T cells is added to the microarray chip. T cell derived cDNA will bind to complementary DNA sequences to cDNA presented on each spot. Green fluorescence will show spots where cDNA from WT L-selectin T cells has exclusively bound. Likewise, red fluorescence displays where only cDNA from I351W L-selectin T cells has associated. Yellow fluorescence would be seen if both WT and I351W T cell derived cDNA binds to the same cDNA presented on a spot. Green spots would therefore represent upregulated genes after L-selectin proteolysis and L-selectin ICD interaction with DNA.

Potentially, L-selectin ICD forms multi-protein complexes which either induce nuclear import or regulate intracellular signalling pathways. Lysates from TCR-activated T cells could be immunoblotted; L-selectin ICD excised and sent for mass spectroscopy for protein partners. Alternatively, lysates from TCR-activated T cells expressing a synthetic peptide of L-selectin ICD V5 His could be run by affinity chromatography containing agarose beads attached to nickel atoms. Bound L-selectin ICD would be eluted using imidazole which would compete with the His tag for nickel binding. Protein partners of eluted L-selectin ICD would be analysed using mass spectroscopy. Additionally, protein binding partners for L-selectin ICD could be elucidated using a yeast hybrid system (Fig 7.5).

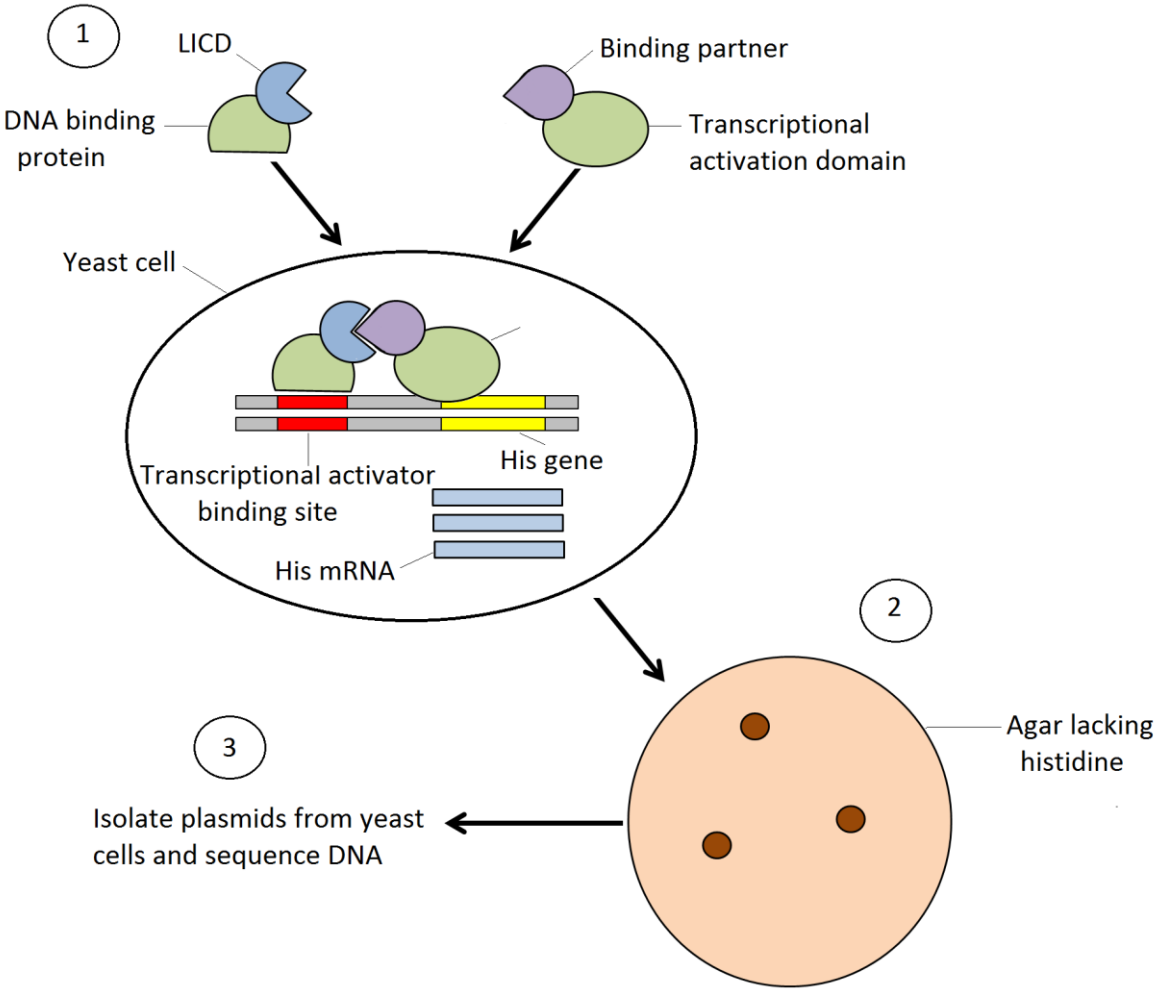

Figure 7.5: Using yeast hybrid system to determine protein binding partners of the L-selectin ICD. (1) Yeast cells are co-transfected with two different plasmids, one containing a DNA binding protein conjugated to L-selectin ICD and the other including a transcriptional activation domain fused to a potential binding partner from a library of proteins which are later transcribed. Any protein that binds to L-selectin ICD will activate transcription of a histidine (His) reporter gene. (2) Cells are plated on agar which lacks histidine. If L-selectin ICD and the binding partner interact, histidine is transcribed allowing the cells to grow on agar. (3) Binding partners from these cells are identified by sequencing the cDNA from isolated plasmids.

8. References

Abbal, C., Lambelet, M., Bertaggia, D., Gerbex, C., Martinez, M., Arcaro, A., & Spertini, O. (2006). Lipid raft adhesion receptors and Syk regulate selectin-dependent rolling under flow conditions. Blood, 108(10), 3352-3359.

Acharyya, S., Oskarsson, T., Vanharanta, S., Malladi, S., Kim, J., Morris, P. G., ... & Norton, L. (2012). A CXCL1 paracrine network links cancer chemoresistance and metastasis. Cell, 150(1), 165-178.

Adrain, C., Zettl, M., Christova, Y., Taylor, N., & Freeman, M. (2012). Tumor necrosis factor signaling requires iRhom2 to promote trafficking and activation of TACE. Science, 335(6065), 225-228.

Agace, W. W. (2006). Tissue-tropic effector T cells: generation and targeting opportunities. Nature Reviews Immunology, 6(9), 682-692.

Ahn, K., Shelton, C. C., Tian, Y., Zhang, X., Gilchrist, M. L., Sisodia, S. S., & Li, Y. M. (2010). Activation and intrinsic γ-secretase activity of PS 1. *Proceedings of the National Academy of Sciences*, *107*(50), 21435-21440.

Alcaide, P., Lim, Y. C., Luscinskas, F. W., & Fresno, M. (2010). Mucin AgC10 from Trypanosoma cruzi Interferes with L-selectin-mediated monocyte adhesion. Infection and immunity, 78(3), 1260-1268.

Alizadeh, D., Trad, M., Hanke, N. T., Larmonier, C. B., Janikashvili, N., Bonnotte, B., ... & Larmonier, N. (2014). Doxorubicin eliminates myeloid-derived suppressor cells and enhances the efficacy of adoptive T-cell transfer in breast cancer. Cancer research, 74(1), 104-118.

Alon, R., Chen, S., Puri, K. D., Finger, E. B., & Springer, T. A. (1997). The kinetics of L-selectin tethers and the mechanics of selectin-mediated rolling. The Journal of cell biology, 138(5), 1169-1180.

Amour, A., Slocombe, P. M., Webster, A., Butler, M., Knight, C. G., Smith, B. J., ... & Docherty, A. J. (1998). TNF-α converting enzyme (TACE) is inhibited by TIMP-3. FEBS letters, 435(1), 39-44.

Ancot, F., Leroy, C., Muharram, G., Lefebvre, J., Vicogne, J., Lemiere, A., ... & Giordano, S. (2012). Shedding-Generated Met Receptor Fragments can be Routed to Either the Proteasomal or the Lysosomal Degradation Pathway. Traffic, 13(9), 1261-1272.

Anders, A., Gilbert, S., Garten, W., Postina, R., & Fahrenholz, F. (2001). Regulation of the α-secretase ADAM10 by its prodomain and proprotein convertases. The FASEB Journal, 15(10), 1837-1839.

Andersson, E. R., & Lendahl, U. (2014). Therapeutic modulation of Notch signalling—are we there yet?. Nature reviews Drug discovery, 13(5), 357-378.

Arbonés, M. L., Ord, D. C., Ley, K., Ratech, H., Maynard-Curry, C., Otten, G., ... & Teddert, T. F. (1994). Lymphocyte homing and leukocyte rolling and migration are impaired in L-selectin-deficient mice. Immunity, 1(4), 247-260.

Arribas, J., & Massagu, J. (1995). Transforming Growth Factor-t and 13-Amyloid Precursor Protein Share a Secretory Mechanism. J. Cell Biol, 128(3), 433-441.

Arumugam, T. V., Magnus, T., Woodruff, T. M., Proctor, L. M., Shiels, I. A., & Taylor, S. M. (2006). Complement mediators in ischemia–reperfusion injury. Clinica Chimica Acta, 374(1), 33-45.

Bajénoff, M., Granjeaud, S., & Guerder, S. (2003). The strategy of T cell antigen-presenting cell encounter in antigen-draining lymph nodes revealed by imaging of initial T cell activation. Journal of Experimental Medicine, 198(5), 715-724.

Bargatze, R. F., Kurk, S., Butcher, E. C., & Jutila, M. A. (1994). Neutrophils roll on adherent neutrophils bound to cytokine-induced endothelial cells via L-selectin on the rolling cells. Journal of Experimental Medicine, 180(5), 1785-1792.

Barreiro, O., Zamai, M., Yáñez-Mó, M., Tejera, E., López-Romero, P., Monk, P. N., ... & Sánchez-Madrid, F. (2008). Endothelial adhesion receptors are recruited to adherent leukocytes by inclusion in preformed tetraspanin nanoplatforms. The Journal of cell biology, 183(3), 527-542.

Barthet, G., Shioi, J., Shao, Z., Ren, Y., Georgakopoulos, A., & Robakis, N. K. (2011). Inhibitors of γ-secretase stabilize the complex and differentially affect processing of amyloid precursor protein and other substrates. The FASEB Journal, 25(9), 2937-2946.

Bass, R., & Edwards, D. R. (2010). ADAMs and protein disulfide isomerase: the key to regulated cell-surface protein ectodomain shedding?. Biochemical Journal, 428(3), e3-e5.

Baumheter, S., Singer, M. S., Henzel, W., Hemmerich, S., Renz, M., Rosen, S. D., & Lasky, L. A. (1993). Binding of L-selectin to the vascular sialomucin CD34. Science, 262(5132), 436-438.

Beel, A. J., & Sanders, C. R. (2008). Substrate specificity of γ-secretase and other intramembrane proteases. Cellular and molecular life sciences, 65(9), 1311-1334

Bennett, T. A., Edwards, B. S., Sklar, L. A., & Rogelj, S. (2000). Sulfhydryl regulation of L-selectin shedding: phenylarsine oxide promotes activation-independent L-selectin shedding from leukocytes. The Journal of Immunology, 164(8), 4120-4129.

Berditchevski, F. (2001). Complexes of tetraspanins with integrins: more than meets the eye. Journal of cell science, 114(23), 4143-4151.

Binder, C. J., & Silverman, G. J. (2005, March). Natural antibodies and the autoimmunity of atherosclerosis. In Springer seminars in immunopathology (Vol. 26, No. 4, pp. 385-404). Springer-Verlag.

Bjerknes, M., Cheng, H., & Ottaway, C. A. (1986). Dynamics of lymphocyte-endothelial interactions *in vivo*. Science, 231, 402-406.

Black, R. A., Rauch, C. T., Kozlosky, C. J., Peschon, J. J., Slack, J. L., Wolfson, M. F., ... & Nelson, N. (1997). A metalloproteinase disintegrin that releases tumour-necrosis factor-alpha from cells. Nature, 385(6618), 729.

Blann, A. D., Sanders, P. A., Herrick, A., & Jayson, M. I. V. (1996). Soluble L-selectin in the connective tissue diseases. British journal of haematology, 95(1), 192-194.

Blidberg, K., Palmberg, L., Dahlén, B., Lantz, A. S., & Larsson, K. (2012). Chemokine release by neutrophils in chronic obstructive pulmonary disease. Innate immunity, 18(3), 503-510.

Blobel, G. (1979). Determinants in Protein Topology. In Biological Functions of Proteinases (pp. 102-108). Springer Berlin Heidelberg.

Boland, B., Smith, D. A., Mooney, D., Jung, S. S., Walsh, D. M., & Platt, F. M. (2010). Macroautophagy is not directly involved in the metabolism of amyloid precursor protein. *Journal of Biological Chemistry*, *285*(48), 37415-37426.

Bozkulak, E. C., & Weinmaster, G. (2009). Selective use of ADAM10 and ADAM17 in activation of Notch1 signaling. Molecular and cellular biology, 29(21), 5679-5695.

Brenner, B., Gulbins, E., Koppenhoefer, U., Lang, F., & Linderkamp, O. (1997). L-selectin-mediated lymphocyte rolling of Jurkat T lymphocytes depends on functional expression of the tyrosine kinase p56lck. Cellular Physiology and Biochemistry, 7(2), 107-118.

Brenner, B., Gulbins, E., Schlottmann, K., Koppenhoefer, U., Busch, G. L., Walzog, B., ... & Lang, F. (1996). L-selectin activates the Ras pathway via the tyrosine kinase p56lck. Proceedings of the National Academy of Sciences, 93(26), 15376-15381.

Brodowicz, T., Wiltschke, C., Budinsky, A. C., Krainer, M., Steger, G. G., & Zielinski, C. C. (1997). Soluble HER-2/neu neutralizes biologic effects of anti-HER-2/neu antibody on breast cancer cells *in vitro*. International journal of cancer, 73, 875-879.

Bruehl, R. E., Springer, T. A., & Bainton, D. F. (1996). Quantitation of L-selectin distribution on human leukocyte microvilli by immunogold labeling and electron microscopy. Journal of Histochemistry & Cytochemistry, 44(8), 835-844.

Brunkan, A. L., & Goate, A. M. (2005). PS function and γ-secretase activity. *Journal of neurochemistry*, *93*(4), 769-792.

Buckley, C. A., Rouhani, F. N., Kaler, M., Adamik, B., Hawari, F. I., & Levine, S. J. (2005). Amino-terminal TACE prodomain attenuates TNFR2 cleavage independently of the cysteine switch. American Journal of Physiology-Lung Cellular and Molecular Physiology, 288(6), L1132-L1138.

Calafat, J., Janssen, H., Knol, E. F., Malm, J., & Egesten, A. (2000). The bactericidal/permeability-increasing protein (BPI) is membrane-associated in azurophil

granules of human neutrophils, and relocation occurs upon cellular activation. Apmis, 108(3), 201-208.

Caligiuri, G., Nicoletti, A., Poirier, B., & Hansson, G. K. (2002). Protective immunity against atherosclerosis carried by B cells of hypercholesterolemic mice. The Journal of clinical investigation, 109(6), 745-753.

Canault, M., Tellier, E., Bonardo, B., Mas, E., Aumailley, M., Juhan-Vague, I., ... & Peiretti, F. (2006). FHL2 interacts with both ADAM-17 and the cytoskeleton and regulates ADAM-17 localization and activity. Journal of cellular physiology, 208(2), 363-372.

Chakravarthy, B., Morley, P., & Whitfield, J. (1999). Ca 2+–calmodulin and protein kinase Cs: a hypothetical synthesis of their conflicting convergences on shared substrate domains. Trends in neurosciences, 22(1), 12-16.

Chanthaphavong, R. S., Loughran, P. A., Lee, T. Y., Scott, M. J., & Billiar, T. R. (2012). A role for cGMP in iNOS-induced TACE/ADAM17 activation, translocation, and TNFR1 shedding in hepatocytes. Journal of Biological Chemistry, jbc-M112.

Chen, A. C., Guo, L. Y., Ostaszewski, B. L., Selkoe, D. J., & LaVoie, M. J. (2010). Aph-1 associates directly with full-length and C-terminal fragments of γ-secretase substrates. Journal of Biological Chemistry, 285(15), 11378-11391.

Chen, A. C., Kim, S., Shepardson, N., Patel, S., Hong, S., & Selkoe, D. J. (2015). Physical and functional interaction between the α-and γ-secretases: A new model of regulated intramembrane proteolysis. J Cell Biol, 211(6), 1157-1176.

Chen, A., Engel, P., & Tedder, T. F. (1995). Structural requirements regulate endoproteolytic release of the L-selectin (CD62L) adhesion receptor from the cell surface of leukocytes. Journal of Experimental Medicine, 182(2), 519-530.

Chen, C., Cui, L., Shang, X., & Zeng, X. (2010). NFAT regulates CSF-1 gene transcription triggered by L-selectin crosslinking. Biocell, 34(2), 57-63.

Chen, C., Shang, X., Cui, L., Xu, T., Luo, J., Ba, X., & Zeng, X. (2008). L-selectin ligation-induced CSF-1 gene transcription is regulated by AP-1 in a c-Abl kinase-dependent manner. Human immunology, 69(8), 501-509.

Chen, F., Yu, G., Arawaka, S., Nishimura, M., Kawarai, T., Yu, H., ... & Milman, P. (2001). Nicastrin binds to membrane-tethered Notch. Nature Cell Biology, 3(8), 751-754.

Choudhary, D., Hegde, P., Voznesensky, O., Choudhary, S., Kopsiaftis, S., Claffey, K. P., ... & Taylor, J. A. (2015, September). Increased expression of L-selectin (CD62L) in high-grade urothelial carcinoma: A potential marker for metastatic disease. In *Urologic Oncology: Seminars and Original Investigations* (Vol. 33, No. 9, pp. 387-e17). Elsevier.

Christova, Y., Adrain, C., Bambrough, P., Ibrahim, A., & Freeman, M. (2013). Mammalian iRhoms have distinct physiological functions including an essential role in TACE regulation. EMBO reports, 14(10), 884-890.

Cohen, S. G., Itkin, T., Chakrabarty, S., Graf, C., Kollet, O., Ludin, A., ... & Niemeyer, E. (2015). PAR1 signaling regulates the retention and recruitment of EPCR-expressing bone marrow hematopoietic stem cells. Nature medicine, 21(11), 1307-1317.

Crockett-Torabi, E., Sulenbarger, B., Smith, C. W., & Fantone, J. C. (1995). Activation of human neutrophils through L-selectin and Mac-1 molecules. The Journal of Immunology, 154(5), 2291-2302.

Crystal, A. S., Morais, V. A., Pierson, T. C., Pijak, D. S., Carlin, D., Lee, V. M. Y., & Doms, R. W. (2003). Membrane topology of γ-secretase component PEN-2. Journal of Biological Chemistry, 278(22), 20117-20123.

Cupers, P., Orlans, I., Craessaerts, K., Annaert, W., & De Strooper, B. (2001). The amyloid precursor protein (APP)-cytoplasmic fragment generated by γ-secretase is rapidly degraded but distributes partially in a nuclear fraction of neurones in culture. Journal of neurochemistry, 78(5), 1168-1178.

Dang, T. P., Gazdar, A. F., Virmani, A. K., Sepetavec, T., Hande, K. R., Minna, J. D., ... & Carbone, D. P. (2000). Chromosome 19 translocation, overexpression of Notch3, and human lung cancer. Journal of the National Cancer Institute, 92(16), 1355-1357.

de Diego, J., Punzon, C., Duarte, M., & Fresno, M. (1997). Alteration of macrophage function by a Trypanosoma cruzi membrane mucin. The Journal of Immunology, 159(10), 4983-4989.

De Strooper, B., Annaert, W., Cupers, P., Saftig, P., Craessaerts, K., Mumm, J. S., ... & Goate, A. (1999). A PS-1-dependent γ-secretase-like protease mediates release of Notch intracellular domain. Nature, 398(6727), 518-522.

De Strooper, B., Iwatsubo, T., & Wolfe, M. S. (2012). PSs and γ-secretase: structure, function, and role in Alzheimer disease. Cold Spring Harbor perspectives in medicine, 2(1), a006304.

De Strooper, B., Saftig, P., Craessaerts, K., Vanderstichele, H., Guhde, G., Annaert, W., ... & Van Leuven, F. (1998). Deficiency of PS-1 inhibits the normal cleavage of amyloid precursor protein. Nature, 391(6665), 387-390.

Demehri, S., Turkoz, A., & Kopan, R. (2009). Epidermal Notch1 loss promotes skin tumorigenesis by impacting the stromal microenvironment.Cancer cell, 16(1), 55-66

Deng, W., Putkey, J. A., & Li, R. (2013). Calmodulin adopts an extended conformation when interacting with L-selectin in membranes. PloS one, 8(5), e62861.

Deng, W., Srinivasan, S., Zheng, X., Putkey, J. A., & Li, R. (2011). Interaction of calmodulin with L-selectin at the membrane interface: implication on the regulation of L-selectin shedding. Journal of molecular biology, 411(1), 220-233.

Deuss, M., Reiss, K., & Hartmann, D. (2008). Part-time α-secretases: the functional biology of ADAM 9, 10 and 17. Current Alzheimer Research, 5(2), 187-201.

Díaz-Rodríguez, E., Montero, J. C., Esparís-Ogando, A., Yuste, L., & Pandiella, A. (2002). Extracellular signal-regulated kinase phosphorylates tumor necrosis factor α-converting enzyme at threonine 735: a potential role in regulated shedding. Molecular biology of the cell, 13(6), 2031.

Díaz-Rodríguez, E., Montero, J. C., Esparís-Ogando, A., Yuste, L., & Pandiella, A. (2002). Extracellular signal-regulated kinase phosphorylates tumor necrosis factor α-converting enzyme at threonine 735: a potential role in regulated shedding. Molecular biology of the cell, 13(6), 2031.

Dombernowsky, S. L., Samsøe-Petersen, J., Petersen, C. H., Instrell, R., Hedegaard, A. M. B., Thomas, L., ... & Fröhlich, C. (2015). The sorting protein PACS-2 promotes ErbB signalling by regulating recycling of the metalloproteinase ADAM17. Nature communications, 6.

Donnelly, S. C., Haslett, C., Robertson, C. E., Carter, D. C., Ross, J. A., Grant, I. S., & Tedder, T. F. (1994). Role of selectiris In development of adult respiratory distress syndrome. The Lancet, 344(8917), 215-219.

Doran, A. C., Lipinski, M. J., Oldham, S. N., Garmey, J. C., Campbell, K. A., Skaflen, M. D., ... & Galkina, E. V. (2011). B-cell aortic homing and atheroprotection depend on Id3. Circulation research, CIRCRESAHA-111.

Dovey, H. F., John, V., Anderson, J. P., Chen, L. Z., de Saint Andrieu, P., Fang, L. Y., ... & Hu, K. L. (2001). Functional γ-secretase inhibitors reduce beta-amyloid peptide levels in brain. Journal of neurochemistry, 76(1), 173-181.

Dries, D. R., Shah, S., Han, Y. H., Yu, C., Yu, S., Shearman, M. S., & Yu, G. (2009). Glu-333 of nicastrin directly participates in γ-secretase activity. Journal of Biological Chemistry, 284(43), 29714-29724.

Düsterhöft, S., Höbel, K., Oldefest, M., Lokau, J., Waetzig, G. H., Chalaris, A., ... & Grötzinger, J. (2014). A disintegrin and metalloprotease 17 dynamic interaction sequence, the sweet tooth for the human interleukin 6 receptor. Journal of Biological Chemistry, 289(23), 16336-16348.

Düsterhöft, S., Jung, S., Hung, C. W., Tholey, A., Sönnichsen, F. D., Grötzinger, J., & Lorenzen, I. (2013). Membrane-proximal domain of a disintegrin and metalloprotease-17 represents the putative molecular switch of its shedding activity operated by protein-disulfide isomerase. Journal of the american chemical society, 135(15), 5776-5781.

Düsterhöft, S., Michalek, M., Kordowski, F., Oldefest, M., Sommer, A., Röseler, J., ... & Lorenzen, I. (2015). Extracellular juxtamembrane segment of ADAM17 interacts with membranes and is essential for its shedding activity. Biochemistry, 54(38), 5791-5801.

Edbauer, D., Willem, M., Lammich, S., Steiner, H., & Haass, C. (2002). Insulin-degrading enzyme rapidly removes the β-amyloid precursor protein intracellular domain (AICD). Journal of Biological Chemistry, 277(16), 13389-13393.

Edbauer, D., Winkler, E., Regula, J. T., Pesold, B., Steiner, H., & Haass, C. (2003). Reconstitution of γ-secretase activity. Nature cell biology, 5(5), 486-488.

Edwards, D. R., Handsley, M. M., & Pennington, C. J. (2008). The ADAM metalloproteinases. Molecular aspects of medicine, 29(5), 258-289.

Ellerbroek, P. M., E Annemiek, M., Hoepelman, A. I., & Coenjaerts, F. E. (2004). Effects of the Capsular Polysaccharides of Cryptococcus neoformans on Phagocyte Migration and Inflammatory Mediators [General Articles]. Current medicinal chemistry, 11(2), 253-266.

Ellisen, L. W., Bird, J., West, D. C., Soreng, A. L., Reynolds, T. C., Smith, S. D., & Sklar, J. (1991). TAN-1, the human homolog of the Drosophila notch gene, is broken by chromosomal translocations in T lymphoblastic neoplasms. Cell, 66(4), 649-661.

Elson, H. F., Dimitrov, D. S., & Blumenthal, R. (1994). A trans-dominant mutation in human immunodeficiency virus type 1 (HIV-1) envelope glycoprotein gp41 inhibits membrane fusion when expressed in target cells. Molecular membrane biology, 11(3), 165-169.

Esaguy, N., Aguas, A. P., & Silva, M. T. (1989). High-resolution localization of lactoferrin in human neutrophils: labeling of secondary granules and cell heterogeneity. Journal of leukocyte biology, 46(1), 51-62.

Eskelinen, E. L., & Saftig, P. (2009). Autophagy: a lysosomal degradation pathway with a central role in health and disease. Biochimica et Biophysica Acta (BBA)-Molecular Cell Research, 1793(4), 664-673.

Evans, B. J., McDowall, A., Taylor, P. C., Hogg, N., Haskard, D. O., & Landis, R. C. (2006). Shedding of lymphocyte function–associated antigen-1 (LFA-1) in a human inflammatory response. Blood, 107(9), 3593-3599.

Fan, H., & Derynck, R. (1999). Ectodomain shedding of TGF-α and other transmembrane proteins is induced by receptor tyrosine kinase activation and MAP kinase signaling cascades. The EMBO Journal, 18(24), 6962-6972.

Fan, H., Turck, C. W., & Derynck, R. (2003). Characterization of growth factor-induced serine phosphorylation of tumor necrosis factor-α converting enzyme and of an alternatively translated polypeptide. Journal of Biological Chemistry, 278(20), 18617-18627.

Fan, H., Turck, C. W., & Derynck, R. (2003). Characterization of growth factor-induced serine phosphorylation of tumor necrosis factor-α converting enzyme and of an alternatively translated polypeptide. Journal of Biological Chemistry, 278(20), 18617-18627.

Faurschou, M., & Borregaard, N. (2003). Neutrophil granules and secretory vesicles in inflammation. Microbes and Infection, 5(14), 1317-1327.

Fiaturi, N., Castellot, J. J., & Nielsen, H. C. (2014). Neuregulin-ErbB4 signaling in the developing lung alveolus: a brief review. *Journal of cell communication and signaling*, *8*(2), 105-111.

Fiscus, L. C., Van Herpen, J., Steeber, D. A., Tedder, T. F., & Tang, M. L. (2001). L-Selectin is required for the development of airway hyperresponsiveness but not airway inflammation in a murine model of asthma. Journal of allergy and clinical immunology, 107(6), 1019-1024.

Fors, B. P., Goodarzi, K., & von Andrian, U. H. (2001). L-selectin shedding is independent of its subsurface structures and topographic distribution. The Journal of Immunology, 167(7), 3642-3651.

Fortna, R. R., Crystal, A. S., Morais, V. A., Pijak, D. S., Lee, V. M. Y., & Doms, R. W. (2004). Membrane topology and nicastrin-enhanced endoproteolysis of APH-1, a component of the γ-secretase complex. Journal of Biological Chemistry, 279(5), 3685-3693.

Fryer, C. J., White, J. B., & Jones, K. A. (2004). Mastermind recruits CycC: CDK8 to phosphorylate the Notch ICD and coordinate activation with turnover. *Molecular cell*, *16*(4), 509-520.

Fukumori, A., Fluhrer, R., Steiner, H., & Haass, C. (2010). Three-amino acid spacing of PS endoproteolysis suggests a general stepwise cleavage of γ-secretase-mediated intramembrane proteolysis. The Journal of Neuroscience, 30(23), 7853-7862.

Galkina, E., Florey, O., Zarbock, A., Smith, B. R., Preece, G., Lawrence, M. B., ... & Ager, A. (2007). T lymphocyte rolling and recruitment into peripheral lymph nodes is regulated by a saturable density of L-selectin (CD62L). European journal of immunology, 37(5), 1243-1253.

Galkina, E., Kadl, A., Sanders, J., Varughese, D., Sarembock, I. J., & Ley, K. (2006). Lymphocyte recruitment into the aortic wall before and during development of atherosclerosis is partially L-selectin dependent. Journal of Experimental Medicine, 203(5), 1273-1282.

Galkina, E., Tanousis, K., Preece, G., Tolaini, M., Kioussis, D., Florey, O., ... & Ager, A. (2003). L-selectin shedding does not regulate constitutive T cell trafficking but controls the migration pathways of antigen-activated T lymphocytes. Journal of Experimental Medicine, 198(9), 1323-1335.

Gallatin, W. M., Weissman, I. L., & Butcher, E. C. (1983). A cell-surface molecule involved in organ-specific homing of lymphocytes. Nature, 304(5921), 30.

Garton, K. J., Gough, P. J., & Raines, E. W. (2006). Emerging roles for ectodomain shedding in the regulation of inflammatory responses. Journal of leukocyte biology, 79(6), 1105-1116.

Gasparini, L., Rusconi, L., Xu, H., Del Soldato, P., & Ongini, E. (2004). Modulation of β-amyloid metabolism by non-steroidal anti-inflammatory drugs in neuronal cell cultures. Journal of neurochemistry, 88(2), 337-348.

Gerendasy, D. D., & Sutcliffe, J. G. (1997). RC3/neurogranin, a postsynaptic calpacitin for setting the response threshold to calcium influxes. Molecular neurobiology, 15(2), 131-163.

Giblin, P. A., Hwang, S. T., Katsumoto, T. R., & Rosen, S. D. (1997). Ligation of L-selectin on T lymphocytes activates beta1 integrins and promotes adhesion to fibronectin. The Journal of Immunology, 159(7), 3498-3507.

Gifford, J. L., Ishida, H., & Vogel, H. J. (2012). Structural insights into calmodulin-regulated Lselectin ectodomain shedding. Journal of Biological Chemistry, 287(32), 26513-26527

Gjurich, B. N., Taghavie-Moghadam, P. L., Ley, K., & Galkina, E. V. (2014). L-selectin deficiency decreases aortic B1a and Breg subsets and promotes atherosclerosis. Thrombosis and haemostasis, 112(4), 803.

Gómez-Gaviro, M., Domínguez-Luis, M., Canchado, J., Calafat, J., Janssen, H., Lara-Pezzi, E., ... & Sánchez-Madrid, F. (2007). Expression and regulation of the metalloproteinase ADAM-8 during human neutrophil pathophysiological activation and its catalytic activity on L-selectin shedding. The Journal of Immunology, 178(12), 8053-8063.

Gomis-Rüth, F. X. (2003). Structural aspects of the metzincin clan of metalloendopeptidases. Molecular biotechnology, 24(2), 157-202.

Gonzales, P. E., Solomon, A., Miller, A. B., Leesnitzer, M. A., Sagi, I., & Milla, M. E. (2004). Inhibition of the tumor necrosis factor-α-converting enzyme by its pro domain. Journal of Biological Chemistry, 279(30), 31638-31645.

Gooz, M. (2010). ADAM-17: the enzyme that does it all. Critical reviews in biochemistry and molecular biology, 45(2), 146-169.

Göőz, M., Göőz, P., Luttrell, L. M., & Raymond, J. R. (2006). 5-HT2A receptor induces ERK phosphorylation and proliferation through ADAM-17 tumor necrosis factor-α-converting enzyme (TACE) activation and heparin-bound epidermal growth factor-like growth factor (HB-EGF) shedding in mesangial cells. Journal of Biological Chemistry, 281(30), 21004-21012.

Gopalan, P. K., Smith, C. W., Lu, H., Berg, E. L., McIntire, L. V., & Simon, S. I. (1997). Neutrophil CD18-dependent arrest on intercellular adhesion molecule 1 (ICAM-1) in shear flow can be activated through L-selectin. The Journal of Immunology, 158(1), 367-375.

Grabher, C., von Boehmer, H., & Look, A. T. (2006). Notch 1 activation in the molecular pathogenesis of T-cell acute lymphoblastic leukaemia. Nature Reviews Cancer, 6(5), 347-359.

Gretz, J. E., Anderson, A. O., & Shaw, S. (1997). Cords, channels, corridors and conduits: critical architectural elements facilitating cell interactions in the lymph node cortex. Immunological reviews, 156(1), 11-24.

Grewal, I. S., Foellmer, H. G., Grewal, K. D., Wang, H., Lee, W. P., Tumas, D., ... & Flavell, R. A. (2001). CD62L is required on effector cells for local interactions in the CNS to cause myelin damage in experimental allergic encephalomyelitis. Immunity, 14(3), 291-302.

Groot, A. J., Habets, R., Yahyanejad, S., Hodin, C. M., Reiss, K., Saftig, P., ... & Vooijs, M. (2014). Regulated proteolysis of NOTCH2 and NOTCH3 receptors by ADAM10 and PSs. *Molecular and cellular biology*, *34*(15), 2822-2832.

Grosely, R., Kopanic, J. L., Nabors, S., Kieken, F., Spagnol, G., Al-Mugotir, M., ... & Sorgen, P. L. (2013). Effects of phosphorylation on the structure and backbone dynamics of the

intrinsically disordered connexin43 C-terminal domain. Journal of Biological Chemistry, 288(34), 24857-24870.

Guenin-Macé, L., Carrette, F., Asperti-Boursin, F., Le Bon, A., Caleechurn, L., Di Bartolo, V., ... & Demangel, C. (2011). Mycolactone impairs T cell homing by suppressing microRNA control of L-selectin expression. Proceedings of the National Academy of Sciences, 108(31), 12833-12838.

Gupta-Rossi, N., Le Bail, O., Gonen, H., Brou, C., Logeat, F., Six, E., ... & Israël, A. (2001). Functional interaction between SEL-10, an F-box protein, and the nuclear form of activated Notch1 receptor. *Journal of Biological Chemistry*, *276*(37), 34371-34378.

Gutiérrez-López, M. D., Gilsanz, A., Yáñez-Mó, M., Ovalle, S., Lafuente, E. M., Domínguez, C., ... & Cabañas, C. (2011). The sheddase activity of ADAM17/TACE is regulated by the tetraspanin CD9. Cellular and Molecular Life Sciences, 68(19), 3275-3292.

Gutiérrez-López, M. D., Gilsanz, A., Yáñez-Mó, M., Ovalle, S., Lafuente, E. M., Domínguez, C., ... & Cabañas, C. (2011). The sheddase activity of ADAM17/TACE is regulated by the tetraspanin CD9. *Cellular and Molecular Life Sciences*, *68*(19), 3275-3292.

Haass, C., & Selkoe, D. J. (1993). Cellular processing of β-amyloid precursor protein and the genesis of amyloid β-peptide. Cell, 75(6), 1039-1042.

Hafezi-Moghadam, A., & Ley, K. (1999). Relevance of L-selectin shedding for leukocyte rolling *in vivo*. Journal of Experimental Medicine, 189(6), 939-948.

Hafezi-Moghadam, A., Thomas, K. L., Prorock, A. J., Huo, Y., & Ley, K. (2001). L-selectin shedding regulates leukocyte recruitment. Journal of Experimental Medicine, 193(7), 863-872.

Hahn, D., Pischitzis, A., Roesmann, S., Hansen, M. K., Leuenberger, B., Luginbuehl, U., & Sterchi, E. E. (2003). Phorbol 12-myristate 13-acetate-induced ectodomain shedding and phosphorylation of the human meprinβ metalloprotease. *Journal of Biological Chemistry*, *278*(44), 42829-42839.

Hall, K. C., & Blobel, C. P. (2012). Interleukin-1 stimulates ADAM17 through a mechanism independent of its cytoplasmic domain or phosphorylation at threonine 735. PLoS One, 7(2), e31600.

Han, M., Liu, M., Wang, Y., Chen, X., Xu, J., Sun, Y., ... & Wu, C. (2012). Antagonism of miR-21 reverses epithelial-mesenchymal transition and cancer stem cell phenotype through AKT/ERK1/2 inactivation by targeting PTEN. *PloS one*, *7*(6), e39520.

Hanson, R. D., Connolly, N. L., Burnett, D., Campbell, E. J., Senior, R. M., & Ley, T. J. (1990). Developmental regulation of the human cathepsin G gene in myelomonocytic cells. Journal of Biological Chemistry, 265(3), 1524-1530.

Hara, T., Nakamura, K., Matsui, M., Yamamoto, A., Nakahara, Y., Suzuki-Migishima, R., ... & Mizushima, N. (2006). Suppression of basal autophagy in neural cells causes neurodegenerative disease in mice. Nature, 441(7095), 885-889.

Harhaj, E. W., & Sun, S. C. (1997). The Serine/Threonine Phosphatase Inhibitor Calyculin A Induces Rapid Degradation of IκBβ REQUIREMENT OF BOTH THE N-AND C-TERMINAL SEQUENCES. Journal of Biological Chemistry, 272(9), 5409-5412.

Hartmann, M., Herrlich, A., & Herrlich, P. (2013). Who decides when to cleave an ectodomain?. Trends in biochemical sciences, 38(3), 111-120.

Hartmann, M., Parra, L. M., Ruschel, A., Böhme, S., Li, Y., Morrison, H., ... & Herrlich, P. (2015). Tumor suppressor NF2 blocks cellular migration by inhibiting ectodomain cleavage of CD44. *Molecular Cancer Research*, *13*(5), 879-890.

Hartmann, T. N., Grabovsky, V., Pasvolsky, R., Shulman, Z., Buss, E. C., Spiegel, A., ... & Alon, R. (2008). A crosstalk between intracellular CXCR7 and CXCR4 involved in rapid CXCL12-triggered integrin activation but not in chemokine-triggered motility of human T lymphocytes and CD34+ cells. Journal of leukocyte biology, 84(4), 1130-1140.

Hay, J. B., & Hobbs, B. B. (1977). The flow of blood to lymph nodes and its relation to lymphocyte traffic and the immune response. *J Exp Med*, *145*(1), 31-44.

Hemler, M. E. (2003). Tetraspanin proteins mediate cellular penetration, invasion, and fusion events and define a novel type of membrane microdomain. Annual review of cell and developmental biology, 19(1), 397-422.

Hemler, M. E. (2003). Tetraspanin proteins mediate cellular penetration, invasion, and fusion events and define a novel type of membrane microdomain. Annual review of cell and developmental biology, 19(1), 397-422.

Hemler, M. E. (2014). Tetraspanin proteins promote multiple cancer stages. Nature reviews Cancer, 14(1), 49-60.

Herreman, A., Hartmann, D., Annaert, W., Saftig, P., Craessaerts, K., Serneels, L., ... & Baekelandt, V. (1999). Presenilin 2 deficiency causes a mild pulmonary phenotype and no changes in amyloid precursor protein processing but enhances the embryonic lethal phenotype of presenilin 1 deficiency. Proceedings of the National Academy of Sciences, 96(21), 11872-11877.

Herron, L. R., Hill, M., Davey, F., & Gunn-Moore, F. J. (2009). The intracellular interactions of the L1 family of cell adhesion molecules. Biochemical Journal, 419(3), 519-531.

Hickey, M. J., Forster, M., Mitchell, D., Kaur, J., De Caigny, C., & Kubes, P. (2000). L-selectin facilitates emigration and extravascular locomotion of leukocytes during acute inflammatory responses *in vivo*. The Journal of Immunology, 165(12), 7164-7170.

Higashiyama, M., Taki, T., Ieki, Y., Adachi, M., Huang, C. L., Koh, T., ... & Miyake, M. (1995). Reduced motility related protein-1 (MRP-1/CD9) gene expression as a factor of poor prognosis in non-small cell lung cancer. Cancer Research, 55(24), 6040-6044.

Hoebe, K., Janssen, E., & Beutler, B. (2004). The interface between innate and adaptive immunity. Nature immunology, 5(10), 971-974.

Hoeing, K., Zscheppang, K., Mujahid, S., Murray, S., Volpe, M. V., Dammann, C. E., & Nielsen, H. C. (2011). PS-1 processing of ErbB4 in fetal type II cells is necessary for control of fetal lung maturation. Biochimica et Biophysica Acta (BBA)-Molecular Cell Research, 1813(3), 480-491.

Holgate, S. T., Yang, Y., Haitchi, H. M., Powell, R. M., Holloway, J. W., Yoshisue, H., ... & Davies, D. E. (2006). The genetics of asthma: ADAM33 as an example of a susceptibility gene. Proceedings of the American Thoracic Society, 3(5), 440-443.

Holmes, O., Paturi, S., Wolfe, M. S., & Selkoe, D. J. (2014). Functional analysis and purification of a Pen-2 fusion protein for γ-secretase structural studies. Journal of neurochemistry, 131(1), 94-100

Honda, T., Yasutake, K., Nihonmatsu, N., Mercken, M., Takahashi, H., Murayama, O., ... & Saido, T. C. (1999). Dual roles of proteasome in the metabolism of PS 1. *Journal of neurochemistry*, *72*(1), 255-261.

Horiuchi, K., Kimura, T., Miyamoto, T., Takaishi, H., Okada, Y., Toyama, Y., & Blobel, C. P. (2007). Cutting edge: TNF-α-converting enzyme (TACE/ADAM17) inactivation in mouse myeloid cells prevents lethality from endotoxin shock. The Journal of Immunology, 179(5), 2686-2689.

Horiuchi, K., Le Gall, S., Schulte, M., Yamaguchi, T., Reiss, K., Murphy, G., ... & Blobel, C. P. (2007). Substrate selectivity of epidermal growth factor-receptor ligand sheddases and their regulation by phorbol esters and calcium influx. Molecular biology of the cell, 18(1), 176-188.

Huang, K., Geoffroy, J. S., Singer, M. S., & Rosen, S. D. (1991). A lymphocyte homing receptor (L-selectin) mediates the *in vitro* attachment of lymphocytes to myelinated tracts of the central nervous system. Journal of Clinical Investigation, 88(5), 1778.

Huang, K., Kikuta, A., & Rosen, S. D. (1994). Myelin localization of a central nervous system ligand for L-selectin. Journal of neuroimmunology, 53(2), 133-141.

Huang, T. T., & D'Andrea, A. D. (2006). Regulation of DNA repair by ubiquitylation. Nature Reviews Molecular Cell Biology, 7(5), 323-334.

Huynh, C., Poliseno, L., Segura, M. F., Medicherla, R., Haimovic, A., Menendez, S., ... & Boylan, J. F. (2011). The novel γ secretase inhibitor RO4929097 reduces the tumor initiating potential of melanoma. PloS one, 6(9), e25264.

Imai, Y., Singer, M. S., Fennie, C., Lasky, L. A., & Rosen, S. D. (1991). Identification of a carbohydrate-based endothelial ligand for a lymphocyte homing receptor. J Cell Biol, 113(5), 1213-1221.

Inui, S., Higashiyama, S., Hashimoto, K., Higashiyama, M., Yoshikawa, K., & Taniguchi, N. (1997). Possible role of coexpression of CD9 with membrane-anchored heparin-binding EGF-like growth factor and amphiregulin in cultured human keratinocyte growth. Journal of cellular physiology, 171(3), 291-298.

Ip, W. E., Sokolovska, A., Charriere, G. M., Boyer, L., Dejardin, S., Cappillino, M. P., ... & Stuart, L. M. (2010). Phagocytosis and phagosome acidification are required for pathogen processing and MyD88-dependent responses to Staphylococcus aureus. The Journal of Immunology, 184(12), 7071-7081.

Ivetic, A., & Ridley, A. J. (2004). Ezrin/radixin/moesin proteins and Rho GTPase signalling in leucocytes. Immunology, 112(2), 165-176.

Ivetic, A., Deka, J., Ridley, A., & Ager, A. (2002). The cytoplasmic tail of l-selectin interacts with members of the ezrin-radixin-moesin (ERM) family of proteins cell activation-dependent binding of moesin but not ezrin. Journal of Biological Chemistry, 277(3), 2321-2329.

Kahn, J., Walcheck, B., Migaki, G. I., Jutila, M. A., & Kishimoto, T. K. (1998). Calmodulin regulates L-selectin adhesion molecule expression and function through a proteasedependent mechanism. Cell, 92(6), 809-818.

Kaiser, M., Wiggin, G. R., Lightfoot, K., Arthur, J. S. C., & Macdonald, A. (2007). MSK regulate TCR-induced CREB phosphorylation but not immediate early gene transcription. European journal of immunology, 37(9), 2583-2595.

Kalinowski, A., Plowes, N. J., Huang, Q., Berdejo-Izquierdo, C., Russell, R. R., & Russell, K. S. (2010). Metalloproteinase-dependent cleavage of neuregulin and autocrine stimulation of vascular endothelial cells. The FASEB Journal, 24(7), 2567-2575.

Kansas, G. S. (1992). Structure and function of L-selectin. Apmis, 100(1-6), 287-293.

Karlsson, A., & Dahlgren, C. (2002). Assembly and activation of the neutrophil NADPH oxidase in granule membranes. Antioxidants and Redox Signaling, 4(1), 49-60.

Kawashima, H., Li, Y. F., Watanabe, N., Hirose, J., Hirose, M., & Miyasaka, M. (1999). Identification and characterization of ligands for L-selectin in the kidney. I. Versican, a large chondroitin sulfate proteoglycan, is a ligand for L-selectin. International immunology, 11(3), 393-405.

Kawashima, H., Watanabe, N., Hirose, M., Sun, X., Atarashi, K., Kimura, T., ... & Rehn, M. (2003). Collagen XVIII, a basement membrane heparan sulfate proteoglycan, interacts with L-selectin and monocyte chemoattractant protein-1. Journal of Biological Chemistry, 278(15), 13069-13076.

Kennedy, A. D., & DeLeo, F. R. (2009). Neutrophil apoptosis and the resolution of infection. Immunologic research, 43(1-3), 25-61.

Kettle, A. J., & Winterbourn, C. C. (1990). Superoxide enhances hypochlorous acid production by stimulated human neutrophils. Biochimica et Biophysica Acta (BBA)-Molecular Cell Research, 1052(3), 379-385.

Kiefel, H., Bondong, S., Hazin, J., Ridinger, J., Schirmer, U., Riedle, S., & Altevogt, P. (2012). L1CAM: a major driver for tumor cell invasion and motility. *Cell adhesion & migration*, *6*(4), 374-384.

Kilian, K., Dernedde, J., Mueller, E. C., Bahr, I., & Tauber, R. (2004). The interaction of protein kinase C isozymes α, ι, and θ with the cytoplasmic domain of L-selectin is modulated by phosphorylation of the receptor. Journal of Biological Chemistry, 279(33), 34472-34480.

Killock, D. J., & Ivetić, A. (2010). The cytoplasmic domains of TNFα-converting enzyme (TACE/ADAM17) and L-selectin are regulated differently by p38 MAPK and PKC to promote ectodomain shedding. Biochemical Journal, 428(2), 293-304.

Killock, D. J., Parsons, M., Zarrouk, M., Ameer-Beg, S. M., Ridley, A. J., Haskard, D. O., ... & Ivetić, A. (2009). *In vitro* and *in vivo* characterization of molecular interactions between calmodulin, ezrin/radixin/moesin, and L-selectin. Journal of Biological Chemistry, 284(13), 8833-8845.

Kim, S. H., & Sisodia, S. S. (2005). Evidence that the "NF" motif in transmembrane domain 4 of PS 1 is critical for binding with PEN-2. Journal of Biological Chemistry, 280(51), 41953-41966.

Kimberly, W. T., LaVoie, M. J., Ostaszewski, B. L., Ye, W., Wolfe, M. S., & Selkoe, D. J. (2003). γ-Secretase is a membrane protein complex comprised of PS, nicastrin, Aph-1, and Pen-2. Proceedings of the National Academy of Sciences, 100(11), 6382-6387.

Kitaya, K., & Yasuo, T. (2009). Dermatan sulfate proteoglycan biglycan as a potential selectin L/CD44 ligand involved in selective recruitment of peripheral blood CD16 (−) natural killer cells into human endometrium. Journal of leukocyte biology, 85(3), 391-400.

Klinger, A., Gebert, A., Bieber, K., Kalies, K., Ager, A., Bell, E. B., & Westermann, J. (2009). Cyclical expression of L-selectin (CD62L) by recirculating T cells. International immunology, 21(4), 443-455.

Kobawala, T. P., Trivedi, T. I., Gajjar, K. K., Patel, D. H., Patel, G. H., & Ghosh, N. R. (2016). Significance of TNF-α and the adhesion molecules: L-Selectin and VCAM-1 in papillary thyroid carcinoma. Journal of thyroid research, 2016.

Komatsu, M., Waguri, S., Chiba, T., Murata, S., Iwata, J. I., Tanida, I., ... & Tanaka, K. (2006). Loss of autophagy in the central nervous system causes neurodegeneration in mice. Nature, 441(7095), 880-884.

KONICEK, B. W., Xia, X., Rajavashisth, T., & Harrington, M. A. (1998). Regulation of mouse colony-stimulating factor-1 gene promoter activity by AP1 and cellular nucleic acid-binding protein. DNA and cell biology, 17(9), 799-809.

Korkmaz, B., Horwitz, M. S., Jenne, D. E., & Gauthier, F. (2010). Neutrophil elastase, proteinase 3, and cathepsin G as therapeutic targets in human diseases. Pharmacological reviews, 62(4), 726-759.

Kourtis, A. P., Nesheim, S. R., Thea, D., Ibegbu, C., Nahmias, A. J., & Lee, F. K. (2000). Correlation of virus load and soluble L-selectin, a marker of immune activation, in pediatric HIV-1 infection. Aids, 14(16), 2429-2436.

Ku, A. W., Muhitch, J. B., Powers, C. A., Diehl, M., Kim, M., Fisher, D. T., ... & Messmer, M. N. (2016). Tumor-induced MDSC act via remote control to inhibit L-selectin-dependent adaptive immunity in lymph nodes. eLife, 5, e17375.

Kyaw, T., Tipping, P., Toh, B. H., & Bobik, A. (2011). Current understanding of the role of B cell subsets and intimal and adventitial B cells in atherosclerosis. Current opinion in lipidology, 22(5), 373-379.

Lacy, P. (2006). Mechanisms of degranulation in neutrophils. Allergy, Asthma & Clinical Immunology, 2(3), 98.

Lange, A., Mills, R. E., Devine, S. E., & Corbett, A. H. (2008). A PY-NLS nuclear targeting signal is required for nuclear localization and function of the Saccharomyces cerevisiae mRNA-binding protein Hrp1. *Journal of Biological Chemistry*, *283*(19), 12926-12934.

Lasky, L. A. (1992). Selectins: Interpreters of Cell-Specific Carbohydrate. *Science*, *258*, 6NOVEMBER.

Laudon, H., Hansson, E. M., Melén, K., Bergman, A., Farmery, M. R., Winblad, B., ... & Näslund, J. (2005). A nine-transmembrane domain topology for PS 1. Journal of Biological Chemistry, 280(42), 35352-35360.

LaVoie, M. J., Ostaszewski, B. L., Ye, W., Wolfe, M. S., & Selkoe, D. J. (2003). γ-Secretase is a membrane protein complex comprised of PS, nicastrin, Aph-1, and Pen-2. Proceedings of the National Academy of Sciences, 100(11), 6382-6387.

Le Gall, S. M., Bobé, P., Reiss, K., Horiuchi, K., Niu, X. D., Lundell, D., ... & Blobel, C. P. (2009). ADAMs 10 and 17 represent differentially regulated components of a general shedding machinery for membrane proteins such as transforming growth factor α, L-selectin, and tumor necrosis factor α. Molecular biology of the cell, 20(6), 1785-1794.

Le Gall, S. M., Maretzky, T., Issuree, P. D., Niu, X. D., Reiss, K., Saftig, P., ... & Blobel, C. P. (2010). ADAM17 is regulated by a rapid and reversible mechanism that controls access to its catalytic site. J Cell Sci, 123(22), 3913-3922.

Lefrançois, L., & Marzo, A. L. (2006). The descent of memory T-cell subsets. Nature Reviews Immunology, 6(8), 618-623.

Lemberg, M. K., & Freeman, M. (2007). Functional and evolutionary implications of enhanced genomic analysis of rhomboid intramembrane proteases. Genome research, 17(11), 1634-1646.

Levy-Lahad, E., Wasco, W., Poorkaj, P., & Romano, D. M. (1995). Candidate gene for the chromosome 1 familial Alzheimer's disease locus. Science, 269(5226), 973.

Ley, K., Gaehtgens, P., Fennie, C., Singer, M. S., Lasky, L. A., & Rosen, S. D. (1991). Lectin-like cell adhesion molecule 1 mediates leukocyte rolling in mesenteric venules *in vivo*. Blood, 77(12), 2553-2555.

Li, X., Maretzky, T., Weskamp, G., Monette, S., Qing, X., Issuree, P. D. A., ... & Blobel, C. P. (2015). iRhoms 1 and 2 are essential upstream regulators of ADAM17-dependent EGFR signaling. Proceedings of the National Academy of Sciences, 112(19), 6080-6085.

Li, Y., Brazzell, J., Herrera, A., & Walcheck, B. (2006). ADAM17 deficiency by mature neutrophils has differential effects on L-selectin shedding. Blood, 108(7), 2275-2279.

Lichtenthaler, S. F. (2011). Alpha-secretase in Alzheimer's disease: molecular identity, regulation and therapeutic potential. Journal of neurochemistry, 116(1), 10-21.

Lipp, M., & Müller, G. (2002). Shaping up adaptive immunity: the impact of CCR7 and CXCR5 on lymphocyte trafficking. Verhandlungen der Deutschen Gesellschaft fur Pathologie, 87, 90-101.

Liu, C. Y., Wang, Y. M., Wang, C. L., Feng, P. H., Ko, H. W., Liu, Y. H., ... & Lee, K. Y. (2010). Population alterations of L-arginase-and inducible nitric oxide synthase-expressed CD11b+/CD14−/CD15+/CD33+ myeloid-derived suppressor cells and CD8+ T lymphocytes in patients with advanced-stage non-small cell lung cancer. Journal of cancer research and clinical oncology, 136(1), 35-45.

Liu, F. L., Wu, C. C., & Chang, D. M. (2014). TACE-dependent amphiregulin release is induced by IL-1β and promotes cell invasion in fibroblast-like synoviocytes in rheumatoid arthritis. Rheumatology, 53(2), 260-269.

Liu, H., Chi, A. W., Arnett, K. L., Chiang, M. Y., Xu, L., Shestova, O., ... & Blacklow, S. C. (2010). Notch dimerization is required for leukemogenesis and T-cell development. *Genes & development*, *24*(21), 2395-2407.

Loers, G., & Schachner, M. (2007). Recognition molecules and neural repair. Journal of neurochemistry, 101(4), 865-882

Loria, V., Dato, I., Graziani, F., & Biasucci, L. M. (2008). Myeloperoxidase: a new biomarker of inflammation in ischemic heart disease and acute coronary syndromes. Mediators of inflammation, 2008.

Lyu, J., Wesselschmidt, R. L., & Lu, W. (2009). Cdc37 regulates Ryk signaling by stabilizing the cleaved Ryk intracellular domain. Journal of Biological Chemistry, 284(19), 12940-12948.

Ma, X. L., Weyrich, A. S., Lefer, D. J., Buerke, M., Albertine, K. H., Kishimoto, T. K., & Lefer, A. M. (1993). Monoclonal antibody to L-selectin attenuates neutrophil accumulation and protects ischemic reperfused cat myocardium. Circulation, 88(2), 649-658.

Major, A. S., Fazio, S., & Linton, M. F. (2002). B-lymphocyte deficiency increases atherosclerosis in LDL receptor–null mice. Arteriosclerosis, thrombosis, and vascular biology, 22(11), 1892-1898.

Mao, G., Cui, M. Z., Li, T., Jin, Y., & Xu, X. (2012). Pen-2 is dispensable for endoproteolysis of PS 1, and nicastrin-Aph subcomplex is important for both γ-secretase assembly and substrate recruitment. Journal of neurochemistry, 123(5), 837-844.

Marambaud, P., Shioi, J., Serban, G., Georgakopoulos, A., Sarner, S., Nagy, V., ... & Wisniewski, T. (2002). A PS-1/γ-secretase cleavage releases the E-cadherin intracellular domain and regulates disassembly of adherens junctions. The EMBO journal, 21(8), 1948-1956.

Marambaud, P., Shioi, J., Serban, G., Georgakopoulos, A., Sarner, S., Nagy, V., ... & Wisniewski, T. (2002). A PS-1/γ-secretase cleavage releases the E-cadherin intracellular domain and regulates disassembly of adherens junctions. *The EMBO journal*, *21*(8), 1948-1956.

Maretzky, T., McIlwain, D. R., Issuree, P. D. A., Li, X., Malapeira, J., Amin, S., ... & Blobel, C. P. (2013). iRhom2 controls the substrate selectivity of stimulated ADAM17-dependent ectodomain shedding. Proceedings of the National Academy of Sciences, 110(28), 11433-11438.

Masopust, D., & Picker, L. J. (2012). Hidden memories: frontline memory T cells and early pathogen interception. The Journal of Immunology, 188(12), 5811-5817.

Matala, E., Alexander, S. R., Kishimoto, T. K., & Walcheck, B. (2001). The cytoplasmic domain of L-selectin participates in regulating L-selectin endoproteolysis. The Journal of Immunology, 167(3), 1617-1623.

Matsuoka, Y., Hughes, C. A., & Bennett, V. (1996). Adducin regulation definition of the calmodulin-binding domain and sites of phosphorylation by protein kinases A and C. Journal of Biological Chemistry, 271(41), 25157-25166.

Matthews, A. L., Noy, P. J., Reyat, J. S., & Tomlinson, M. G. (2016). Regulation of A disintegrin and metalloproteinase (ADAM) family sheddases ADAM10 and ADAM17: The emerging role of tetraspanins and rhomboids. Platelets, 1-9.

McDermott, M. F., Aksentijevich, I., Galon, J., McDermott, E. M., Ogunkolade, B. W., Centola, M., ... & McCarthy, J. (1999). Germline mutations in the extracellular domains of the 55 kDa TNF receptor, TNFR1, define a family of dominantly inherited autoinflammatory syndromes. Cell, 97(1), 133-144.

Mertins, P., Qiao, J. W., Patel, J., Udeshi, N. D., Clauser, K. R., Mani, D. R., ... & Carr, S. A. (2013). Integrated proteomic analysis of post-translational modifications by serial enrichment. Nature methods, 10(7), 634-637.

Micchelli, C. A., Esler, W. P., Kimberly, W. T., Jack, C., Berezovska, O., Kornilova, A., ... & Wolfe, M. S. (2003). γ-Secretase/PS inhibitors for Alzheimer's disease phenocopy Notch mutations in Drosophila. The FASEB Journal, 17(1), 79-81.

Migaki, G. I., Kahn, J., & Kishimoto, T. K. (1995). Mutational analysis of the membrane-proximal cleavage site of L-selectin: relaxed sequence specificity surrounding the cleavage site. Journal of Experimental Medicine, 182(2), 549-558.

Milla, M. E., Gonzales, P. E., & Leonard, J. D. (2006). The TACE zymogen. Cell biochemistry and biophysics, 44(3), 342-348.

Mitchell, D. J., Li, P., Reinhardt, P. H., & Kubes, P. (2000). Importance of L-selectin–dependent leukocyte–leukocyte interactions in human whole blood. Blood, 95(9), 2954-2959.

Möller-Hackbarth, K., Dewitz, C., Schweigert, O., Trad, A., Garbers, C., Rose-John, S., & Scheller, J. (2013). A disintegrin and metalloprotease (ADAM) 10 and ADAM17 are major sheddases of T cell immunoglobulin and mucin domain 3 (Tim-3). *Journal of Biological Chemistry*, *288*(48), 34529-34544.

Mora, J. R., & von Andrian, U. H. (2006). T-cell homing specificity and plasticity: new concepts and future challenges. Trends in immunology, 27(5), 235-243.

Morohashi, Y., Kan, T., Tominari, Y., Fuwa, H., Okamura, Y., Watanabe, N., ... & Tomita, T. (2006). C-terminal fragment of PS is the molecular target of a dipeptidic γ-secretase-specific inhibitor DAPT (N-[N-(3, 5-difluorophenacetyl)-L-alanyl]-S-phenylglycine t-butyl ester). Journal of Biological Chemistry, 281(21), 14670-14676.

Moss, M. L., Jin, S. C., Milla, M. E., Burkhart, W., Carter, H. L., Chen, W. J., ... & Kost, T. A. (1997). Cloning of a disintegrin metalloproteinase that processes precursor tumour-necrosis factor-alpha. Nature, 385(6618), 733.

Mulligan, M. S., Lowe, J. B., Larsen, R. D., Paulson, J., Zheng, Z. L., Defrees, S., ... & Ward, P. A. (1993). Protective effects of sialylated oligosaccharides in immune complex-induced acute lung injury. Journal of Experimental Medicine, 178, 623-623.

Murphy, G. (2009, April). Regulation of the proteolytic disintegrin metalloproteinases, the 'Sheddases'. In *Seminars in cell & developmental biology* (Vol. 20, No. 2, pp. 138-145). Academic Press.

Needham, L. K., & Schnaar, R. L. (1993). The HNK-1 reactive sulfoglucuronyl glycolipids are ligands for L-selectin and P-selectin but not E-selectin. Proceedings of the National Academy of Sciences, 90(4), 1359-1363.

Neel, V. A., & Young, M. W. (1994). Igloo, a GAP-43-related gene expressed in the developing nervous system of Drosophila. *DEVELOPMENT-CAMBRIDGE-*, *120*, 2235-2235.

Nelson, R. M., Cecconi, O., Roberts, W. G., Aruffo, A., Linhardt, R. J., & Bevilacqua, M. P. (1993). Heparin oligosaccharides bind L-and P-selectin and inhibit acute inflammation. Blood, 82(11), 3253-3258.

Ni, C. Y., Murphy, M. P., Golde, T. E., & Carpenter, G. (2001). γ-Secretase cleavage and nuclear localization of ErbB-4 receptor tyrosine kinase. *Science*, *294*(5549), 2179-2181.

Nishi, E., Hiraoka, Y., Yoshida, K., Okawa, K., & Kita, T. (2006). Nardilysin enhances ectodomain shedding of heparin-binding epidermal growth factor-like growth factor through activation of tumor necrosis factor-α-converting enzyme. Journal of Biological Chemistry, 281(41), 31164-31172.

Nyabi, O., Bentahir, M., Horré, K., Herreman, A., Gottardi-Littell, N., Van Broeckhoven, C., ... & De Strooper, B. (2003). PSs mutated at Asp-257 or Asp-385 restore Pen-2 expression and

Nicastrin glycosylation but remain catalytically inactive in the absence of wild type PS. Journal of Biological Chemistry, 278(44), 43430-43436.

Öberg, C., Li, J., Pauley, A., Wolf, E., Gurney, M., & Lendahl, U. (2001). The Notch intracellular domain is ubiquitinated and negatively regulated by the mammalian Sel-10 homolog. Journal of Biological Chemistry, 276(38), 35847-35853.

Oh, K., Lee, O. Y., Shon, S. Y., Nam, O., Ryu, P. M., Seo, M. W., & Lee, D. S. (2013). A mutual activation loop between breast cancer cells and myeloid-derived suppressor cells facilitates spontaneous metastasis through IL-6 trans-signaling in a murine model. Breast cancer research, 15(5), R79.

Ovalle, S., Gutiérrez-López, M. D., Monjas, A., & Cabañas, C. (2007). Implication of the tetraspanin CD9 in the immune system and cancer. Inmunología, 26(2), 65-72.

Palacino, J. J., Berechid, B. E., Alexander, P., Eckman, C., Younkin, S., Nye, J. S., & Wolozin, B. (2000). Regulation of amyloid precursor protein processing by PS 1 (PS1) and PS2 in PS1 knockout cells. *Journal of Biological Chemistry*, *275*(1), 215-222.

Park, J. T., Li, M., Nakayama, K., Mao, T. L., Davidson, B., Zhang, Z., ... & Wang, T. L. (2006). Notch3 gene amplification in ovarian cancer. Cancer research, 66(12), 6312-6318.

Parker, K. H., Sinha, P., Horn, L. A., Clements, V. K., Yang, H., Li, J., ... & Ostrand-Rosenberg, S. (2014). HMGB1 enhances immune suppression by facilitating the differentiation and suppressive activity of myeloid-derived suppressor cells. Cancer research, 74(20), 5723-5733.

Pear, W. S., & Aster, J. C. (2004). T cell acute lymphoblastic leukemia/lymphoma: a human cancer commonly associated with aberrant NOTCH1 signaling. *Current opinion in hematology*, *11*(6), 426-433.

Peiretti, F., Deprez-Beauclair, P., Bonardo, B., Aubert, H., Juhan-Vague, I., & Nalbone, G. (2003). Identification of SAP97 as an intracellular binding partner of TACE. Journal of cell science, 116(10), 1949-1957.

Peschon, J. J., Slack, J. L., Reddy, P., Stocking, K. L., Sunnarborg, S. W., Lee, D. C., ... & Boyce, R. W. (1998). An essential role for ectodomain shedding in mammalian development. *Science*, *282*(5392), 1281-1284.

Phong, M. C., Gutwein, P., Kadel, S., Hexel, K., Altevogt, P., Linderkamp, O., & Brenner, B. (2003). Molecular mechanisms of L-selectin-induced co-localization rafts and shedding. Biochemical and biophysical research communications, 300(2), 563-569

Pietromonaco, S. F., Simons, P. C., Altman, A., & Elias, L. (1998). Protein kinase C-θ phosphorylation of moesin in the actin-binding sequence. *Journal of Biological Chemistry*, *273*(13), 7594-7603.

Pinnix, C. C., & Herlyn, M. (2007). The many faces of Notch signaling in skin-derived cells. *Pigment cell research*, *20*(6), 458-465.

Podlisny, M. B., Citron, M., Amarante, P., Sherrington, R., Xia, W., Zhang, J., ... & Koo, E. H. (1997). PS proteins undergo heterogeneous endoproteolysis between Thr 291 and Ala 299 and occur as stable N-and C-terminal fragments in normal and Alzheimer brain tissue. Neurobiology of disease, 3(4), 325-337.

Prenzel, N., Zwick, E., Daub, H., Leserer, M., Abraham, R., Wallasch, C., & Ullrich, A. (1999). EGF receptor transactivation by G-protein-coupled receptors requires metalloproteinase cleavage of proHB-EGF. Nature, 402(6764), 884-888.

Prokop, S., Haass, C., & Steiner, H. (2005). Length and overall sequence of the PEN-2 C-terminal domain determines its function in the stabilization of PS fragments. Journal of neurochemistry, 94(1), 57-62.

Prokop, S., Shirotani, K., Edbauer, D., Haass, C., & Steiner, H. (2004). Requirement of PEN-2 for stabilization of the PS N-/C-terminal fragment heterodimer within the γ-secretase complex. Journal of Biological Chemistry, 279(22), 23255-23261.

Qian, M., Shen, X., & Wang, H. (2016). The distinct role of ADAM17 in APP proteolysis and microglial activation related to Alzheimer's disease. Cellular and molecular neurobiology, 36(4), 471-482.

Reddy, P., Slack, J. L., Davis, R., Cerretti, D. P., Kozlosky, C. J., Blanton, R. A., ... & Black, R. A. (2000). Functional analysis of the domain structure of tumor necrosis factor-α converting enzyme. *Journal of Biological Chemistry*, *275*(19), 14608-14614.

Reiss, K., Maretzky, T., Ludwig, A., Tousseyn, T., De Strooper, B., Hartmann, D., & Saftig, P. (2005). ADAM10 cleavage of N-cadherin and regulation of cell–cell adhesion and β-catenin nuclear signalling. *The EMBO journal*, *24*(4), 742-752.

Reyes-Moreno, C., Girouard, J., Lapointe, R., Darveau, A., & Mourad, W. (2004). CD40/CD40 homodimers are required for CD40-induced phosphatidylinositol 3-kinase-dependent expression of B7. 2 by human B lymphocytes. *Journal of Biological Chemistry*, *279*(9), 7799-7806.

Ribes, S., Ebert, S., Regen, T., Agarwal, A., Tauber, S. C., Czesnik, D., ... & Hammerschmidt, S. (2010). Toll-like receptor stimulation enhances phagocytosis and intracellular killing of nonencapsulated and encapsulated Streptococcus pneumoniae by murine microglia. Infection and immunity, 78(2), 865-871.

Richards, F. M., Tape, C. J., Jodrell, D. I., & Murphy, G. (2012). Anti-tumour effects of a specific anti-ADAM17 antibody in an ovarian cancer model *in vivo*. *PloS one*, *7*(7), e40597.

Robinson, J. M. (2008). Reactive oxygen species in phagocytic leukocytes. Histochemistry and cell biology, 130(2), 281.

Rogaev, E. I., Sherrington, R., Rogaeva, E. A., Levesque, G., Ikeda, M., Liang, Y., ... & Mar, L. (1995). Familial Alzheimer's disease in kindreds with missense mutations in a gene on chromosome 1 related to the Alzheimer's disease type 3 gene. Nature, 376(6543), 775-778.

Rogaev, E. I., Sherrington, R., Rogaeva, E. A., Levesque, G., Ikeda, M., Liang, Y., ... & Mar, L. (1995). Familial Alzheimer's disease in kindreds with missense mutations in a gene on chromosome 1 related to the Alzheimer's disease type 3 gene. Nature, 376(6543), 775.

Rovida, E., Paccagnini, A., Del Rosso, M., Peschon, J., & Sbarba, P. D. (2001). TNF-α-converting enzyme cleaves the macrophage colony-stimulating factor receptor in macrophages undergoing activation. The Journal of Immunology, 166(3), 1583-1589.

Rozenberg, I., Sluka, S. H., Mocharla, P., Hallenberg, A., Rotzius, P., Boren, J., ... & Eriksson, E. E. (2011). Deletion of L-selectin increases atherosclerosis development in ApoE−/− mice. PloS one, 6(7), e21675.

Rzeniewicz, K., Newe, A., Gallardo, A. R., Davies, J., Holt, M. R., Patel, A., ... & Parsons, M. (2015). L-selectin shedding is activated specifically within transmigrating pseudopods of monocytes to regulate cell polarity *in vitro*. Proceedings of the National Academy of Sciences, 112(12), E1461-E1470.

Sahin, U., Weskamp, G., Kelly, K., Zhou, H. M., Higashiyama, S., Peschon, J., ... & Blobel, C. P. (2004). Distinct roles for ADAM10 and ADAM17 in ectodomain shedding of six EGFR ligands. The Journal of cell biology, 164(5), 769-779.

Sako, D., Chang, X. J., Barone, K. M., Vachino, G., White, H. M., Shaw, G., ... & Cumming, D. A. (1993). Expression cloning of a functional glycoprotein ligand for P-selectin. Cell, 75(6), 1179-1186.

Sallusto, F., Geginat, J., & Lanzavecchia, A. (2004). Central memory and effector memory T cell subsets: function, generation, and maintenance. Annu. Rev. Immunol., 22, 745-763.

Sallusto, F., Mackay, C. R., & Lanzavecchia, A. (2000). The role of chemokine receptors in primary, effector, and memory immune responses. Annual review of immunology, 18(1), 593-620.

Sallusto, F., Palermo, B., Hoy, A., & Lanzavecchia, A. (1999). The role of chemokine receptors in directing traffic of naive, type 1 and type 2 T cells. In Mechanisms of B Cell Neoplasia 1998 (pp. 123-129). Springer Berlin Heidelberg.

Sassetti, C., Tangemann, K., Singer, M. S., Kershaw, D. B., & Rosen, S. D. (1998). Identification of podocalyxin-like protein as a high endothelial venule ligand for L-selectin: parallels to CD34. Journal of Experimental Medicine, 187(12), 1965-1975.

Sato, C., Takagi, S., Tomita, T., & Iwatsubo, T. (2008). The C-terminal PAL motif and transmembrane domain 9 of PS 1 are involved in the formation of the catalytic pore of the γ-secretase. The Journal of Neuroscience, 28(24), 6264-6271

Scapini, P., Lapinet-Vera, J. A., Gasperini, S., Calzetti, F., Bazzoni, F., & Cassatella, M. A. (2000). The neutrophil as a cellular source of chemokines. Immunological reviews, 177(1), 195-203.

Schleiffenbaum, B., Spertini, O., & Tedder, T. F. (1992). Soluble L-selectin is present in human plasma at high levels and retains functional activity. The Journal of Cell Biology, 119(1), 229-238.

Schlöndorff, J., Becherer, J. D., & Blobel, C. P. (2000). Intracellular maturation and localization of the tumour necrosis factor α convertase (TACE). Biochemical Journal, 347(1), 131-138.

Schroeter, E. H., Kisslinger, J. A., & Kopan, R. (1998). Notch-1 signalling requires ligand-induced proteolytic release of intracellular domain. Nature, 393(6683), 382-386.

Schulz, J. G., Annaert, W., Vandekerckhove, J., Zimmermann, P., De Strooper, B., & David, G. (2003). Syndecan 3 intramembrane proteolysis is PS/γ-secretase-dependent and modulates cytosolic signaling. Journal of Biological Chemistry, 278(49), 48651-48657.

Schweisguth, F. (2004). Regulation of notch signaling activity. Current biology, 14(3), R129-R138.

Scott, A. J., O'Dea, K. P., O'Callaghan, D., Williams, L., Dokpesi, J. O., Tatton, L., ... & Takata, M. (2011). Reactive oxygen species and p38 mitogen-activated protein kinase mediate tumor necrosis factor α-converting enzyme (TACE/ADAM-17) activation in primary human monocytes. Journal of Biological Chemistry, 286(41), 35466-35476.

Segal, A. W. (2005). How neutrophils kill microbes. Annu. Rev. Immunol., 23, 197-223.

Selders, G. S., Fetz, A. E., Radic, M. Z., & Bowlin, G. L. (2017). An overview of the role of neutrophils in innate immunity, inflammation and host-biomaterial integration. Regenerative Biomaterials, 4(1), 55-68.

Selkoe, D. J. (1994). Cell biology of the amyloid beta-protein precursor and the mechanism of Alzheimer's disease. Annual review of cell biology, 10(1), 373-403.

Selkoe, D., & Kopan, R. (2003). Notch and PS: regulated intramembrane proteolysis links development and degeneration. *Annual review of neuroscience*, *26*(1), 565-597.

Serhan, C. N., & Savill, J. (2005). Resolution of inflammation: the beginning programs the end. Nature immunology, 6(12), 1191-1197.

Shah, S., Lee, S. F., Tabuchi, K., Hao, Y. H., Yu, C., LaPlant, Q., ... & Yu, G. (2005). Nicastrin functions as a γ-secretase-substrate receptor. Cell, 122(3), 435-447.

Shearman, M. S., Beher, D., Clarke, E. E., Lewis, H. D., Harrison, T., Hunt, P., ... & Castro, J. L. (2000). L-685,458, an aspartyl protease transition state mimic, is a potent inhibitor of amyloid β-protein precursor γ-secretase activity. Biochemistry, 39(30), 8698-8704.

Sherrington, R., Rogaev, E. I., Liang, Y. A., & Rogaeva, E. A. (1995). Cloning of a gene bearing missense mutations in early-onset familial Alzheimer's disease. Nature, 375(6534), 754.

Shi, W., Fan, H., Shum, L., & Derynck, R. (2000). The tetraspanin CD9 associates with transmembrane TGF-α and regulates TGF-α–induced EGF receptor activation and cell proliferation. The Journal of cell biology, 148(3), 591-602.

Shirotani, K., Edbauer, D., Capell, A., Schmitz, J., Steiner, H., & Haass, C. (2003). γ-Secretase activity is associated with a conformational change of nicastrin. Journal of Biological Chemistry, 278(19), 16474-16477.

Sica, A., Matsushima, K., Van Damme, J., Wang, J. M., Polentarutti, N., Dejana, E., ... & Mantovani, A. (1990). IL-1 transcriptionally activates the neutrophil chemotactic factor/IL-8 gene in endothelial cells. Immunology, 69(4), 548.

Simon, S. I., Burns, A. R., Taylor, A. D., Gopalan, P. K., Lynam, E. B., Sklar, L. A., & Smith, C. W. (1995). L-selectin (CD62L) cross-linking signals neutrophil adhesive functions via the Mac-1 (CD11b/CD18) beta 2-integrin. The Journal of Immunology, 155(3), 1502-1514.

Smolen, J. E., Petersen, T. K., Koch, C., O'Keefe, S. J., Hanlon, W. A., Seo, S., ... & Simon, S. I. (2000). L-selectin signaling of neutrophil adhesion and degranulation involves p38 mitogen-activated protein kinase. Journal of Biological Chemistry, 275(21), 15876-15884.

Sommer, A., Kordowski, F., Büch, J., Maretzky, T., Evers, A., Andrä, J., ... & Tholey, A. (2016). Phosphatidylserine exposure is required for ADAM17 sheddase function. Nature communications, 7.

Soond, S. M., Everson, B., Riches, D. W., & Murphy, G. (2005). ERK-mediated phosphorylation of Thr735 in TNFα-converting enzyme and its potential role in TACE protein trafficking. Journal of cell science, 118(11), 2371-2380.

Spertini, O., Cordey, A. S., Monai, N., Giuffrè, L., & Schapira, M. (1996). P-selectin glycoprotein ligand 1 is a ligand for L-selectin on neutrophils, monocytes, and CD34+ hematopoietic progenitor cells. The Journal of cell biology, 135(2), 523-531.

Spertini, O., Schleiffenbaum, B., White-Owen, C., Ruiz, P., & Tedder, T. F. (1992). ELISA for quantitation of L-selectin shed from leukocytes *in vivo*. Journal of immunological methods, 156(1), 115-123.

Steadman, R., Petersen, M. M., & Williams, J. D. (1996). Human neutrophil secondary granule exocytosis is independent of protein kinase activation and is modified by calmodulin activity. The international journal of biochemistry & cell biology, 28(7), 777-786.

Steiner, H., Duff, K., Capell, A., Romig, H., Grim, M. G., Lincoln, S., ... & Citron, M. (1999). A loss of function mutation of PS-2 interferes with amyloid β-peptide production and Notch signaling. Journal of Biological Chemistry, 274(40), 28669-28673.

Stoddart, J. H., Jasuja, R. R., Sikorski, M. A., Von Andrian, U. H., & Mier, J. W. (1996). Protease-resistant L-selectin mutants. Down-modulation by cross-linking but not cellular activation. The Journal of Immunology, 157(12), 5653-5659.

Stoyanova, T., Goldstein, A. S., Cai, H., Drake, J. M., Huang, J., & Witte, O. N. (2012). Regulated proteolysis of Trop2 drives epithelial hyperplasia and stem cell self-renewal via β-catenin signaling. Genes & development, 26(20), 2271-2285.

Streeter, P. R., Rouse, B. T., & Butcher, E. C. (1988). Immunohistologic and functional characterization of a vascular addressin involved in lymphocyte homing into peripheral lymph nodes. The Journal of Cell Biology, 107(5), 1853-1862.

Struhl, G., & Adachi, A. (2000). Requirements for PS-dependent cleavage of notch and other transmembrane proteins. Molecular cell, 6(3), 625-636.

Stylianou, S., Clarke, R. B., & Brennan, K. (2006). Aberrant activation of notch signaling in human breast cancer. *Cancer research*, *66*(3), 1517-1525.

Suh, Jaehong, *et al*. "FE65 proteins regulate NMDA receptor activation-induced amyloid precursor protein processing." Journal of neurochemistry 119.2 (2011): 377-388.

Sundvall, M., Veikkolainen, V., Kurppa, K., Salah, Z., Tvorogov, D., van Zoelen, E. J., ... & Elenius, K. (2010). Cell death or survival promoted by alternative isoforms of ErbB4. *Molecular biology of the cell*, *21*(23), 4275-4286.

Surena, A. L., de Faria, G. P., Studler, J. M., Peiretti, F., Pidoux, M., Camonis, J., ... & Junier, M. P. (2009). DLG1/SAP97 modulates transforming growth factor α bioavailability. Biochimica et Biophysica Acta (BBA)-Molecular Cell Research, 1793(2), 264-272.

Swendeman, S., Mendelson, K., Weskamp, G., Horiuchi, K., Deutsch, U., Scherle, P., ... & Blobel, C. P. (2008). VEGF-A stimulates ADAM17-dependent shedding of VEGFR2 and crosstalk between VEGFR2 and ERK signaling. Circulation research, 103(9), 916-918.

Tachida Y., Nakagawa K., Saito T. *et al*. (2008) Interleukin-1 beta upregulates TACE to enhance alpha-cleavage of APP in neurons:resulting decrease in Abeta production. J. Neurochem. 104, 1387–1393

Takasugi, N., Tomita, T., Hayashi, I., Tsuruoka, M., Niimura, M., Takahashi, Y., ... & Iwatsubo, T. (2003). The role of PS cofactors in the γ-secretase complex. Nature, 422(6930), 438-441.

Tammam, J., Ware, C., Efferson, C., O'neil, J., Rao, S., Qu, X., ... & Kunii, K. (2009). Down-regulation of the Notch pathway mediated by a γ-secretase inhibitor induces anti-tumour effects in mouse models of T-cell leukaemia. British journal of pharmacology, 158(5), 1183-1195.

Tan, Belinda H., et al. "Macrophages acquire neutrophil granules for antimicrobial activity against intracellular pathogens." The Journal of Immunology 177.3 (2006): 1864-1871.

Tang, M. L., Hale, L. P., Steeber, D. A., & Tedder, T. F. (1997). L-selectin is involved in lymphocyte migration to sites of inflammation in the skin: delayed rejection of allografts in L-selectin-deficient mice. The Journal of Immunology, 158(11), 5191-5199.

Tang, M. L., Steeber, D. A., Zhang, X. Q., & Tedder, T. F. (1998). Intrinsic differences in L-selectin expression levels affect T and B lymphocyte subset-specific recirculation pathways. The Journal of Immunology, 160(10), 5113-5121.

Taylor, P. A., Panoskaltsis-Mortari, A., Swedin, J. M., Lucas, P. J., Gress, R. E., Levine, B. L., ... & Blazar, B. R. (2004). L-Selectinhi but not the L-selectinlo CD4+ 25+ T-regulatory cells are potent inhibitors of GVHD and BM graft rejection. Blood, 104(12), 3804-3812.

Tedder, T. F., Steeber, D. A., & Pizcueta, P. (1995). L-selectin-deficient mice have impaired leukocyte recruitment into inflammatory sites. Journal of Experimental Medicine, 181(6), 2259-2264.

Tellier, E., Canault, M., Rebsomen, L., Bonardo, B., Juhan-Vague, I., Nalbone, G., & Peiretti, F. (2006). The shedding activity of ADAM17 is sequestered in lipid rafts. Experimental cell research, 312(20), 3969-3980.

Thinakaran G., Borchelt D. R., Lee M. K. *et al*. (1996) Endoproteolysis of PS 1 and accumulation of processed derivatives *in vivo*. Neuron 17, 181–190.

Tolia, A., Horré, K., & De Strooper, B. (2008). Transmembrane domain 9 of PS determines the dynamic conformation of the catalytic site of γ-secretase. Journal of Biological Chemistry, 283(28), 19793-19803.

Tousseyn, T., Thathiah, A., Jorissen, E., Raemaekers, T., Konietzko, U., Reiss, K., ... & Annaert, W. (2009). ADAM10, the rate-limiting protease of regulated intramembrane proteolysis of Notch and other proteins, is processed by ADAMS-9, ADAMS-15, and the γ-secretase. Journal of Biological Chemistry, 284(17), 11738-11747.

Trinite, B., Chan, C. N., Lee, C. S., Mahajan, S., Luo, Y., Muesing, M. A., ... & Levy, D. N. (2014). Suppression of Foxo1 activity and down-modulation of CD62L (L-selectin) in HIV-1 infected resting CD4 T cells. PLoS One, 9(10), e110719.

Trotman, L. C., Wang, X., Alimonti, A., Chen, Z., Teruya-Feldstein, J., Yang, H., ... & Tempst, P. (2007). Ubiquitination regulates PTEN nuclear import and tumor suppression. Cell, 128(1), 141-156.

Troyanovsky, S. (2005). Cadherin dimers in cell–cell adhesion. European journal of cell biology, 84(2), 225-233.

Tsang, Y. T., Neelamegham, S., Hu, Y., Berg, E. L., Burns, A. R., Smith, C. W., & Simon, S. I. (1997). Synergy between L-selectin signaling and chemotactic activation during neutrophil adhesion and transmigration. The Journal of Immunology, 159(9), 4566-4577.

Tsukamoto, S., Takeuchi, M., Kawaguchi, T., Togasaki, E., Yamazaki, A., Sugita, Y., ... & Sakaida, E. (2014). Tetraspanin CD9 modulates ADAM17-mediated shedding of LR11 in leukocytes. Experimental & molecular medicine, 46(4), e89.

Tu, L., Chen, A., Delahunty, M. D., Moore, K. L., Watson, S. R., McEver, R. P., & Tedder, T. F. (1996). L-selectin binds to P-selectin glycoprotein ligand-1 on leukocytes: interactions between the lectin, epidermal growth factor, and consensus repeat domains of the selectins determine ligand binding specificity. The Journal of Immunology, 157(9), 3995-4004.

Tu, L., Poe, J. C., Kadono, T., Venturi, G. M., Bullard, D. C., Tedder, T. F., & Steeber, D. A. (2002). A functional role for circulating mouse L-selectin in regulating leukocyte/endothelial cell interactions *in vivo*. The Journal of Immunology, 169(4), 2034-2043.

Van Itallie, C. M., & Anderson, J. M. (2014, December). Architecture of tight junctions and principles of molecular composition. In *Seminars in cell & developmental biology* (Vol. 36, pp. 157-165). Academic Press.

Van Niel, G., Charrin, S., Simoes, S., Romao, M., Rochin, L., Saftig, P., ... & Raposo, G. (2011). The tetraspanin CD63 regulates ESCRT-independent and-dependent endosomal sorting during melanogenesis. Developmental cell, 21(4), 708-721.

Van Zante, A., & Rosen, S. D. (2003). Sulphated endothelial ligands for L-selectin in lymphocyte homing and inflammation.

Vassena, L., Giuliani, E., Koppensteiner, H., Bolduan, S., Schindler, M., & Doria, M. (2015). HIV-1 Nef and Vpu interfere with L-selectin (CD62L) cell surface expression to inhibit adhesion and signaling in infected CD4+ T lymphocytes. Journal of virology, 89(10), 5687-5700.

Venturi, G. M., Tu, L., Kadono, T., Khan, A. I., Fujimoto, Y., Oshel, P., ... & Steeber, D. A. (2003). Leukocyte migration is regulated by L-selectin endoproteolytic release. Immunity, 19(5), 713-724.

Vestweber, D., & Blanks, J. E. (1999). Mechanisms that regulate the function of the selectins and their ligands. Physiological reviews, 79(1), 181-213.

von Andrian, U. H., Chambers, J. D., McEvoy, L. M., Bargatze, R. F., Arfors, K. E., & Butcher, E. C. (1991). Two-step model of leukocyte-endothelial cell interaction in inflammation: distinct roles for LECAM-1 and the leukocyte beta 2 integrins *in vivo*. Proceedings of the National Academy of Sciences, 88(17), 7538-7542.

von Rotz, R. C., Kohli, B. M., Bosset, J., Meier, M., Suzuki, T., Nitsch, R. M., & Konietzko, U. (2004). The APP intracellular domain forms nuclear multiprotein complexes and regulates the transcription of its own precursor. Journal of cell science, 117(19), 4435-4448.

Waddell, T. K., Fialkow, L., Chan, C. K., Kishimoto, T. K., & Downey, G. P. (1994). Potentiation of the oxidative burst of human neutrophils. A signaling role for L-selectin. Journal of Biological Chemistry, 269(28), 18485-18491.

Waddell, T. K., Fialkow, L., Chan, C. K., Kishimoto, T. K., & Downey, G. P. (1995). Signaling functions of L-selectin enhancement of tyrosine phosphorylation and activation of MAP kinase. Journal of Biological Chemistry, 270(25), 15403-15411.

Walcheck, B., Alexander, S. R., Hill, C. A. S., & Matala, E. (2003). ADAM-17-independent shedding of L-selectin. Journal of leukocyte biology, 74(3), 389-394.

Walcheck, B., Kahn, J., Fisher, J. M., & Wang, B. B. (1996). Neutrophil rolling altered by inhibition of L-selectin shedding *in vitro*. Nature, 380(6576), 720.

Wang, R., Zhang, Y. W., Sun, P., Liu, R., Zhang, X., Zhang, X., ... & Zhang, Z. (2006). Transcriptional regulation of PEN-2, a key component of the γ-secretase complex, by CREB. Molecular and cellular biology, 26(4), 1347-1354.

Wang, Y., Herrera, A. H., Li, Y., Belani, K. K., & Walcheck, B. (2009). Regulation of mature ADAM17 by redox agents for L-selectin shedding. The Journal of Immunology, 182(4), 2449-2457.

Wang, Y., Zhang, A. C., Ni, Z., Herrera, A., & Walcheck, B. (2010). ADAM17 activity and other mechanisms of soluble L-selectin production during death receptor-induced leukocyte apoptosis. The Journal of Immunology, 184(8), 4447-4454.

Wang, Y., Zhang, Y., & Ha, Y. (2006). Crystal structure of a rhomboid family intramembrane protease. Nature, 444(7116), 179-180.

Wanger, T. M., Dewitt, S., Collins, A., Maitland, N. J., Poghosyan, Z., & Knäuper, V. (2015). Differential regulation of TROP2 release by PKC isoforms through vesicles and ADAM17. *Cellular signalling*, *27*(7), 1325-1335.

Weber, S., & Saftig, P. (2012). Ectodomain shedding and ADAMs in development. Development, 139(20), 3693-3709.

Weiss, A. (1993). T cell antigen receptor signal transduction: a tale of tails and cytoplasmic protein-tyrosine kinases. *Cell*, *73*(2), 209-212.

Weiss, G., & Schaible, U. E. (2015). Macrophage defense mechanisms against intracellular bacteria. Immunological reviews, 264(1), 182-203.

Westermann, J., Ehlers, E. M., Exton, M. S., Kaiser, M., & Bode, U. (2001). Migration of naive, effector and memory T cells: implications for the regulation of immune responses. *Immunological reviews*, *184*(1), 20-37.

Willems, S. H., Tape, C. J., Stanley, P. L., Taylor, N. A., Mills, I. G., Neal, D. E., ... & Murphy, G. (2010). Thiol isomerases negatively regulate the cellular shedding activity of ADAM17. Biochemical Journal, 428(3), 439-450.

Wirth, T. C., Badovinac, V. P., Zhao, L., Dailey, M. O., & Harty, J. T. (2009). Differentiation of central memory CD8 T cells is independent of CD62L-mediated trafficking to lymph nodes. The Journal of Immunology, 182(10), 6195-6206.

Wolfe, M. S., Xia, W., Ostaszewski, B. L., Diehl, T. S., Kimberly, W. T., & Selkoe, D. J. (1999). Two transmembrane aspartates in PS-1 required for PS endoproteolysis and γ-secretase activity. Nature, 398(6727), 513-517.

Xia, W., Zhang, J., Perez, R., Koo, E. H., & Selkoe, D. J. (1997). Interaction between amyloid precursor protein and PSs in mammalian cells: implications for the pathogenesis of Alzheimer disease. *Proceedings of the National Academy of Sciences*, *94*(15), 8208-8213.

Xu, P., & Derynck, R. (2010). Direct activation of TACE-mediated ectodomain shedding by p38 MAP kinase regulates EGF receptor-dependent cell proliferation. Molecular cell, 37(4), 551-566.

Xu, P., Liu, J., Sakaki-Yumoto, M., & Derynck, R. (2012). TACE activation by MAPK-mediated regulation of cell surface dimerization and TIMP3 association. Science signaling, 5(222), ra34.

Xu, T., Chen, L., Shang, X., Cui, L., Luo, J., Chen, C., ... & Zeng, X. (2008). Critical role of Lck in L-selectin signaling induced by sulfatides engagement. *Journal of leukocyte biology*, *84*(4), 1192-1201.

Yáñez-Mó, M., Barreiro, O., Gordon-Alonso, M., Sala-Valdés, M., & Sánchez-Madrid, F. (2009). Tetraspanin-enriched microdomains: a functional unit in cell plasma membranes. Trends in cell biology, 19(9), 434-446.

Youn, J. I., Collazo, M., Shalova, I. N., Biswas, S. K., & Gabrilovich, D. I. (2012). Characterization of the nature of granulocytic myeloid-derived suppressor cells in tumor-bearing mice. Journal of leukocyte biology, 91(1), 167-181.

Yu, G., Nishimura, M., Arawaka, S., Levitan, D., Zhang, L., Tandon, A., ... & Supala, A. (2000). Nicastrin modulates PS-mediated notch/glp-1 signal transduction and βAPP processing. Nature, 407(6800), 48-54.

Zaidel-Bar, R. (2013). Cadherin adhesome at a glance.

Zakrzewicz, A., Gräfe, M., Terbeek, D., Bongrazio, M., Auch-Schwelk, W., Walzog, B., ... & Gaehtgens, P. (1997). L-selectin–dependent leukocyte adhesion to microvascular but not to macrovascular endothelial cells of the human coronary system. Blood, 89(9), 3228-3235.

Zeng, F., Xu, J., & Harris, R. C. (2009). Nedd4 mediates ErbB4 JM-a/CYT-1 ICD ubiquitination and degradation in MDCK II cells. The FASEB Journal, 23(6), 1935-1945.

Zhang, C. C., Pavlicek, A., Zhang, Q., Lira, M. E., Painter, C. L., Yan, Z., ... & Zong, Q. (2012). Biomarker and pharmacologic evaluation of the γ-secretase inhibitor PF-03084014 in breast cancer models. Clinical Cancer Research, 18(18), 5008-5019.

Zhao, L. C., Edgar, J. B., & Dailey, M. O. (2001). Characterization of the rapid proteolytic shedding of murine L-selectin. Journal of Immunology Research, 8(3-4), 267-277.

Zheng, Y., Schlöndorff, J., & Blobel, C. P. (2002). Evidence for regulation of the tumor necrosis factor α-convertase (TACE) by protein-tyrosine phosphatase PTPH1. Journal of Biological Chemistry, 277(45), 42463-42470.

Zimmerman, G. A., McIntyre, T. M., Mehra, M., & Prescott, S. M. (1990). Endothelial cell-associated platelet-activating factor: a novel mechanism for signaling intercellular adhesion. J Cell Biol, 110(2), 529-540.

Appendix I: Solutions and buffer

Buffer	Recipe
Agarose gel (1 %)	2g agarose 200 mL of 1 X TBE buffer 10 µL ethidium bromide
Binding/wash buffer	100 mM sodium phosphate (pH 8.0) 600 mM sodium chloride 0.02 % Tween 20 (v/v)
Elution buffer	300 mM Imidazole 50 mM sodium phosphate (pH 8.0) 300 mM NaCl 0.01 % Tween 20 (v/v)
FACs buffer	Phosphate buffered saline 1 % Fetal Calf Serum (v/v)
LB Agar	1 L of LB Broth 15 g agar
Luria-Bertani broth (LB) medium	10g tryptone 5g yeast extract 10g NaCl
Orange G loading buffer	0.25% Orange G (w/v) 30 % glycerol (v/v) in dH_2O
pH 7.1 medium	Serum free DMEM 25 mM HEPES pH adjusted to 7.1 and filtered through 0.22 µM filter
pH 7.9 medium	D10 25 mM HEPES pH adjusted to 7.9 and filtered through 0.22 µM

Phosphate buffered saline	10 PBS tablets (OXOID)/1L dH_2O
Cell lysis buffer	25 mM HEPES (pH 7.5) 150 mM NaCl 10 mM $MgCl_2$ 1 mM EDTA 2 % glycerol (v/v) 1 % Triton X-100 (v/v) 8 mg/mL 1,10 Phenathroline 1 mM sodium orthovanadate one Roche complete ULTRA Tablet
SDS (4X) reducing buffer/Laemmli buffer	660 mM Tris-HCl (pH 6.8) 26 % glycerol (v/v) 4 % SDS (w/v) 0.01 % bromophenol blue (w/v) 5 % β2-meracaptoethanol (v/v).
SDS reducing buffer (2X)	660 mM Tris-HCl (pH 6.8) 26 % glycerol (v/v) 2 % SDS (w/v) 0.01 % bromophenol blue (w/v) 5 % β2-meracaptoethanol (v/v).
TBE buffer	0.45 M Tris 0.45 M Boric acid 10 mM EDTA (pH 8.0)
TBS-T	PBS 1% Tween-20 (v/v)

Appendix II: Chemicals

Chemical	Manufacturer
1,10 Phenathroline	Sigma Aldrich Company Ltd, Dorset, UK
Agar	Fisher Scientific, Loughborough, UK
Boric acid	Fisher Scientific, Loughborough, UK
Bromophenol blue	Fisher Scientific, Loughborough, UK
dNTPs	New England Biolabs, Hitchin, UK
EDTA	Fisher Scientific, Loughborough, UK
Ethidium bromide	Sigma Aldrich Company Ltd, Dorset, UK
Glycerol	Fisher Scientific, Loughborough, UK
HEPES	Fisher Scientific, Loughborough, UK
Hydrochloric acid	Fisher Scientific, Loughborough, UK
Imidazole	Sigma Aldrich Company Ltd, Dorset, UK
Magnesium chloride	Fisher Scientific, Loughborough, UK
Orange G	Sigma Aldrich Company Ltd, Dorset, UK
Paraformaldehyde	Fisher Scientific, Loughborough, UK
Skimmed milk powder	Milbona, Lidl, UK
Sodium chloride	Fisher Scientific, Loughborough, UK
Sodium dodecyl sulphate SDS	Fisher Scientific, Loughborough, UK
Sodium Orthovanadate	Sigma Aldrich Company Ltd, Dorset, UK
Sodium phosphate	Sigma Aldrich Company Ltd, Dorset, UK
Tris Base	Fisher Scientific, Loughborough, UK
Triton X-100	Fisher Scientific, Loughborough, UK
Tryptone	Fisher Scientific, Loughborough, UK
Tween-20	Sigma Aldrich Company Ltd, Dorset, UK
Yeast extract	Fisher Scientific, Loughborough, UK
β2-mercaptoethanol	Sigma Aldrich Company Ltd, Dorset, UK

Appendix III: Consumables and laboratory equipment

Consumable	Manufacturer
Amicon® Ultra-4 Centrifugal Filter Units	Millipore (U.K) Ltd, Hertfordshire, UK
SuperSignal West Pico Chemiluminescence developing solution	Thermo Fisher Scientific, Paisley, UK
Foams	Bio-Rad Laboratories Ltd, Hertfordshire, UK
Filter paper	Fisher Scientific, Loughborough, UK
Cryo vials	Grenier bio-one, Stonehouse, UK
Clearline pipette tips (10, 100, 200, 1000 µL)	Dutscher Scientific, Essex, UK
Immobilon-PSQ 0.2 µM polyvinyliden-difluorid (PVDF) membrane	Millipore (U.K) Ltd, Hertfordshire, UK
Millex filters (0.45 µM)	Millipore (U.K) Ltd, Hertfordshire, UK

Equipment	Manufacturer
BD FACs Canto II	BD Biosciences, Oxford, UK
Centrifuge Heraeus Megafuge 4R	Thermo Fisher Scientific, Paisley, UK
DynaMag-5 magnet	Thermo Fisher Scientific, Paisley, UK
FLUOstar OPTIMA microplate reader	BMG Labtech, Aylesbury, UK
Freezing container	Nalgene Labware, Thermo Fisher Scientific, Paisley, UK
Heat block	Wolflabs, York, UK
HERA Cell 150 Incubator (cell culture)	Heraeus, Hanau, Germany
Incubator (molecular biology)	Gallenkamp, Weistechnik, Loughborough, UK
Magnetic stirrer	Falc instruments, Tremglio, Italy
Microcentrifuge (Heraeus Biofuge Pico)	DJB Labcare Ltd, Newport Pagnell, UK
Mini Protean 14 –Well Combs	Bio-Rad Laboratories Ltd, Hertfordshire, UK

myECL imager	Thermo Fisher Scientific, Paisley, UK
ND-1000 NanoDrop ™ spectrophotometer	Thermo Fisher Scientific, Paisley, UK
Neubauer cell counting chamber	Cereromics, Valencia, Spain
Optima L-100 XP ultracentrifuge	Beckman Coulter, High Wycombe, UK
Orbital shaker	Gallenkamp, Weistechnik, Loughborough, UK
Oven	Gallenkamp, Weisstechnik, Loughborough, UK
Peltier DNA Engine Dyad Thermal Cycler	Bio-Rad Laboratories Ltd, Hertfordshire, UK
Peqlab gel electrophoresis tank	VWR, Darmstadt, Germany
pH meter	Jenway, Staffordshire, UK
Pipettes (P10, 100, 200, 1000)	Mettler-Toledo Ltd, Leicester, UK
Power Supply	Bio-Rad Laboratories Ltd, Hertfordshire, UK
Rocker	Stuart, Staffordshire, UK
Rotator plate	Stuart, Staffordshire, UK
SLA-3000 fixed angle rotor	Thermo Fisher Scientific, Paisley, UK
Sonic Dismembrator model-120	Thermo Fisher Scientific, Paisley, UK
SureLock Mini Cell system	Thermo Fisher Scientific, Paisley, UK
SW28.1 swinging bucket rotor	Beckman Coulter, High Wycombe, UK
Swiftpet Pipette boy	HTL, Lab Solutions, Warszawa, Poland
Thin wall, ultra-clear centrifugation tube (38.5 mL)	Beckman Coulter, High Wycombe, UK
Tweezers	VWR International Inc, Chicago, UK
Optima L-100 XP Ultracentrifuge	Beckman Coulter, High Wycombe, UK
UV transilluminator	UVP, Upland, USA
XCell II™ Blot Module	Thermo Fisher Scientific, Paisley, UK

Appendix IV: Primers

Primer number	Primer sequence		Reference to section
1	TCTGGGTTGGCATTTAAGATTTGGCTGGCAAGG	F	6.4
2	CCTTGCCAGCCAAATCTTAAATGCCAACCCAGA	R	
3	TCTGGGTTGGCATTTTGGATTTGGCTGGCAAGG	F	6.4
4	CCTTGCCAGCCAAATCCAAAATGCCAACCCAGA	R	
5	*CGCCCGGGGG*GGATCCGCCGCCACC**ATG**GGCTGCAGAAGAACTAGAG	F	3.2
6	*CTCGAGCCCG*GGATCC**TCA**ATGGTGATGGTGATG	R	

A1: Primers used for cloning in Chapters 3 and 6. Forward (F) and reverse (R) primers for In-Fusion (yellow) and site directed mutagenesis (red) are shown. For In-fusion reactions, primer sequence homology with the plasmid is shown in italics. The BamHI restriction site (GGATCC) is underlined. Start (ATG) and stop (TCA) codons are illustrated in bold while the kozak consensus sequence is displayed in purple. The forward primer contains a sequence for the N terminus of L-selectin (highlighted in pink) and the reverse primer contains DNA for the C terminal V5 His region (highlighted in grey). For site directed mutagenesis, introduction of lysine (AAG) for I351K L-selectin is highlighted in blue and tryptophan (TGG) for I351W L-selectin in green.

Primer number	Primer sequence		Binding site of primer
7	ATGGGCTGCAGAAGAACTAG	F	L-selectin start codon
8	CTGTGTAATTGTCTCGGCAG	R	L-selectin 206
9	TACACAGCTTCTTGCCAGCC	F	L-selectin 504
10	CCTCCAAAGGCTCACACTGA	R	L-selectin 623
11	GCATGTACCTTCATCTGCTCAG	F	L-selectin 888
12	TATCTCGAGATATGGGTCATTCATACTTCTCTTGGA	R	V5/His stop codon

A2: Primers used to sequence L-selectin.

Appendix V: Plasmid Maps

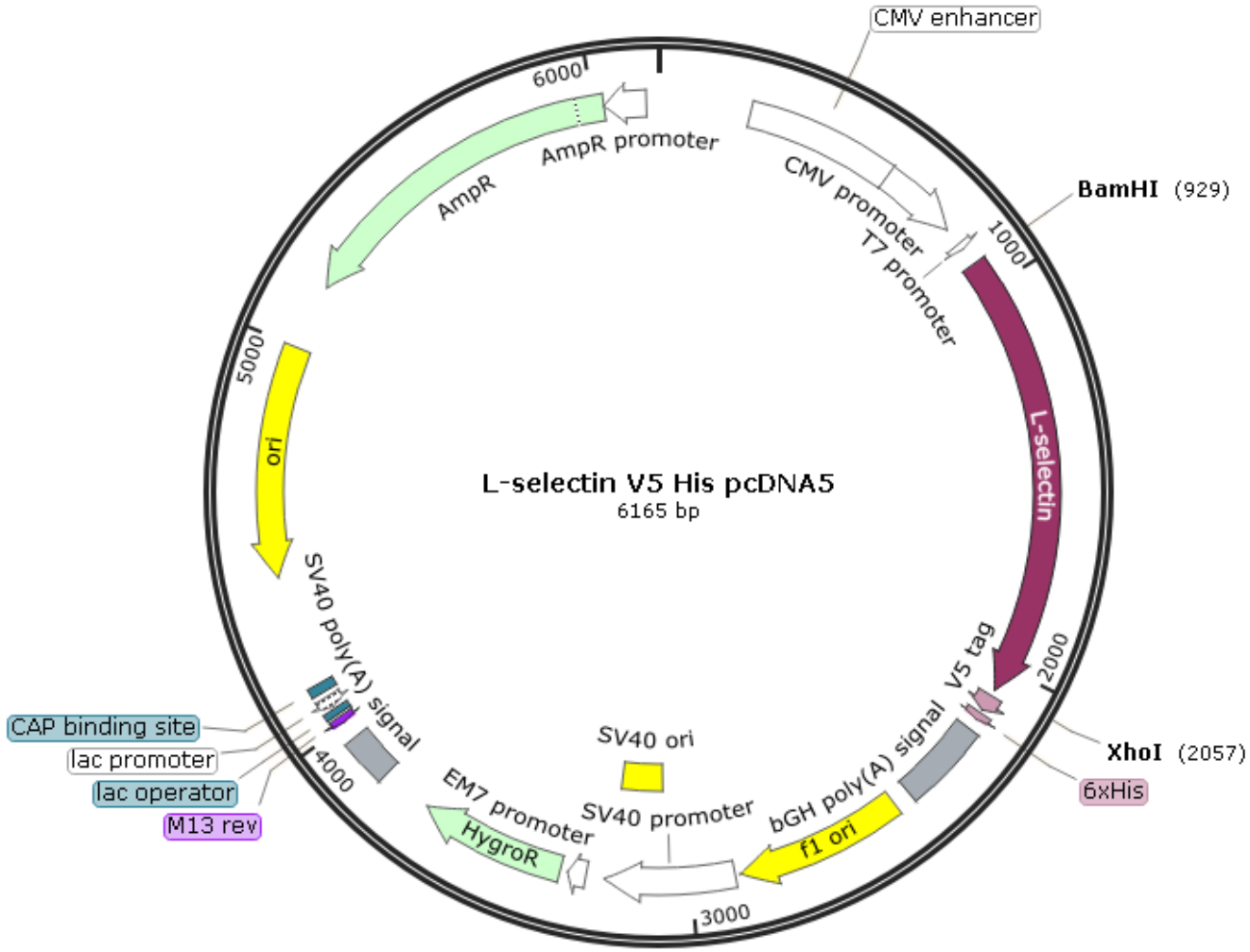

Figure A.1: Circular map of the L-selectin V5 His pcDNA5 plasmid

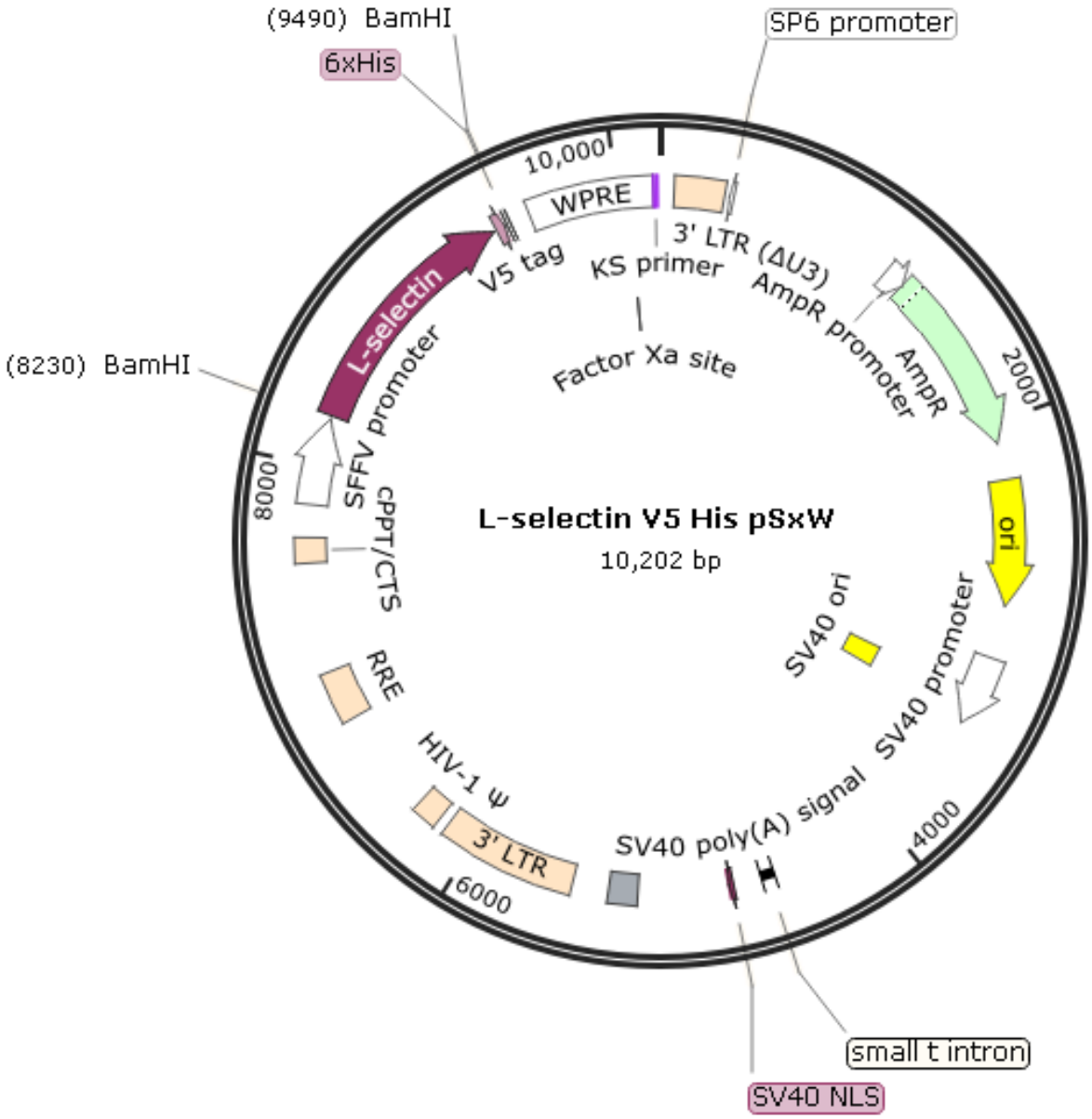

Figure A.2: Circular map of the L-selectin V5 His pSxW plasmid